EFFECTS OF TRAFFIC VARIABILITY ON THE NUMBER AND START TIME OF SIGNAL TIMING PLANS

A Dissertation

by

MUSHTAQ FARHAN HAMID AL-SAIDI

Submitted to the Graduate and Professional School of
Texas A&M University
in partial fulfillment of the requirements for the degree of

DOCTOR OF PHILOSOPHY

Chair of Committee,	Gene Hawkins
Committee Members,	Daren B.H. Cline
	Dominique Lord
	Yunlong Zhang
Head of Department,	Zachary Grasley

December 2021

Major Subject: Civil Engineering

ABSTRACT

Traffic volume at any intersection varies with time. Amount and pattern of variation can differ depending on the nature of the area, population composition, and other factors. Regardless, addressing that variation in traffic volume when designing timing plans at an intersection is essential to optimize its performance. Specifically, selecting when to initiate a timing plan can play a major role in improving the signal's operation. Therefore, in this study, two methodologies were developed to optimize the selection of breakpoints of timing plans at a pretimed signalized intersection based on the minimization of delay. These techniques are the critical zone optimization method and the ΔV optimization method. The developed techniques generate different alternatives of timing plan breakpoints and select the optimal set of breakpoints based on their performance. To validate the proposed methodologies, traffic counts were collected on two consecutive days in two intersections in College Station, TX. The counts were collected by, first, recording videos of the traffic and then analyzing those videos by a computer program, developed by the author, which can detect and count vehicles in the recorded videos. The developed optimization methodologies were applied on the collected data by utilizing a computer program which was also developed by the author based on the proposed optimization techniques. Timing plan breakpoints were generated by the optimization process. The results showed the ability of the developed optimization techniques to minimize delay and select, accordingly, the optimized breakpoints of timing plans. Also, by comparing the results with the results of the

traditional AM peak, PM peak, and off-peak plan set, the developed techniques were found to be more effective in selecting the breakpoints of timing plans.

Furthermore, it was found that the critical zone optimization method performed better than the ΔV optimization method because it produces breakpoints that causes slightly less delay than those found by the ΔV optimization. Additionally and most importantly, the critical zone optimization method produces more alternatives of timing plan breakpoints that might perform relatively similar to the optimal breakpoints. This can help local agencies to freely select the breakpoints that can fit their requirements.

ACKNOWLEDGEMENTS

I would like to thank my committee chair, Dr. Hawkins, and my committee members, Dr. Zhang, Dr. Lord, and Dr. Cline, for their guidance and support throughout the course of this research.

Thanks also go to my friends and colleagues and the department faculty and staff for making my time at Texas A&M University a great experience.

Finally, thanks to my mother and father for their encouragement and to my wife and kids for their patience and love.

CONTRIBUTORS AND FUNDING SOURCES

This work was supervised by a dissertation committee consisting of Professor Gene Hawkins [advisor] and Professors Yunlong Zhang and Dominique Lord of Zachry Department of Civil and Environmental Engineering and Professor Daren Cline of the Department of Statistics.

The videos analyzed for Chapter III were provided by the advisor, Professor Gene Hawkins.

All other work conducted for the dissertation was completed by the student independently.

Graduate study was supported by a scholarship from the Higher Committee for Education Development in Iraq and a graduate assistantship from Texas A&M University.

NOMENCLATURE

a	Acceleration
C	Cycle length
c	Capacity
d	Control delay
D	Total delay
E_{LT}	Equivalent number of through cars for a protected left-turning vehicle
E_R	Equivalent number of through cars for a protected right-turning
EBLT	Eastbound left turn
EBRT	Eastbound Right Turn
EBTH	Eastbound through
f_a	Adjustment factor for area type
f_{bb}	Adjustment factor for blocking effect of local buses that stop within intersection area
f_{HVg}	Adjustment factor for heavy vehicles and grade
f_{Lpb}	Pedestrian adjustment factor for left-turn groups
f_{LT}	Adjustment factor for left-turn vehicle presence in a lane group
f_{LU}	Adjustment factor for lane utilization
f_{ms}	Adjustment factor for downstream lane blockage
f_p	Adjustment factor for existence of a parking lane and parking activity adjacent to lane group
f_{Rpb}	Pedestrian-bicycle adjustment factor for right-turn groups
f_{RT}	Adjustment factor for right-turn vehicle presence in a lane group
f_{SP}	Adjustment factor for sustained spillback
f_w	Adjustment factor for lane width
f_{wz}	Adjustment factor for work zone presence at the intersection,
fps	Frames per second
HCM	Highway Capacity Manual
I	Upstream filtering adjustment factor
k	Incremental delay factor

l	Distance between vehicles
L	Lost time
MUTCD	Manual on Uniform Traffic Control Devices
n	Degree of polynomial
N	Number of lanes
NBLT	Northbound left turn
NBRT	Northbound Right Turn
NBTH	Northbound through
P	Proportion of vehicles arriving during the green indication
pc/h/ln	Passenger car per hour per lane
P_g	Approach grade for the corresponding movement group
P_{HV}	Percentage heavy vehicles in the corresponding movement group
P_R	Proportion of right-turning vehicles in the shared lane
PF	Progression adjustment factor
R	All-Red clearance interval
R_P	Platoon ration
s	Saturation flowrate
s_{sr}	Saturation flow rate in shared right-turn and through lane group with permitted operation
s_{th}	Saturation flow rate of an exclusive through lane
s_o	Base saturation flow rate
SBLT	Southbound left turn
SBRT	Southbound Right Turn
SBTH	Southbound through
T	Study period
t	Time
θ	Angle of direction of a vehicle
TOD	Time of Day
TxDOT	Texas Department of Transportation
v	Speed
V	Traffic volume
veh/h/ln	Vehicle per hour per lane

Vph	Vehicle per hour
W	Intersection width
WBLT	Westbound left turn
WBRT	Westbound Right Turn
WBTH	Westbound through
X	Volume to capacity ratio
y	Critical flow ratio
YOLO	You Only Look Once

TABLE OF CONTENTS

LIST OF FIGURES

LIST OF TABLES

CHAPTER I

INTRODUCTION

Traffic volume changes with time. Within a given day, the traffic volume in the early morning is different than that in the late morning and noon period. In the late afternoon, it is different than that during the night. Over a week, traffic on workdays is different than traffic on the weekend. The same thing happens from month to month. During school season, traffic is different than break seasons. Of course, this depends on the nature of the land use. For example, traffic in industrial areas is different than that in residential areas. Having a traffic control system, namely, traffic signals, that can accommodate this variability in traffic volume is essential to make sure road users experience the lowest possible amount of delay.

Electro-mechanical controllers used to be the only controllers that traffic agencies used for signal operation. Those controllers used dials that could only handle up to three timing plans which ended up being AM peak, off peak, and PM peak. However, signal controllers today have become so advanced they can handle more than 40 timing plans per day. That should provide more flexibility and freedom when selecting the number of timing plans. Nevertheless, many still use only 3 or 4 timing plans in a day. As a result, there is the potential that the full efficiency of modern controllers is not being realized.

Currently, when developing a timing plan for any traffic signal, the main thing that is taken into consideration is that the cycle length is calculated in a way that gives minimum delay during the period that cycle is applied for. Also, the timing plan is calculated based on 15-minute flowrate but that timing plan may be applied for 1 to 4 hours which could result in a higher delay during periods when timing plan is not appropriate. However, changing that time window, for example, starting earlier or later than the original start time of the timing plan can result in a lower value for the delay since the timing plan will cover a different period. That would be more evident with higher variability of traffic volume, at which time selecting the optimal number and start time of timing plans will be more effective in improving the performance of traffic signals. Therefore, selecting the number of plans and when to start a new timing plan is a key factor in the performance of any traffic signal.

Currently, traffic agencies use their engineering judgment to determine the number and start time of the daily timing plans. Although the engineering judgement is needed in most cases, an analytically-based guide is required to get the optimal performance from the traffic system. Hence comes the importance of this research. In this research, a methodology was developed that can optimizes the number of timing plans and decides when each plan should start. By providing the traffic volumes for the analysis period and the use of optimization techniques, it is possible to do that. The optimization was conducted in a way that can give the lowest possible value for the summation of delay throughout the analysis period.

Problem Statement

The traffic volume can change from hour to hour during a day. Also, these variabilities can be noticed from day to day, week to week, month to month and even year to year. This variability needs to be considered when developing timing plans for signalized intersections. Currently, only engineering judgement is used to decide the number and start time of timing plans at any signalized intersection. Selecting the optimal number and start time of a signal timing plan is usually done by following subjective assessment. There is no documented procedure that traffic agencies can use to decide on the optimal number and start time or breakpoints of signal timing plans.

Research Goal and Objectives

The goal of this study is to determine the optimal number and start times of timing plans at a pretimed signalized intersection based on the variability in traffic volumes throughout the day. This goal will be met by answering the following questions.

1. What are the advantages and disadvantages of the current practice in selecting breakpoints of signal timing plans?
2. What is the maximum number of timing plans a signal controller can handle?
3. What is an appropriate way to evaluate traffic variability at an intersection.
4. How to optimize the number and start time of timing plans at an isolated, pretimed signalized intersection.
5. For validation, what is the type and amount of needed data?
6. How to collect the required data.

Assumptions and Limitations

The following assumptions and limitations are considered and followed throughout this dissertation.

1. The methodology is developed for isolated pretimed signalized intersections.
2. The minimum period a timing plan is continually applied for is 1 hour.
3. The optimization methodology is based on minimizing delay.

Outline of the Dissertation

This dissertation is consisted of six chapters. Chapter I was presented in the previous few pages. The next five chapters are as the following:

Chapter II: Literature Review. In this chapter, previous research that is related to the topic of the dissertation was presented and cited.

Chapter III: Data Collection. The data needed for testing and validating the developed methodology was presented in this chapter along with the developed technique for automatically detecting and counting the vehicles in the intersection.

Chapter IV: Theoretical Approach. Chapter IV presents the theory the research is based on and the methodology of time-of-day signal timing optimization.

Chapter V: Application and Validation. In this chapter, the collected data were used to test and validate the developed methodology.

Chapter VI: Conclusions and Recommendations. Chapter VI presents final conclusions, recommendations, and future research, which are related to the dissertation's topic, in addition to the benefits of the study.

CHAPTER II

LITERATURE REVIEW

Traffic Variability and Breakpoints of Signal Timing Plans

Traffic variability can affect the overall performance of any traffic signal. One of the most important tasks that is affected by traffic variability is selecting the appropriate time of day to change the signal timing pattern. In other words, when to change from one signal timing plan to another.

As a variability measure, the earliest reference found that talked about the developing of the peak hour factor formula was (Normann, 1962). Based on that research, “the peak 15-min period was used because it is considered the shortest time interval on which an index of the variation in traffic flow during the peak hour may be used”. This, however, needs to be further investigated because that research was conducted more than 50 years ago, and since then traffic characteristics and components have changed dramatically. Also, the technology used nowadays in traffic signals and controllers is very advanced compared to the technology during the 1960’s.

By looking at the literature, not much research was found regarding the selection of the optimal number and start time of traffic signal timing plans. However, below is a summary of previous research that was found in the literature. Different techniques to find the timing plan breakpoints have been used in the literature, each with its own advantages and disadvantages.

The Signal Timing Manual (Koonce et al., 2008; Urbanik et al., 2015) gives general recommendations on how to determine the time-of-day breakpoints for traffic signal plans. The manual noted that time-of-day plans should be developed for specific outcomes and can be used to help an agency meet its objectives during different time periods. However, it did not give guidelines for how to decide when those time-of-day breakpoints should be.

Wang et al. (X. D. Wang, Cottrell, & Mu, 2005) used K-means clustering to identify TOD breakpoints. The K-means method is a nonhierarchical statistical algorithm, in which the data are divided into K initial clusters and the centroid for each cluster is found. The data then are assigned to each cluster based on their distance from the cluster's centroid. This process is repeated until it converges when there is a minimal or no reassignment happens. Their research involved a case study in which they collected 5-minute turning counts for the period (7:00-10:45) am on a weekday for two-intersection corridor in Salt Lake City, Utah. They used two clusters (K=2), namely AM peak and AM off-peak. By using this method, they were able to determine when the best timing of the breakpoints for the two intersections is. However, their data were collected for a limited period and they suggested to try this method with a bigger set of data and more intersections.

Park et al. (Park, Santra, Yun, & Lee, 2004) used genetic algorithm technique to find the best timing for time-of-day, or TOD breakpoints. They applied two-stage optimizations: outer loop for TOD breakpoints and inner loop for timing plans of corresponding intervals. They used intersection delay as their fitness function. However, their technique did not calculate the optimal number of breakpoints, instead, they assumed that the number of breakpoints is given, and they tested limited number of breakpoints per day. They also assumed that it is not practical to have a timing plan to last for less than two hours because of transition costs. Based on their assumption, any period less than two hours, for which a timing plan is used, would not be sufficient to overcome the disruption in service caused by the transition from one plan to another.

Lee et al. (Lee, Kim, & Park, 2010) based their research on the work of Park et al. (Park et al., 2004) and they used the same data Park et al. (Park et al., 2004) used. However, they used the average cumulative queue instead of delay time as a fitness function for their genetic algorithm optimization. One thing to point here is that in both papers they did not consider all of the possibilities of start time of a timing plan. They predetermined a limited number of possible breakpoints and used genetic algorithm to choose the best breakpoints from the provided set. For an analysis period between 5:00 am to 7:00 pm they assumed that there are only 56 possible 15-min intervals, which are 5:00 am-5:15 am, 5:15 am-5:30 am, …, 6:45 pm-7:00 pm. They used those intervals as their possible start time for a new timing plan. However, they did not consider 14 other possible start times for the intervals. For example, they did not study the periods 5:05 am – 5:20 am, 5:20 am – 5:35 am, …, 6:50 pm – 7:05 pm.

To sum up, all of the techniques listed above found the breakpoints to a limited precision level they assumed to be sufficient. No one of them calculated the required number of plans per day. Instead, they considered it is predetermined. In our research, however, we will suggest a procedure to find the optimal number of plans per day as well as their start time.

Methods of Traffic Volume Data Collection

Traffic data are required to evaluate the performance of any highway system. There are different methods to collect traffic volume data, such as manual counting like tally counters (Randall, 2012), mechanical counting like pneumatic road tubes (Larue & Wullems, 2019), or electrical counters like induction loop (Grote, Williams, Preston, & Kemp, 2018), piezoelectric sensors (Rajab, Al Kalaa, & Refai, 2016), and wireless sensor network (H. Wang, Ouyang, Meng, & Kong, 2020). See Figure 1, Figure 2, and Figure 3 below.

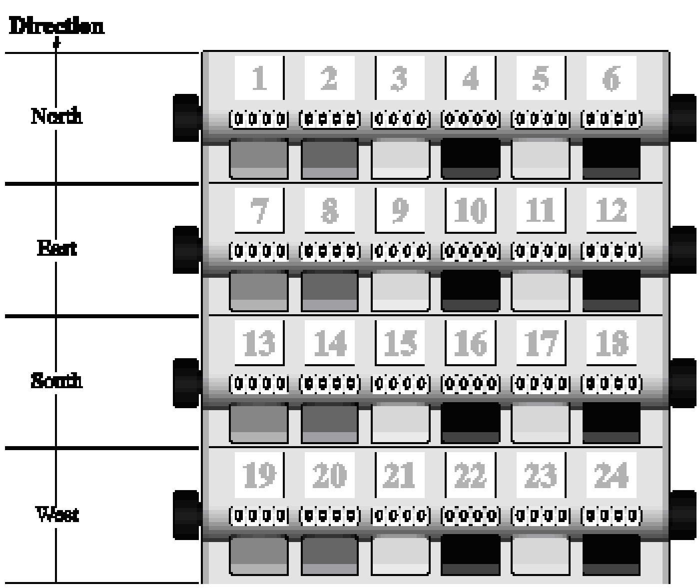

Figure 1: Tally Counter for a Four-Way Count

(Reprinted from (Randall, 2012))

Figure 2: Pneumatic Road Tubes

(Reprinted from (Wordpress, 2014))

Figure 3: Piezoelectric Sensors

(Reprinted from (Counter, 2021))

Additionally, there are some relatively modern methods like radar, Figure 4, and image processing techniques.

Figure 4: Radar Traffic Counter

(Reprinted from (Tri-State, 2021))

All of the previously mentioned techniques of traffic data collection vary in their ability, accuracy, and safety of their users. However, the relatively modern vehicle detection technique, which is image processing technique, can be considered one of the safest, most accurate, and less destructive to the structure of the roadways since it only requires installing cameras at the location under study.

There are different image processing detection techniques which require the use of extensive computer powers and some level of knowledge in programming. One of which was developed by Redmon, et. al. (Redmon, Divvala, Girshick, & Farhadi, 2015) which they called “You Only Look Once” or YOLO for short. It presented a new approach of object detection by framing the objects with spatially separated bounding boxes. After that, with the use of artificial intelligence, those boxes are associated with probabilities which then get translated to whatever the nature of the detected object was.

In this dissertation, a methodology was developed to determine the optimal number of timing plans and starting time of each one. Data were collected to test the developed technology. The method that was used to collect the data was image processing. The following chapters will present the data collection methodology and TOD timing plan optimization technique.

CHAPTER III

DATA COLLECTION

Introduction

To test the validity of the developed technique, turning counts are needed, at least at one intersection. Since the developed technique works on extended periods of time, the data need to be collected during such periods. For most residential areas, 12 hours can be considered a good representative for the fluctuation of traffic volume. However, to get the counts for 12 hours, manual methods are not practical. Therefore, cameras are used to record the traffic movement at the selected locations. Additionally, to get the counts of traffic movements, a computerized image processing technique is developed by the author, a technique that can automatically get the number and directions of the vehicles on the videos. Python ("Python Programing Language," 2020) was used for developing the image processing tool.

Site Selection

To test the developed technique, traffic movement counts are needed for intersections with relatively high traffic volumes and variability. Therefore, two intersections were selected for this study. Data were collected on two days for each intersection which makes four sets of data, in total, for the two intersections. These intersections have high traffic volumes compared to other intersections in College Station, Texas. The selected intersections are:

1. University Drive and Texas Avenue intersection.

2. George Bush Drive and Texas Avenue intersection.

See Figure 5 and Figure 6 below.

Figure 5: Intersection of University Drive and Texas Avenue

(Modified from (Google Earth, 2019, December 29))

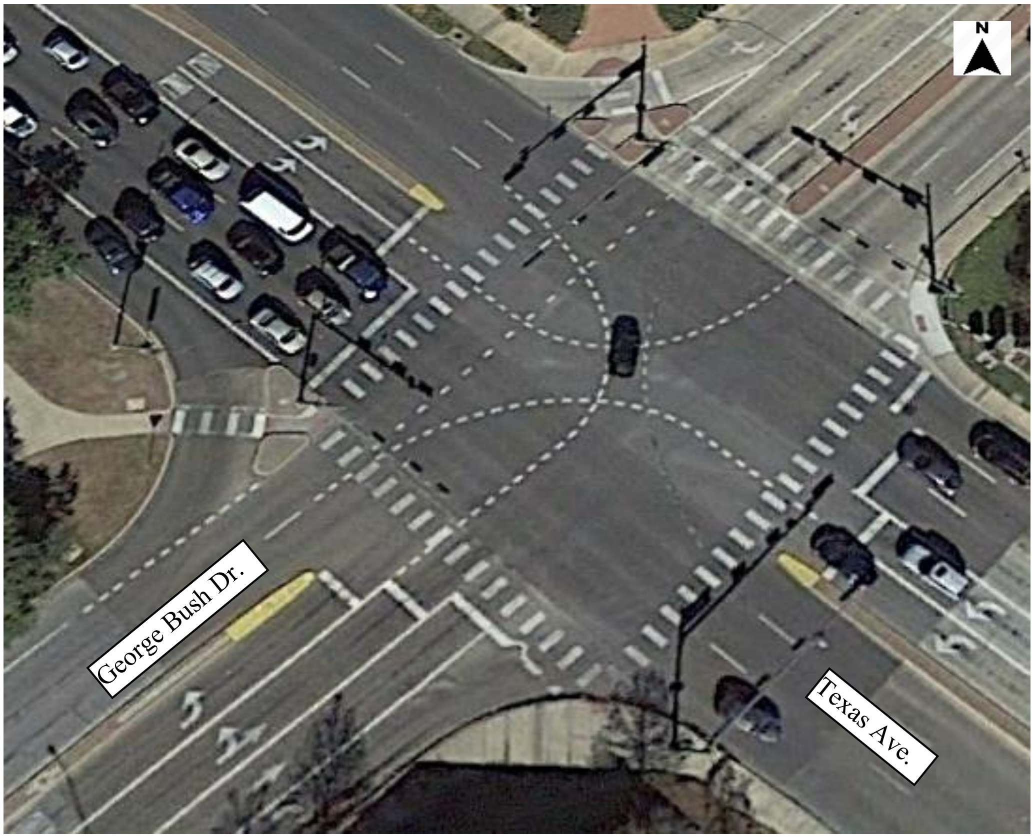

Figure 6: Intersection of George Bush Drive and Texas Avenue

(Modified from (Google Earth, 2019, December 29))

The two intersections are very important to the area due to their locations which are close to the university and the fact that they are both intersections of major roads in College Station. See Figure 7 below which shows locations of the two intersections.

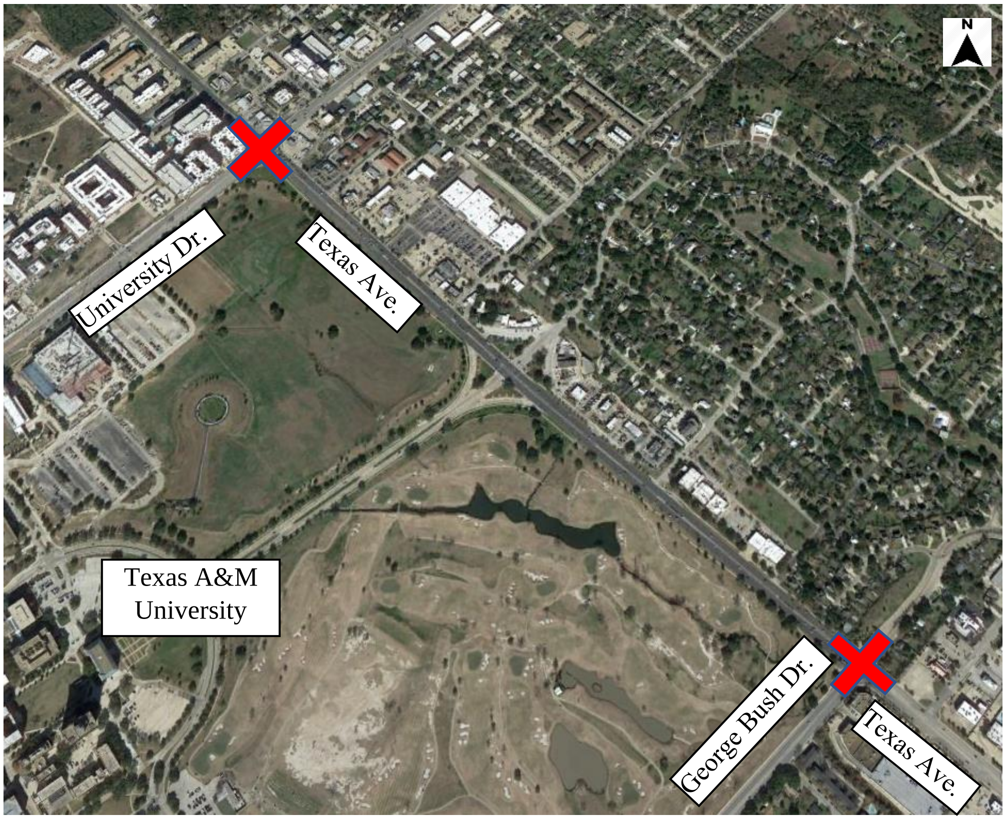

Figure 7: Locations of the Intersection of University Drive and Texas Avenue and the Intersection of George Bush Drive and Texas Avenue (Modified from (Google Earth, 2019, December 29))

Site Description

The first intersection, which is the University Drive and Texas Avenue intersection, is located in the north side of College Station, one of the busiest zones in the city due to the fact that it is very close to Texas A&M University, the main attraction point in the city.

Similarly, the second intersection, which is the intersection of George Bush Dr. and Texas Avenue, is also located at a busy area, which is the south eastern entrance of Texas A&M University.

Traffic volume, at both intersections, is expected to have high fluctuation because it can be affected by the schedule of classes in Texas A&M University.

Dimensions of the two intersections are as shown in Figure 8 and Figure 9 below.

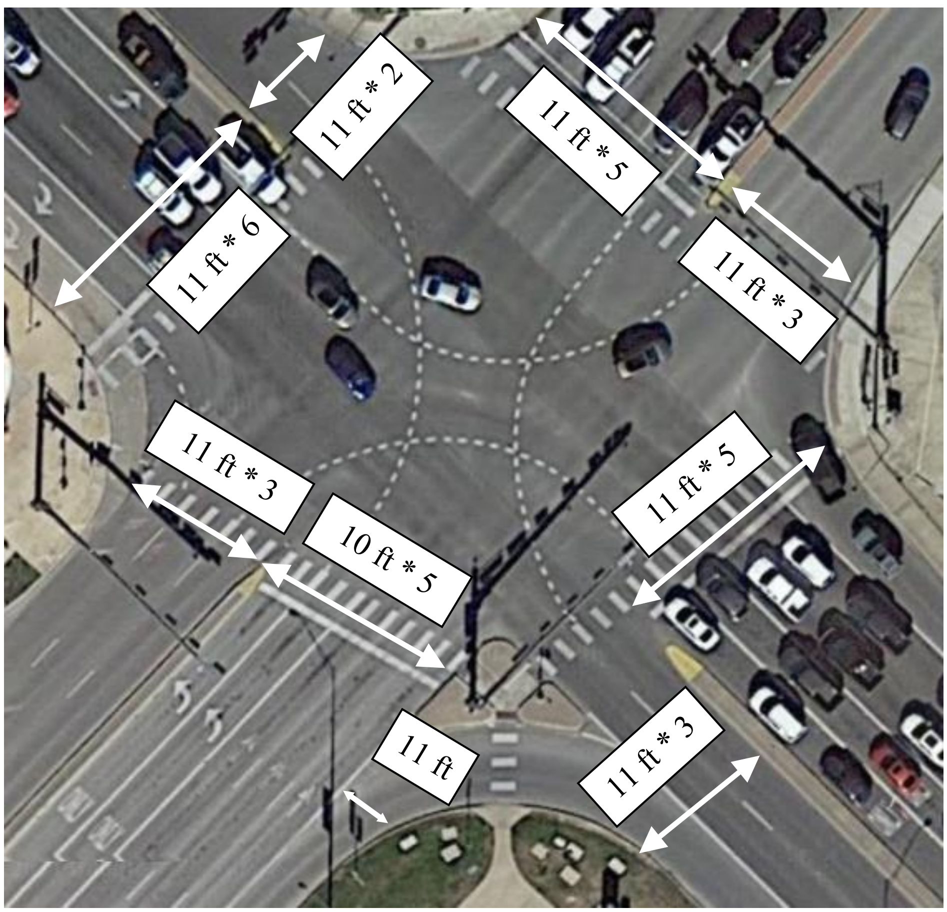

Figure 8: Dimensions of the Intersection of University Drive and Texas Avenue

(Modified from (Google Earth, 2019, December 29))

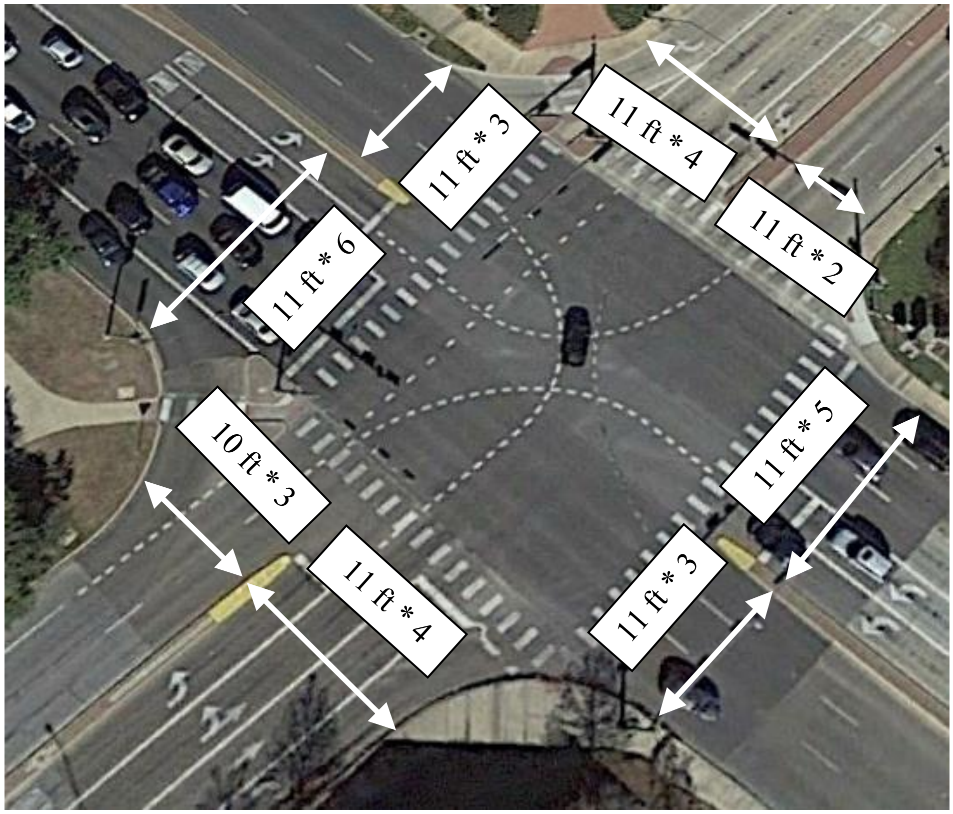

Figure 9: Dimensions of the Intersection of George Bush and Texas Avenue

(Modified from (Google Earth, 2019, December 29))

Speed limit is 40 mph on all approaches of both intersections, except for the westbound of the intersection of George Bush Drive and Texas Avenue which has a 30-mph speed limit.

Traffic Movements

Directions of traffic movements in each intersection are shown in the next two sections.

1. University Dr. and Texas Ave. Intersection

Traffic movements are shown in Figure 10 for the intersection of University Dr. and Texas Ave. All approaches have dedicated lanes for every movement, i.e. separate lanes for right turn movement, through movement, and left turn, except for the westbound which has one shared lane that serves right turn and through movements. Number of lanes for each movement is shown in Figure 10 below.

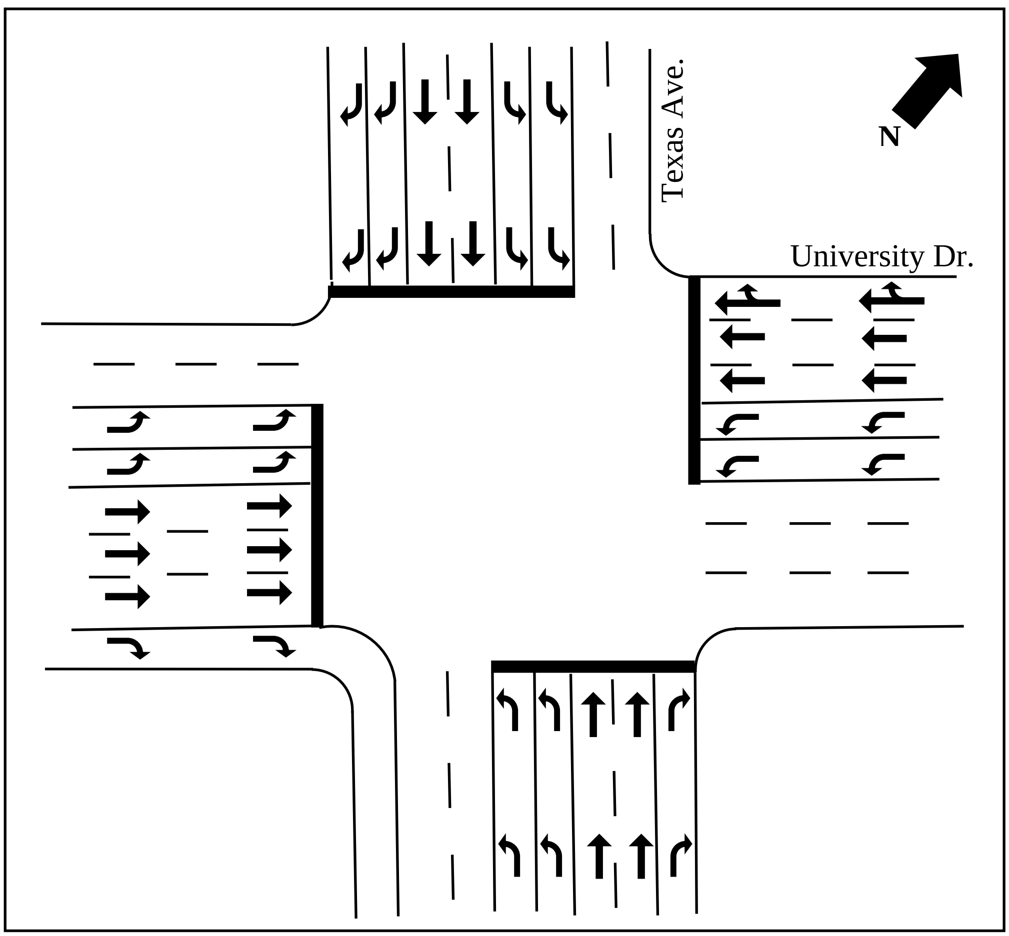

Figure 10: Traffic Movements at the Intersection of University Dr. and Texas Ave.

Lanes are distributed as the following:

1. For northbound, there are one right-turn lane, two through lanes, and two left-turn lanes.
2. For southbound, there are two right-turn lanes, two through lanes, and two left-turn lanes.
3. For eastbound, there are one right-turn lane, three through lanes, and two left-turn lanes.
4. For westbound, there are one right and through shared lane, two dedicated through lanes, and two left-turn lanes.

2. George Bush Dr. and Texas Ave. Intersection

Traffic movements are shown in Figure 11 for the intersection of George Bush Dr. and Texas Ave. All approaches have dedicated lanes for every movement, i.e. separate lanes for right turn movement, through movement, and left turn, except for the northbound which has one shared lane that serves right turn and through movements and the eastbound which has one shared lane that serves left turn and through movements. Number of lanes for each movement is shown in Figure 11 below.

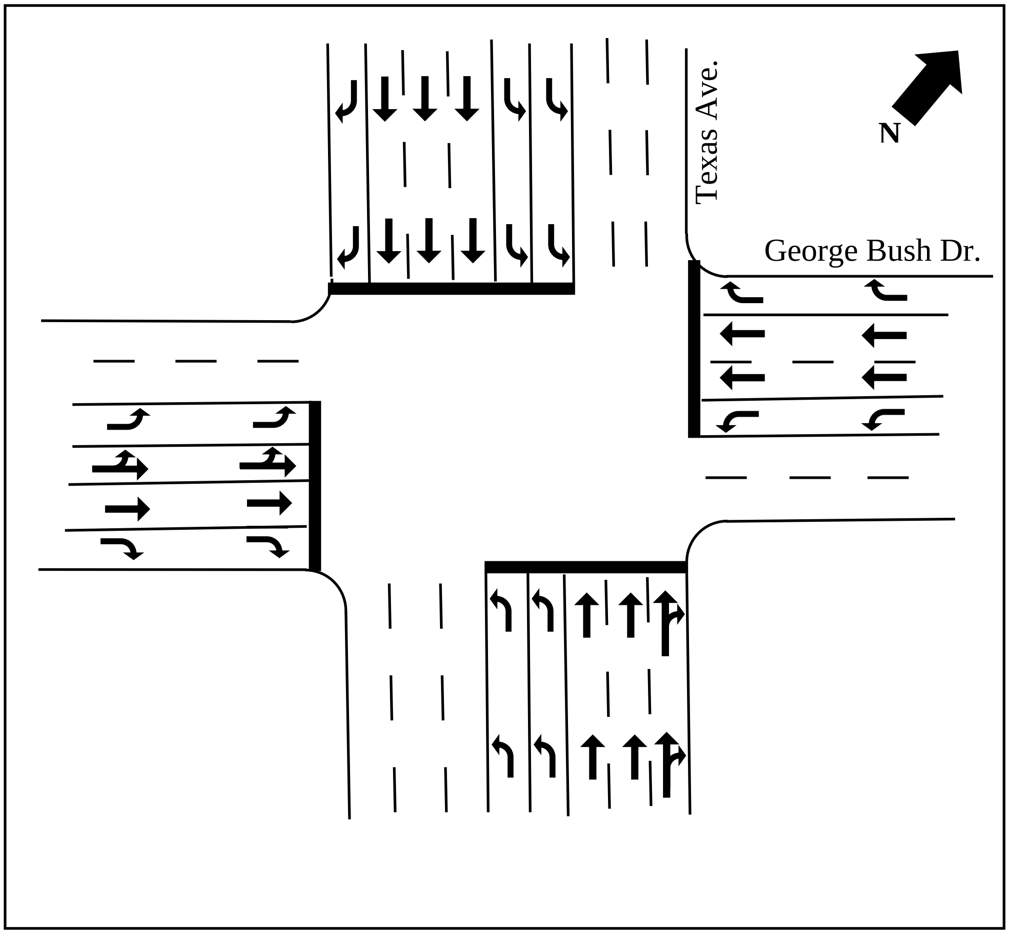

Figure 11: Traffic Movements at the Intersection of George Bush Drive and Texas Avenue

Lanes are distributed as the following:

1. For northbound, there are one right and through shared lane, two dedicated through lanes, and two left-turn lanes.
2. For southbound, there are one right-turn lane, three through lanes, and two left-turn lanes.

3. For eastbound, there are one right-turn lane, one through only lane, one left and through shared lane, and one left-turn only lane.
4. For westbound, there are one right-turn lane, two dedicated through lanes, and one left-turn lane.

Traffic Volumes

For each of the two intersections, traffic data were collected on two days, namely the 12th and the 13th of February, 2019. On each day, at both intersections, two video cameras were placed at the south eastern and the north eastern corners respectively. See Figure 12 through Figure 15 that show the locations and fields of view of cameras in both intersections. Each camera recorded videos of the intersection continuously from 7:00 am until 7:00 pm, which is a continuous 12-hour period on that day. Taking into consideration that during school time and especially during the spring and fall semester, traffic in College Station, in general, is at its highest level. Therefore, these traffic counts, since they were collected in February, are typical for the spring semester. Also, it is worth mentioning that the videos were collected in 2019, which is a pre-Covid-19 pandemic. That means that traffic volume was at its normal level since the majority of classes were held in-class then. While, after the quarantine was announced in March, 2020, traffic volume was at its lowest level.

Figure 12: View of the Camera at the North Eastern Corner of Intersection of

University Dr. And Texas Ave.

Figure 13: View of the Camera at the South Eastern Corner of Intersection of University

Dr. And Texas Ave.

Figure 14: View of the Camera at the North Eastern Corner of Intersection of George Bush Dr. And Texas Ave.

Figure 15: View of the Camera at the South Eastern Corner of Intersection of George Bush Dr. And Texas Ave.

After recording the videos, the next step is to count the vehicles in the videos. Since the videos are 12 hours each which makes a total of 48 hours for the two cameras on each intersection during the two days, or 96 hours for the two intersections together, it is very tasking and almost impractical to manually count the vehicles in the videos. Therefore, the need to develop a computerized tool is necessary. Python programing language ("Python Programing Language," 2020) was used to write a program that can detect and count vehicles in the videos by using special image processing techniques. There are two steps that were followed to get the final counts, namely, detection and counting.

Detection

Detection is the first step in the image processing technique that was developed to get the traffic counts at the selected intersections. The detection technique is based on the method developed by the paper of Redmon et. al. (Redmon et al., 2015). Only minor modification to their python code was necessary to adjust it to be suitable to our needs. The developed detection program does the following:

1. It accepts videos as input.
2. It breaks the video into separate pictures (frames). The number of frames depends on how many frames/second or fps the video has.
3. For each frame, vehicles, pedestrians, and other objects are detected and a rectangle surrounding each detected object is drawn.
4. The coordinates of the rectangles are recorded.

5. The coordinates of the center point of the rectangle are calculated and recorded.
6. The output is a text file with the columns shown below.
    - Column 1: Object Number
    - Column 2: Frame Number
    - Column 3: x-coordinate of the top left corner of the surrounding box
    - Column 4: y-coordinate of the top left corner of the surrounding box
    - Column 5: x-coordinate of the lower right corner of the surrounding box
    - Column 6: y-coordinate of the lower right corner of the surrounding box
    - Column 7: x-coordinate of the center point
    - Column 8: y-coordinate of the center point
    - Column 9: type of the detected object, a car, a truck, a person, …etc.

Counting

As presented in the previous section, the developed program detects objects in each frame of the video separately. For example, let us assume that we are trying to detect the presence of a car in a 2-second-long video and that the video does show the car during the whole 2 seconds. Also, let us assume that the video has 20 fps. That means that the total number of frames in the video is 2 sec × 20 fps = 40 frames. In this case, the car that is shown in the video will be detected 40 times since the detection process works on a frame-by-frame basis. The detection program will show in the output that there are 40 cars in the video when it should be only one. Therefore, to get accurate counts, it is important to track each vehicle in the video from the moment it appears in the video until it leaves.

To track the vehicles that are detected, the process below is followed. See Figure 16 below. In the figure, the dark grey cars are all the same car but shown at different locations at different frames of the video, while light grey cars are other cars also shown at different frames. To find where the location of a vehicle is in the next frame, the following steps are followed:

1. Distance between the location of the car in the current frame and all the close cars in the next frame are first recorded, l in Figure 16 below.
2. The angles between the lines that connect cars in the current frame with the close cars in the previous frame and the lines that connect the cars with the cars in the following frames are recorded, θ in the figure.
3. The value of θ_1 is found by manually measuring the angle between the beginning of the path of vehicles and the stop line as it is displayed in the video. A 90^o angle is reasonable if the cameras are positioned to have a perfect top view as shown in Figure 16. Nevertheless, the value of the angle can change depending on the location of the cameras.
4. To decide what the location of the dark grey car in frame 2 is, two paths are the only possible options, namely, l_2 and l_2' since these are the closest locations of vehicles in frame 2 to the red car in frame 1. Their angles are θ_2 and θ_2' respectively. In general, the angles need to be as close to 180^o as possible because, even if the car is turning to the right or to the left, that turn

would not be noticed between two consecutive frames in a 30 frames/second video for example. Therefore, if the angle is not close to 180^o, the location is not considered. In Figure 16, if any of θ_2 or θ_2' is not close to 180^o, it would automatically be disregarded and the other option is selected. However, if they are roughly at the same distance from 180^o, for example, if they were 160^o and 199^o respectively, the next step is required to determine the direction of the vehicle.

5. The direction of the vehicle should be consistent. In other words, if between frame 1 and frame 2 the car was turning left, in frame 3, we should see a confirmation of the movement to the left direction. In Figure 16, to decide between θ_2 and θ_2', we have to look at θ_3 and θ_3'. We see that when selecting θ_2' and θ_3' direction, the car turns right and then turns left which is not a normal movement at an intersection. However, when looking at θ_2 and θ_3 direction, we see first that the car turns to the left and then it continues turning to the left which shows consistency in the movement. Therefore, θ_2 and θ_3 are selected as the direction of the movement of the selected car.
6. This procedure is applied to all the other cars.
7. After tracking the cars, they are counted and sorted based on their direction and the time they entered the intersection.

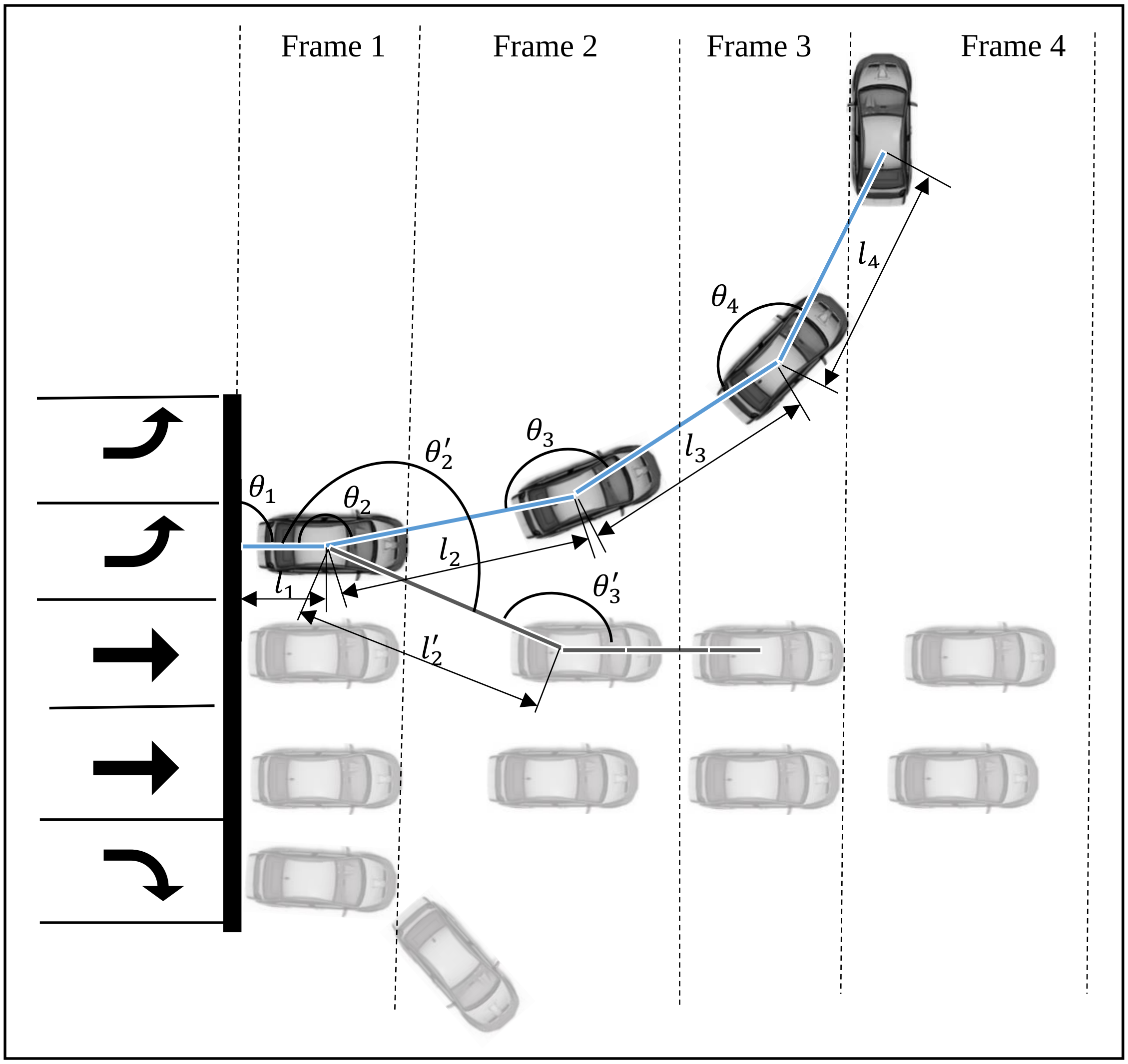

Figure 16: Tracking Detected Vehicles

This technique works for any lane whether it was shared or dedicated since the detection and tracking process can happen at any point if it was visible to the camera with enough clarity.

After applying the developed technique on the videos that were recorded on February 12, 2019, from 7:00 am until 7:00 pm for the intersection of Texas Ave. and University Dr., the following traffic counts were collected. Counts of the other day on this intersection and the two-day counts for the George Bush Dr. and Texas Ave. are available in the Appendix.

Table 1 shows the hourly volumes of traffic for each movement at the intersection.

Table 1: Traffic Volumes for University Dr. and Texas Ave. Intersection on February 12, 2019

	Traffic Volume (vph)											
Time*	8:00	9:00	10:00	11:00	12:00	13:00	14:00	15:00	16:00	17:00	18:00	19:00
Northbound Right Turn	139	184	165	191	278	383	302	309	320	379	467	293
Northbound Left Turn	452	651	483	548	427	470	807	370	377	314	550	574
Northbound Through	595	629	552	720	808	684	818	753	902	742	661	664
Northbound Total	1186	1464	1200	1459	1513	1537	1927	1432	1599	1435	1678	1531
Southbound Right Turn	117	71	51	82	70	104	65	76	57	56	104	71
Southbound Left Turn	153	212	166	215	242	266	272	260	215	249	317	277
Southbound Through	616	550	627	1214	612	841	639	642	649	587	800	665
Southbound Total	887	834	844	1513	925	1212	976	979	922	893	1223	1014
Eastbound Right Turn	160	253	385	470	589	663	598	720	579	497	981	855
Eastbound Left Turn	88	125	100	146	186	225	167	162	112	143	219	208
Eastbound Through	355	791	732	542	807	815	659	812	829	1058	1102	728
Eastbound Total	604	1170	1218	1158	1583	1703	1425	1695	1521	1698	2303	1792
Westbound Right Turn	180	160	120	151	235	232	185	149	159	174	205	179
Westbound Left Turn	193	226	222	227	259	438	369	346	227	224	391	335
Westbound Through	1229	718	477	487	451	701	988	606	437	973	551	599
Westbound Total	1602	1105	820	866	945	1372	1543	1102	824	1372	1148	1113
Intersection Total	4280	4573	4083	4997	4967	5825	5872	5208	4866	5399	6353	5451

* Note: Time indicates end time for the interval

Figure 17 shows a barchart of the traffic volumes for the whole intersection while Figure 18 shows a barchart of hourly traffic volumes for each direction.

These data, in addition to the data from the other intersection, will be used in the validation of the optimization technique in Chapter V.

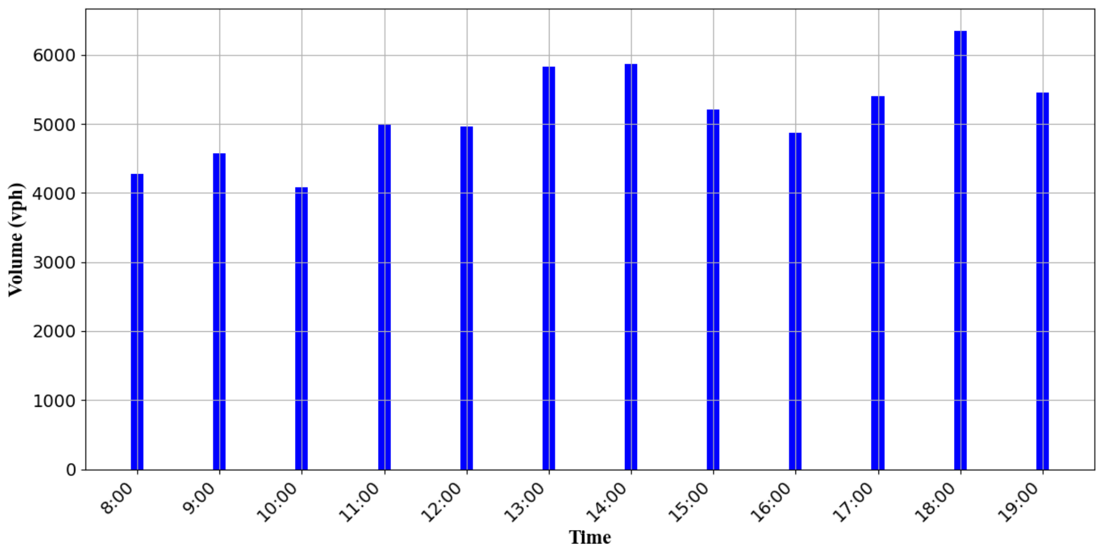

Figure 17: Traffic Volumes Entering the Intersection for University Dr. and Texas Ave. Intersection on February 12, 2019

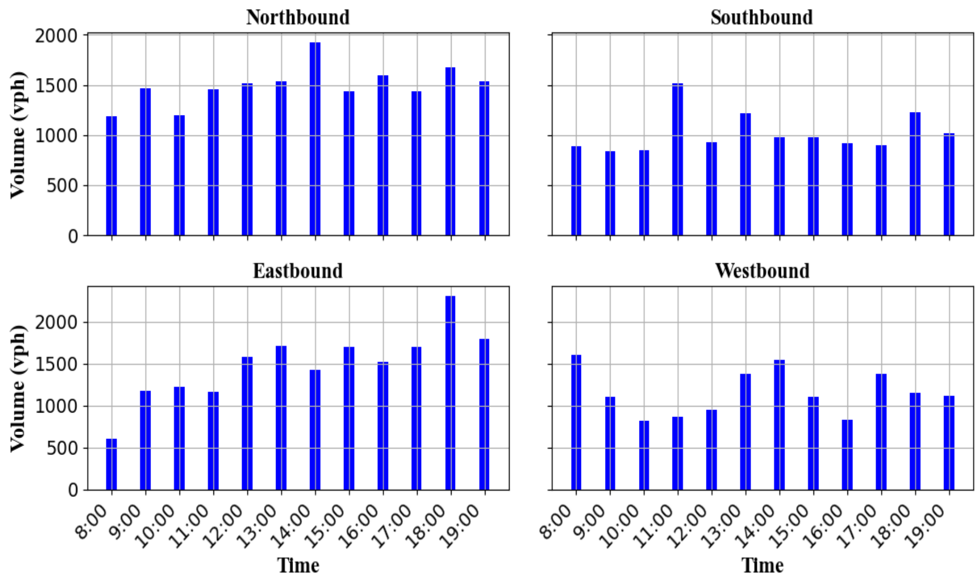

Figure 18: Traffic Volumes for Each Approach for University Dr. and Texas Ave. Intersection on February 12, 2019

Next, to verify that the developed detecting and counting techniques are accurate, part of the same videos was manually calculated, namely the period between 5:00 pm to 6:00 pm. For this period, manual counts vs the counts that were obtained from the developed technique were plotted against each other and compared to each other visually. Two plots are shown below. Figure 19 shows a barchart of the traffic data for each direction at the intersection calculated manually in addition to the computer counts for of the same directions and period mentioned above. Figure 20, on the other hand, shows a quantile-quantile plot of the manual counts vs. computer counts. While Table 2 contains the values of student counts and computer counts in addition to the percent change. The percent change is calculated by using equation (1) below:

$$Change\ \% = \frac{Student\ Counts - Computer\ counts}{Student\ Counts} \times 100 \qquad (1)$$

Table 2: Error Check

Direction	**Student counts**	**Computer counts**	**Percent change**
NBRT	762	760	0.26
NBLT	1082	1124	-3.88
NBTH	1352	1325	2.0
SBRT	176	176	0.0
SBLT	612	595	2.78
SBTH	1474	1466	0.54
EBRT	1769	1836	-3.79
EBLT	441	428	2.95
EBTH	1758	1831	-4.15
WBRT	392	384	2.04
WBLT	730	727	0.41
WBTH	1090	1150	-5.5

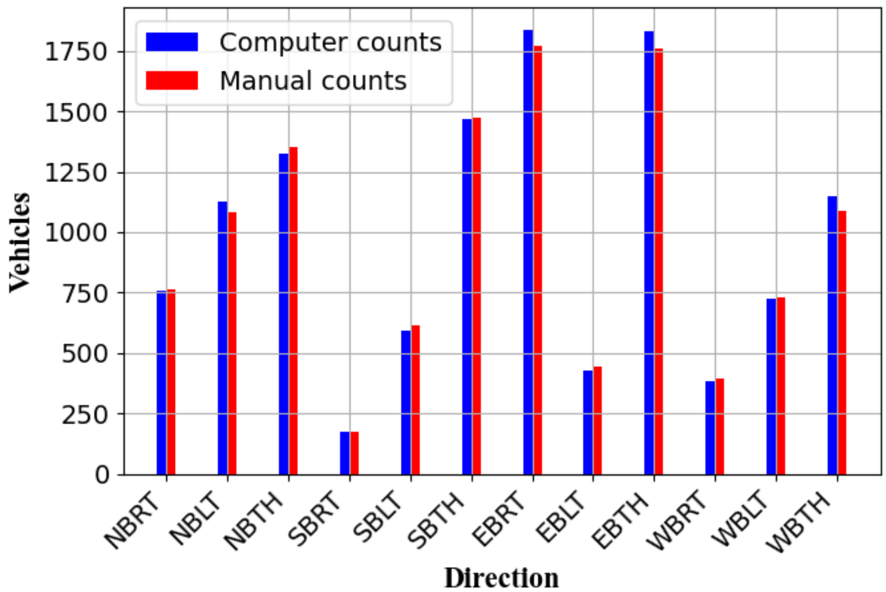

Figure 19: Barchart of Computer Counts and Manual Counts

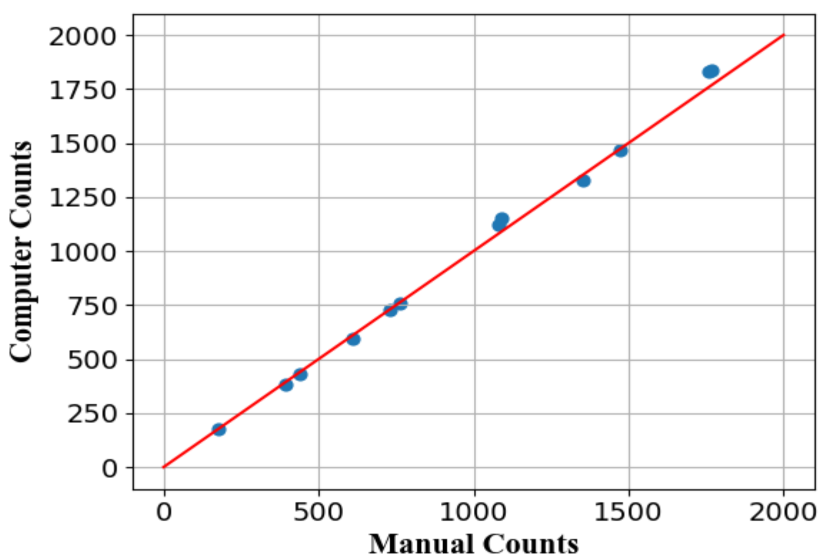

Figure 20: q-q Plot of Computer Counts vs Manual Counts

Both figures and the table above show that the two sets of data match each other almost perfectly. However, there are still some differences that can be seen between them. Those differences are due to, first, the fact that human error is possible when counting vehicles. Second, if the quality of the videos is not high, computer detection can miss some of the frames. The developed algorithm is written in a way that predicts the location of the vehicle even if it wasn't detected at a specific frame by interpolating its location between the previous frame and the next frame. However, if that continues for several frames the vehicle will not be detected. That case is rare, however, at least with the videos of the intersection under study, even though that the videos had only 10 frames per second and the resolution was very low. There is one case though that can cause a vehicle not to be detected even with videos with high quality. That case is when a vehicle is blocked by a bigger vehicle, like a truck. This issue is not associated with computer detection only. Human counters can miss those vehicles, too, if they were blocked from their view. In fact, cameras might have the advantage here since they are placed higher than the human height which provides better field of view.

A final note on the detection and counting processes is that the quality of videos should be as high as possible to make sure that everything is recorded in a way that makes it easy to detect the vehicles. As mentioned above, resolution of the videos is a very important factor that can affect the detection step. In addition, frame rate plays a major role in the tracking process. A video with a low frame per second (fps) rate has a higher chance that a vehicle would not get tracked properly if it wasn't detected in some of the frames. While tracking a vehicle in a video with a high fps would be more successful.

Additionally, placement of cameras is another important factor that needs to be considered. There should be at least one camera at each corner of the intersection to guarantee that all vehicles get captured since all angles are covered by cameras. Finally, the height at which the cameras are placed at can affect the accuracy of detection, since the field of view can get blocked by high vehicles. The height can be determined on a case-by-case basis depending on the dimensions of the intersection and safety considerations.

In conclusion, if cameras, with the required specifications, are available and placed properly, auto detection and tracking would be done successfully which would reduce the cost of traffic counting significantly because a smaller number of people would be needed.

Also, safety of traffic counting would be improved since there is a minimal human interaction when using cameras. It would be limited to the time of placing the cameras and removing them. While, with manual counts, individuals need to be physically available at the location of counting during the whole period which might not be safe.

CHAPTER IV

THEORETICAL APPROACH

Introduction

Traffic at almost any intersection fluctuates and changes in volume depending on different factors including, but not limited to, location and time. The location of an intersection affects the amount traffic volume it receives in a way that if it was at a busy area, the traffic volume would be higher than that if the intersection were in a small quite town. Location, however, is not the focus of this research although it is an important factor. Time, on the other hand, is the focus of this dissertation. Time can play a major role in the change in traffic volume at any intersection. For example, during the day, traffic volume is expected to be different than traffic volume at night. Also, morning volume might be different than it at noon or afternoon. Additionally, traffic volumes change from day to day. For, example, the weekday traffic is different than that during the weekend. The changes can also be affected by changes in the months during the year. For instance, traffic in March or February is expected to be higher than traffic volume in June and July in a college city like College Station, TX for example.

Therefore, managing those changes in traffic volumes is essential to have an efficiently controlled operation of traffic. At a signalized intersection, traffic is controlled by traffic signals. Those signals direct the traffic based on timing plans that are designed based on the traffic volume. Different traffic volumes and characteristics require different timing plans. Since traffic volume changes with time, different timing plans need to be used throughout any relatively extended period that experience fluctuation in traffic volume. However, selecting when to shift from one timing plan to another has not been controlled by any guidance or regulations. Therefore, this dissertation developed a procedure to provide local agencies guidance to follow when deciding on when to initiate a new timing plan.

This procedure optimizes the number of plans and the start time of each plan by minimizing delay. The following sections will show in detail how this procedure is developed and used.

This chapter presents the general fundamentals and logic that are used in this dissertation. Real-world traffic data for the intersection of University Dr and Texas Ave at College Station, TX are used and presented in the next chapter. The details and techniques used to collect these data are presented in the data collection chapter.

Delay

To find the optimal number of signal timing plans (n) and their start time (t), the criterion that is followed is that the optimal n and t are those that cause the least amount of delay throughout the study period. Therefore, delay needs to be calculated for each possible value of n and t to decide on their optimal values.

Delay is calculated by using HCM's equation (*HCM*, 2016), Equation (2) below:

$$d = d_1 + d_2 + d_3 \tag{2}$$

where,

d = control delay (s/veh)

d_1 = uniform delay (s/veh) $= \frac{0.5\ C\ (1-g/C)^2}{1-[\min(1,X)g/C]}$ (3)

d_2 = incremental delay (s/veh), and

d_3 = initial queue delay (s/veh).

d_3 will be considered 0 seconds because if it is larger than 0 seconds, this means that the system has failed. Therefore, the value of d_3 will not be considered in this dissertation.

The procedure used to calculate the delay is illustrated in Figure 21 below. The steps shown in the figure are implemented in detail in the following sections.

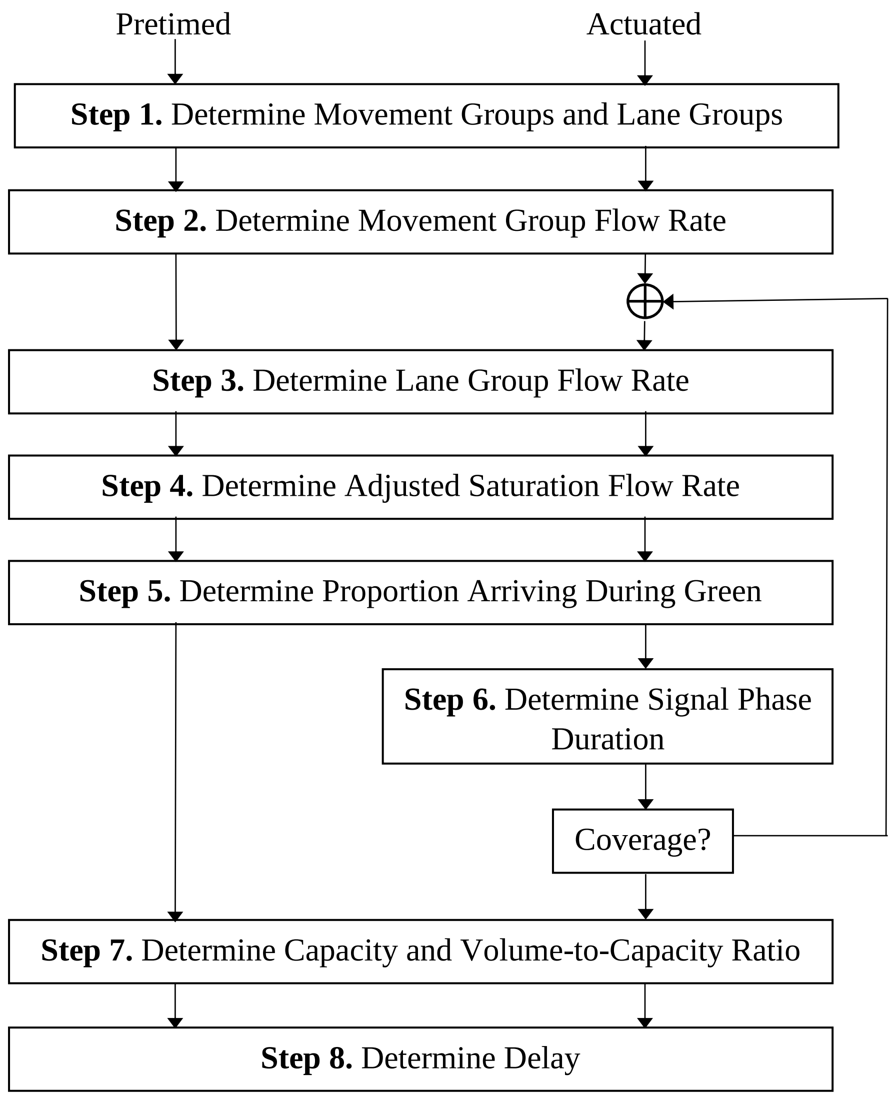

Figure 21: HCM's Motorized Vehicle Methodology for Signalized Intersections

Source: (*HCM*, 2016)

Cycle Time:

Cycle length is calculated by using the HCM's equation. Equation (4) below:

$$C_{min} = \frac{L \times X_c}{X_c - \sum_{i=1}^{n} \left(\frac{v}{s}\right)_{ci}} \tag{4}$$

where,

C_{min}	=	estimated minimum cycle length (seconds)
L	=	total lost time per cycle (seconds)
$\left(\frac{v}{s}\right)_{ci}$	=	flow ratio for critical lane group i (seconds)
X_c	=	critical $\frac{v}{c}$ ratio for the intersection

Lost Time Intervals:

All-red and yellow clearance intervals are calculated by considering different factors, which are: the intersection geometric design, speed limit, driver's reaction time, and the characteristics of vehicles.

Pedestrian Interval:

Pedestrian interval is calculated using the MUTCD procedure (*Manual on Uniform Traffic Control Devices (MUTCD)*, 2009).

Green Time:

Green time is calculated as a percentage of the cycle time. The HCM procedure is followed in the dissertation.

Developing of Optimization Process

Traffic volume changes during different periods of time. Depending on the amount of change, a different timing plan might be required for each different period.

Figure 22 below represents a traffic volume vs time relationship. The data shown in the figure are not real-world data. They were generated for illustration purposes only to emphasize the concept of peak and off-peak traffic. Traditionally, to determine the breakpoint of a timing plan, which is the time of day at which the timing plan is started, traffic engineer would, visually, inspect the time vs volume diagram and determine where the peak and off-peak are located. Then, they determine the breakpoints accordingly. Additionally, timing plans are only designed for either peak or off-peak periods while the transitional period is not focused on and is usually merged with the peak or off-peak periods. However, in this dissertation, the transitional period is considered and treated as a third zone that needs to be studied and might need a separate timing plan because the transitional period might be extended for a relatively long period of time, during which the volume can change to a point that requires a new timing plan. Additionally, in this dissertation, the breakpoints of timing plans are determined based on the performance of the total timing scheme. Specifically, the selected breakpoints are those that cause the least amount of delay during the study period.

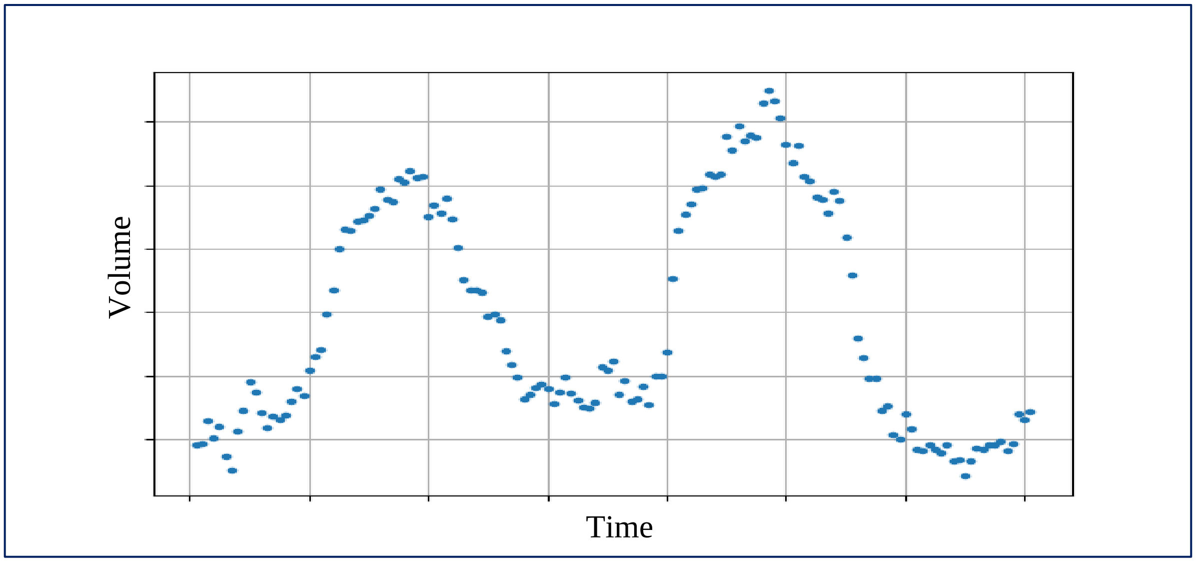

Figure 22: Time vs. Volume

Regression

To do the calculations that are required to find the breakpoints of timing plans, first, we need to find the formula $V(t)$ for volume curve, see Figure 23. To do that, regression analysis is applied to the traffic volume data. $V(t)$ will be an nth degree polynomial having the form shown in equation (5).

$$V(t) = a_n t^n + a_{n-1} t^{n-1} + \cdots + a_2 t^2 + a_1 t + a_0 \quad (5)$$

where,

a = coefficient

n = degree of polynomial

t = time

The degree of the equation is determined by taking into consideration that a too high degree would overfit the data which would cause the developed formula to be hard to generalize. On the other hand, a very low degree would not represent the data very well. Therefore, when selecting the degree of the formula, we need to plot the formula with the data and see that it follows the general shape of the data. In other words, it needs to show the peak and off-peak zones, but it should not follow every minor oscillation in the data. The formula does not need to be the best fit for the data since we are not using it to predict the values of the data. We are only using it to represent the general shape of the data to locate the major critical zones in the data. By doing that, we are, in a way, following the traditional method since in the traditional method, the critical zones are determined visually.

Although polynomial regression is used in this dissertation, spline regression can also be used to find the best fit for the data. However, for the purpose of our research, polynomial regression is sufficient in representing the general shape of the data.

Figure 23 shows a plot of traffic volume data. These generated data are used to develop a regression model $V(t)$ that fits the points.

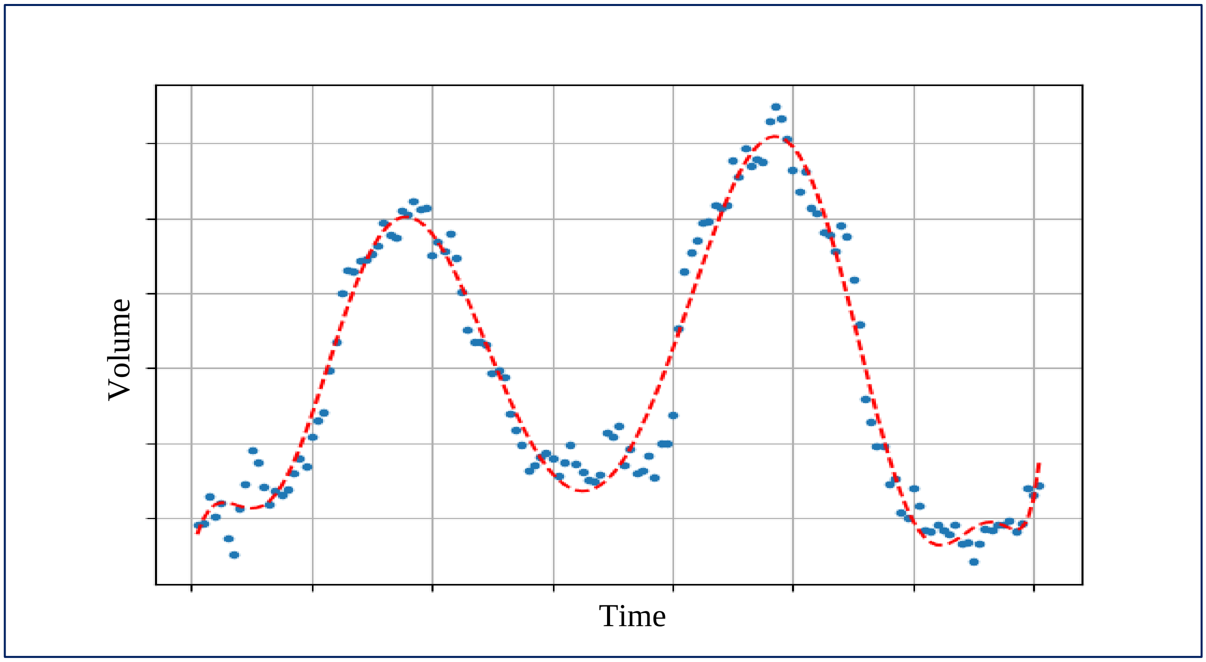

Figure 23: Curve Fitting

Optimization Methods

Two optimization methods were developed in this dissertation. They are:

1. Critical zone optimization method
2. ΔV optimization method.

These two methods are explained in the following sections.

Critical Zone Optimization Method

This optimization method follows the traditional method by focusing on the critical points which are the peak and off-peak points. However, it adds to that a third zone which is the transitional area.

Unlike the traditional method which depends on the visual inspection and the engineering judgement which can be different from one person to another, the critical zone optimization method determines the location of the breakpoints by following a procedure that is mostly automated which can make the process consistent and easier compared to the traditional method.

In general, for a better performance and to reduce delay, a timing plan needs to be changed or adjusted according to the changes of traffic volume at an intersection (Urbanik et al., 2015). Therefore, for the data in Figure 24, a different timing plan might be required for each of the following:

1. an off-peak plan (the blue shaded area),
2. a transitional plan (the orange shaded area), and
3. a peak plan (the red shaded area).

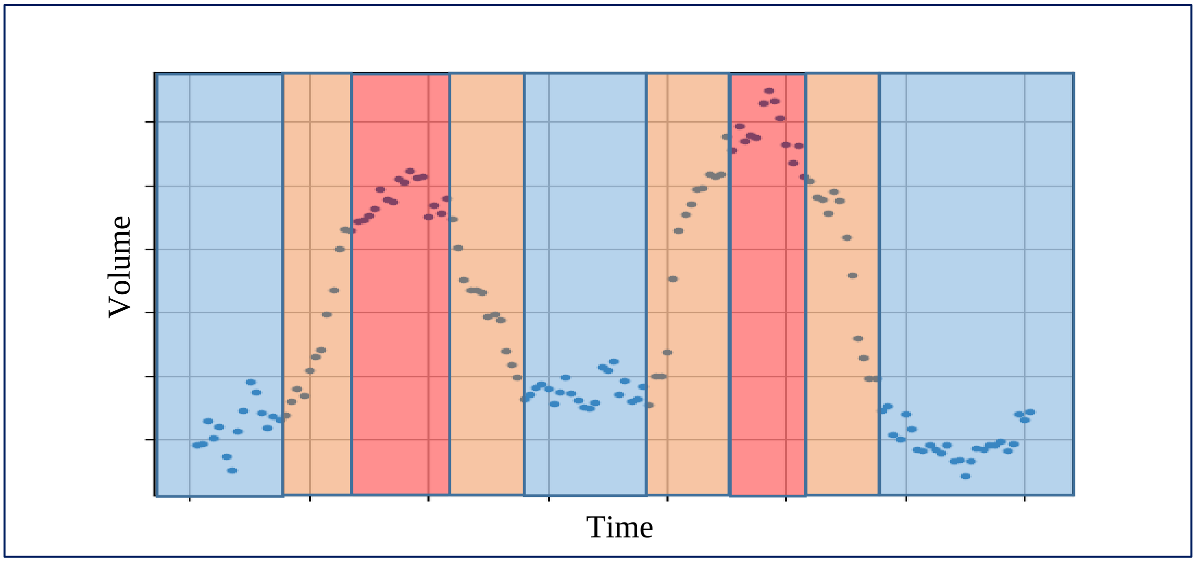

Figure 24: Critical Zones of Time vs. Volume Plot

Additionally, for each zone of the three zones above, we need to determine the following:

1. location of each zone, and
2. size of the zone.

The following two sections explain how to determine the location and size of the critical zones.

Location of Critical Zones:

The general location of critical zones, especially the peak and off-peak zones, can be determined visually by inspecting the volume vs. time plot. However, in this dissertation, instead of only inspecting the data, we are developing a formula that represents the data. Details on how to find $V(t)$ are available in the regression section that was presented earlier.

Mathematically, what differentiates the transitional, orange area from both the peak and off-peak areas, in Figure 24 above, is that the slope of the curve in the transitional area is higher than all the other areas while the slope is zero at the peak and off-peak zones. Therefore, and to find the location of those critical points, the first derivative of $V(t)$ is calculated. See equation (6) below.

$$V'(t) = n\, a_n\, t^{n-1} + (n-1)\, a_{n-1}\, t^{n-2} + \cdots + 2\, a_2\, t + a_1 \tag{6}$$

The transitional zones would have either a high positive $V'(t)$ value for the increasing zone, or a low negative value for the decreasing zone. However, since we are interested only in determining the transitional zone in general regardless of its direction, the absolute value of $V'(t)$ is calculated. Hence, now any peak in the $|V'(t)|$ plot represents a transitional zone. See Figure 25 below.

Now, the locations of the critical zones are determined mathematically since, in the $V'(t)$ plot, Figure 25, the peaks represent the transitional zones, while when the value of the derivative is zero, it is either a peak or an off-peak in the original $V(t)$ plot. The next step is to determine how far each zone is extended to.

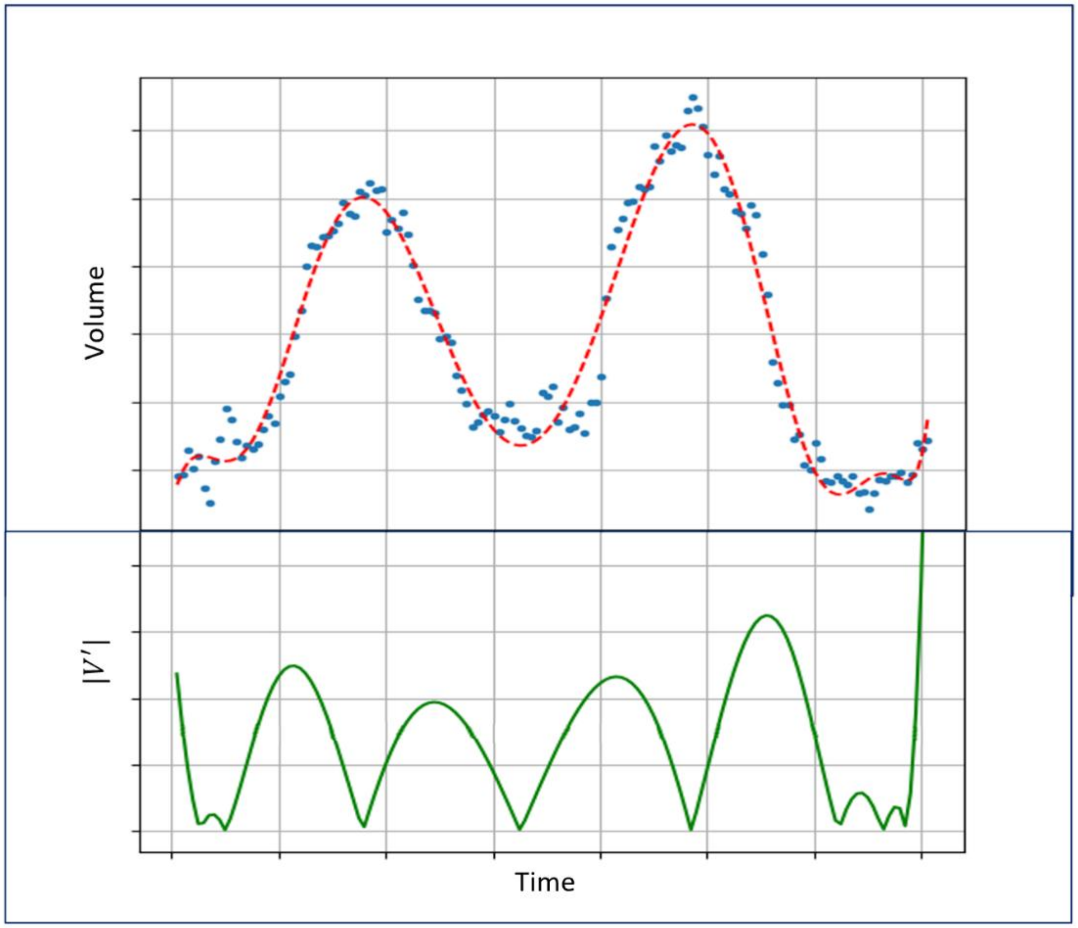

Figure 25: Critical Zones

Size of Critical Zones:

After finding the locations of the critical zones in the previous step, in this step we determine the limits of each zone. Since whenever a zone ends, the next zone starts immediately, the limits that are found in this step are considered the separations between the zones or the points at which the traffic volume changes from one condition to another. In other words, any two consecutive points will have between them either a peak, an off-peak, or a transitional zone. Therefore, considering these points as the breakpoints for timing plans is going to help in improving the performance of a traffic signal since the timing plans will, then, be designed for periods with relatively uniform traffic volume.

The search for these zone limits, or the breakpoints, is conducted by scanning the plot of $|V'(t)|$ for different alternatives. Those alternatives will be evaluated based on their performance. The scanning process is done by drawing a horizontal line on the plot of $|V'(t)|$. Initially, the line will start at zero and its value will be increased incrementally. The increments can be decided upon by considering the time increments by which the traffic data were collected.

For each increment, the horizontal line which represents the critical value of $V'(t)$, or $V'(t)_{critical}$, when it intersects with the $|V'(t)|$ plot, the x-coordinates of the intersection points are considered a potential set of breakpoints. See Figure 26 below.

Before using this set, however, one step needs to be done. The first breakpoint, t_0, might not be equal to zero initially. If so, it needs to be moved to zero to make sure the whole study period is covered. Same thing is done to the last breakpoint, t_n, which needs to be moved to the end of the study period.

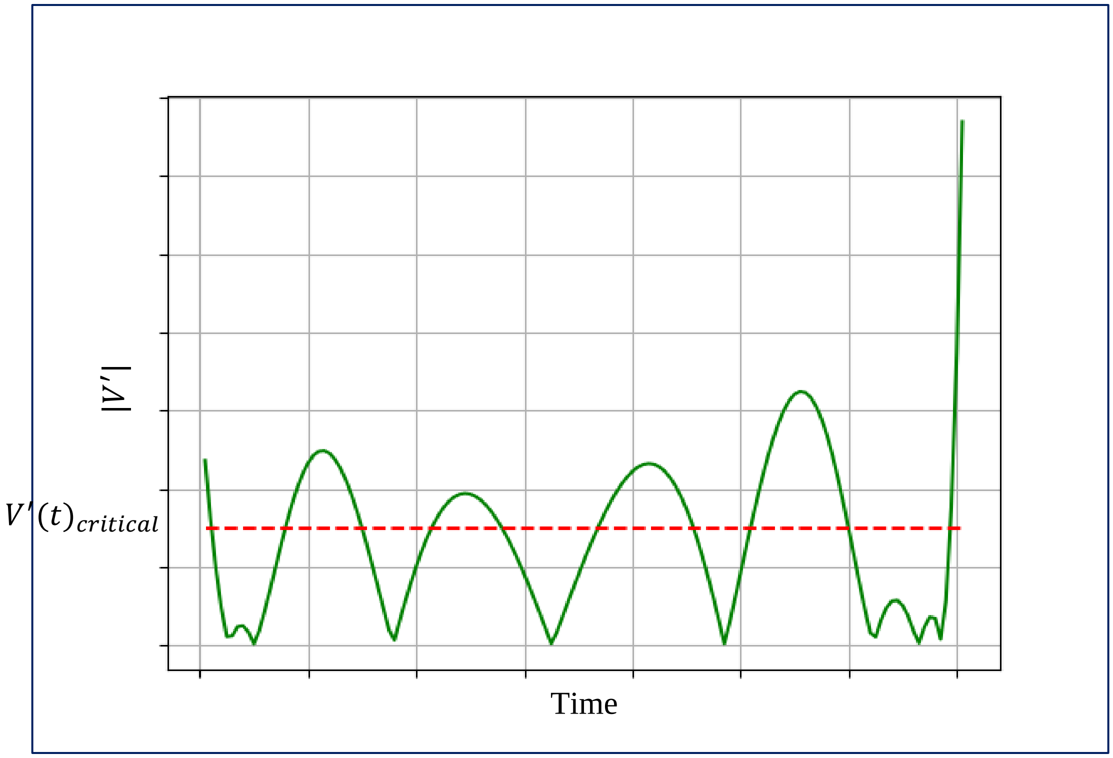

Figure 26: Time vs. Absolute ($V'(t)$)

Additionally, for each value of $V'(t)_{critical}$, we need to check that the periods between any two consecutive breakpoints is not less than the minimum period any timing plan is applied for. In this research, the minimum period is assumed to be one hour. However, this is a decision that needs to be made by local agencies and it can be different from one situation to another.

Nevertheless, if any suggested period, which is the period between any two consecutive suggested breakpoints, is less than the minimum period, the following treatment is conducted.

Let us assume that the period (t_i to t_{i+1}) is less than one hour.

1. If the period is the first or the last period in the study period, we merge that period with the neighboring period and update the breakpoint set.
2. If that period is not the first or the last and it is a transitional period, then we break that period into two halves and add each of the resulting sub-period to its neighboring period. The resulting breakpoint will be between t_i and t_{i+1} and found by the following equation.

$$t_m = (t_i + t_{i+1})/2 \tag{7}$$

   where,

   t_m = the mid-breakpoint.

   The reason for choosing to divide the transitional period and add each half to its neighboring period is that each half is close in value to the neighboring period.
3. If that period is not the first or the last and it is a peak or an off-peak period, first we delete t_i and merge the period (t_i to t_{i+1}) with the previous period. We record the resulting breakpoints, after deleting t_i, as one alternative of breakpoint sets. Then, we keep t_i and delete t_{i+1} and record the resulting set of breakpoints as another alternative of breakpoint sets.
   The reason not to break the period into two halves, in this condition, is that any peak or off-peak period when broken in half would create two similar periods which do not need to be added to two different periods.

After generating multiple alternatives of breakpoint sets, it is time to select only one set. The criterion that is followed to find the optimal breakpoints of timing plans is that the selected breakpoints are those that cause the least amount of delay throughout the study period. Therefore, delay is calculated for each timing plan period in every increment of $V'(t)_{critical}$.

Figure 27 below represents the distribution of the breakpoints for one iteration or increment of $V'(t)_{critical}$. t_i is a timing plan breakpoint or the time of day at which the selected timing plan starts. Timing plan (1) is implemented from t_0 to t_1. Timing plan (2) will be implemented from t_1 to t_2, and so on. As stated earlier, the time periods have a minimum value of 1 hour to decrease the effect of transitioning from one timing plan to another. That is one of the assumptions of this dissertation, which are listed in Chapter I.

Delay is calculated throughout each timing plan period. d_1 is the delay that is calculated during the implementation of timing plan (1). d_2 is the delay that is calculated during the implementation of timing plan (2), and so on.

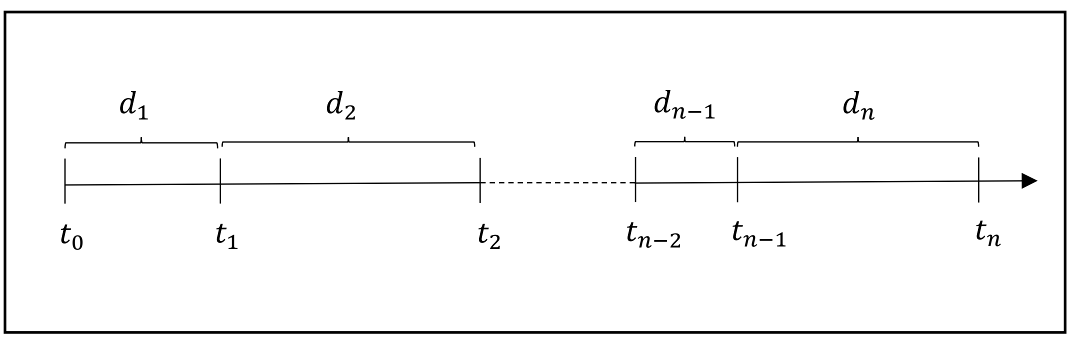

Figure 27: Delay Throughout the Study Period

Next, the weighted average delay is calculated for the whole study period by using equation (8) below.

$$Total\ delay\ (D) = \frac{\sum_{i=1}^{n}(d_i * V_i)}{\sum_{i=1}^{n} V_i} \tag{8}$$

where,

d_i	=	delay in (sec/veh) for time period (i)
V_i	=	volume during time period (i) (veh/hr)
$Total\ delay\ (D)$	=	total intersection delay in (sec/veh) for the whole study period

The following steps are to select a different combination of time breakpoints (t_1 to t_2). As noted earlier, this is done by incrementally increasing the value of $V'(t)_{critical}$ and getting the points where it intersects with $|V'(t)|$ plot, Figure 28 below. The x-coordinates of the intersection points represent the new set of (t_0 to t_n). After that, a new total delay (D) is calculated by using equation (8) above.

The whole process is repeated several times by changing the value of $V'(t)_{critical}$ and getting new values of total delay (D).

The final time set that is selected is the one corelated with the minimum value of D since it provides the best level of service based on the HCM analysis (*HCM*, 2016). The selection of the best set is dependent on its performance.

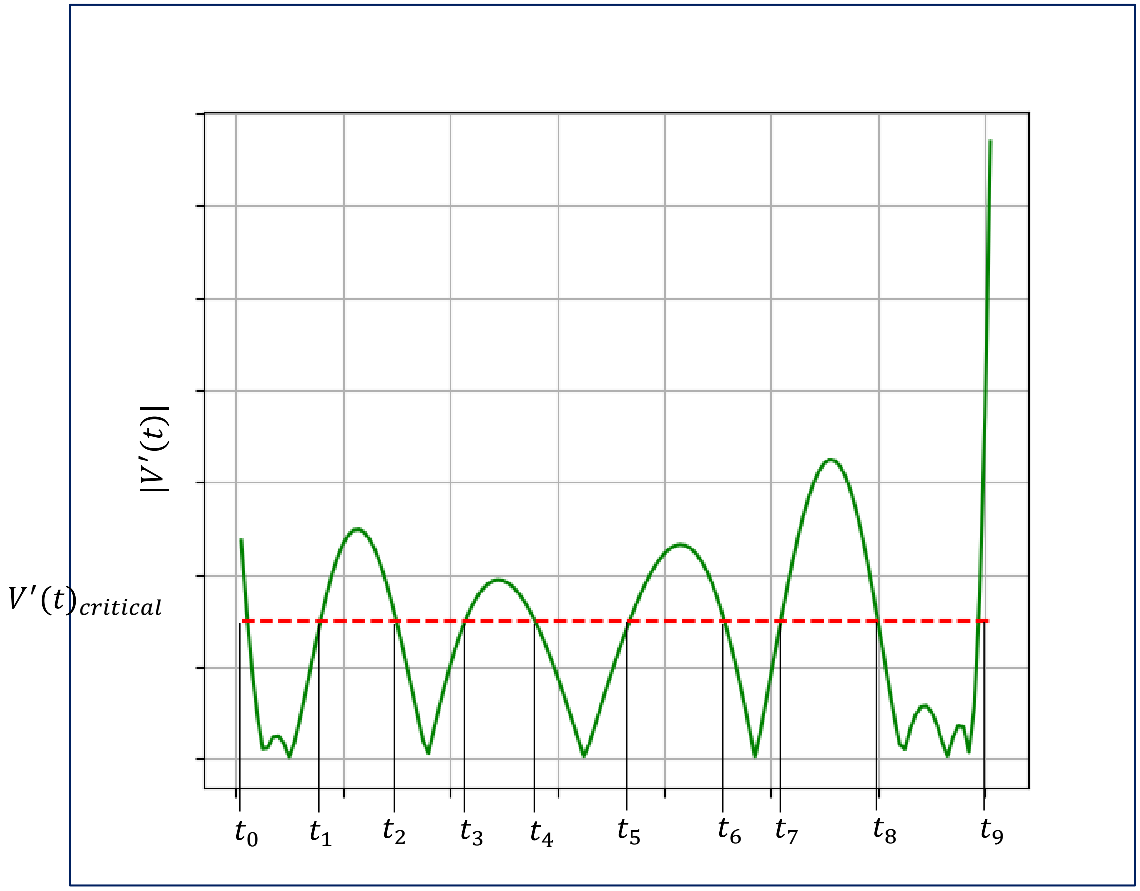

Figure 28: Breakpoints of Timing Plans

ΔV Optimization Method:

In this method, the traffic volume plot will be divided into different zones depending on the amount of traffic volume. Each zone will have a different timing plan that is designed based on the traffic characteristics for that zone. Since the traffic volume will be more homogeneous within each zone, timing plan can be more efficient which, as a result, will reduce delay. The ΔV optimization method can be executed by applying the following steps. A flowchart of the steps is shown in Figure 29 below.

1. Start a step counter that will be used in calculations. For the first iteration, $step\ counter = 1$, but it will be increased by 1 at each iteration.
2. The initial iteration is to calculate one timing plan for the whole study period. That is one alternative which will be evaluated and compared to other alternatives in the following steps. In Figure 30, t_0 and t_1 represent the initial proposed breakpoints.

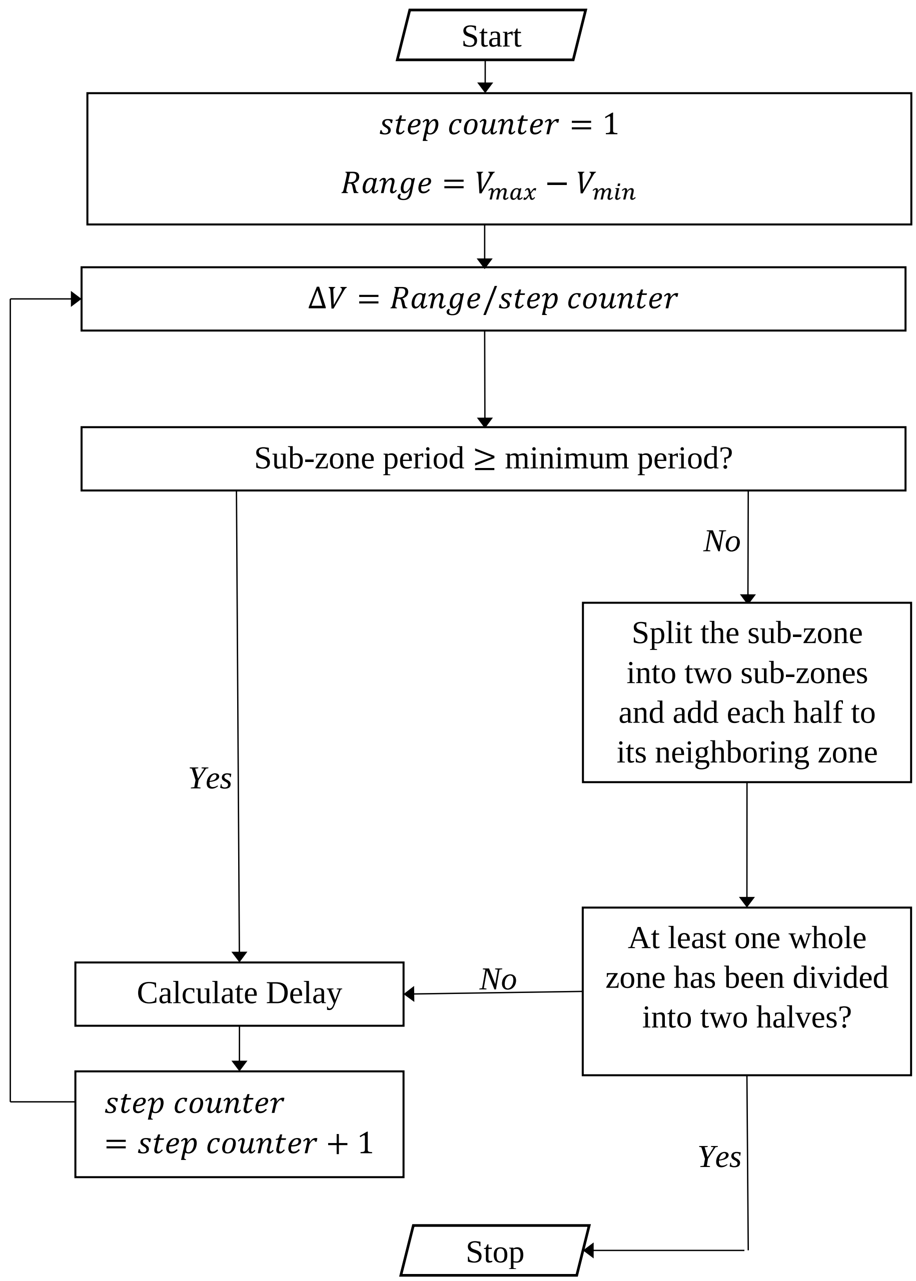

Figure 29: Flowchart of ΔV Optimization Method

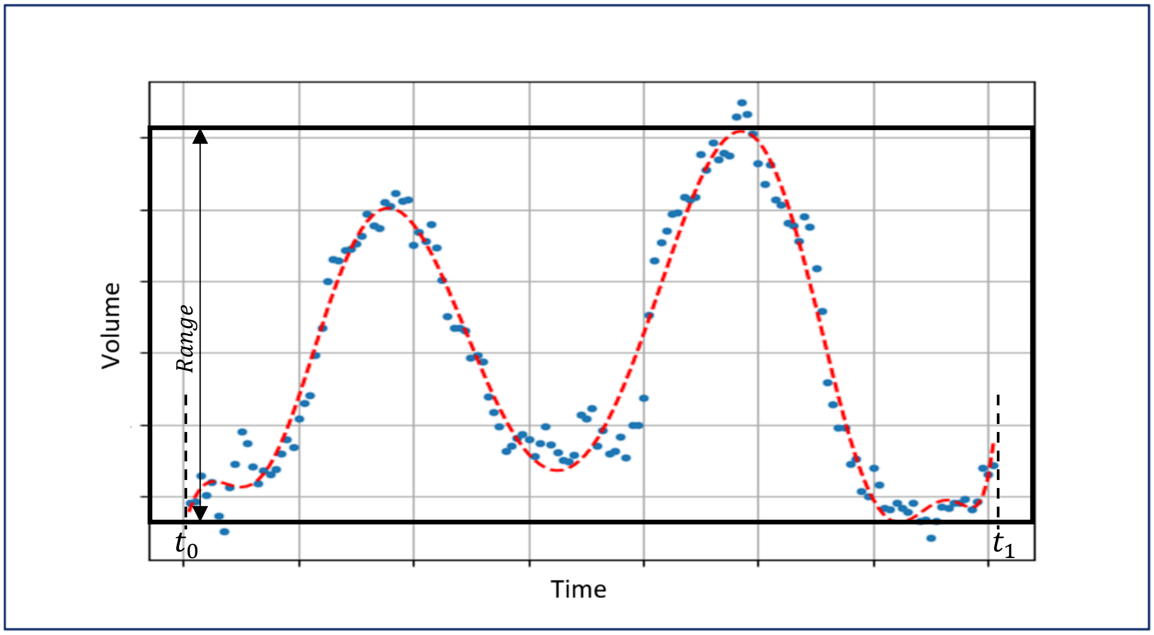

Figure 30: Range of Traffic Volume ($step\ counter = 1$)

3. Calculate the range of the traffic volume by using equation (9).

$$Range = V_{max} - V_{min} \tag{9}$$

where,

V_{max} = maximum value of the volume vs time curve.

V_{min} = minimum value of the volume vs time curve.

4. Calculate ΔV by dividing the range by the $step\ counter$,

$$\Delta V = range/step\ counter \tag{10}$$

The idea of dividing the range by the step number is to separate different levels of traffic volume. Each level will have its own timing plan. Therefore, a horizontal line is drawn every ΔV increase in traffic volume, the y-axis, on the volume vs time plot. Then, the time, or x-coordinate, at which the horizontal lines intersect with the volume curve is considered a potential breakpoint of a timing plan. The next steps will determine whether those points are selected as breakpoints or not. Figure 31 shows the suggested breakpoints when $step\ counter = 2$, while Figure 32 presents the suggested breakpoints when $step\ counter = 3$, and Figure 33 the suggested breakpoints when $step\ counter = 4$.

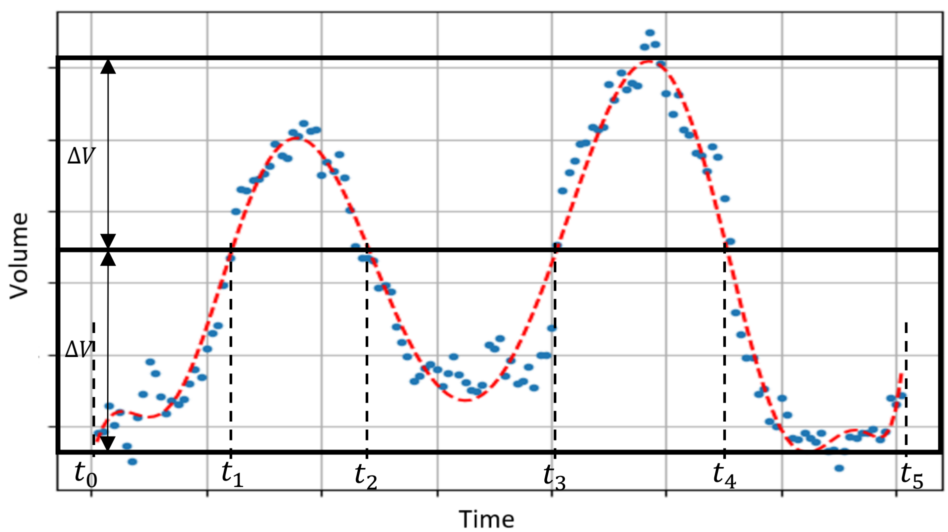

Figure 31: $step\ counter = 2$

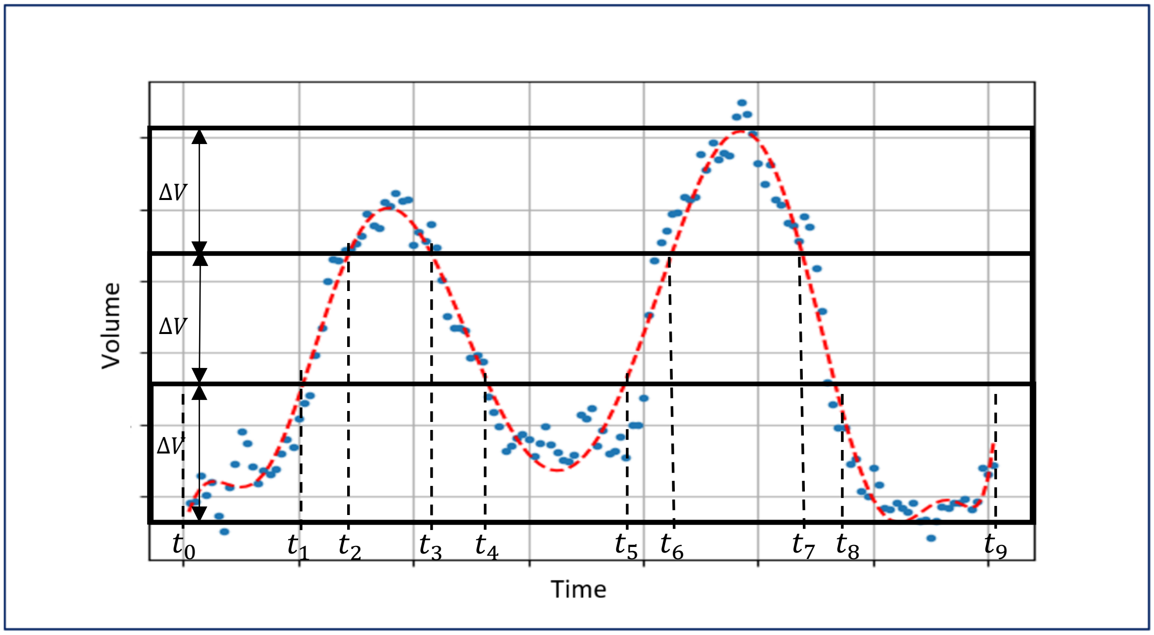

Figure 32: $step\ counter = 3$

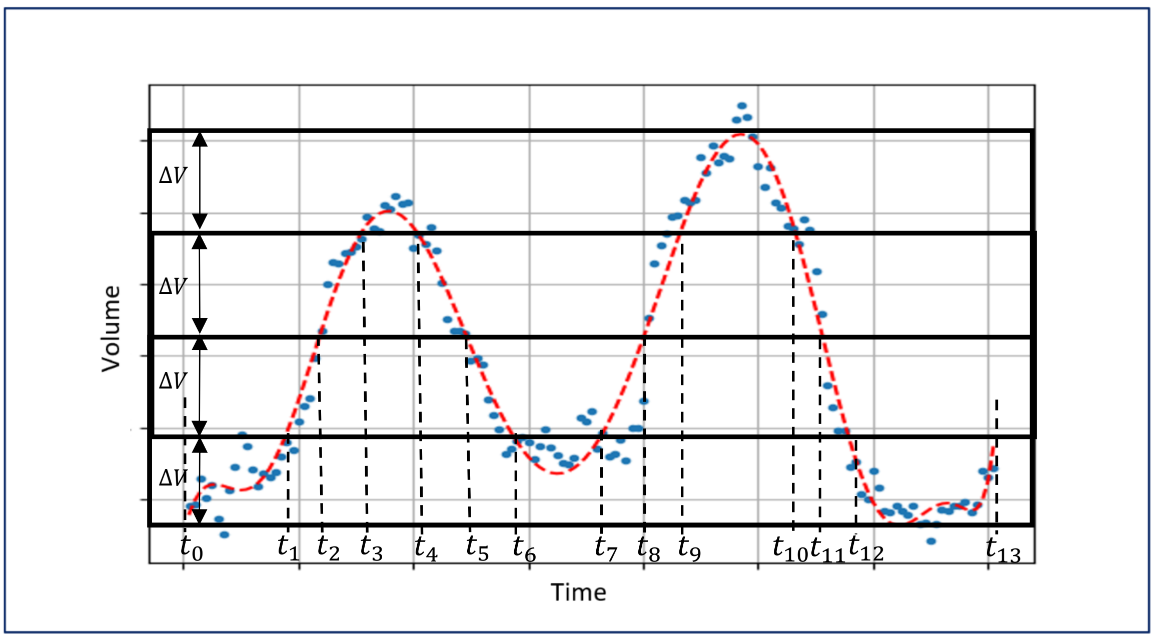

Figure 33: $step\ counter = 4$

5. We need to check that any suggested period, or in other words the distance between any two consecutive t's, is larger or equal to the minimum period a timing plan is proposed to be applied through. In this research, the minimum period is assumed to be one hour. However, this is a decision that needs to be made by local agencies.

   If any period happens to be less than the minimum period, the same procedure that is used in the previous optimization method is used here. It is as the following

   Let us assume that the period (t_i to t_{i+1}) is less than one hour.

   - If the period is the first or the last period in the study period, we merge that period with the neighboring period and update the breakpoint set.
   - If that period is not the first or the last and it is a transitional period, then we break that period into two halves and add each of the resulting sub-period to its neighboring period. The resulting breakpoint will be between t_i and t_{i+1} and found by equation (7) .
   - If that period is not the first or the last and it is a peak or an off-peak period, first we delete t_i and merge the period (t_i to t_{i+1}) with the previous period. We record the resulting breakpoints, after deleting t_i, as one alternative of breakpoint sets. Then, we keep t_i and delete t_{i+1} and record the resulting set of breakpoints as another alternative of breakpoint sets.

When a whole zone of ΔV is divided because each single sub-zone is smaller than the minimum period, then that is an indication that no further reduction in the value of ΔV is required.

6. In this step, we calculate delay for the whole study period by using equation (8).
7. In this step, the $step\ counter$ is increased by 1.
8. Same process is repeated starting at step number 4 above until the stopping criterion in step 5 is true.

By following the steps above, different sets of breakpoints along with their calculated delay values. The selected set of breakpoints is the one that causes the least amount of delay.

Final Note on the Developed Optimization Methods

A final note that needs to be considered when using either of the two optimization methods that were presented in this dissertation, the critical zone optimization method and the ΔV optimization method, is that the ΔV optimization method depends directly on the change in traffic volume. The other method, which is the critical zone optimization method, although it depends on the value of the rate of change in volume when selecting the potential breakpoints, the final decision when selecting the breakpoints is taken after calculating delay which depends on the volume in its calculation. Therefore, the rate of change in volume only initiates the process of the selection in this optimization method but the decision is made after inspecting the volume.

Both methods are implemented in this dissertation. The choice of one method over the other is decided upon based on its performance in reducing delay. In Chapter V, both methods are applied on real-world data and compared to each other based on their effectiveness in lowering the amount of delay in the selected intersections.

Additionally, compared to the other methods that were presented in Chapter II, the two optimization methods that were developed in this dissertation have the ability of proposing both the number and the start time of timing plans, while when using the methods in the literature, you need to assume the number of timing plans first, and then find their start time.

Computer Program Developing

Since the previously mentioned procedures include multiple steps with repetitive calculations, it is time consuming to be implemented manually. Therefore, a computer program is needed do these calculations. The program was developed by the author to implement this task. Python is the programing language that was used to code the program ("Python Programing Language," 2020). The input into the developed program is the traffic turning counts, geometry of the intersection, and speed limit. In addition to the minimum values and default values, if any.

The developed computer program does the following.

1. It accepts the input data mentioned above.
2. Plots the data vs any time scale (i.e. 5-minute, 15-minute, … etc.) taking into consideration that the data should be collected by time increments less or equal to the plotting time increments.
3. Calculates $V'(t)$.
4. Calculates yellow time, all-red, and pedestrian intervals.
5. Calculates a timing plan for each time period.
6. Calculates total delay (D) for each time period.
7. Iterates the value of $V'(t)_{critical}$ and gets different sets of (t_0 to t_n) and D.
8. Changes the value of ΔV based on the procedure in the ΔV optimization method.
9. Adjust the values of (t_0 to t_n) based on the criteria mentioned earlier where t_0 should be at time = 0 and t_n at the end of the study period.
10. Finds the minimum D and the optimal (t_0 to t_n) set based on the critical zone method.
11. It finds the minimum D and the optimal (t_0 to t_n) set based on the ΔV optimization method.
12. Compares the two results from the two optimization methods and suggests the optimal solution between the two

The following chapter, Chapter V, shows in detail the implementation of the developed techniques on real-world data and the utilization of the computer program.

CHAPTER V

APPLICATION AND VALIDATION

Introduction

After developing the optimization techniques that were presented in the previous chapter, in this chapter, real-world data are used to test the developed techniques. The data and the data collection were presented in chapter three, Data Collection.

Data

Traffic counts were collected for the intersection of University Drive and Texas Avenue and the intersection of George Bush Drive and Texas Avenue. Both intersections are in College Station, Texas. The data were collected for two 12-hour periods on two successive days for each of the two intersections. These data are used in this chapter as an input for the optimization techniques that were developed in the previous chapter. The results will show whether the technique can minimize the delay experienced by vehicles at these intersections. The breakpoints of timing plans are calculated by using the developed optimization techniques. As mentioned in chapter IV, the developed techniques are the critical zone optimization method and ΔV optimization method. In the first method, the breakpoints are determined by finding the time of day at which $V'_{critical}$ intersects with the curve of the absolute value of $V'(t)$. After that, we calculate Total delay (D) by using equation (8). Finally the selected time-of-day breakpoints will be the set with the lowest Total delay (D).

However, in the other optimization method, which is the ΔV optimization method, the traffic volume plot is divided into different zones depending on the amount of traffic volume. Each zone will have a different timing plan that is designed based on the traffic characteristics for that zone. The selected breakpoints are those that cause the lowest amount of delay, which is calculated by using equation (8) and the procedure in the following section.

Calculation of Delay

The HCM procedure was the adopted guidelines to calculate delay as shown in chapter IV. Steps 1 through 8 below were followed to calculate delay for every suggested time period. The calculations and values shown in this section are for the data that were collected for the intersection of University Dr. and Texas Ave. on February 12, 2019. The calculations of the other three cases, however, are not included in this section since they follow the same procedure. Therefore, there is no need to repeat them here. However, a summary of the results and their analysis and discussion are included in the following sections. Additionally, more detailed results of the optimization process for all the other three data sets are available in the appendix.

Below are the steps that are followed to calculate delay.

Step 1. Determine Movement Groups and Lane Groups

Movement groups and lane groups are determined by following the HCM procedure. "In general, a separate lane group is established for *(a)* each lane (or combination of adjacent lanes) that exclusively serves one movement and (*b*) each lane shared by two or more movements. While a separate movement group is established for *(a)* each turn movement with one or more exclusive turn lanes and (*b*) the through movement (inclusive of any turn movements that share a lane)". (HCM, 2016).

Lane groups are shown in Figure 34 while movement groups are shown in Figure 35 below for the University Dr. and Texas Ave. intersection.

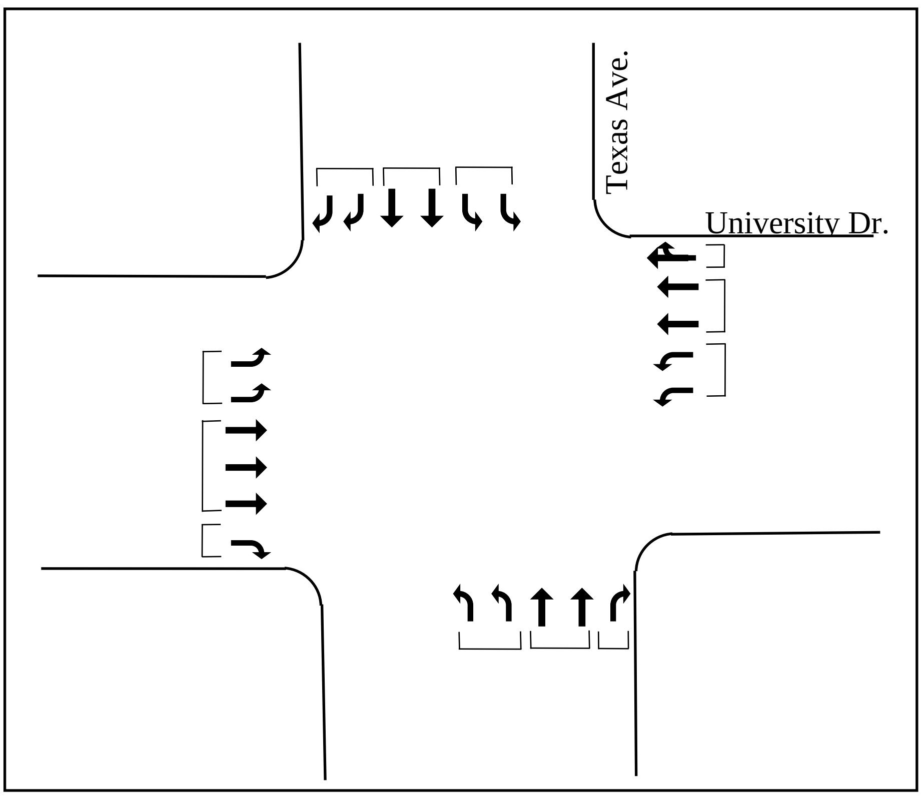

Figure 34: Lane Groups for the Intersection

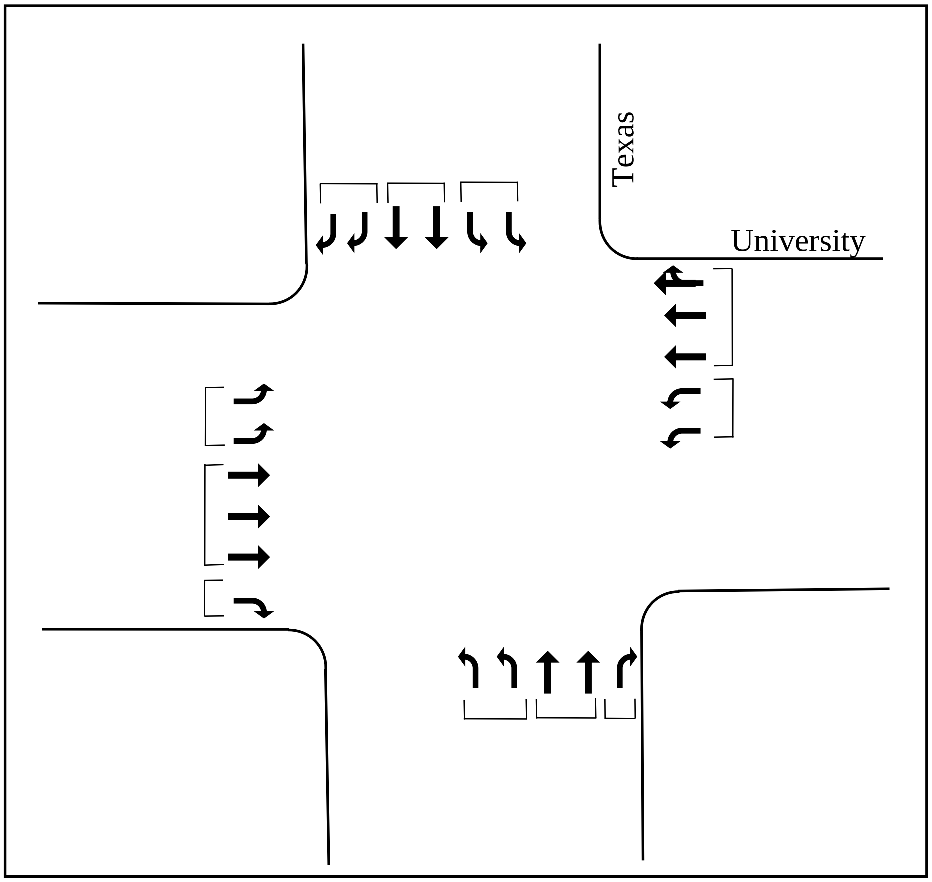

Figure 35: Movement Groups for the Intersection

Step 2. Determine Movement Group Flow Rate

The flow rates are going to be different for different time of day. Since our technique covers an extended period, different values of flow rates are used for different time frames.

Step 3. Determine Lane Group Flow Rate

Flow rates of the lane groups are also going to be different for different time of day because the analysis technique covers multiple periods.

Step 4. Determine Adjusted Saturation Flow Rate

To calculate the saturation flow rate, the following equation is used, equation (11) (*HCM*, 2016):

$$s = s_o \, f_w \, f_{HVg} \, f_p \, f_{bb} \, f_a \, f_{LU} \, f_{LT} \, f_{RT} \, f_{Lpb} \, f_{Rpb} \, f_{wz} \, f_{ms} \, f_{sp} \qquad (11)$$

where,

s = adjusted saturation flow rate (veh/h/ln),

s_o = base saturation flow rate (pc/h/ln),

f_w = adjustment factor for lane width,

f_{HVg} = adjustment factor for heavy vehicles and grade,

f_p = adjustment factor for existence of a parking lane and parking activity adjacent to lane group,

f_{bb} = adjustment factor for blocking effect of local buses that stop within intersection area,

f_a = adjustment factor for area type,

f_{LU} = adjustment factor for lane utilization,

f_{LT} = adjustment factor for left-turn vehicle presence in a lane group,

f_{RT} = adjustment factor for right-turn vehicle presence in a lane group,

f_{Lpb} = pedestrian adjustment factor for left-turn groups,

f_{Rpb} = pedestrian-bicycle adjustment factor for right-turn groups,

f_{wz} = adjustment factor for work zone presence at the intersection,

f_{ms} = adjustment factor for downstream lane blockage, and

f_{sp} = adjustment factor for sustained spillback.

Below is how each factor in equation (11) was found for the intersection of Texas Ave. and University Dr. based on the HCM recommendations (*HCM*, 2016).

- s_o = 1900 pc/h/ln because the College Station-Bryan, TX Metro Area population was larger than 250,000 during the time of study. ("U.S. Census Bureau, American Community Survey 1-year estimates," 2019)
- f_w = 1.00 since all lanes are within the range, $(\geq 10.0 - 12.9)$ ft.
- f_{HVg} = adjustment factor for heavy vehicles and grade is calculated by using equations (12) and (13).

  If the grade is negative (i.e., downhill), then the factor is computed with Equation (12).

$$f_{HVg} = \frac{(100 - .79\, P_{HV} - 2.07\, P_g)}{100} \tag{12}$$

  If the grade is not negative (i.e., level or uphill), then the factor is computed with Equation (13)

$$f_{HVg} = \frac{(100 - 0.78\, P_{HV} - 0.31\, {P_g}^2)}{100} \tag{13}$$

  where,

  P_{HV} = percentage heavy vehicles in the corresponding movement group (%), and

  P_g = approach grade for the corresponding movement group (%).

- f_p = 1.00 because there is no parking in the intersection area.
- f_{bb} = 1.00 since there is no bus stop within 250 ft from the intersection.
- f_a = 1, because the headway is normal.
- f_{LU} values are from Exhibit 19-15, HCM. They are shown below.

Table 3: Values of f_{LU}

factor	**Eastbound**			**Westbound**			**Northbound**			**Southbound**		
Lane Group	L	T	R	L	T	T+R	L	T	R	L	T	R
No. of lanes	2	3	1	2	2	1	2	2	1	2	2	2
$\boldsymbol{f_{LU}}$	0.971	0.908	1.00	0.971	0.952	1.00	0.971	0.952	1.00	0.971	0.952	0.885

- f_{LT} is calculated with equation (14).

$$f_{LT} = \frac{1}{E_{LT}} \tag{14}$$

where,

E_{LT} = equivalent number of through cars for a protected left-turning vehicle (= 1.05). Therefore, the values of f_{LT} for all left turns in the intersection are all equal to ($\frac{1}{1.05} = 0.95$).

- f_{RT} is calculated with equation (15) for all right turn directions except for westbound right-turn because the lane is shared with through movement.

$$f_{RT} = \frac{1}{E_{RT}} \tag{15}$$

The adjusted saturation flow rate for this lane group is computed by using equation (16) below.

$$s_{sr} = \frac{s_{th}}{1 + P_R(\frac{E_R}{f_{Rpb}} - 1)} \tag{16}$$

where,

s_{sr}	=	saturation flow rate in shared right-turn and through lane group with permitted operation (veh/h/ln),
s_{th}	=	saturation flow rate of an exclusive through lane (veh/h/ln),
P_R	=	proportion of right-turning vehicles in the shared lane (decimal),
E_R	=	equivalent number of through cars for a protected right-turning vehicle = 1.18, and
f_{Rpb}	=	pedestrian–bicycle adjustment factor for right-turn groups.

- f_{Rpb} for southbound right turn is 1 because it is a protected direction. For the other right turn lanes, however, it is calculated by following the procedure in HCM, Chapter 31, the section named "Right-Turn Movements and Left-Turn Movements from One-Way Street" (*HCM*, 2016). The procedure is straight forward. However, it requires the cycle length to be known. But we know until this point, we have not calculated the cycle length yet because, to do so, the adjusted saturation flowrates are needed, which in turn requires f_{Rpb} as an input. Therefore, iterations need to be conducted as the following:

1. Assume f_{Rpb} = 1.
2. Calculate s and then C.
3. Calculate f_{Rpb} by using C above
4. Repeat steps 2 and 3 until C starts converging.

- f_{Lpb} is 1 for all left turns because they are all protected movements.
- f_{wz} = 1.00 because there is no work zone in the area when the data were collected.
- f_{ms} = 1.00 because there is no downstream lane blockage, and
- f_{sp} = 1.00 because there was no spillback.

By using equation (11), adjusted saturation flow can now be calculated for all lane groups except for the westbound shared lane group, which is calculated by using equation (16).

Next, we calculate the cycle time.

Cycle Time:

Cycle length calculation is an iterative process as explained above. The formula that is used for the iterations calculations is the HCM's equation. Equation (17) below:

$$C_{min} = \frac{L \times X_c}{X_c - \sum_{i=1}^{n} \left(\frac{v}{s}\right)_{ci}} \tag{17}$$

Where,

C_{min} = estimated minimum cycle length (seconds)

L = total lost time per cycle (seconds)

$\left(\frac{v}{s}\right)_{ci}$ = flow ratio for critical lane group i

X_c = critical v/c ratio for the intersection. It is assumed to be 0.8 for the intersection based on the HCM's recommendation.

All-Red Clearance Interval

All-red clearance interval was calculated using the following equation:

$$R = max\left[\frac{W + Length}{1.47v} - 1, 1.0\right] \tag{18}$$

Where,

W = intersection width (feet)

$Length$ = vehicle length, (use 20 ft.)

v = 85^{th} percentile speed, which is considered as the following:

- If not available, posted speed limit + 7 will be used. Therefore, for the current case it is considered 47 mph since the posted speed is 40 mph for all approaches.
- For left turn, 20 mph will be used

Yellow Interval:

Yellow interval was calculated using the following equation:

$$Y = t + \frac{1.47v}{2a + (64.4 \times g)} \tag{19}$$

Where,

t = reaction time (1.0 sec)

a = deceleration (10.0 ft/sec^2)

v = 85^{th} percentile speed, which is considered as the following:

- If not available, posted speed limit + 7 will be used, which is 47 mph.
- For left turn, posted speed – 5 mph was used, 35 mph.

g = grade (as decimal)

Effective Green

Effective green is calculated using equation (20) below:

$$g_i = \frac{y_{ci}}{\sum_{i=1}^{n} y_{ci}} C \qquad (20)$$

where,

g_i = effective green for phase i

y_i = critical flow ratio for phase $i = v_i/(N\ s_i)$ (sec)

C = cycle length (sec)

Pedestrian Interval:

Pedestrian interval will be calculated using the MUTCD procedure (*Manual on Uniform Traffic Control Devices (MUTCD)*, 2009).

Step 5. Determine Proportion Arriving During Green

To determine proportion arriving during green time (P), equation (21) below is used:

$$P = R_p \left(\frac{g}{C}\right) \tag{21}$$

where,

P = proportion of vehicles arriving during the green indication (decimal),

R_p= platoon ration. Based on the HCM, if the spacing between signals is less or equal to 800 ft, which is the case in the University Dr. and Texas Ave. intersection, then the value of R_p= 2.00.

g = effective green time (s), and

C = cycle length (s).

Step 6. Determine Signal Phase Duration

The signal phase duration is calculated by following the HCM procedure for pretimed signals as was shown above.

Step 7. Determine Capacity and Volume-to-Capacity Ratio

The capacity is calculated with equation (22).

$$c = N\, s \left(\frac{g}{C}\right) \tag{22}$$

where c is the capacity (veh/h), and all other variables are as previously defined.

The volume to capacity ratio is calculated with equation (23) below

$$X = \frac{v}{c} \tag{23}$$

where X is the volume to capacity ratio, and all other variables are as previously defined.

Step 8. Determine Delay

Delay is calculated by using the following equation

$$d = d_1 + d_2 + d_3 \qquad (24)$$

where,

d_1 = uniform delay (s/veh) = $PF \frac{0.5\, C\, (1-g/C)^2}{1-[\min(1,X) g/C]}$, (25)

d_2 = incremental delay (s/veh)

$$= 900\, T \left[(X_A - 1) + \sqrt{(X_A - 1)^2 + \frac{8kIX_A}{c_A T}}\right], \qquad (26)$$

PF = progression adjustment factor,

$$= \frac{1-P}{1-g/C} \times \frac{1-y}{1-\min(1,X)\, P} \times \left[1 + y\frac{1-PC/g}{1-g/C}\right] \qquad (27)$$

$$y = \min(1,X)\, g/C \qquad (28)$$

C = cycle time,

g = effective green time (sec),

X = Volume-to-capacity ratio,

T = study period = 1 hour for our case.

X_A = the average volume-to-capacity ratio,

k = incremental delay factor = 0.50 as recommended by the HCM for pretimed phases

I = upstream filtering adjustment factor = 0.09 based on HCM's recommendation.

c_A = the average capacity (veh/h),

d_3 = initial queue delay (s/veh) = 0 sec/veh, and

d = control delay (s/veh).

d_3 will be considered 0 seconds because if it is larger than 0 seconds, this means that the system has failed. Therefore, the value of d_3 is not considered in this dissertation.

Regression

Based on the developed procedures and before we start the analysis, we need to develop a formula. Regression is used to develop a polynomial that represents the collected data. As mentioned in chapter IV, the degree of the polynomial is selected so the developed formula represents the general shape or major movements in the data. However, to get the optimal degree of the polynomial, different alternatives are tested. The optimal alternative that is selected is the one that causes the least amount of delay. The following steps are followed to determine the degree of polynomial.

1. A range of possible values for the degree of the formula is selected. The limits of the range may be extreme. For example, it can start at one which represents a straight line, and the maximum value of the range can be the value that, when used and the polynomial was plotted, we would see it follow every possible oscillation in the data. This, however, is not needed. The range can be shortened to be limited to only the values that represent the general shape of the data. If this decision is not preferable or not easily made, however, the extreme option, mentioned earlier, can be selected. The only disadvantage in the extreme option is it requires a relatively long time to analyze, depending on the specifications of the computer used in the analysis.
2. For each value of the range that was determined in the previous step, a polynomial is developed by using regression.
3. The optimization techniques are applied using each polynomial and the value of delay is calculated for each developed set of timing plan breakpoints by using equation (8). After that, the minimum value of the calculated delay values is recorded for each polynomial.
4. The selected degree of polynomial is the one that causes the least amount of delay.

The procedure above might not result in the best degree of the polynomial from a statistical point of view because the polynomial, then, might overfit or underfit the collected data. However, the goal in this study is not to select a predictor for the data. The goal is to select a formula that represents the general shape of the data. Additionally, and as will be shown later in this section, a higher degree of the polynomial would not give the best results of delay. The reason for that is when the polynomial starts to follow minor movements in the data, that will create a possible breakpoint of a timing plan. However, that breakpoint might not be at the optimal time. The focus of the oscillation might be driven away from the major areas which need to be focused on in the analysis, like the peak and off-peak hours.

For the traffic counts of the intersection of University Dr. and Texas Ave. which were collected on February 12, 2019, different polynomials were generated with degrees ranging from 3 to 14. This range is considered as extreme since it starts at 3, which can be considered a poor representative for the data as it is apparent in Figure 36. We could have started at 1; however, it would not add any value to the study and would only add more analysis effort with no benefit. After the 3rd degree, other degrees up to 14 were tested. See Figure 37 through Figure 47 below. We can see in Figure 43, the 10th degree polynomial started to oscillate and follow minor movements in the data which do not represent the major movements in the data. However, we continue beyond that to test higher degrees because the goal is to automate the process wherever possible.

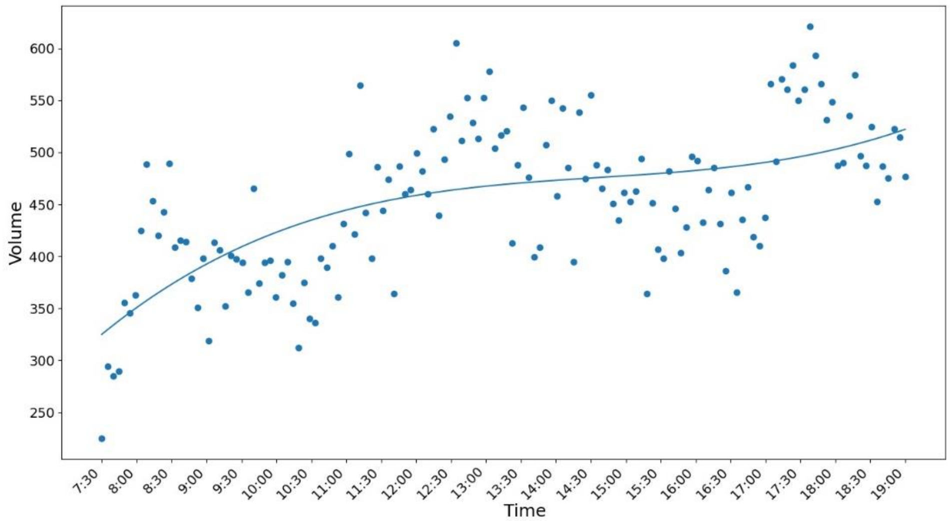

Figure 36: Plot of the Traffic Counts and Their 3rd Degree Polynomial

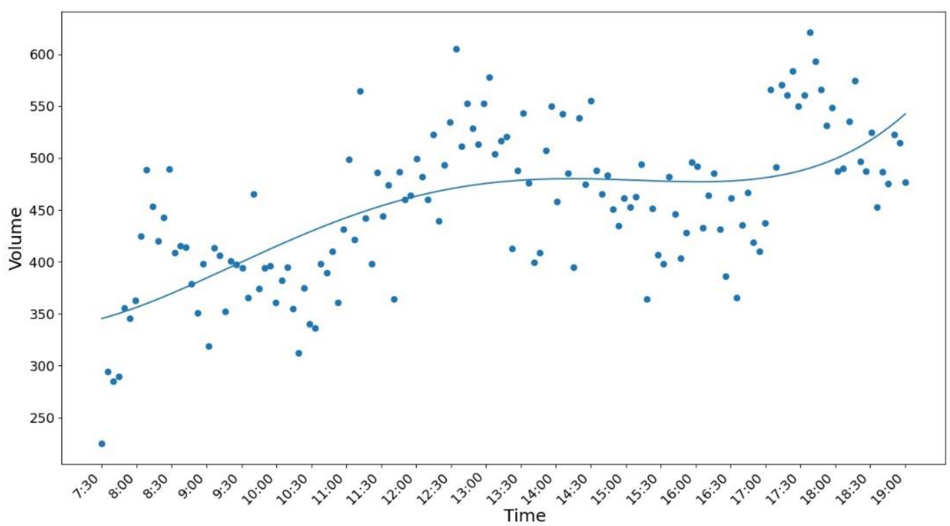

Figure 37: Plot of the Traffic Counts and Their 4th Degree Polynomial

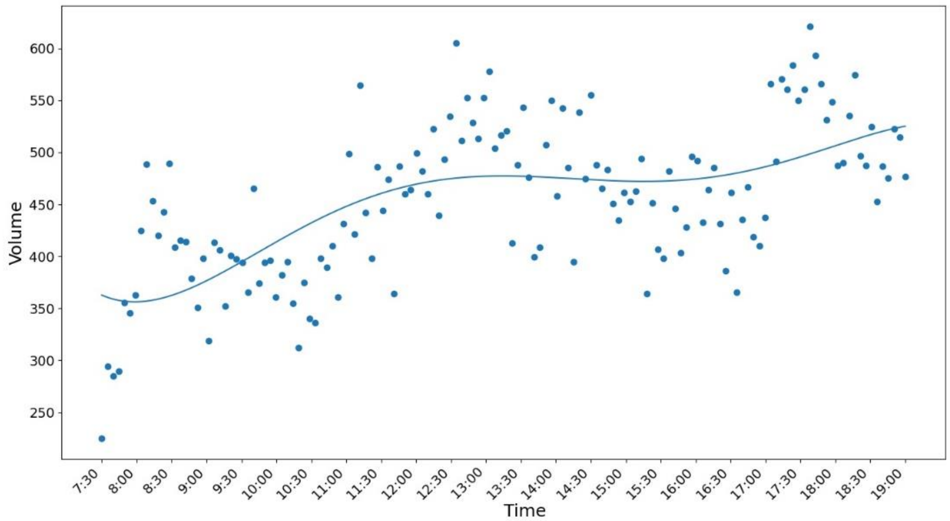

Figure 38: Plot of the Traffic Counts and Their 5th Degree Polynomial

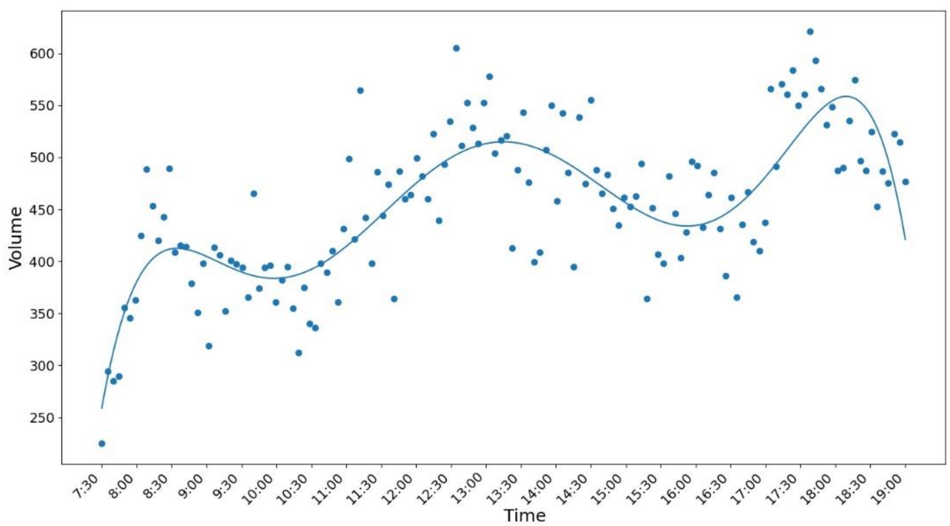

Figure 39: Plot of the Traffic Counts and Their 6th Degree Polynomial

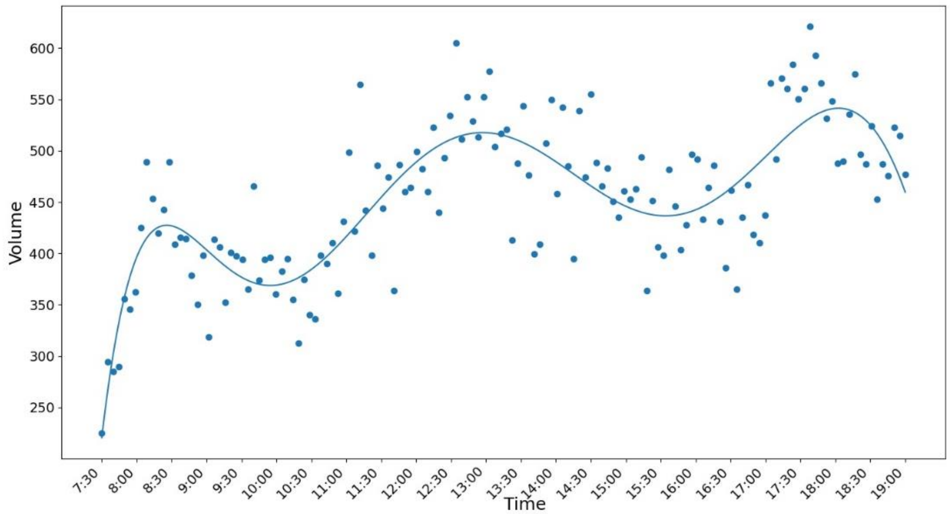

Figure 40: Plot of the Traffic Counts and Their 7th Degree Polynomial

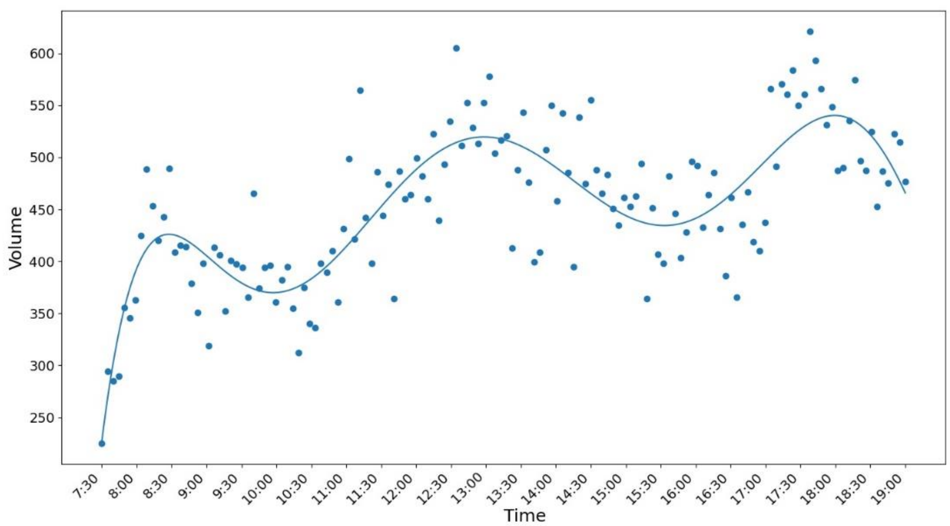

Figure 41: Plot of the Traffic Counts and Their 8th Degree Polynomial

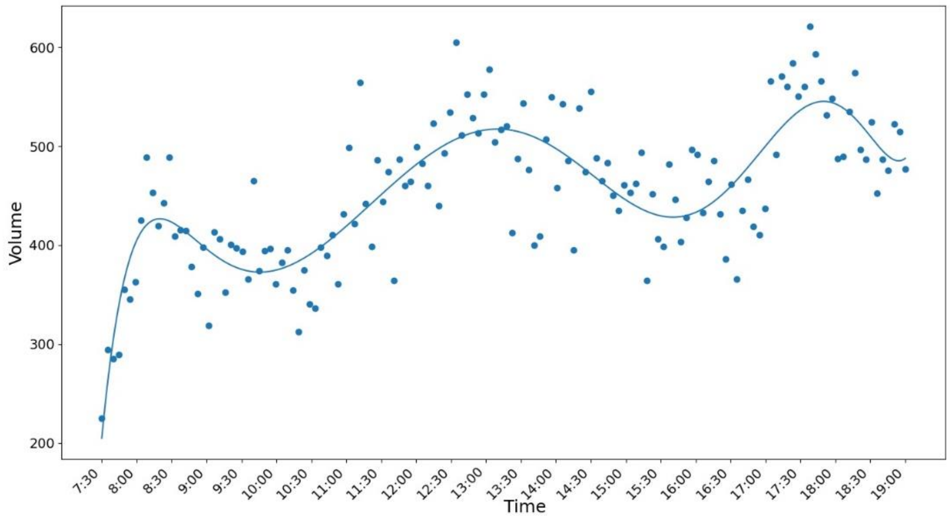

Figure 42: Plot of the Traffic Counts and Their 9th Degree Polynomial

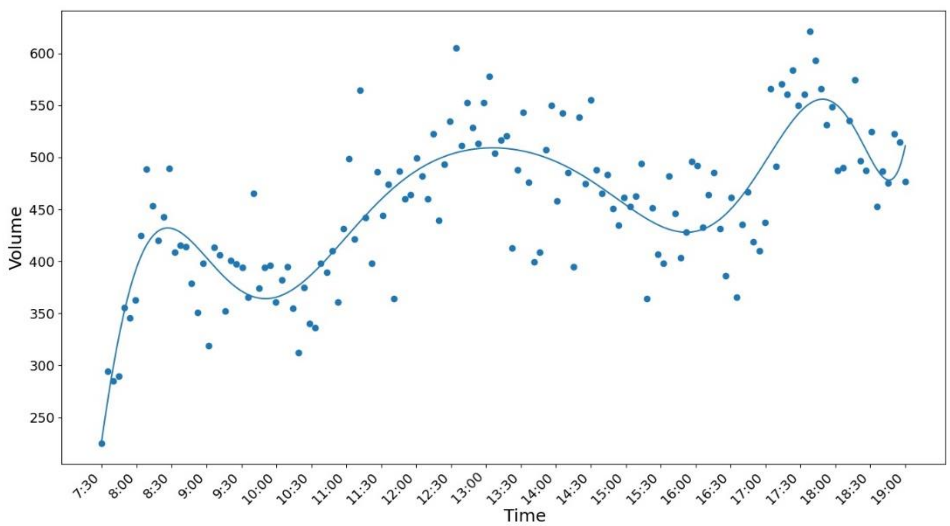

Figure 43: Plot of the Traffic Counts and Their 10th Degree Polynomial

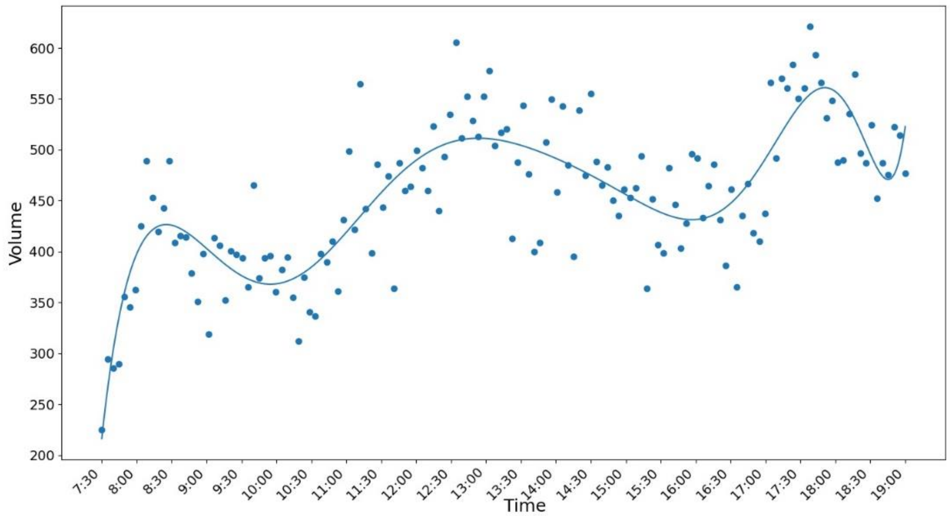

Figure 44: Plot of the Traffic Counts and Their 11th Degree Polynomial

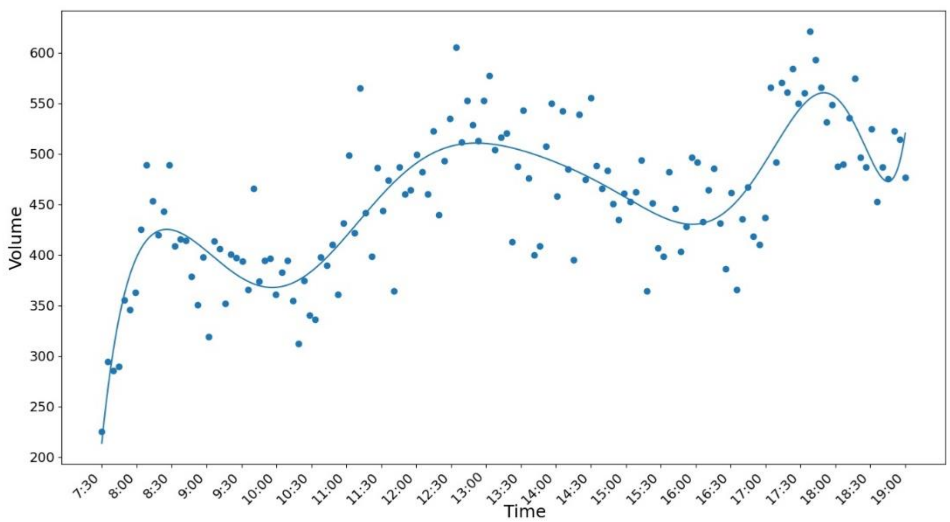

Figure 45: Plot of the Traffic Counts and Their 12th Degree Polynomial

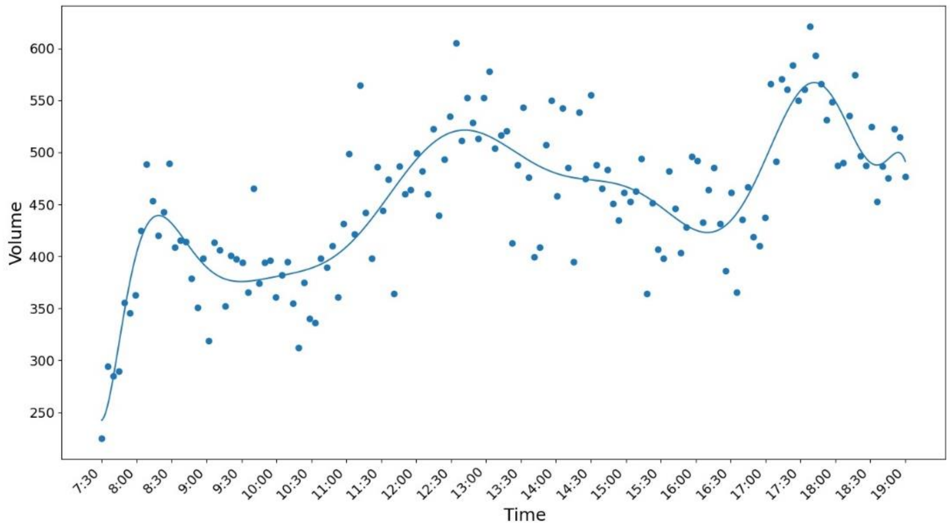

Figure 46: Plot of the Traffic Counts and Their 13th Degree Polynomial

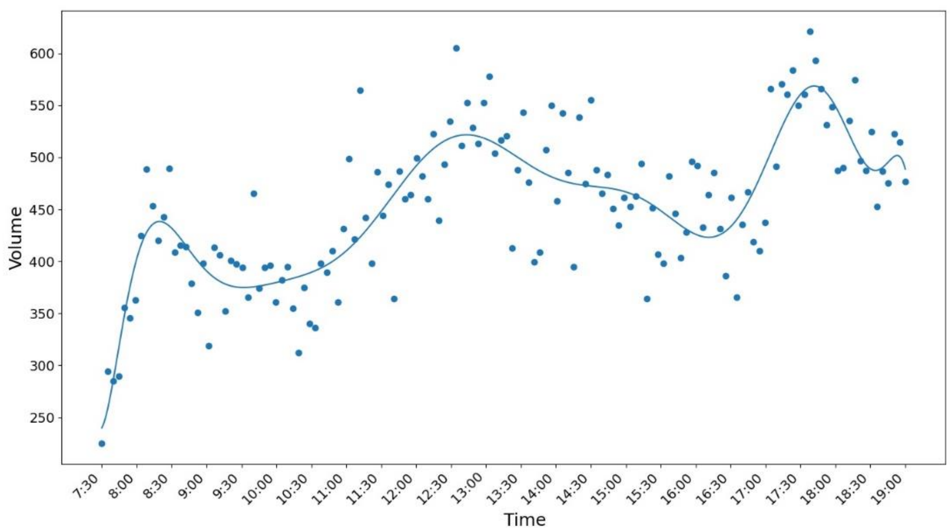

Figure 47: Plot of the Traffic Counts and Their 14th Degree Polynomial

After determining the range of the alternatives of degrees of the polynomial, a polynomial is generated for each degree in the range of degrees. For each polynomial, the timing plan breakpoints are calculated based on the procedure which was presented in Chapter IV and applied in the next section in this chapter. Then, for every polynomial, we find the breakpoints that cause the least amount of delay and record that minimum delay. For the traffic counts of the intersection of University Dr. and Texas Ave. which were collected on February 12, 2019, Table 4 shows, for every degree of polynomial, the value of the minimum delay that were obtained by using the developed optimization techniques. Figure 48 shows a plot of minimum delay vs. degree of polynomial. By inspecting both the table and figure below, we conclude that a 6th degree polynomial would be a better representation of the data since, when using it in the analysis, the minimum value of delay was obtained. Therefore, in the analysis in the following sections, the used polynomial degree is 6 and it is shown in Figure 39 above.

Table 4: Minimum Delay for Each Polynomial Degree

Degree of Polynomial	Minimum Delay	Figure Number
3	24.7	Figure 36
4	23.5	Figure 37
5	22.8	Figure 38
6	21.4	Figure 39
7	22.7	Figure 40
8	22.7	Figure 41
9	23.4	Figure 42
10	22.5	Figure 43
11	22.5	Figure 44
12	22.5	Figure 45
13	23.2	Figure 46
14	24	Figure 47

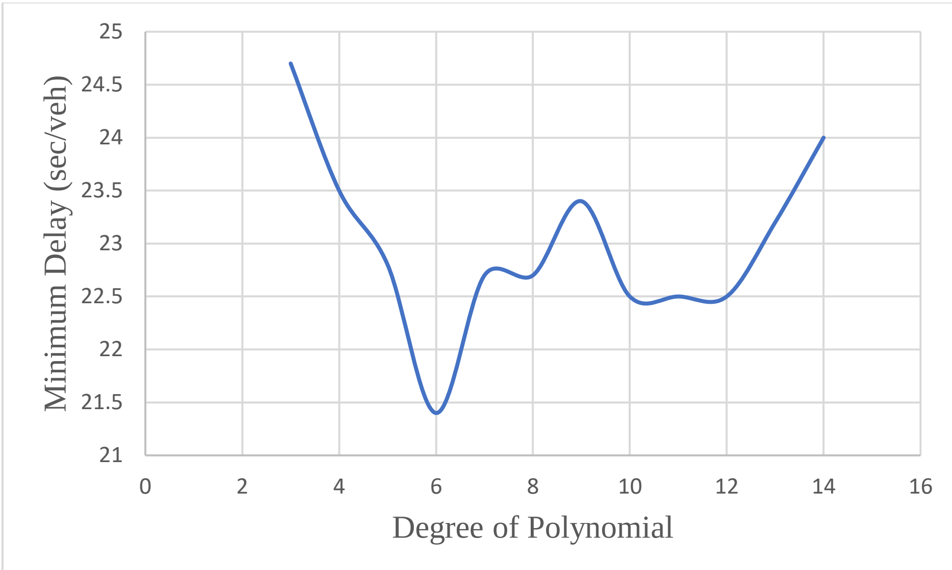

Figure 48: Minimum Delay vs. Degree of Polynomial

Results

To apply the developed procedures, the tool that is used is the program that was written by the author based on the logic that was presented in the previous chapter and earlier in this chapter. The developed program does the following tasks:

1. It accepts the input data mentioned above.
2. Plots the data vs any time scale (i.e. 5-minute, 15-minute, … etc.) taking into consideration that the data should be collected by time increments less or equal to the plotting time increments.
3. Calculates $V'(t)$.
4. Calculates yellow time, all-red, and pedestrian intervals.

5. Calculates a timing plan for each time period.
6. Calculates total delay (D) for each time period.
7. Iterates the value of $V'(t)_{critical}$ and gets different sets of (t_0 to t_n) and D.
8. Changes the value of ΔV based on the procedure in the ΔV optimization method.
9. Adjust the values of (t_0 to t_n) based on the criteria mentioned earlier where t_0 should be at time = 0 and t_n at the end of the study period.
10. Finds the minimum D and the optimal (t_0 to t_n) set based on the critical zone method.
11. It finds the minimum D and the optimal (t_0 to t_n) set based on the ΔV optimization method.
12. Compares the two results from the two optimization methods and suggests the optimal solution between the two

The two developed optimization techniques are applied on the data. The results are shown for each technique.

Critical Zone Optimization Method

As explained in Chapter IV, the first derivative of the generated polynomial is found, and its absolute value is plotted. Then, a horizontal line is drawn on the plot. That line is called $V'(t)_{critical}$. The x-axis coordinates at which $V'(t)_{critical}$ intersects with the absolute value of V' represents potential breakpoints of a timing plan. Different values are generated for $V'(t)_{critical}$ and different sets of breakpoints are thus found. The range of values of $V'(t)_{critical}$ can be predetermined manually by inspecting the plot of the absolute value of V' vs time of day. For the intersection under study, the range of $V'(t)_{critical}$ is (0 to 1.4). That range was chosen because, beyond it, the values of the breakpoints are going to be impractical. When $V'(t)_{critical}$ = 1.4, there is only one time period which is the minimum number of periods. See Figure 70.

After using the collected data in the program and running it, the following results are obtained. The potential sets of breakpoints are shown in the Appendix as the following. For the intersection of University Dr. and Texas Ave. Figure 70 to Figure 113 show the generated sets of potential breakpoints for the data that were collected on February 12 (day 1), and Figure 121 to Figure 167 for the data that were collected on February 13 (day 2). While for the intersection of George Bush Dr. and Texas Ave., Figure 172 to Figure 203 show the generated sets of potential breakpoints for the data that were collected on February 12 (day 1), and Figure 218 to Figure 255 for the data that were collected on February 13 (day 2). Each one of these figures has a plot of the absolute value of $V'(t)$ vs time of day. For every figure, the x-coordinates of the intersection points are recorded and selected as a candidate for a set of the timing plan breakpoints.

However, if any two successive breakpoints are less than one hour apart from each other, they need to be adjusted because the assumption is that any period is at least one hour. The adjustment is conducted by following the procedure shown in Chapter IV. Due to the adjustment, different alternatives can be generated for one value of $V'(t)_{critical}$. For example, Figure 71 to Figure 86 all represent different combinations of the breakpoints due to the fact that the initial intersection points of $V'(t)_{critical} = 0.1$ and the plot of the absolute value of V' has some periods that are less than 1 hour. The adjustment of those breakpoints generated 16 different sets of breakpoints for $V'(t)_{critical} = 0.1$.

For every set of breakpoints, delay is calculated by following the HCM procedure that was presented earlier. A summary of all the generated breakpoints along with their corresponding value of delay and the figure numbers that show their plot is available in the Appendix as the following. For the intersection of University Dr. and Texas Ave, Table 7 for day 1, and Table 9 for day 2. While for the intersection of George Bush Dr. and Texas Ave., Table 11 for day 1, and Table 13 for day 2.

ΔV Optimization Method:

ΔV optimization technique is explained in detail in Chapter IV. The first step is to calculate the range of the data and then calculate ΔV by using equations (9) and (10) respectively. Their values are shown on the plots of the polynomial shown in the Appendix. For the intersection of University Dr. and Texas Ave. Figure 114 to Figure 120 show the generated sets of potential breakpoints for the data that were collected on February 12 (day 1), and Figure 168 to Figure 171 for the data that were collected on February 13 (day 2). While for the intersection of George Bush Dr. and Texas Ave.,

Figure 204 to Figure 217 show the generated sets of potential breakpoints for the data that were collected on February 12 (day 1), and Figure 256 to Figure 261 for the data that were collected on February 13 (day 2).. On each of these figures, the distance between the top and bottom red lines represents the range, while the distance between every two consecutive lines represents ΔV. The potential breakpoints are the x-coordinates of the intersection points of the red horizontal lines and the plot of the polynomial. If any period is less than 1 hour, the adjustment procedure shown in Chapter IV is used to treat those periods. The analysis continued until ΔV is equal to $range/5$, because beyond that, all the periods in at least one zone are less than one hour, which is considered a trigger to stop the analysis based on the developed procedure.

For every set of breakpoints, delay is calculated by following the HCM procedure that was presented earlier. A summary of all the generated breakpoints along with their corresponding value of delay and the figure numbers that show their plot is available in the Appendix as the following. For the intersection of University Dr. and Texas Ave, Table 8 for day 1, and Table 10 for day 2. While for the intersection of George Bush Dr. and Texas Ave., Table 12 for day 1, and Table 14 for day 2.

Selected Breakpoints

The criterion of selecting the optimal breakpoints that is followed in this dissertation is that the optimal set of breakpoints is the one that causes the least amount of delay. Therefore, and after inspecting the values of delay that are shown in the Appendix, the breakpoints can be selected. Figure 49 through Figure 52 show the breakpoints that cause the least delay for the intersection of University Dr. and Texas Ave. (day 1), intersection of University Dr. and Texas Ave. (day 2), intersection of George Bush Dr. and Texas Ave. (day 1), and intersection of George Bush Dr. and Texas Ave. (day 2), respectively, by using the critical zone method. While Figure 53 through Figure 56 show the breakpoints that cause the least delay for the intersection of University Dr. and Texas Ave. (day 1), intersection of University Dr. and Texas Ave. (day 2), intersection of George Bush Dr. and Texas Ave. (day 1), and intersection of George Bush Dr. and Texas Ave. (day 2), respectively, by using ΔV method.

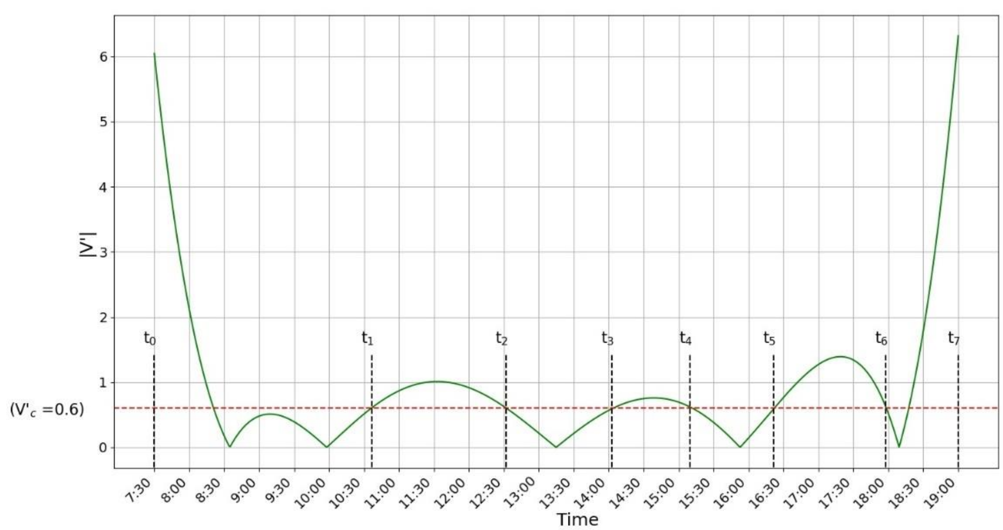

Figure 49: Selected Breakpoints for the Intersection of University Dr. and Texas Ave. (Day 1) by Using the Critical Zone Optimization Technique

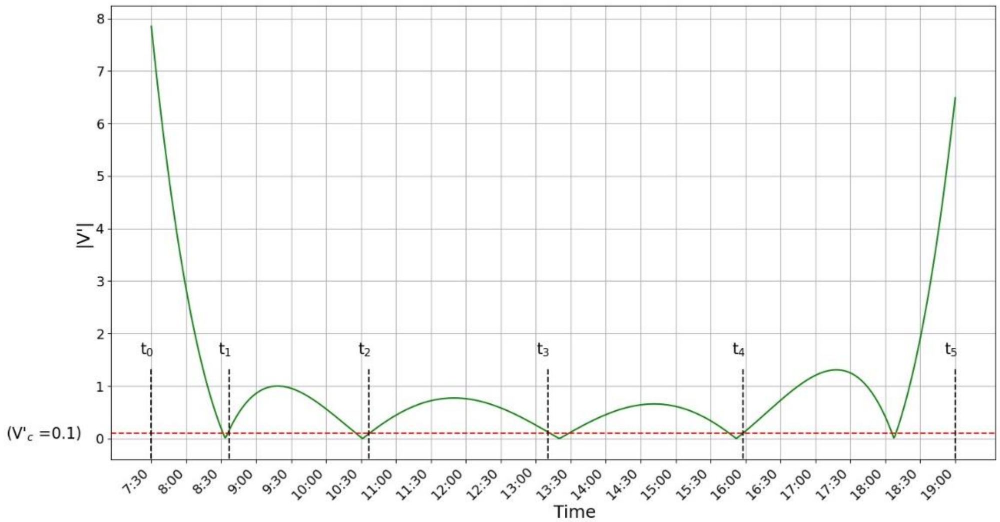

Figure 50: Selected Breakpoints for the Intersection of University Dr. and Texas Ave. (Day 2) by Using the Critical Zone Optimization Technique

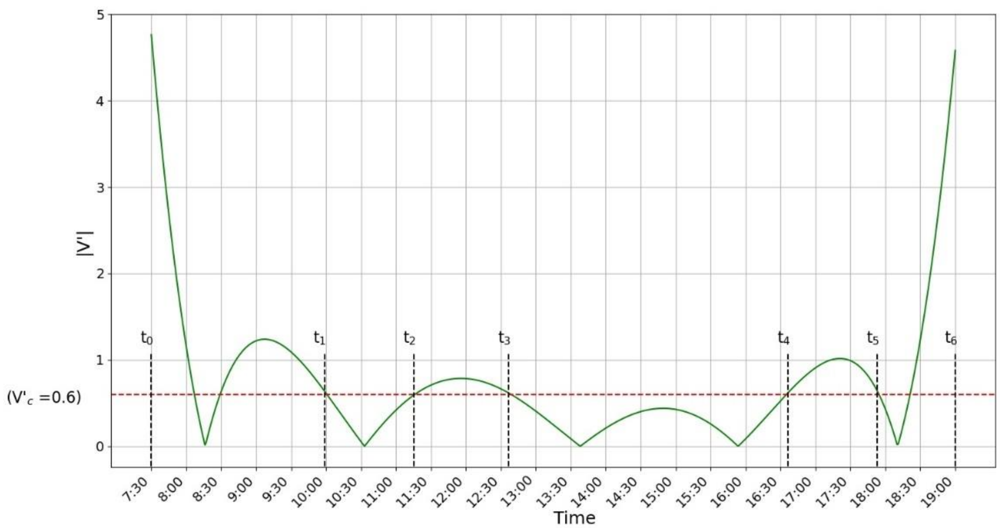

Figure 51: Selected Breakpoints for the Intersection of George Bush Dr. and Texas Ave. (Day 1) by Using the Critical Zone Optimization Technique

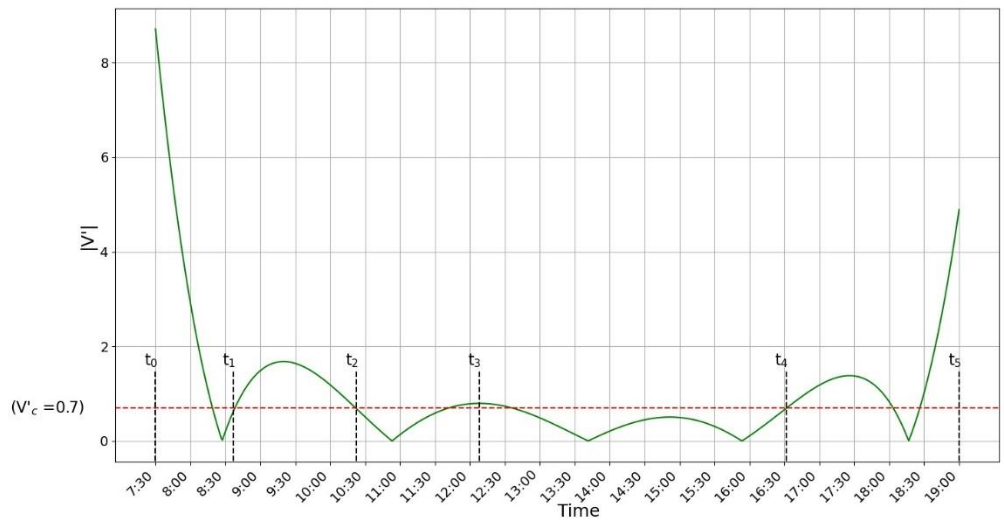

Figure 52: Selected Breakpoints for the Intersection of University Dr. and Texas Ave. (Day 2) by Using the Critical Zone Optimization Technique

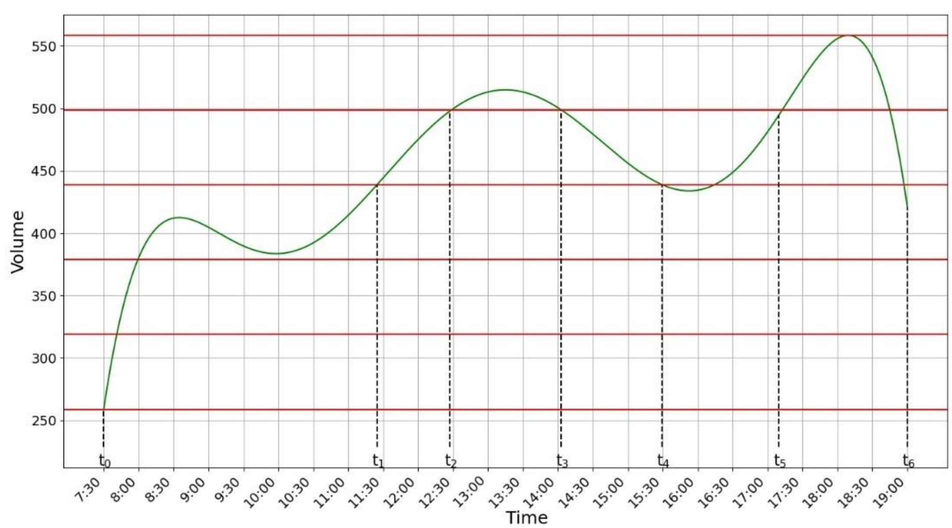

Figure 53: Selected Breakpoints for the Intersection of University Dr. and Texas Ave. (Day 1) by Using the ΔV Optimization Technique

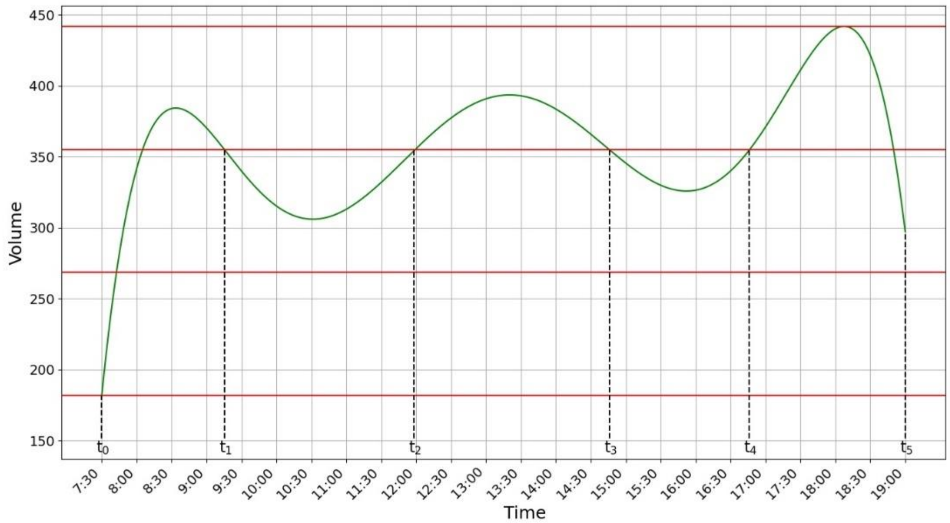

Figure 54: Selected Breakpoints for the Intersection of University Dr. and Texas Ave. (Day 2) by Using the ΔV Optimization Technique

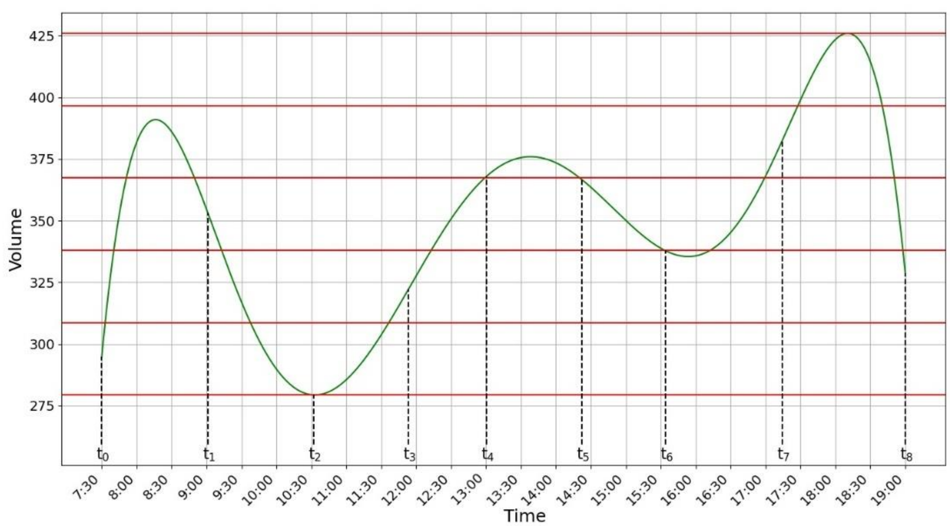

Figure 55: Selected Breakpoints for the Intersection of George Bush Dr. and Texas Ave. (Day 1) by Using the ΔV Optimization Technique

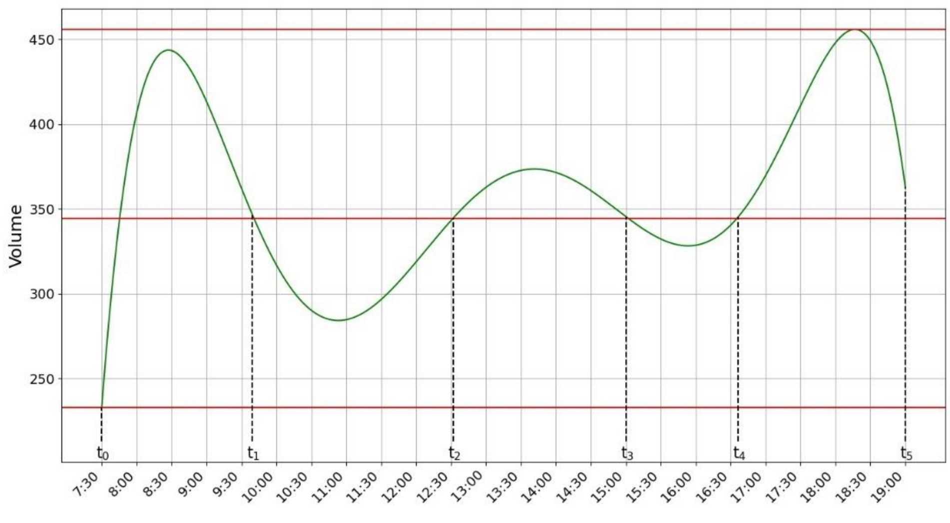

Figure 56: Selected Breakpoints for the Intersection of George Bush Dr. and Texas Ave. (Day 2) by Using the ΔV Optimization Technique

Table 5 shows the values of delay for the selected breakpoints above along with their figure number.

Table 5: Results of other Intersections

Intersection	Date of Data Collection	Optimization Method	Minimum Delay (sec/veh)	Figure Number
TX. Ave & Univ. Dr.	02-12-2019	Critical Zone	21.4	Figure 49
		ΔV	21.8	Figure 53
	02-13-2019	Critical Zone	22.8	Figure 50
		ΔV	23.5	Figure 54
TX. Ave & George Bush Dr.	02-12-2019	Critical Zone	26.8	Figure 51
		ΔV	27.1	Figure 55
	02-13-2019	Critical Zone	25.4	Figure 52
		ΔV	25.3	Figure 56

These breakpoints can be used on the intersections to enhance the performance of the traffic signals. For example, for the data that were collected on February 12, 2019 for the intersection of University Dr. and Texas Ave., the timing plan breakpoints that cause the minimum delay, which is 21.4 sec/veh, are shown in Figure 57 below. These breakpoints represent the optimal time of day points at which a new timing plan needs to be initiated. A different timing plan is used for every period shown in the figure below.

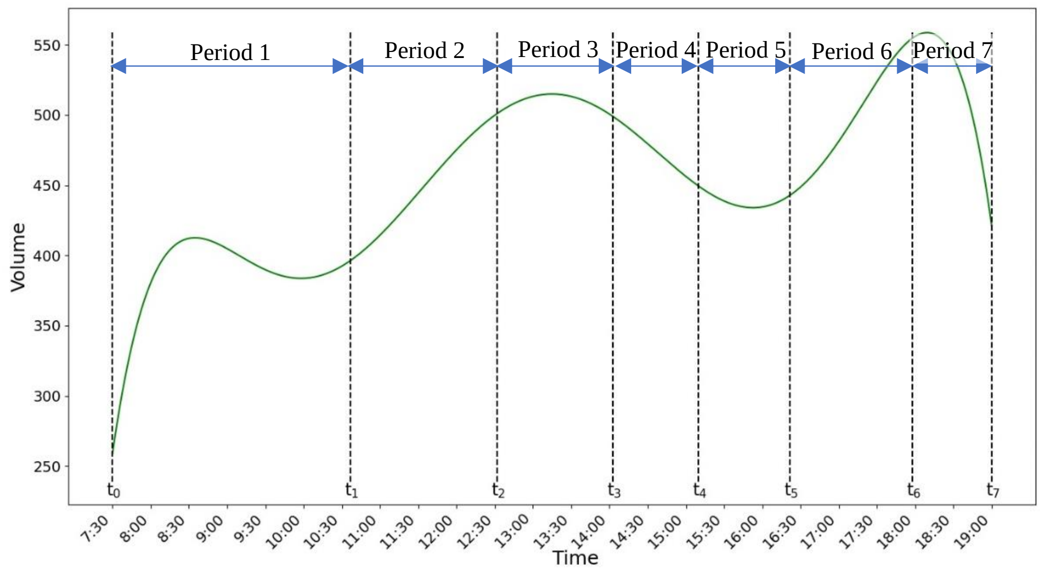

Figure 57: Selected Breakpoints

However, this does not mean that these breakpoints are the only set of breakpoints that should be selected. In fact, there are other options that can perform relatively similar to the selected breakpoints. Depending on what is considered acceptable delay by the local agency, different alternatives are generated by the developed optimization techniques. Those alternatives are available in the Appendix.

Sensitivity Analysis

After applying the developed optimization techniques on the collected data and to test the possibility of the use of the developed timing plans on the same intersections but on different days with similar traffic properties, a sensitivity analysis is conducted on the collected data. If the traffic behavior is relatively the same on multiple days, it is important to determine whether the developed timing plans, by using the data from one day, would work efficiently on the other days. Therefore, for each set of the data that were collected in this dissertation, different sets of data were generated. The generated data were within $\pm$5% of the original data to replicate the case that if the data on other days are close in values and properties to those of the original data. The values were randomly generated within the range above. For every set of the original data, three sets of data were generated, which makes a total of 12 sets of generated data. Moreover, the optimal set of timing plans that was found for every set of the original data was applied on the three corresponding sets of data. Finally, delay was calculated for the generated sets of data and was compared to the delay that was calculated by using the original data.

As mentioned earlier, the data were collected for two intersections during two days for each intersection. Figure 58 through Figure 69 show plots of the original data vs. their three corresponding generated sets of data.

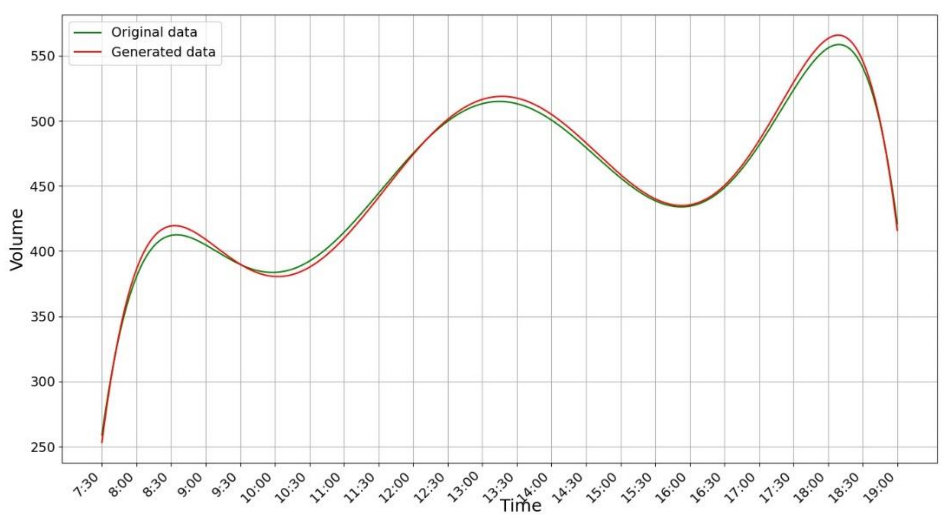

Figure 58: Generated Data Set 1 of the Intersection of University Dr. and Texas Ave (Day 1)

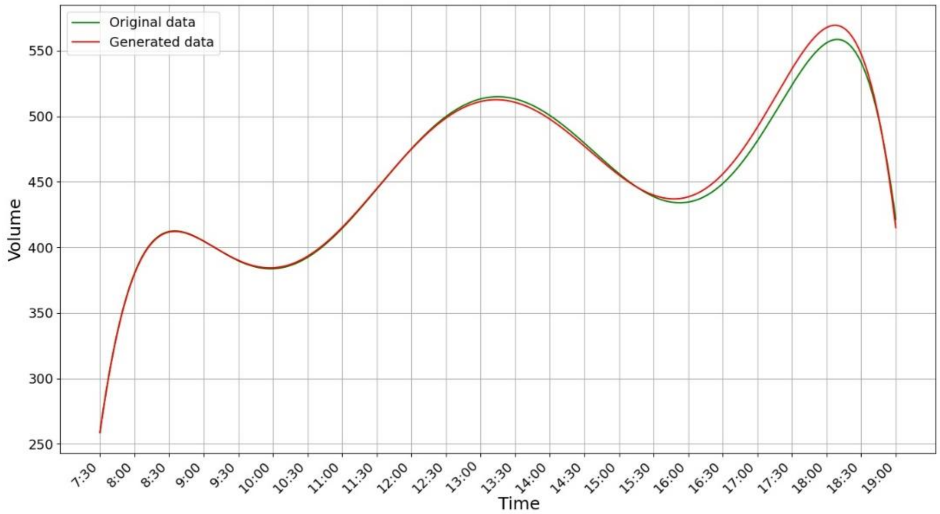

Figure 59: Generated Data Set 2 of the Intersection of University Dr. and Texas Ave (Day 1)

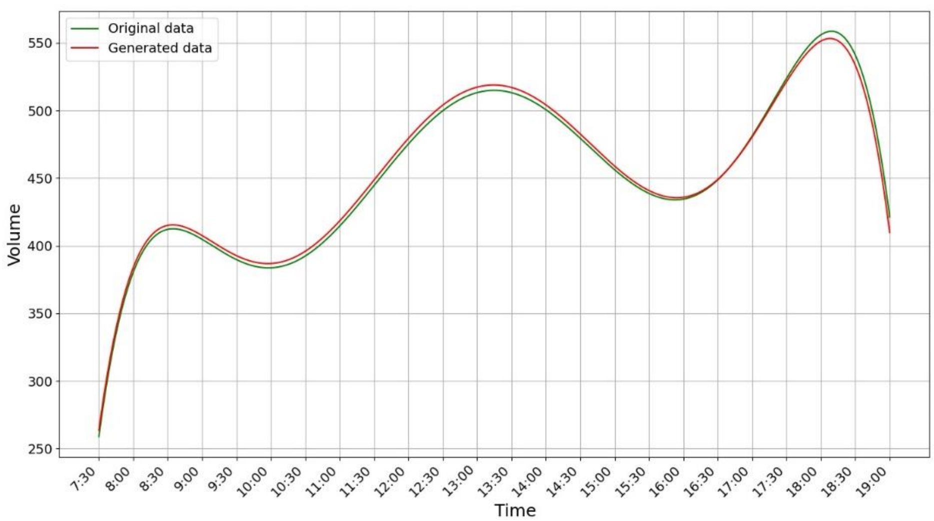

Figure 60: Generated Data Set 3 of the Intersection of University Dr. and Texas Ave (Day 1)

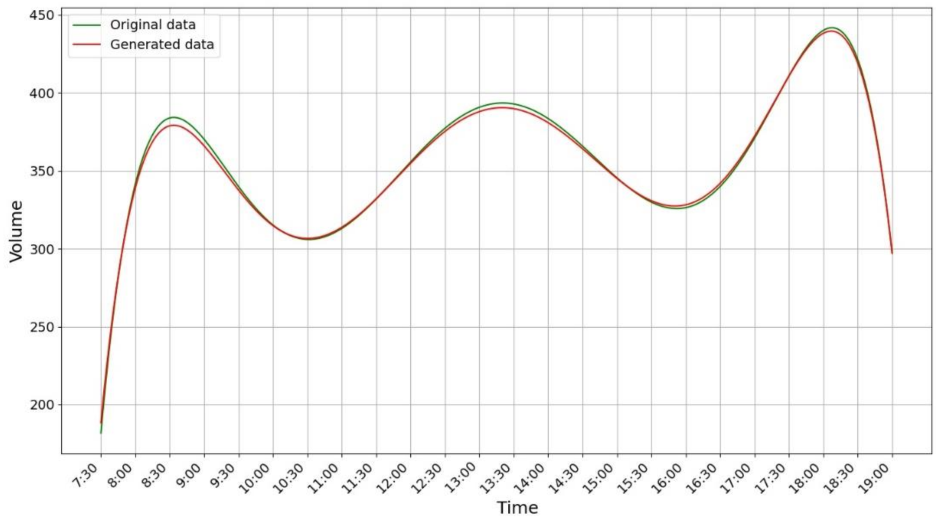

Figure 61: Generated Data Set 1 of the Intersection of University Dr. and Texas Ave (Day 2)

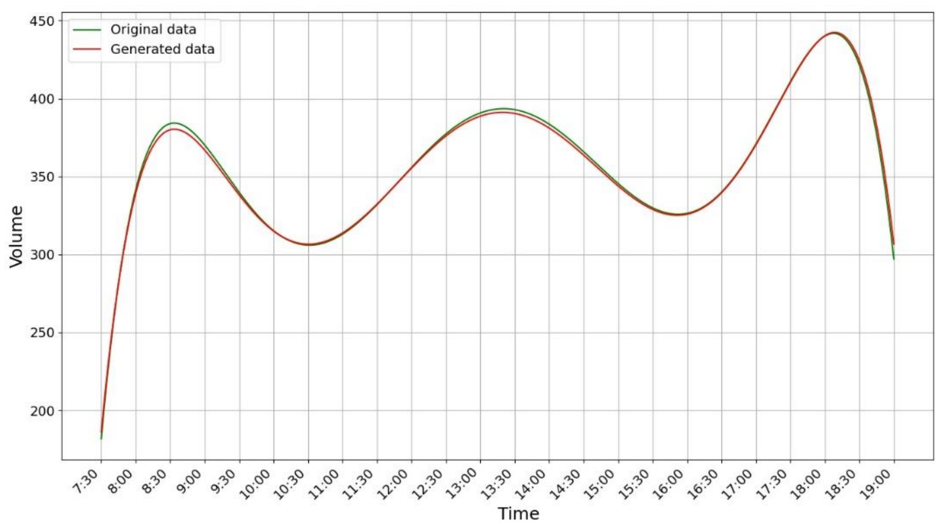

Figure 62: Generated Data Set 2 of the Intersection of University Dr. and Texas Ave (Day 2)

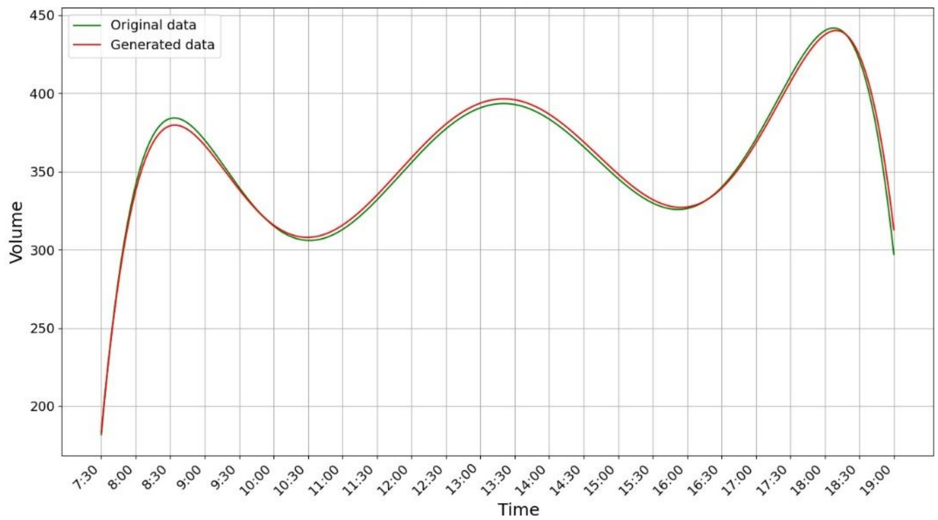

Figure 63: Generated Data Set 3 of the Intersection of University Dr. and Texas Ave (Day 2)

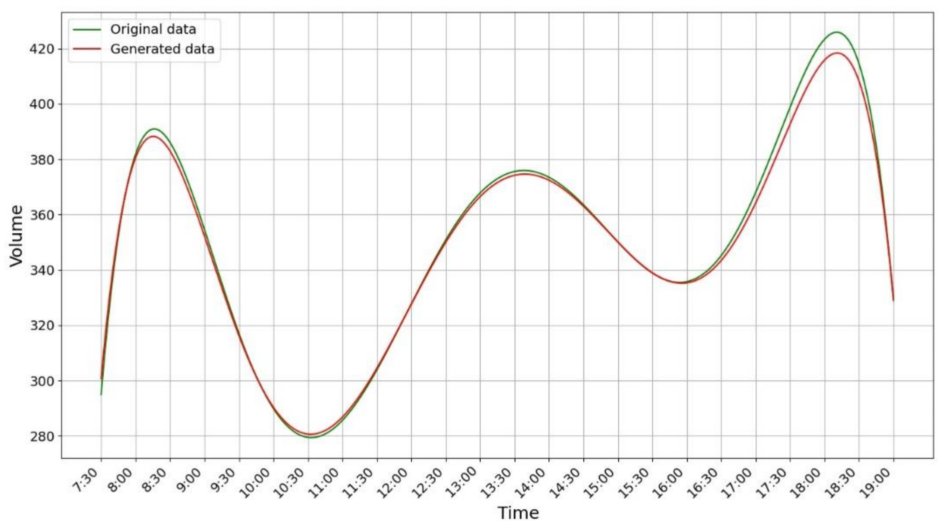

Figure 64: Generated Data Set 1 of the Intersection of George Bush Dr. and Texas Ave (Day 1)

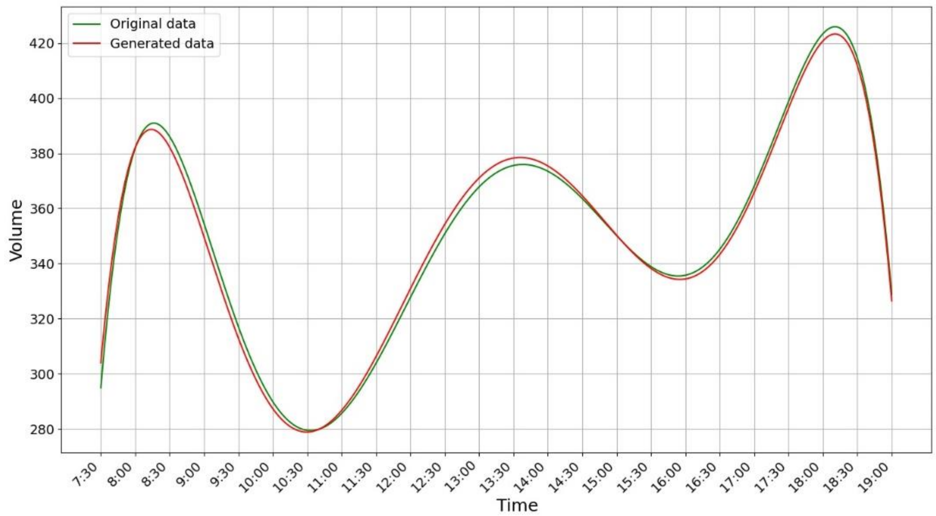

Figure 65: Generated Data Set 2 of the Intersection of George Bush Dr. and Texas Ave (Day 1)

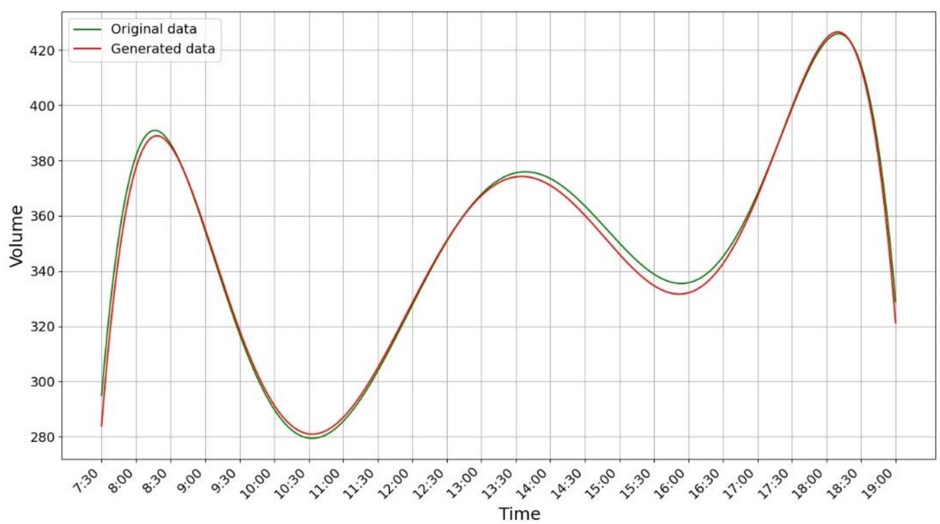

Figure 66: Generated Data Set 3 of the Intersection of George Bush Dr. and Texas Ave (Day 1)

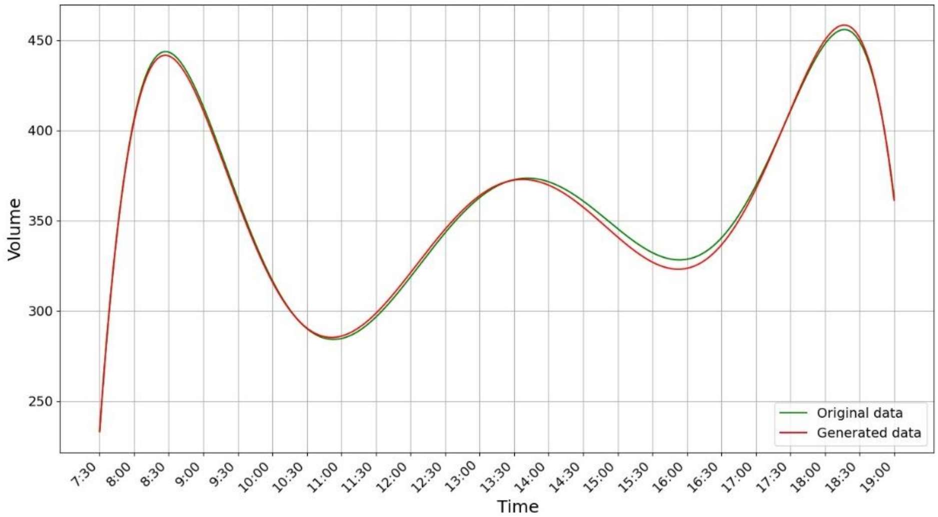

Figure 67: Generated Data Set 1 of the Intersection of George Bush Dr. and Texas Ave (Day 2)

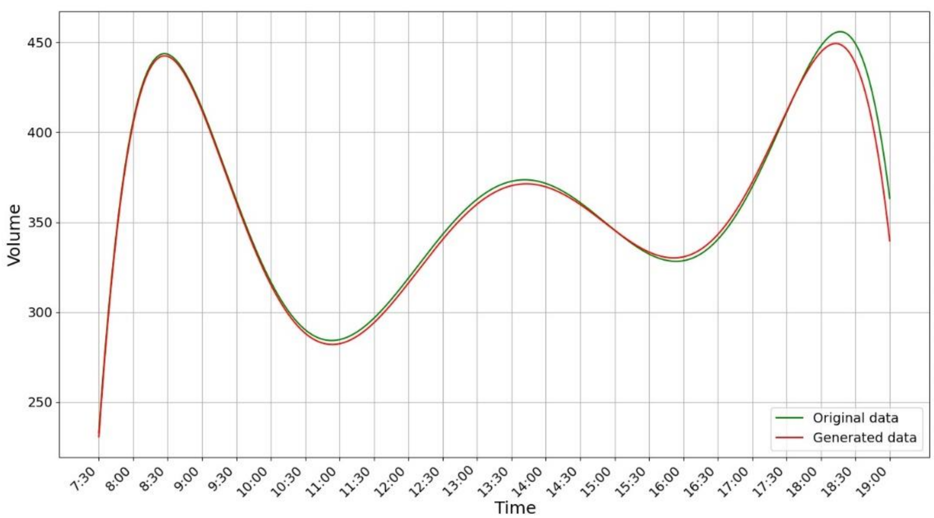

Figure 68: Generated Data Set 2 of the Intersection of George Bush Dr. and Texas Ave (Day 2)

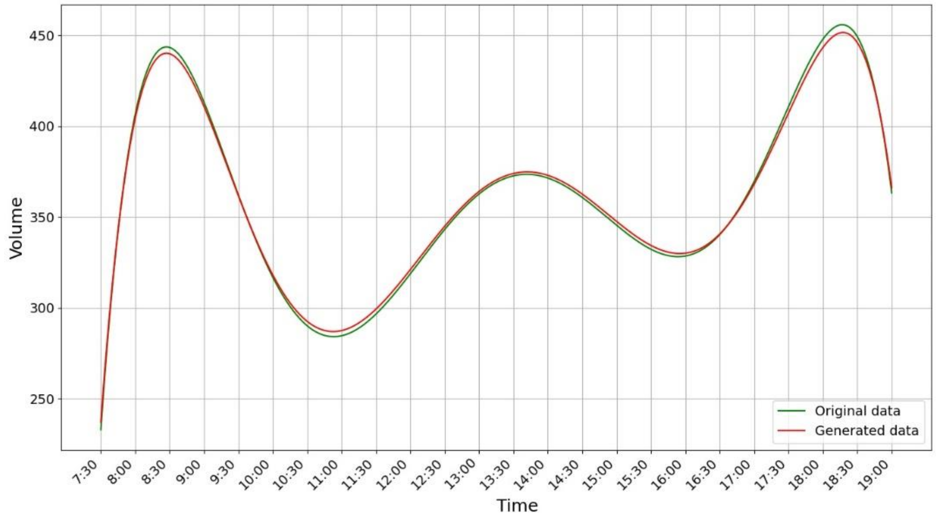

Figure 69: Generated Data Set 3 of the Intersection of George Bush Dr. and Texas Ave (Day 2)

After applying the optimal timing plan breakpoints on the generated data, delay was calculated for each case and the percent difference in delay was calculated by using equation (29) below.

$$Percen\ Difference\ in\ Delay = \frac{Delay_{Generated\ Data} - Delay_{Original\ Data}}{Delay_{Generated\ Data}} \times 100 \qquad (29)$$

The results are shown in Table 6 below.

Table 6: Results of the Sensitivity Analysis

Intersection	Date of Data Collection	Minimum Delay Using Original Data	Generated Data Set Number	Minimum Delay Using Generated Data	% Difference in Delay
TX. Ave & Univ. Dr.	02-12-2019	21.4	1	23.7	9.70%
			2	23.5	8.94%
			3	23.2	7.76%
	02-13-2019	22.8	1	25.1	9.16%
			2	23.9	4.60%
			3	24.5	6.94%
TX. Ave & George Bush Dr.	02-12-2019	26.8	1	28.1	4.63%
			2	29.2	8.22%
			3	28.3	5.30%
	02-13-2019	25.3	1	26.4	4.17%
			2	27.2	6.99%
			3	27.1	6.64%

We can see in the table above that when using the optimal breakpoints of timing plans on the generated data, delay is increased slightly. However, in all of the cases, the increase in delay did not exceed 3 sec/veh or 10%, which can be considered acceptable. This means that the calculated breakpoints of timing plans can be used on different days if the traffic volume is within ∓5% of the original data.

Interpretation of Results

By studying the optimization results that were presented earlier, we can see clearly the difference in performance between different sets of breakpoints. The minimum delay ranges between 21.4 sec/veh to 27.1 for all of the four intersection data sets.

Comparing the Developed Techniques to the Traditional Method

As stated in chapter IV, the traditional method of selecting timing plans for a pretimed intersection is to manually determine the breakpoints. The timing plan usually consist of three periods, which are AM peak, PM peak and off-peak. To compare the results of the developed techniques to the traditional method, we need, first, to replicate the results of the traditional method. However, since that method consists of manual selection of the breakpoints, its results will be subjective because it is not consistent, which is the main drawback that initiated this research. Therefore, instead of manually selecting the breakpoints and to eliminate the factor of inconsistent results, we will look at some of the generated breakpoints that resemble the traditionally selected breakpoints. Since the developed techniques generate a wide range of possible breakpoints, some of them will replicate the traditional AM, PM, off-peak plans. This does not only overcome the comparison to inconsistent results but also adds other alternatives to compare to. For example, if we look at Figure 116 or Figure 117, we can see that the generated breakpoints represent typical am, pm, off peak plan set. Even Figure 118 can be considered similar to an am, pm, off peak set with the exception of adding one transitional period between t_2 and t_3, which is not usual in a traditional breakpoint set. The delay values, in the three formerly mentioned figures, are (30, 26.4, and 25.3) sec/veh respectively. Those values are higher than the minimum value which is 21.4 sec/veh. This proves that the developed technique is effective in selecting the breakpoints of timing plans. However, even if the minimum value of delay was for a set of breakpoints that resembles a traditional set of breakpoints, this does not mean that the developed techniques were not effective. On the contrary, that would only mean that the traditional system works for the current intersection. However, the breakpoints for the timing plans in that intersection would not be selected manually. They would be calculated by using the developed techniques.

Comparison of the Developed Optimization Techniques

By comparing the two developed optimization method, we can see a slight advantage of the critical zone method over the ΔV method. However, the difference might not be effective in most cases. There is another more important advantage of the critical zone method, however, which is the number of the generated alternatives of the breakpoints of timing plans. This gives other options to select breakpoints other than the one that causes the minimum delay, especially that there might be other breakpoints that cause delay close to the minimum value. For example, if for some reason like some local constraints or coordination purposes, the optimal breakpoints do not fit the system, the traffic engineer can choose from the other options that are provided through the critical zone optimization method that cause slightly higher delay. This option is limited with the ΔV optimization method since the number of the generated alternatives is less than that in the critical zone optimization method.

It is important to note here that the optimization and selection of the timing plan breakpoint might not be the only solution an intersection needs to solve its traffic operation issues. Factors other than signal timing might be the reason that the operation is not ideal. If, after running this technique at a pretimed controlled intersection and getting the optimal breakpoints, the intersection still had traffic problems, it is likely that merely changing when timing plans start is not enough. Probably, actuation needs to be considered or even some constructional changes like adding lanes or interchanges. However, the goal of this study is to provide a guidance to select the best breakpoints for timing plans at an intersection by using the optimization techniques which are based on minimizing delay. Other considerations might still be needed after getting the optimal breakpoints, however, they are out of the scope of this dissertation. After getting the timing plan breakpoints, engineering judgement and other guidelines should be followed. If the decision is to have a pretimed signal operation at the intersection, then, the developed techniques can be effectively used to decide on when to change from one timing plan to another.

CHAPTER VI

CONCLUSIONS AND RECOMMENDATIONS

Conclusions

This dissertation covers the selection of the time-of-day breakpoints of timing plans at an isolated pretimed signalized intersection based on the minimization of delay at the intersection. Two techniques were developed to implement this task. They are the critical zone optimization method and the ΔV optimization method.

To test and validate the developed techniques, a computer program was developed by the author. That program was written, by using Python programming language ("Python Programing Language," 2020), based on the suggested optimization techniques. The application of the program was conducted on four sets of traffic data. Two intersections were selected which are the intersection of Texas Ave. and University Dr. and the intersection of Texas Ave. and George Bush Dr. Both intersections are in College Station, TX. Traffic counts were collected on two days for each intersection, which makes a total of four sets of data. Traffic counts were not collected manually, however. Video cameras were placed at the south eastern and north eastern corners of each intersection and 12 hours (7:00 am – 7:00 pm) of video were recorded on each camera during each day. The data then were counted by a detection and tracking computer program that was also developed by the author by using Python programing language. The accuracy of the detection and counting program was validated by comparing it to manual counts of parts of the same recorded videos. The developed comparison plots showed high accuracy of the developed detection and counting program.

After that, the turning counts were used to test the optimization techniques. The results showed the ability of the developed optimization techniques to minimize delay and select, accordingly, the optimized breakpoints of timing plans. Also, by comparing the results with the results of the traditional AM peak, PM peak, and off-peak plan set, the developed techniques were found to be more effective in selecting the breakpoints of timing plans.

Additionally, a sensitivity analysis was conducted by generating different data sets from the original data and applying the breakpoints that were found by using the original data. The analysis showed that these breakpoints can be efficiently used on the generated data.

It was also found that the critical zone optimization method performed better than the ΔV optimization method because it produces breakpoints that causes slightly less delay than those found by the ΔV optimization. Additionally and most importantly, the critical zone optimization method produces more alternatives of timing plan breakpoints that might perform relatively similar to the optimal breakpoints. This can help local agencies to freely select the breakpoints that can fit their requirements.

Recommendations

Although the developed technique showed that the suggested techniques were effective in minimizing delay of a pretimed intersection, it is important to note that the optimization and selection of the timing plan breakpoint might not be the only solution an intersection needs to solve its traffic operation issues. If the operation of an intersection is not optimal even after applying our optimization technique, it is likely that factors other than signal timing might be the reason that the operation is not ideal. Perhaps, only changing when timing plans start is not enough. It is possible, then, that actuation needs to be considered or even some constructional changes, like adding lanes or interchanges.

However, the goal of this study is to provide a guidance to select the optimal breakpoints for timing plans at an intersection by using the optimization technique which is based on minimizing delay. Other considerations might still be needed after getting the optimal breakpoints, but they are out of the scope of this dissertation. Also, if there are any system requirements like a predetermined cycle length or offsets, then the intersection needs to be analyzed differently.

Additionally, after getting the timing plan breakpoints, engineering judgement and other guidelines should be followed. If the decision is to have a pretimed signal operation at the intersection, then, the optimization technique that was developed in this dissertation can be effectively used to decide on when to change from one timing plan to another.

Regarding data collection, high quality videos with high frame rate, a minimum of 30 fps, are required. Also, when placing the cameras at the intersection, at least one camera, at each corner of the intersection, is required to guarantee a full coverage of the intersection. Additionally, high end computers are also necessary to analyze the videos efficiently.

Future Research

Although the objectives of this research have been achieved, further research can still be of a great value in the future. This research was conducted on pretimed intersections; therefore, it is recommended that further research is conducted to expand the application to more complex systems like actuated and/or coordinated systems.

Additionally, when choosing a regression formula, for this research, polynomial regression was chosen as a method of estimating the formula that represents the collected data. As an extension to this research, the author will test other forms of regression, like spline regression for example. The author will also investigate estimating $V'(t)$ rather than calculating it by deriving $V(t)$.

Finally, regarding vehicles detection and tracking, the possibility of using artificial intelligence (AI) to develop a tracking technique of vehicles needs to be studied. A comparison between AI method and the currently used algorithmic analysis is recommended as it would determine which method is more efficient.

Benefits of the Study

The benefits of the study can be summarized in the following points.

1. Reducing delay. Reducing delay is the main objective of this study
2. Reducing cost. Cost will be reduced as a direct result to the reduced delay, since saving time means saving money depending on the value of time for the road users.
3. Safety. An optimized traffic signal will have the lowest possible stopping time which can lower the possibility of the rear-end collisions.
4. Environmental. Gas emission will be reduced because delay and travel time, in general, will be reduced.

REFERENCES

Counter, S. T. (2021). Traffic Counter Store, Piezoelectric Sensor. Retrieved from https://trafficcounterstore.com/product/6-class-i-bl-piezo-100-lead-in/

Google Earth. (2019, December 29). Intersection of University Drive and Texas Avenue Retrieved from https://earth.google.com/web/@30.62783779,-96.33488153,103.13999203a,144.88700949d,35y,-0h,0t,0r

Grote, M., Williams, I., Preston, J., & Kemp, S. (2018). A practical model for predicting road traffic carbon dioxide emissions using Inductive Loop Detector data. *Transportation Research Part D: Transport and Environment, 63*, 809-825. doi:https://doi.org/10.1016/j.trd.2018.06.026

Highway Capacity Manual. (2016). (Sixth ed.): Washington, D.C. : Transportation Research Board©.

Koonce, P., Rodegerdts, L., Lee, K., Quayle, S., Beaird, S., Braud, C., . . . Urbanik, T. (2008). *Traffic signal timing manual*: Washington, D.C. : U.S. Department of Transportation, Federal Highway Administration, 2008.

Larue, G. S., & Wullems, C. (2019). A new method for evaluating driver behavior and interventions for passive railway level crossings with pneumatic tubes. *Journal of Transportation Safety & Security, 11*(2), 150-166. doi:10.1080/19439962.2017.1365316

Lee, J., Kim, J., & Park, B. (2010). A genetic algorithm-based procedure for determining optimal time-of-day break points for coordinated actuated traffic signal systems. *KSCE Journal of Civil Engineering, 15*(1), 197-203. doi:10.1007/s12205-011-1093-0

Manual on Uniform Traffic Control Devices (MUTCD). (2009). United States: U.S. Department of Transportation, Federal Highway Administration (FHWA).

Normann, O. K. (1962). Variations in Flow at Intersections as Related to Size of City, Type of Facility and Capacity Utilization. *HRB Bull*(352), 55-99.

Park, B., Santra, P., Yun, I., & Lee, D.-H. (2004). Optimization of Time-of-Day Breakpoints for Better Traffic Signal Control. *Transportation Research Record: Journal of the Transportation Research Board, 1867*, 217-223. doi:10.3141/1867-25

. Python Programing Language (Version 3.8). (2020): Python Software Foundation. Retrieved from https://www.python.org/

Rajab, S., Al Kalaa, M. O., & Refai, H. (2016). Classification and speed estimation of vehicles via tire detection using single-element piezoelectric sensor. *Journal of Advanced Transportation, 50*(7), 1366-1385. doi:10.1002/atr.1406

Randall, J. (2012). *Traffic Recorder Instruction Manual* (2nd ed.). Texas: Texas Department of Transportation.

Redmon, J., Divvala, S., Girshick, R., & Farhadi, A. (2015). You Only Look Once: Unified, Real-Time Object Detection. arXiv:1506.02640. Retrieved from https://ui.adsabs.harvard.edu/abs/2015arXiv150602640R

Tri-State, T. D. (2021). Radar Traffic Counter. Retrieved from https://tstdata.com/technology.html

U.S. Census Bureau, American Community Survey 1-year estimates. (2019). Retrieved from http://censusreporter.org/profiles/31000US17780-college-station-bryan-tx-metro-area/

Urbanik, T., Tanaka, A., Lozner, B., Lindstrom, E., Lee, K., Quayle, S., . . . Bullock, D. (2015). *Signal timing manual* (2nd ed.): Washington, D.C. : Transportation Research Board, 2015.

Wang, H., Ouyang, M., Meng, Q., & Kong, Q. (2020). A traffic data collection and analysis method based on wireless sensor network. *EURASIP Journal on Wireless Communications and Networking, 2020*(1), 2. doi:10.1186/s13638-019-1628-5

Wang, X. D., Cottrell, W., & Mu, S. C. (2005). Using K-Means Clustering to Identify Time-of-Day Break Points for Traffic Signal Timing. *2005 IEEE Intelligent Transportation Systems Conference (ITSC)*, 519-524. doi:10.1109/itsc.2005.1520102

Wordpress. (2014). Black Rubber Tubes in the Roadway: Helping to Understand Your Neighborhood. Retrieved from https://bellevuentss.wordpress.com/2014/01/27/black-rubber-tubes-in-the-roadway-helping-to-understand-your-neighborhood/

APPENDIX

OPTIMIZATION RESULTS

In this appendix, a summary of data and the analysis results is presented for the four cases that were analyzed and presented in Chapter V. These cases are:

1. University Dr. and Texas Ave intersection. Data were collected on February 12, 2019.
2. University Dr. and Texas Ave intersection. Data were collected on February 13, 2019.
3. George Bush and Texas Ave. intersection. Data were collected on February 12, 2019.
4. George Bush and Texas Ave. intersection. Data were collected on February 13, 2019.

There optimization results are shown in the following sections. A detailed discussion about the results was presented in Chapter V.

University Dr. and Texas Ave Intersection, Feb 12, 2019:

Below are the optimization results by using both of the developed optimization techniques for the traffic counts data of the intersection of University Dr. and Texas Ave. that were collected on February 12, 2019

Critical Zone Optimization Technique:

Figure 70 through Figure 113 show the developed breakpoints by using the critical zone optimization method.

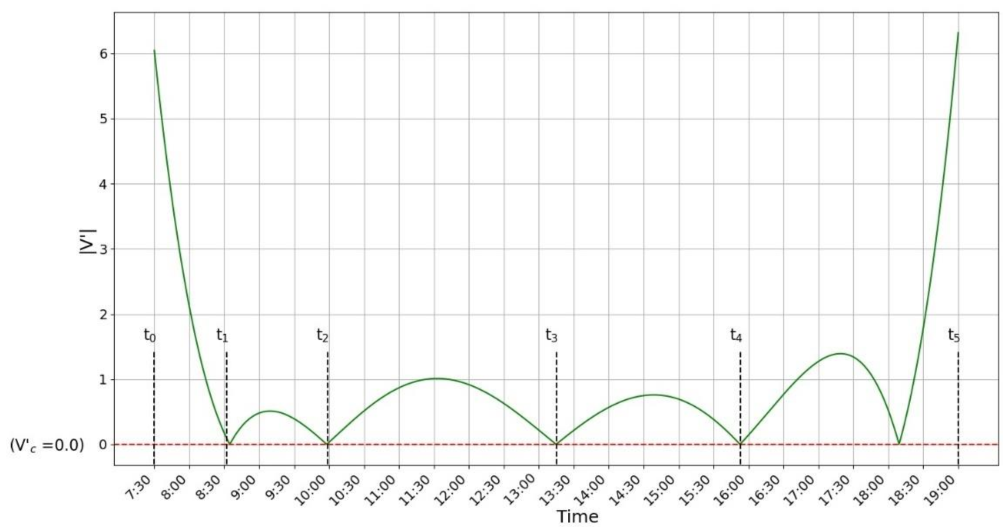

Figure 70: $V'(t)_{critical}$ = 0.0

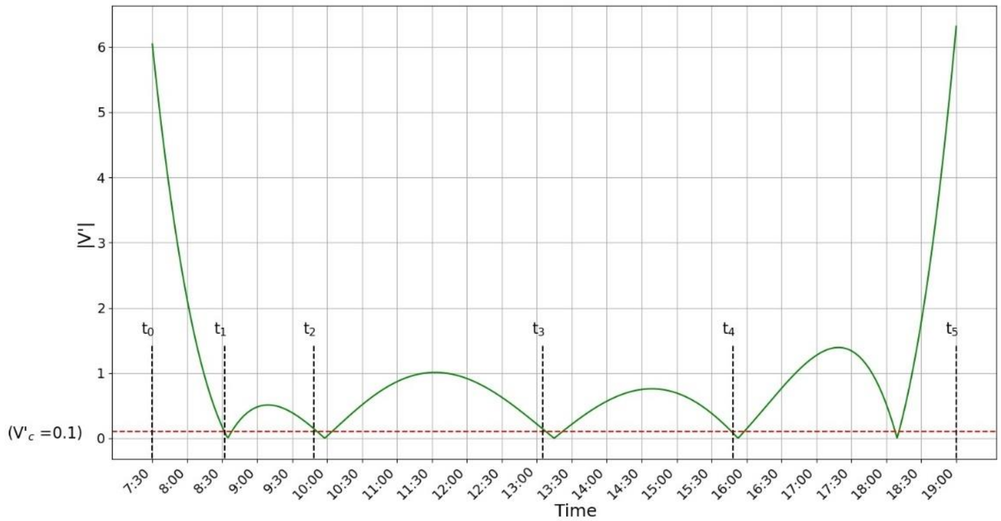

Figure 71: $V'(t)_{critical}$ = 0.1, Breakpoint Set 1

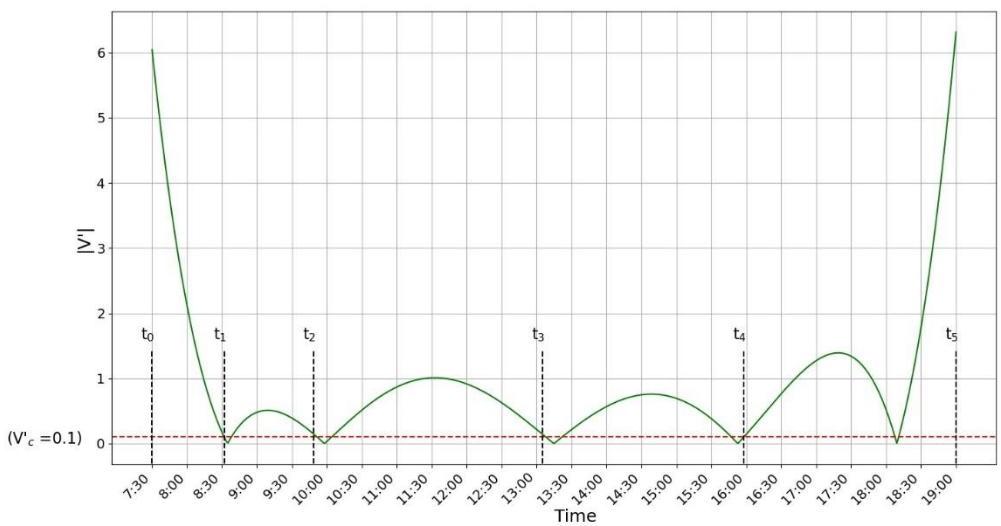

Figure 72: $V'(t)_{critical}$ = 0.1, Breakpoint Set 2

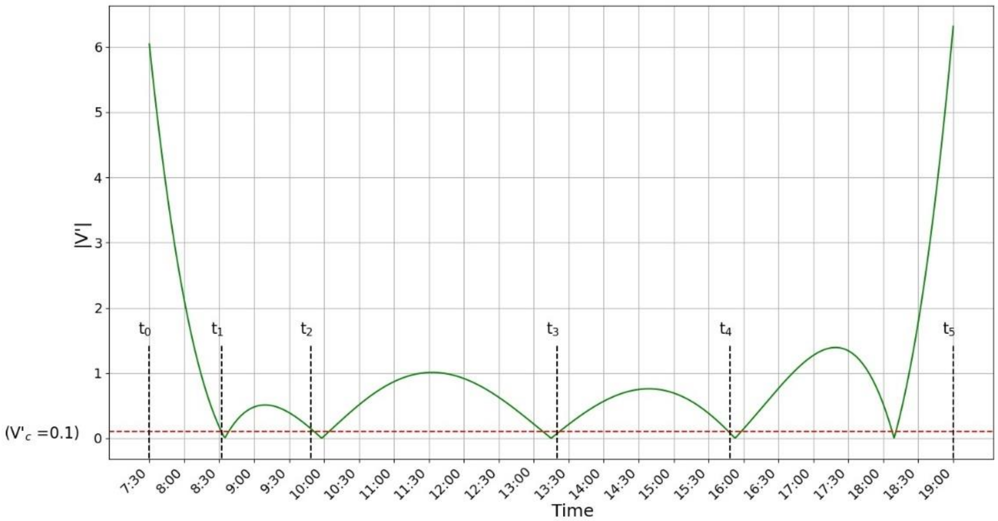

Figure 73: $V'(t)_{critical}$ = 0.1, Breakpoint Set 3

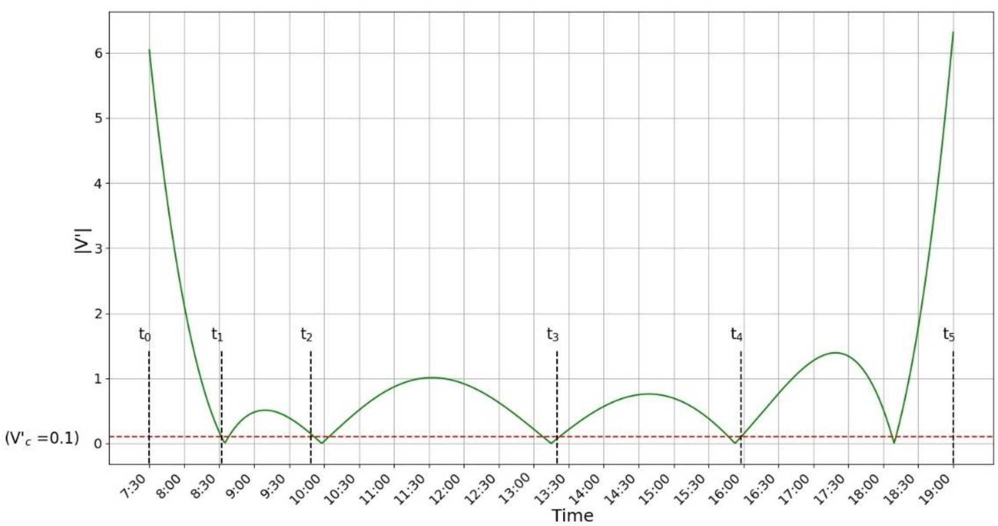

Figure 74: $V'(t)_{critical}$ = 0.1, Breakpoint Set 4

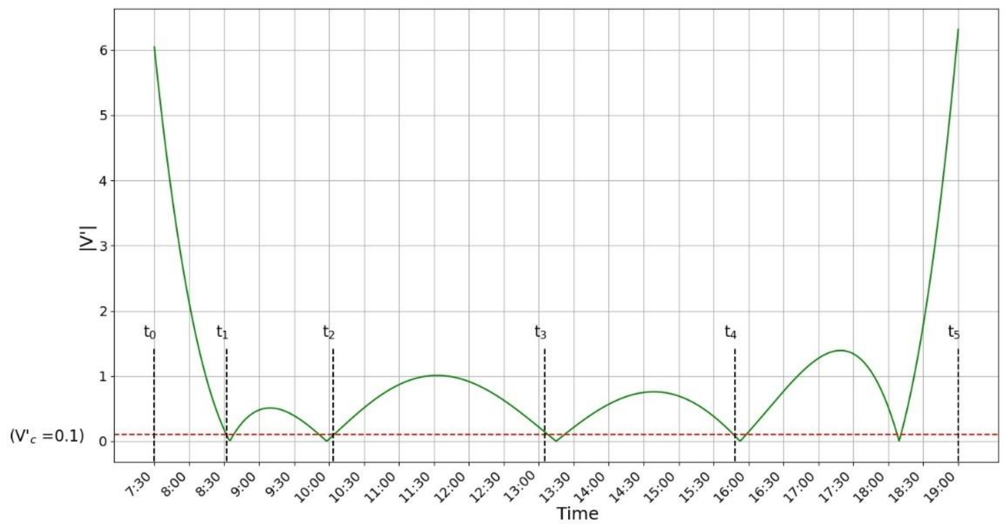

Figure 75: $V'(t)_{critical}$ = 0.1, Breakpoint Set 5

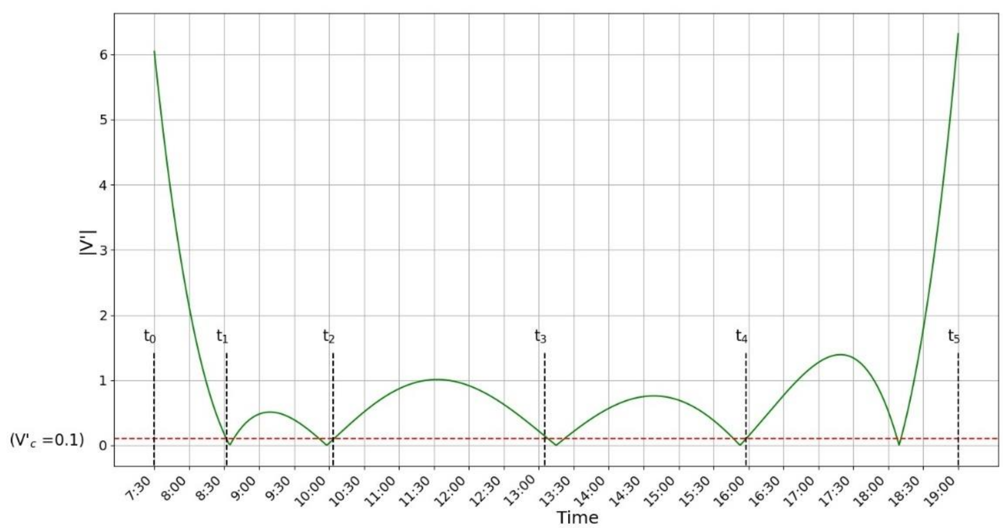

Figure 76: $V'(t)_{critical}$ = 0.1, Breakpoint Set 6

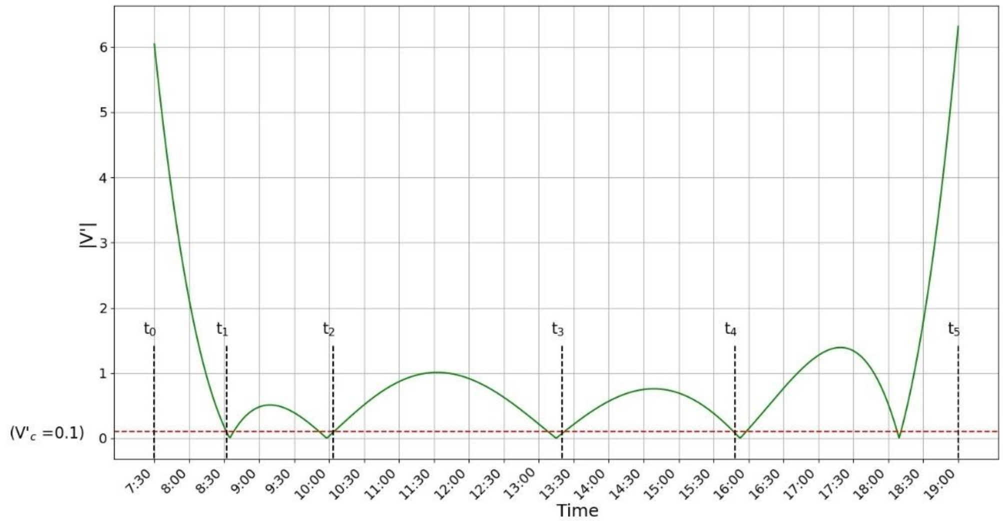

Figure 77: $V'(t)_{critical}$ = 0.1, Breakpoint Set 7

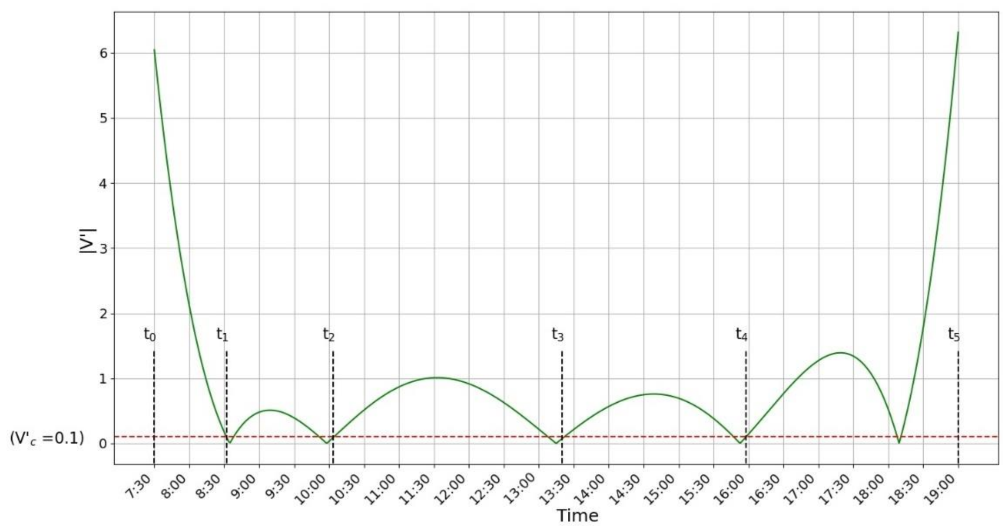

Figure 78: $V'(t)_{critical}$ = 0.1, Breakpoint Set 8

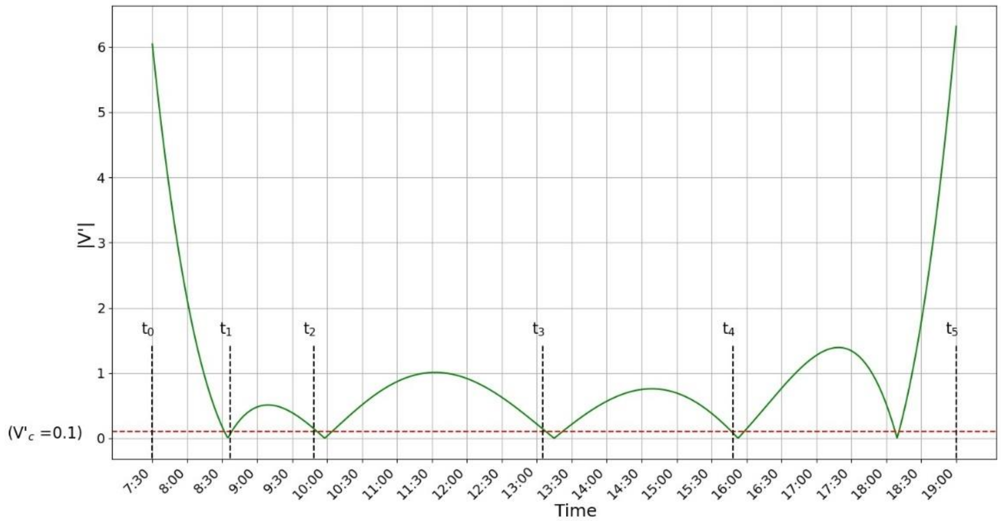

Figure 79: $V'(t)_{critical}$ = 0.1, Breakpoint Set 9

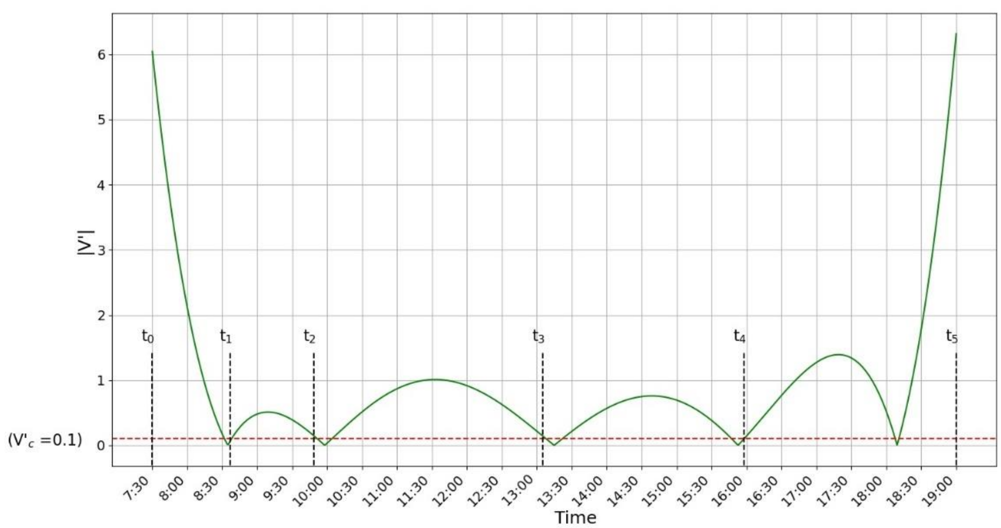

Figure 80: $V'(t)_{critical}$ = 0.1, Breakpoint Set 10

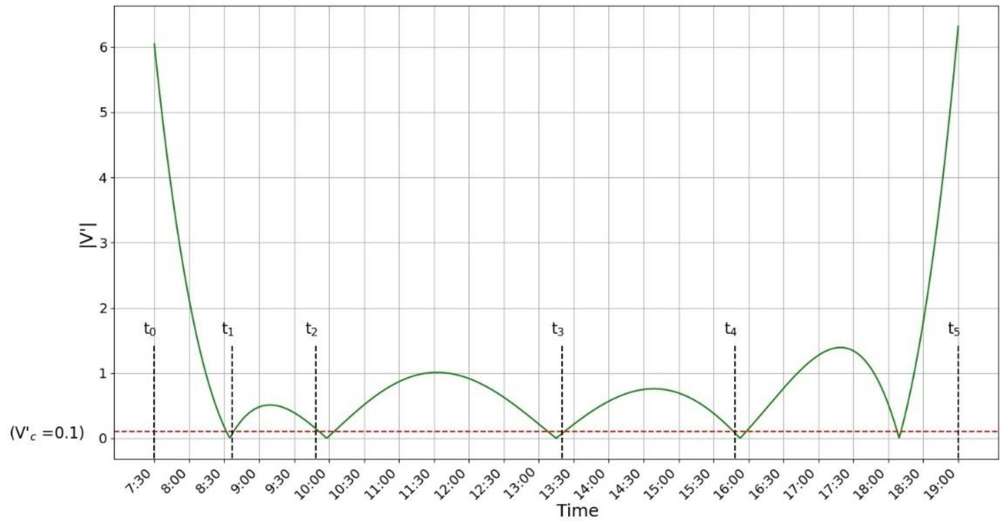

Figure 81: $V'(t)_{critical}$ = 0.1, Breakpoint Set 12

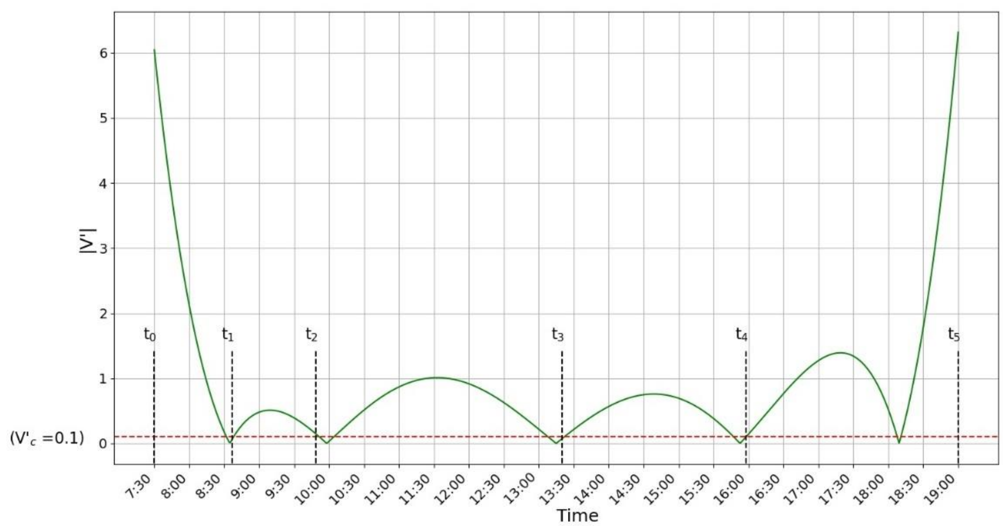

Figure 82: $V'(t)_{critical}$ = 0.1, Breakpoint Set 13

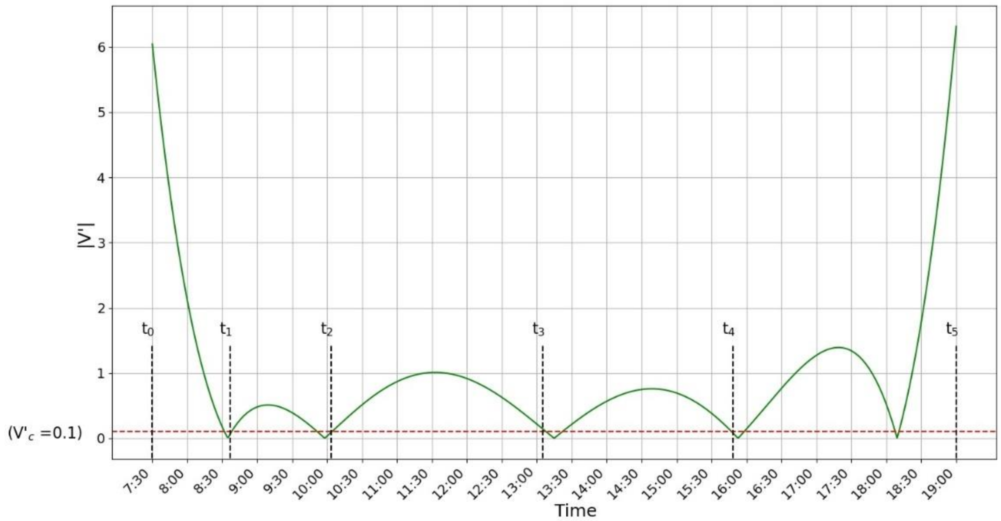

Figure 83: $V'(t)_{critical}$ = 0.1, Breakpoint Set 14

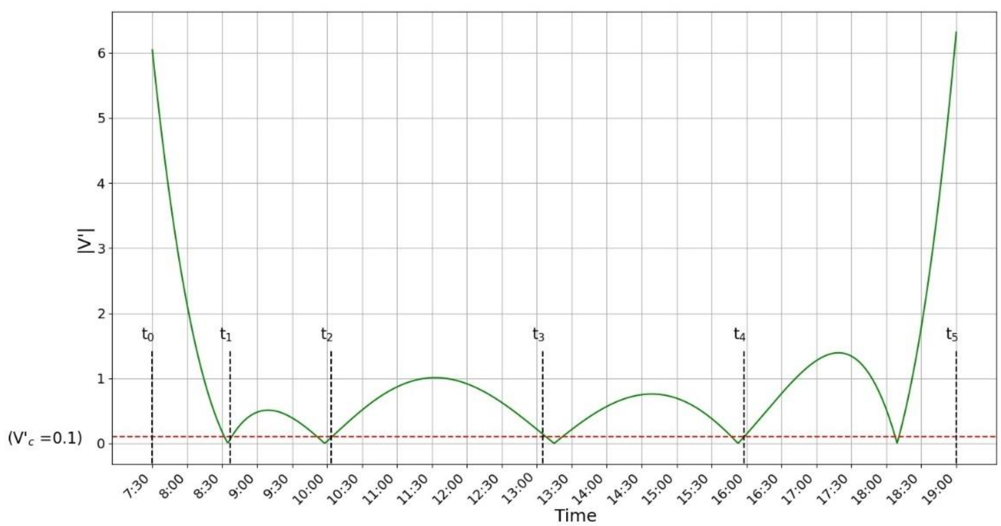

Figure 84: $V'(t)_{critical}$ = 0.1, Breakpoint Set 15

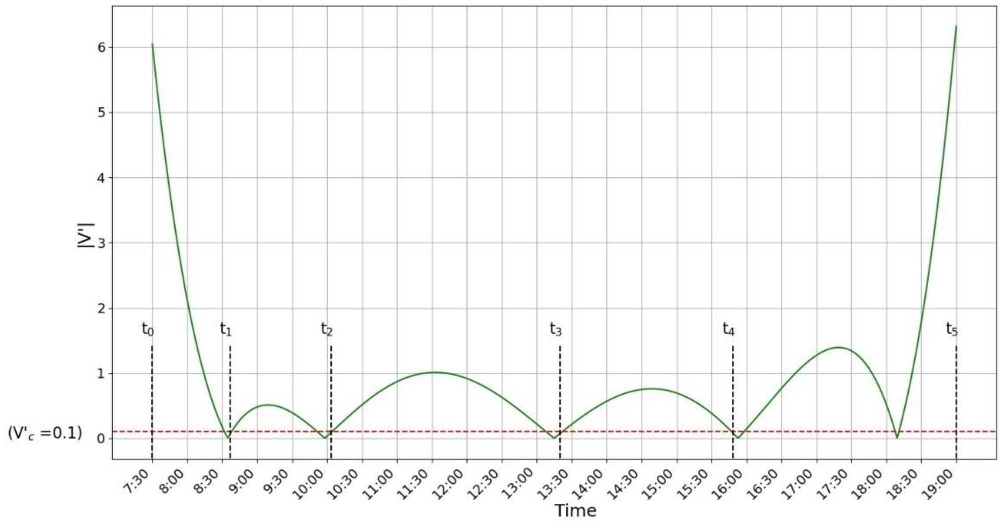

Figure 85: $V'(t)_{critical}$ = 0.1, Breakpoint Set 16

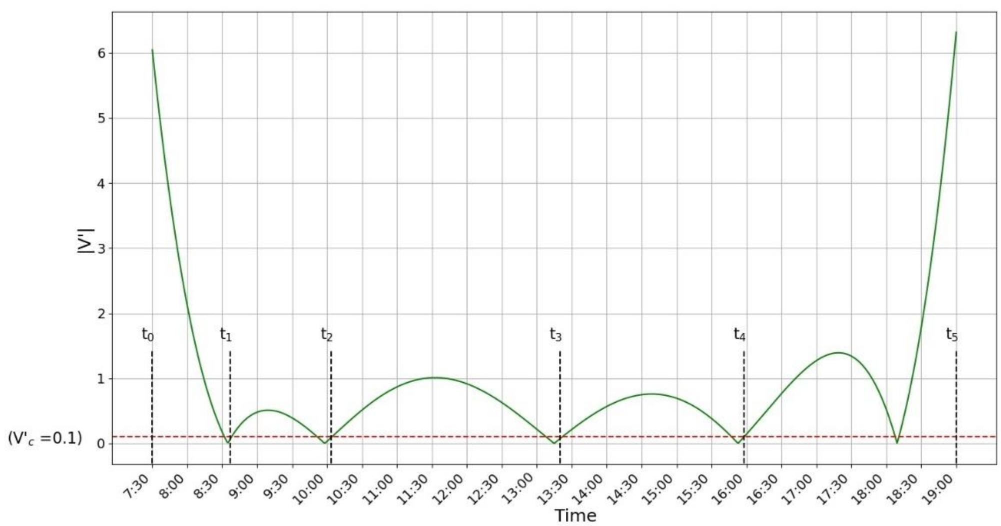

Figure 86: $V'(t)_{critical}$ = 0.1, Breakpoint Set 17

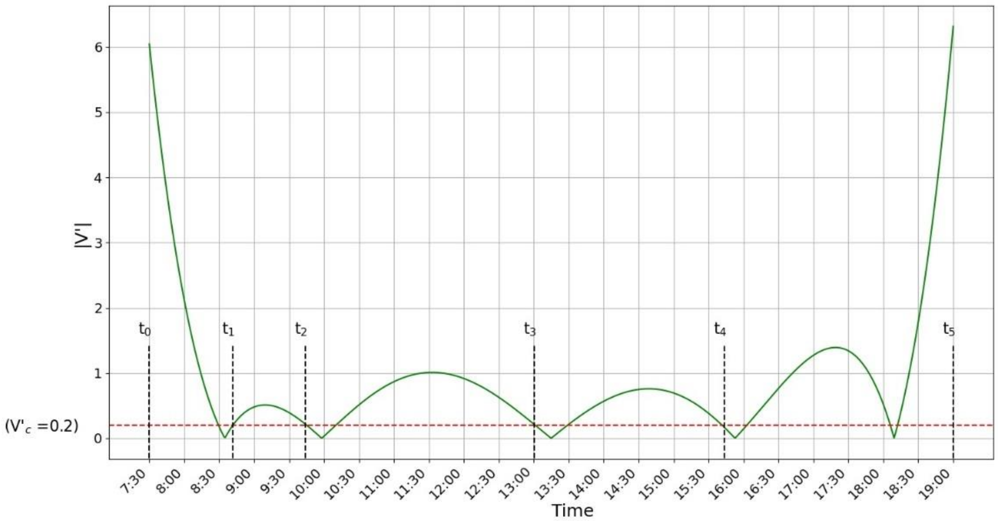

Figure 87: $V'(t)_{critical}$ = 0.2, Breakpoint Set 1

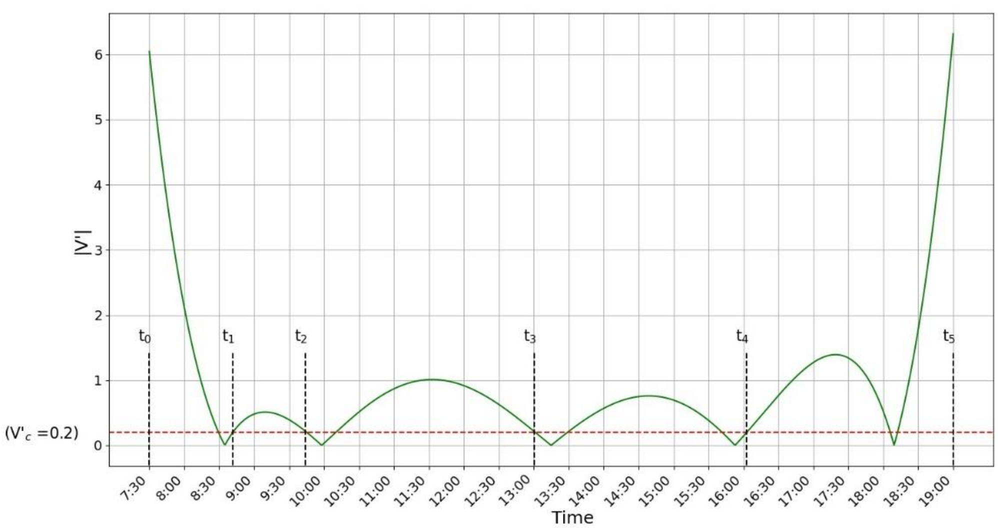

Figure 88: $V'(t)_{critical}$ = 0.2, Breakpoint Set 2

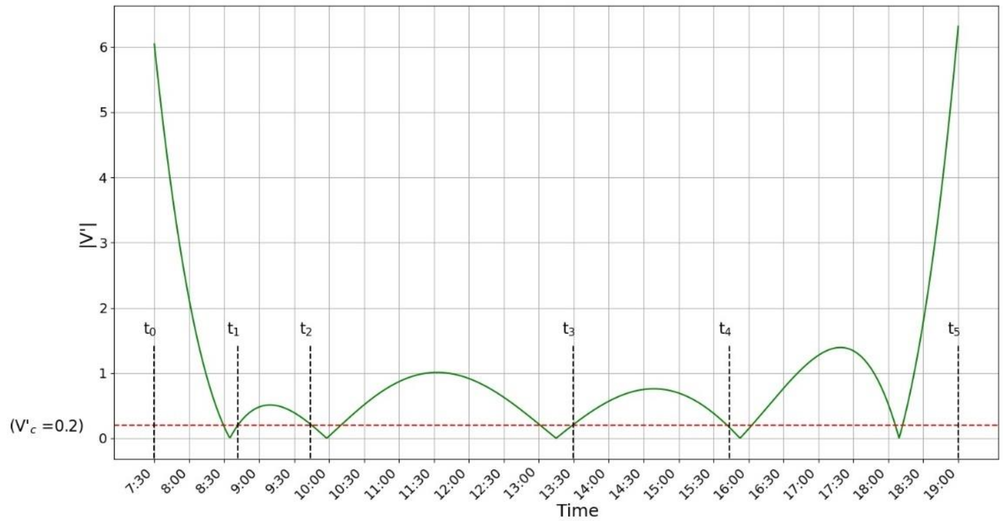

Figure 89: $V'(t)_{critical}$ = 0.2, Breakpoint Set 3

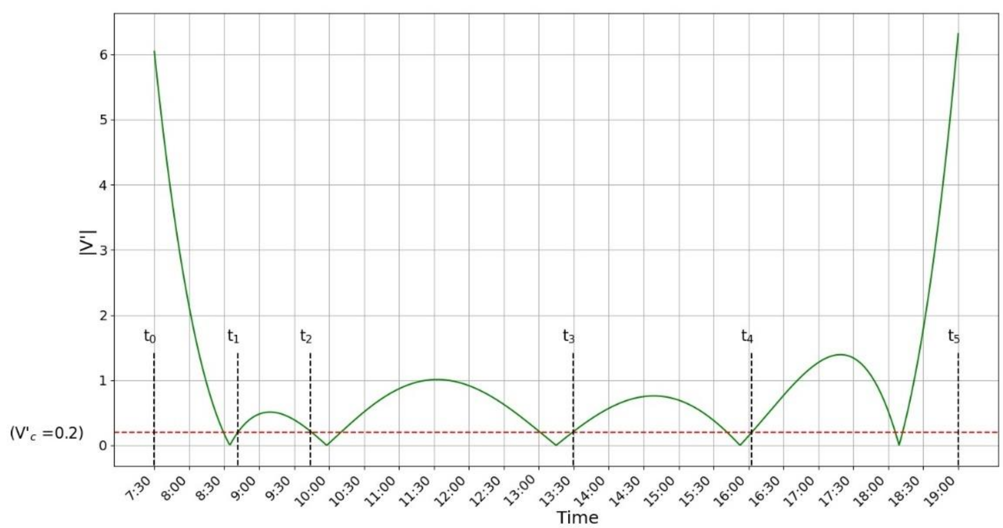

Figure 90: $V'(t)_{critical}$ = 0.2, Breakpoint Set 4

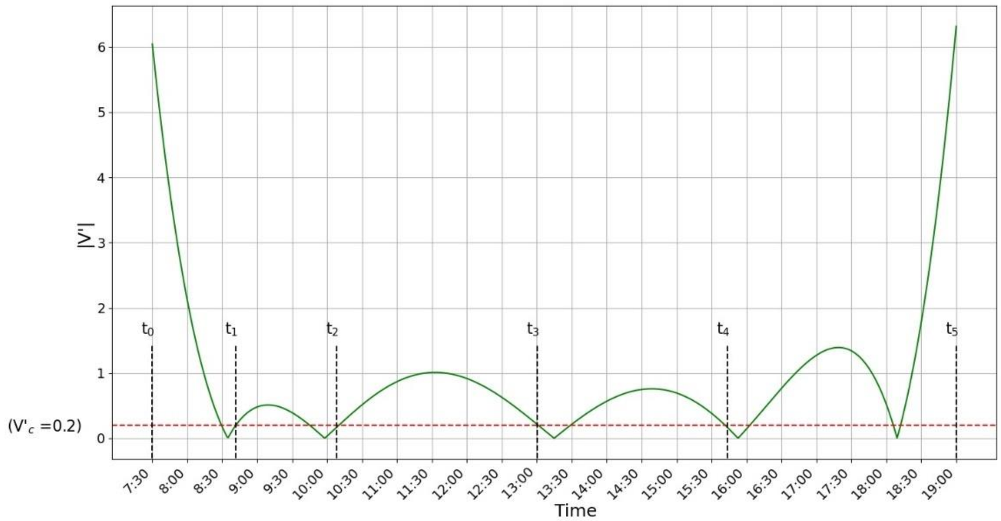

Figure 91: $V'(t)_{critical}$ = 0.2, Breakpoint Set 5

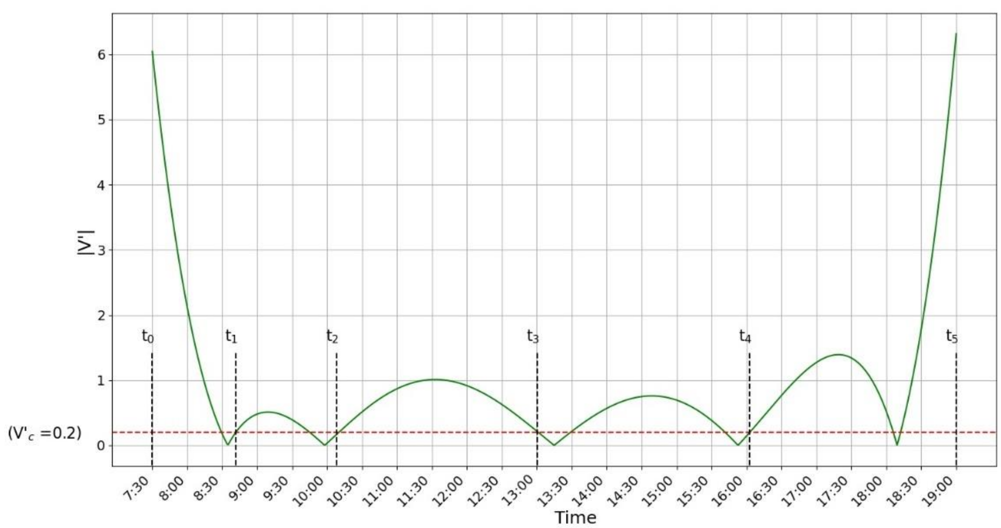

Figure 92: $V'(t)_{critical}$ = 0.2, Breakpoint Set 6

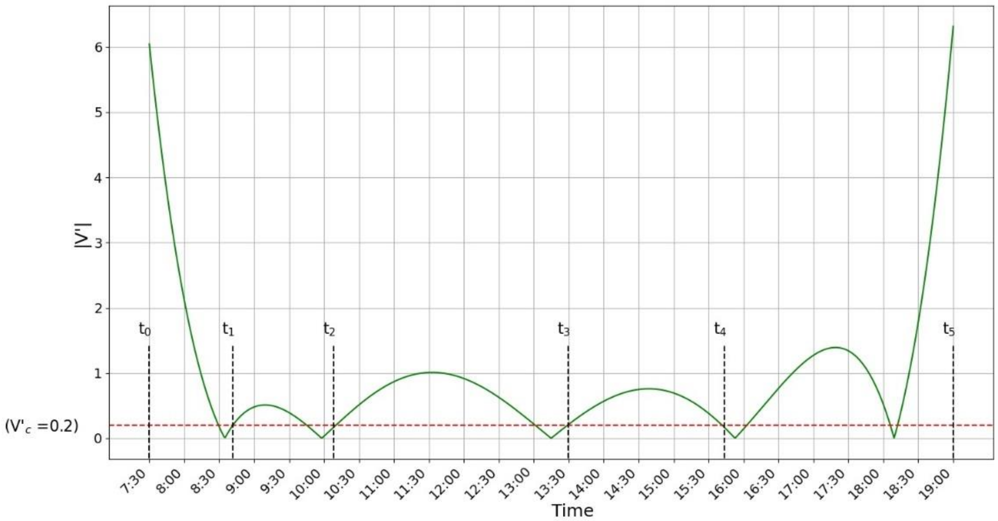

Figure 93: $V'(t)_{critical}$ = 0.2, Breakpoint Set 7

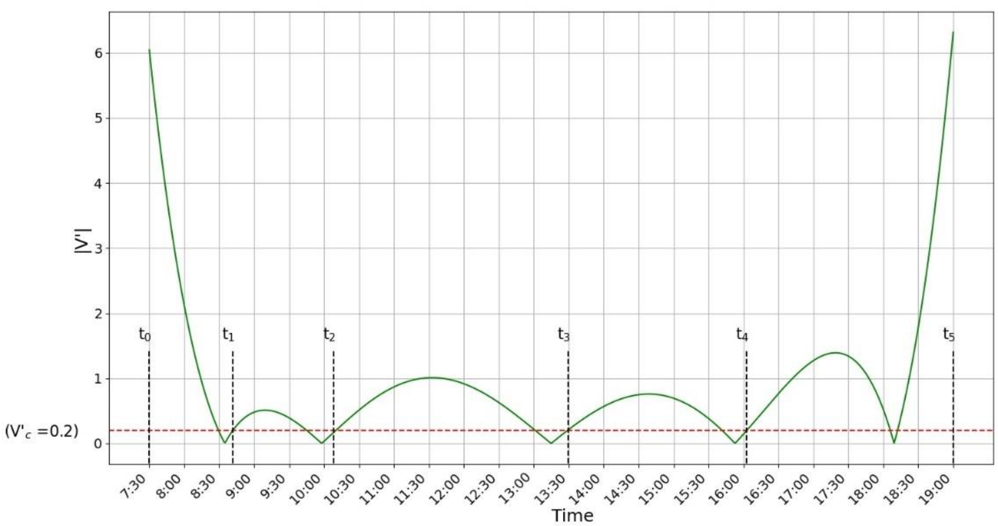

Figure 94: $V'(t)_{critical}$ = 0.2, Breakpoint Set 8

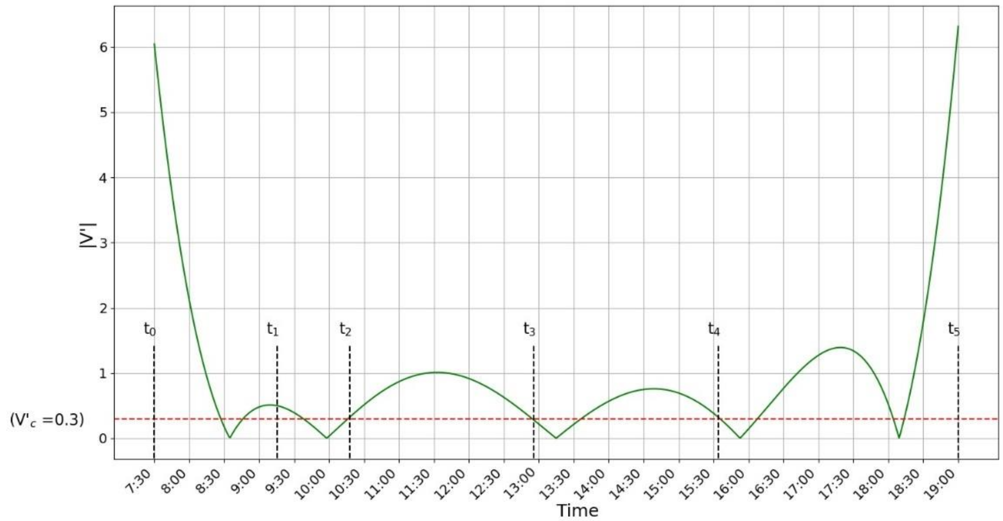

Figure 95: $V'(t)_{critical}$ = 0.3, Breakpoint Set 1

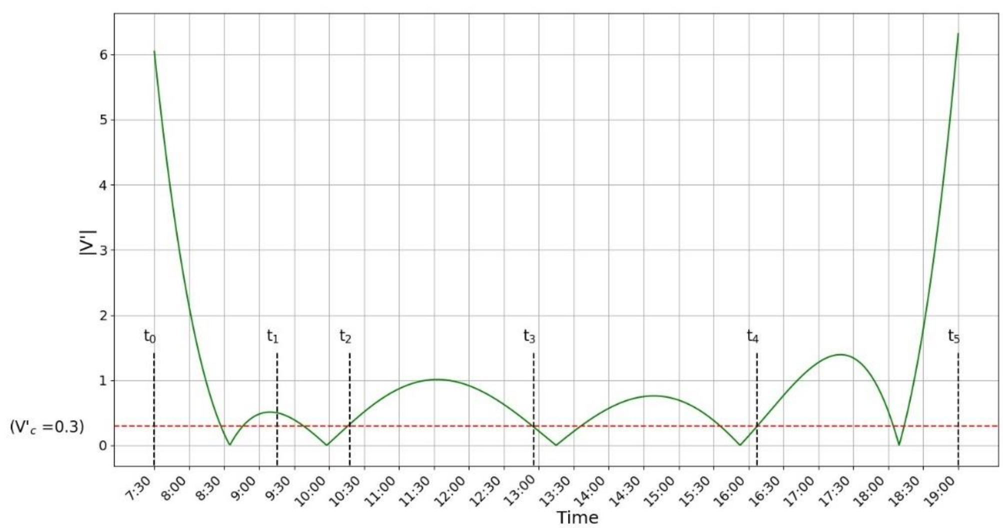

Figure 96: $V'(t)_{critical}$ = 0.3, Breakpoint Set 2

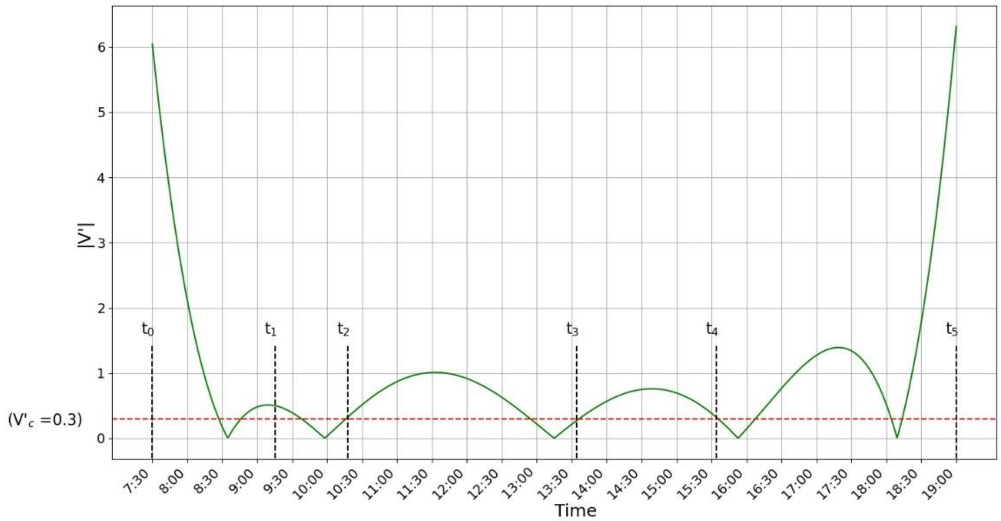

Figure 97: $V'(t)_{critical}$ = 0.3, Breakpoint Set 3

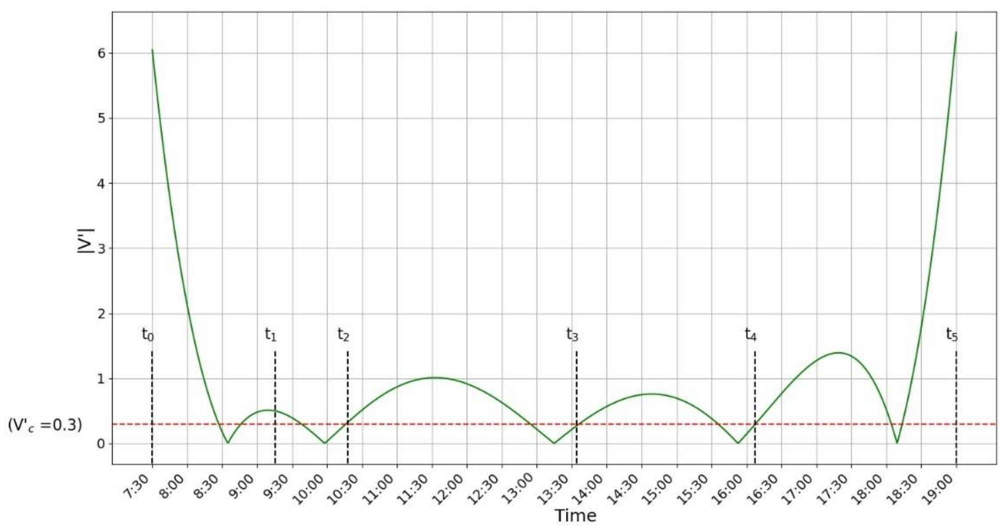

Figure 98: $V'(t)_{critical}$ = 0.3, Breakpoint Set 4

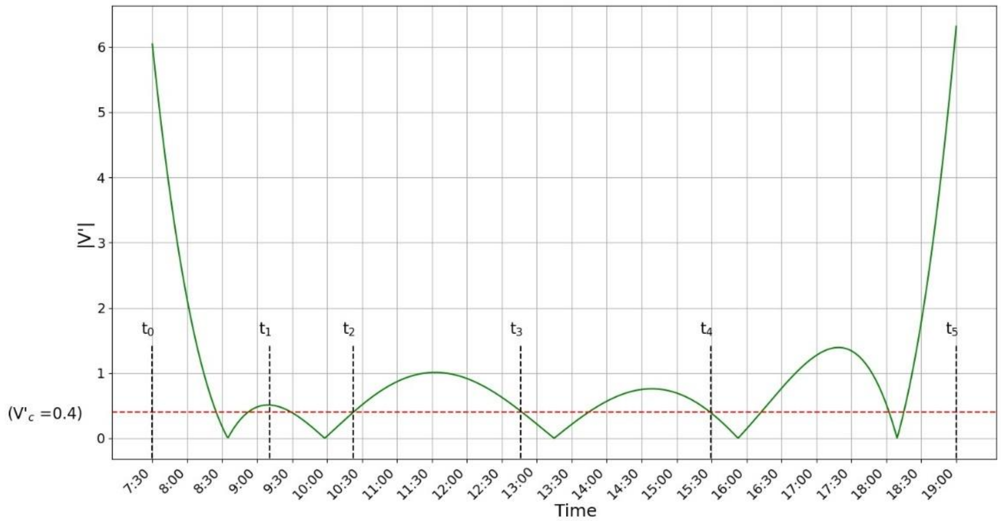

Figure 99: $V'(t)_{critical}$ = 0.4, Breakpoint Set 1

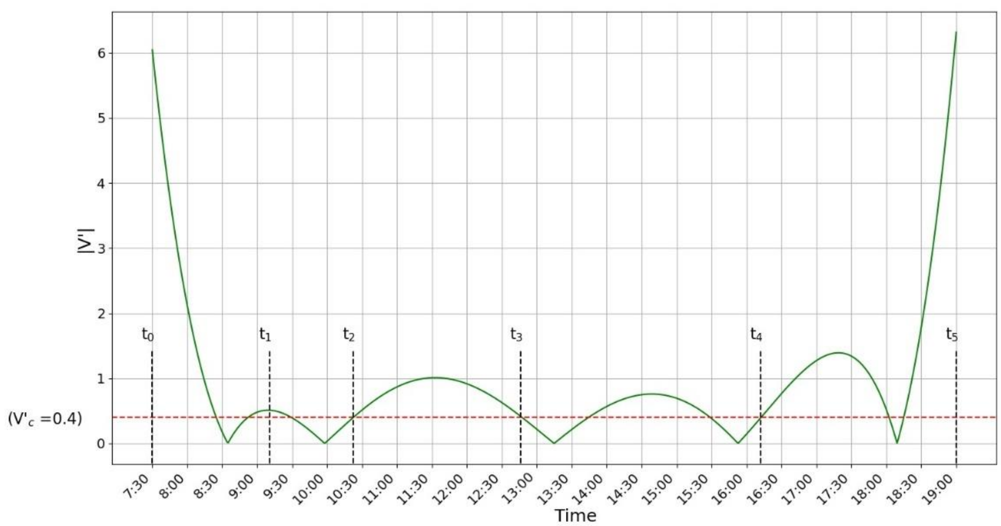

Figure 100: $V'(t)_{critical}$ = 0.4, Breakpoint Set 2

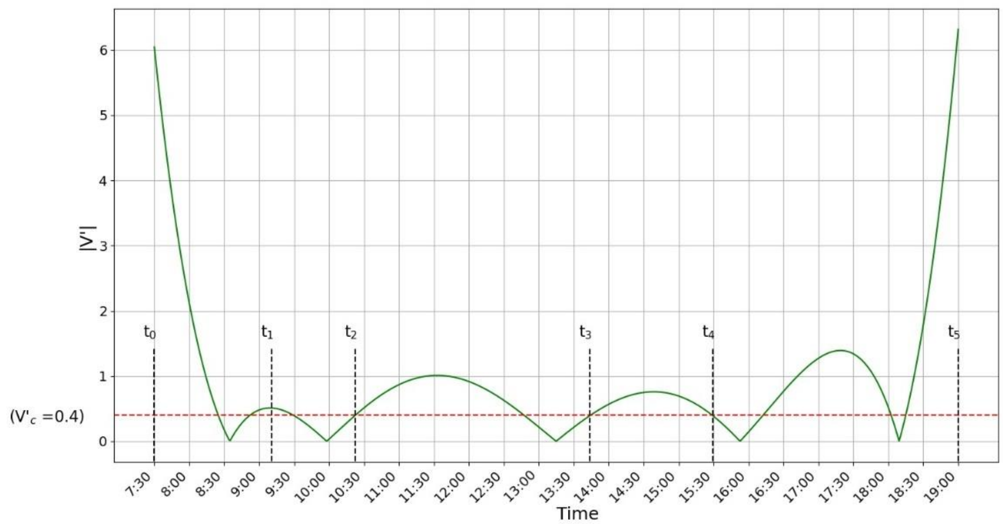

Figure 101: $V'(t)_{critical}$ = 0.4, Breakpoint Set 3

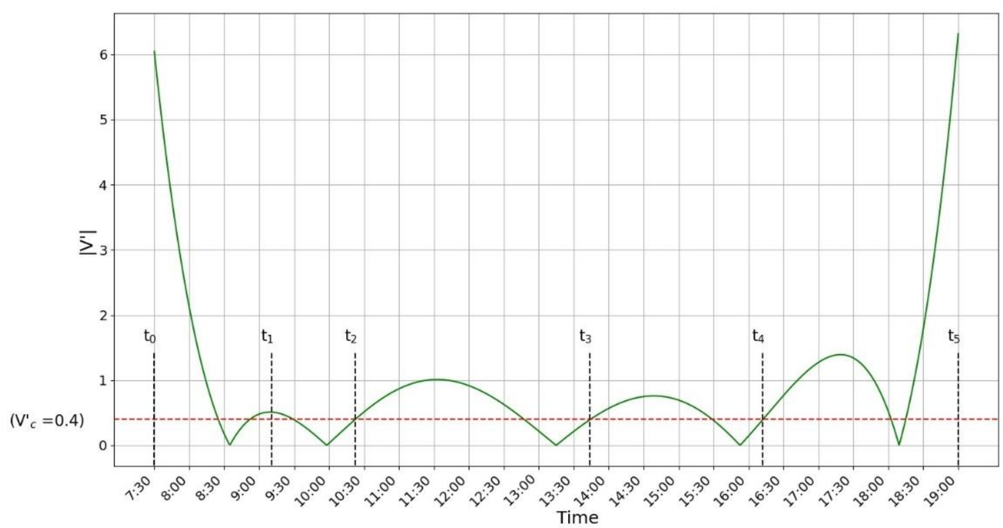

Figure 102: $V'(t)_{critical}$ = 0.4, Breakpoint Set 4

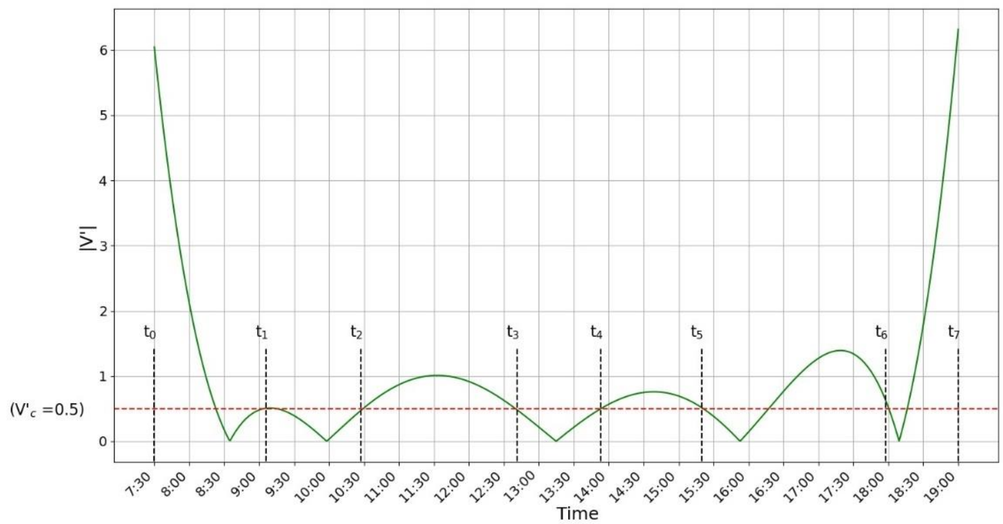

Figure 103: $V'(t)_{critical}$ = 0.5, Breakpoint Set 1

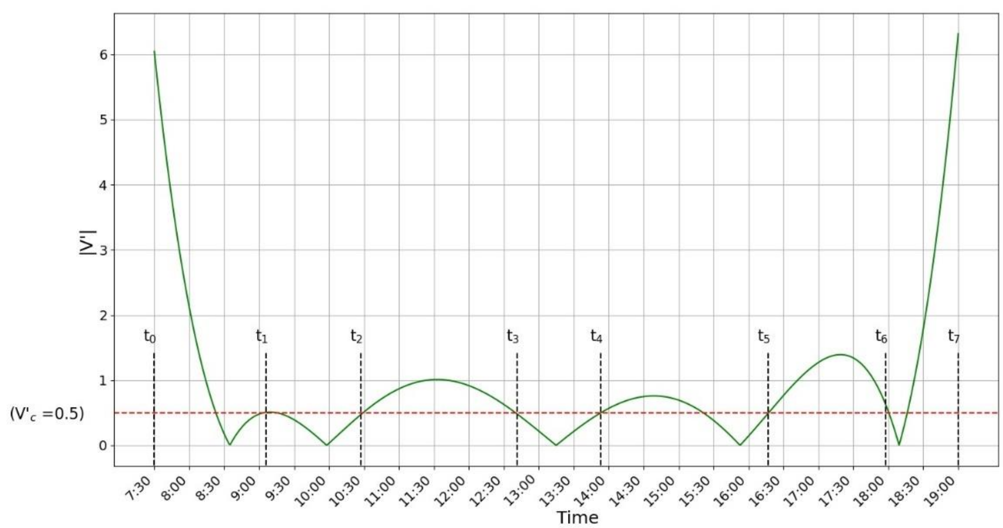

Figure 104: $V'(t)_{critical}$ = 0.5, Breakpoint Set 2

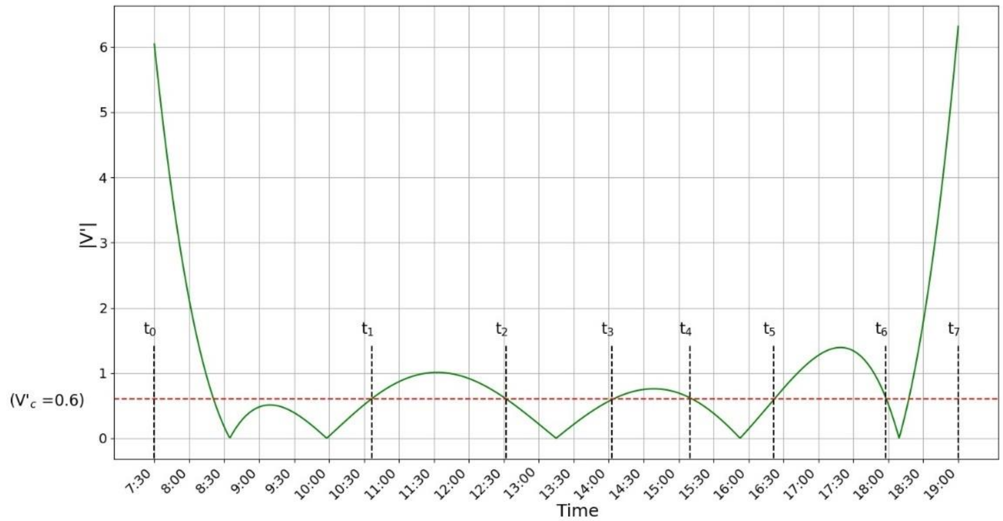

Figure 105: $V'(t)_{critical}\ =\ 0.6$

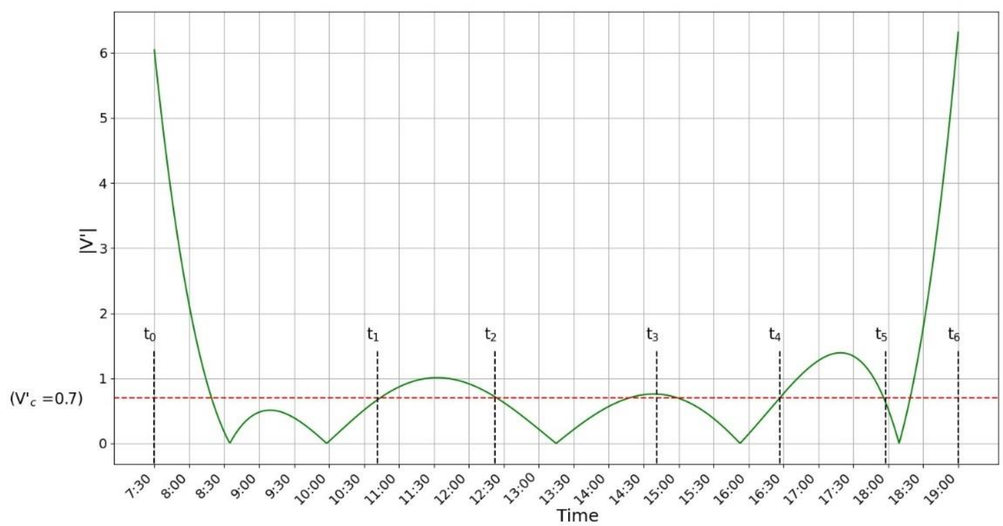

Figure 106: $V'(t)_{critical}\ = 0.7$

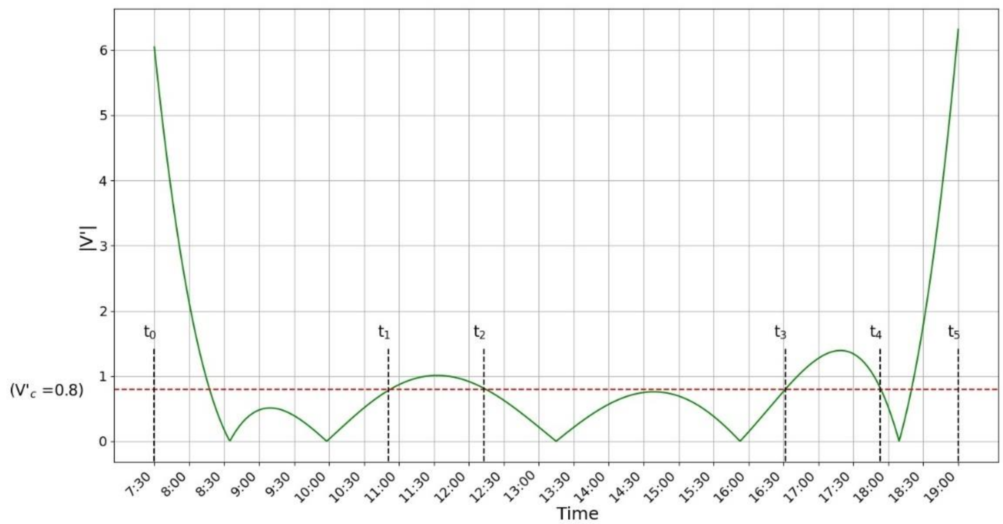

Figure 107: $V'(t)_{critical}$ = 0.8

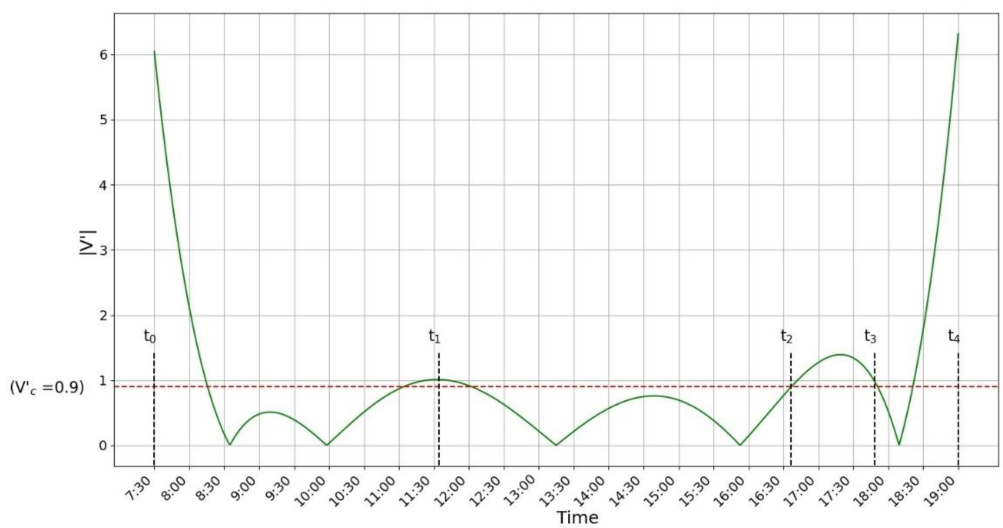

Figure 108: $V'(t)_{critical}$ = 0.9

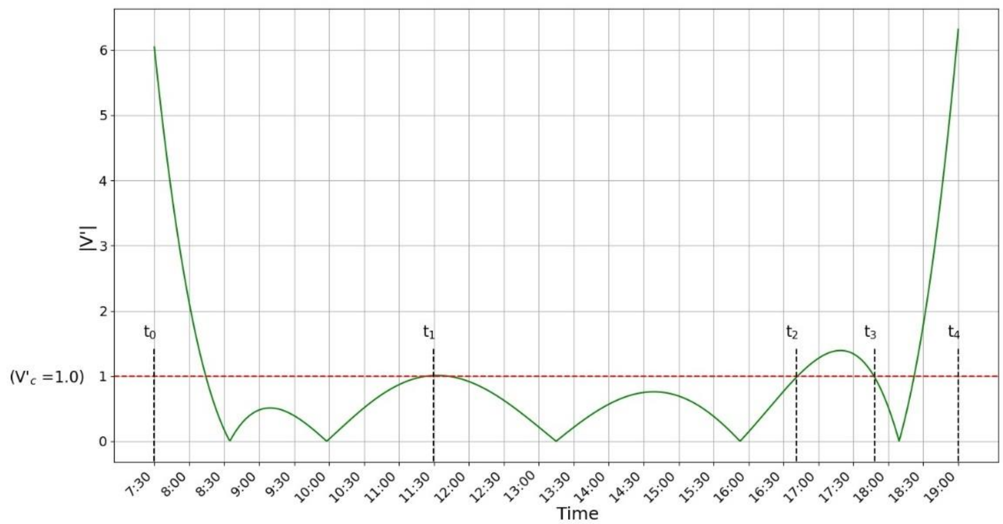

Figure 109: $V'(t)_{critical}$ = 1.0

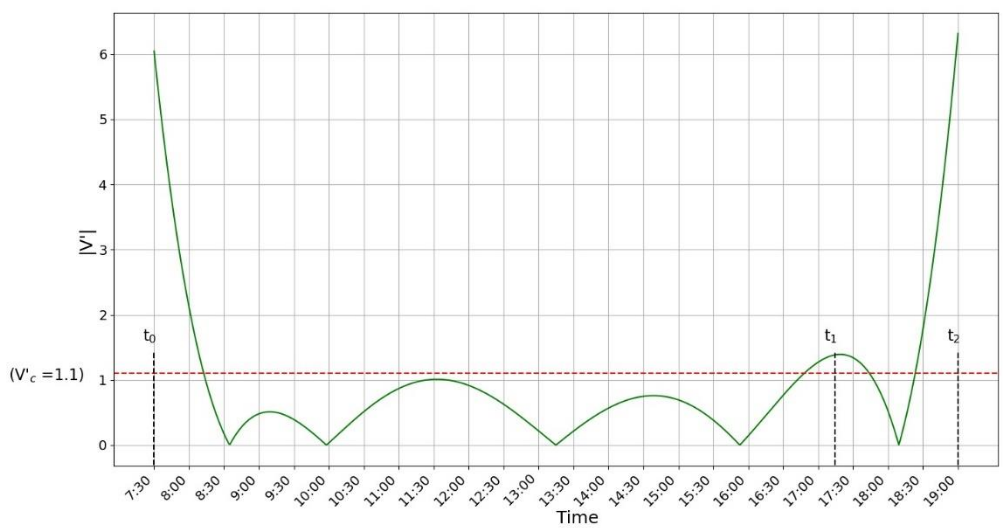

Figure 110: $V'(t)_{critical}$ = 1.1

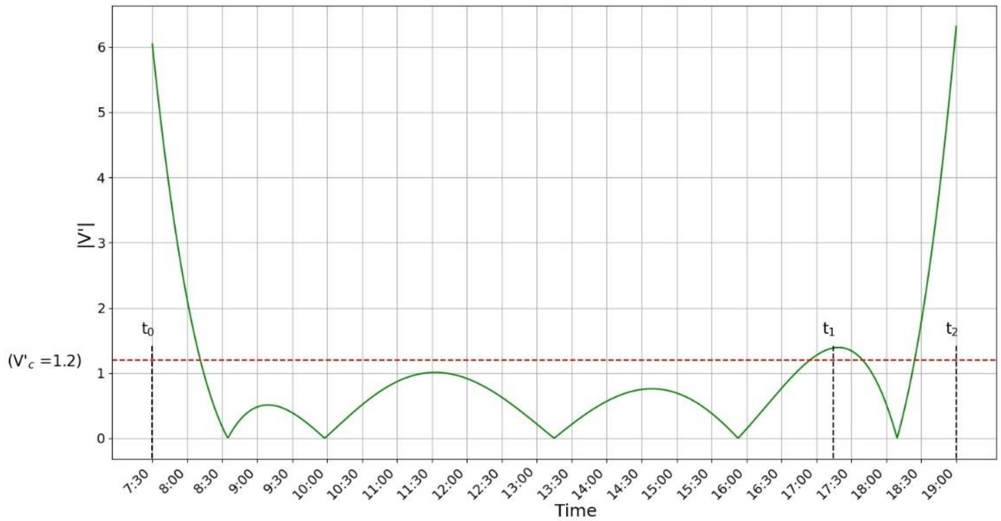

Figure 111: $V'(t)_{critical}$ = 1.2

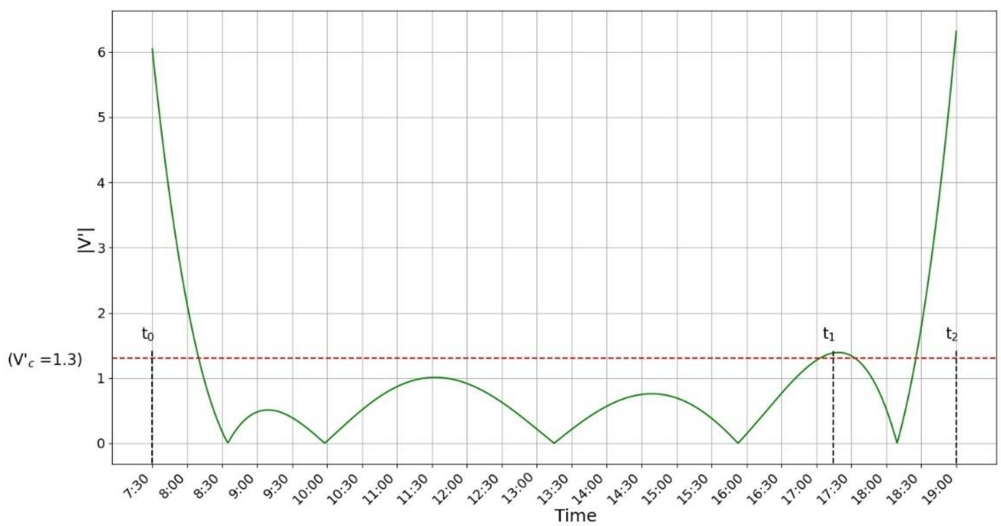

Figure 112: $V'(t)_{critical}$ = 1.3

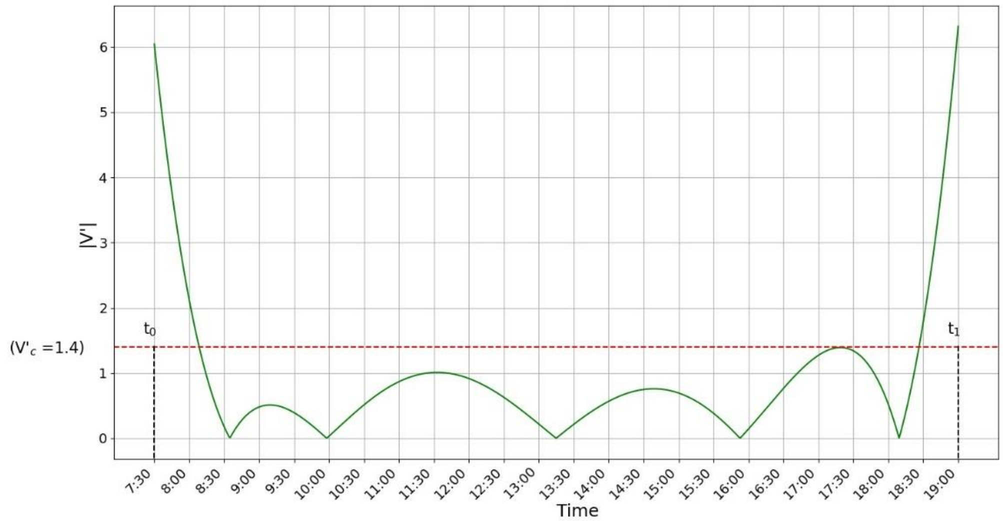

Figure 113: $V'(t)_{critical}$ = 1.4

Table 7 includes the developed breakpoints along with the values of delay and the figure number of each set of timing plan breakpoints.

Table 7: Results of the Critical Zone Optimization Method

$V'(t)_{critical}$	Start time	End time	Total Delay (sec)	Figure Number
0	07:00	08:30	26.8	Figure 70
	08:30	10:00		
	10:00	13:15		
	13:15	16:00		
	16:00	19:00		
0.1	07:00	08:30	26.6	Figure 71
	08:30	09:50		
	09:50	13:05		
	13:05	15:50		
	15:50	19:00		
0.1	07:00	08:30	27.1	Figure 72
	08:30	09:50		
	09:50	13:05		
	13:05	16:00		
	16:00	19:00		
0.1	07:00	08:30	26.6	Figure 73
	08:30	09:50		
	09:50	13:20		
	13:20	15:50		
	15:50	19:00		
0.1	07:00	08:30	27.1	Figure 74
	08:30	09:50		
	09:50	13:20		
	13:20	16:00		
	16:00	19:00		
0.1	07:00	08:30	26.6	Figure 75
	08:30	10:05		
	10:05	13:05		
	13:05	15:50		
	15:50	19:00		
0.1	07:00	08:30	27.1	Figure 76
	08:30	10:05		
	10:05	13:05		
	13:05	16:00		
	16:00	19:00		
0.1	07:00	08:30	26.6	Figure 77

Table 7: Results of the Critical Zone Optimization Method (Continued)

$V'(t)_{critical}$	Start time	End time	Total Delay (sec)	Figure Number
	08:30	10:05		
	10:05	13:20		
	13:20	15:50		
	15:50	19:00		
0.1	07:00	08:30	27.1	Figure 78
	08:30	10:05		
	10:05	13:20		
	13:20	16:00		
	16:00	19:00		
0.1	07:00	08:35	26.6	Figure 79
	08:35	09:50		
	09:50	13:05		
	13:05	15:50		
	15:50	19:00		
0.1	07:00	08:35	27	Figure 80
	08:35	09:50		
	09:50	13:05		
	13:05	16:00		
	16:00	19:00		
0.1	07:00	08:35	26.5	Figure 81
	08:35	09:50		
	09:50	13:20		
	13:20	15:50		
	15:50	19:00		
0.1	07:00	08:35	27	Figure 82
	08:35	09:50		
	09:50	13:20		
	13:20	16:00		
	16:00	19:00		
0.1	07:00	08:35	26.7	Figure 83
	08:35	10:05		
	10:05	13:05		
	13:05	15:50		
	15:50	19:00		
0.1	07:00	08:35	27.2	Figure 84
	08:35	10:05		

Table 7: Results of the Critical Zone Optimization Method (Continued)

$V'(t)_{critical}$	Start time	End time	Total Delay (sec)	Figure Number
	10:05	13:05		
	13:05	16:00		
	16:00	19:00		
0.1	07:00	08:35	26.7	Figure 85
	08:35	10:05		
	10:05	13:20		
	13:20	15:50		
	15:50	19:00		
0.1	07:00	08:35	27.2	Figure 86
	08:35	10:05		
	10:05	13:20		
	13:20	16:00		
	16:00	19:00		
0.2	07:00	08:40	25.8	Figure 87
	08:40	09:45		
	09:45	13:00		
	13:00	15:45		
	15:45	19:00		
0.2	07:00	08:40	26	Figure 88
	08:40	09:45		
	09:45	13:00		
	13:00	16:05		
	16:05	19:00		
0.2	07:00	08:40	25.8	Figure 89
	08:40	09:45		
	09:45	13:30		
	13:30	15:45		
	15:45	19:00		
0.2	07:00	08:40	26	Figure 90
	08:40	09:45		
	09:45	13:30		
	13:30	16:05		
	16:05	19:00		
0.2	07:00	08:40	25.7	Figure 91
	08:40	10:10		
	10:10	13:00		

Table 7: Results of the Critical Zone Optimization Method (Continued)

$V'(t)_{critical}$	Start time	End time	Total Delay (sec)	Figure Number
	13:00	15:45		
	15:45	19:00		
0.2	07:00	08:40	25.9	Figure 92
	08:40	10:10		
	10:10	13:00		
	13:00	16:05		
	16:05	19:00		
0.2	07:00	08:40	25.6	Figure 93
	08:40	10:10		
	10:10	13:30		
	13:30	15:45		
	15:45	19:00		
0.2	07:00	08:40	25.9	Figure 94
	08:40	10:10		
	10:10	13:30		
	13:30	16:05		
	16:05	19:00		
0.3	07:00	09:15	26.5	Figure 95
	09:15	10:20		
	10:20	13:00		
	13:00	15:35		
	15:35	19:00		
0.3	07:00	09:15	26.4	Figure 96
	09:15	10:20		
	10:20	13:00		
	13:00	16:10		
	16:10	19:00		
0.3	07:00	09:15	26.8	Figure 97
	09:15	10:20		
	10:20	13:35		
	13:35	15:35		
	15:35	19:00		
0.3	07:00	09:15	26.7	Figure 98
	09:15	10:20		
	10:20	13:35		
	13:35	16:10		

Table 7: Results of the Critical Zone Optimization Method (Continued)

$V'(t)_{critical}$	Start time	End time	Total Delay (sec)	Figure Number
	16:10	19:00		
0.4	07:00	09:10	25.1	Figure 99
	09:10	10:20		
	10:20	12:45		
	12:45	15:30		
	15:30	19:00		
0.4	07:00	09:10	25.8	Figure 100
	09:10	10:20		
	10:20	12:45		
	12:45	16:10		
	16:10	19:00		
0.4	07:00	09:10	25.8	Figure 101
	09:10	10:20		
	10:20	13:45		
	13:45	15:30		
	15:30	19:00		
0.4	07:00	09:10	26.5	Figure 102
	09:10	10:20		
	10:20	13:45		
	13:45	16:10		
	16:10	19:00		
0.5	07:00	09:05	22.7	Figure 103
	09:05	10:25		
	10:25	12:40		
	12:40	14:00		
	14:00	15:20		
	15:20	18:00		
	18:00	19:00		
0.5	07:00	09:05	22.6	Figure 104
	09:05	10:25		
	10:25	12:40		
	12:40	14:00		
	14:00	16:15		
	16:15	18:00		
	18:00	19:00		
0.6	07:00	10:35	21.4	Figure 105

Table 7: Results of the Critical Zone Optimization Method (Continued)

$V'(t)_{critical}$	Start time	End time	Total Delay (sec)	Figure Number
	10:35	12:30		
	12:30	14:05		
	14:05	15:10		
	15:10	16:20		
	16:20	18:00		
	18:00	19:00		
0.7	07:00	10:40	23.1	Figure 106
	10:40	12:20		
	12:20	14:40		
	14:40	16:25		
	16:25	18:00		
	18:00	19:00		
0.8	07:00	10:50	23.6	Figure 107
	10:50	12:15		
	12:15	16:30		
	16:30	18:00		
	18:00	19:00		
0.9	07:00	11:35	24.5	Figure 108
	11:35	16:35		
	16:35	17:50		
	17:50	19:00		
1	07:00	11:30	25	Figure 109
	11:30	16:40		
	16:40	17:50		
	17:50	19:00		
1.1	07:00	17:15	32.8	Figure 110
	17:15	19:00		
1.2	07:00	17:15	32.8	Figure 111
	17:15	19:00		
1.3	07:00	17:15	32.8	Figure 112
	17:15	19:00		
1.4	07:00	19:00	41.3	Figure 113

ΔV Optimization Method:

Figure 114 to Figure 120 show the developed breakpoints by using the ΔV optimization method.

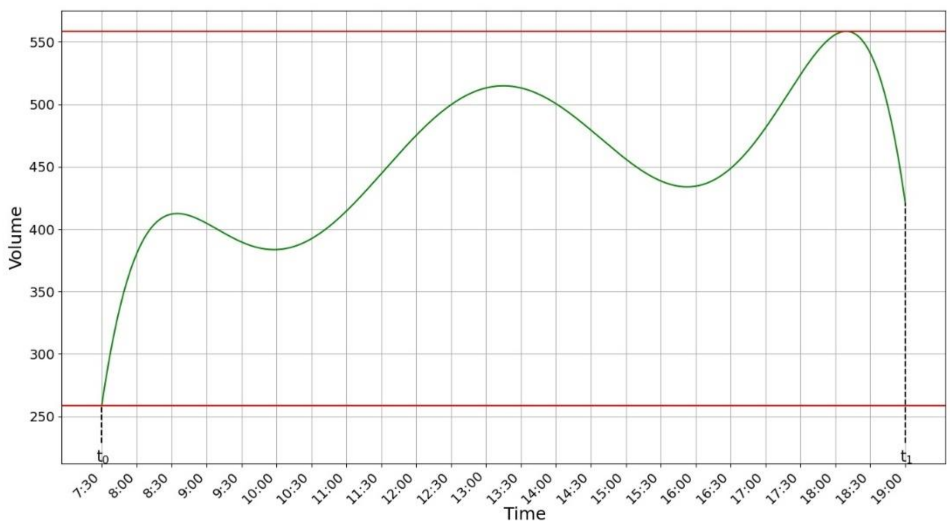

Figure 114: $\Delta V = Range/1$

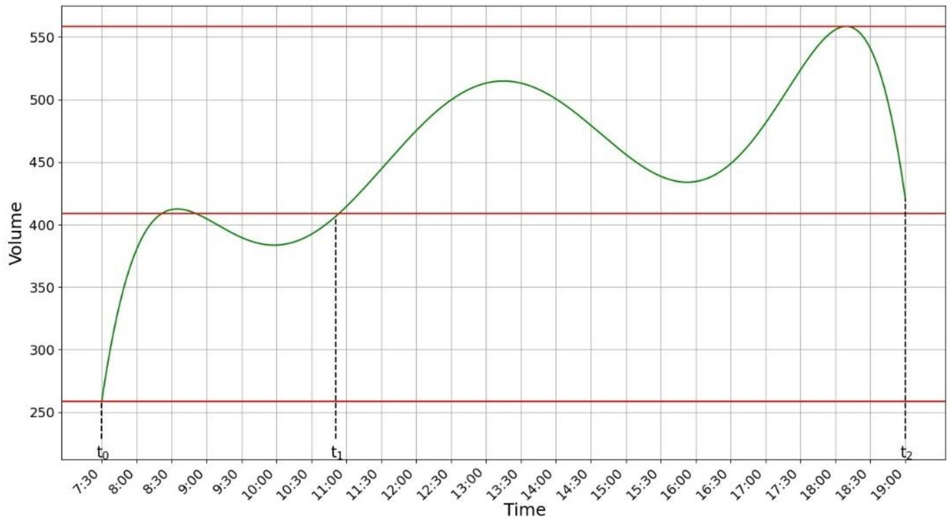

Figure 115: $\Delta V = Range/2$, Breakpoint Set 1

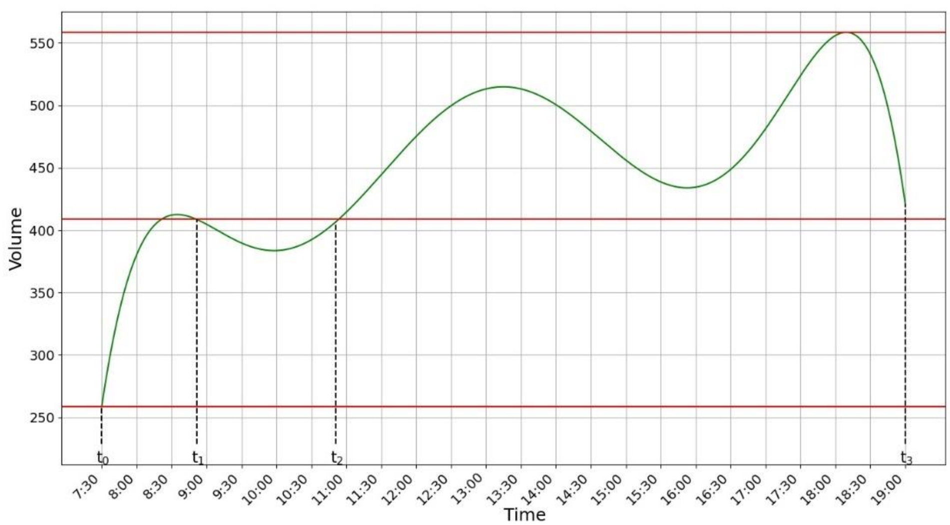

Figure 116: $\Delta V = Range/2$, Breakpoint Set 2

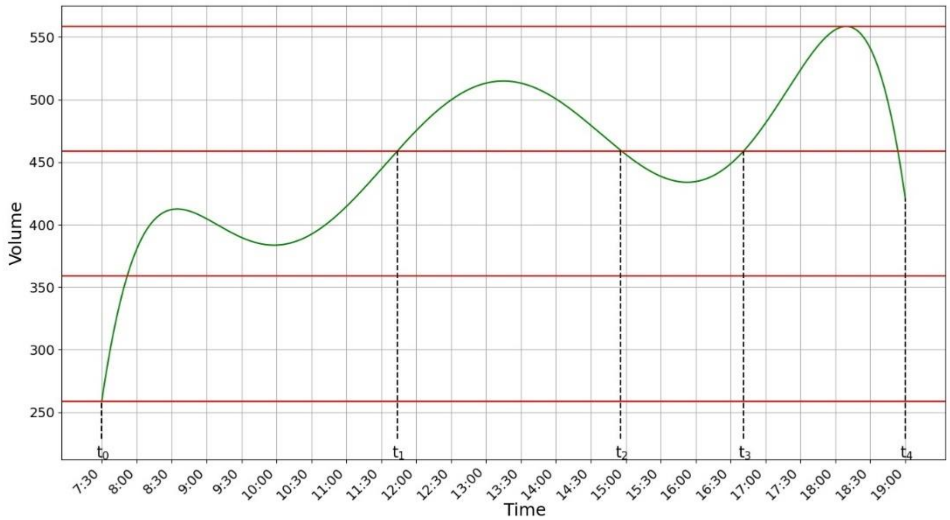

Figure 117: $\Delta V = Range/3$

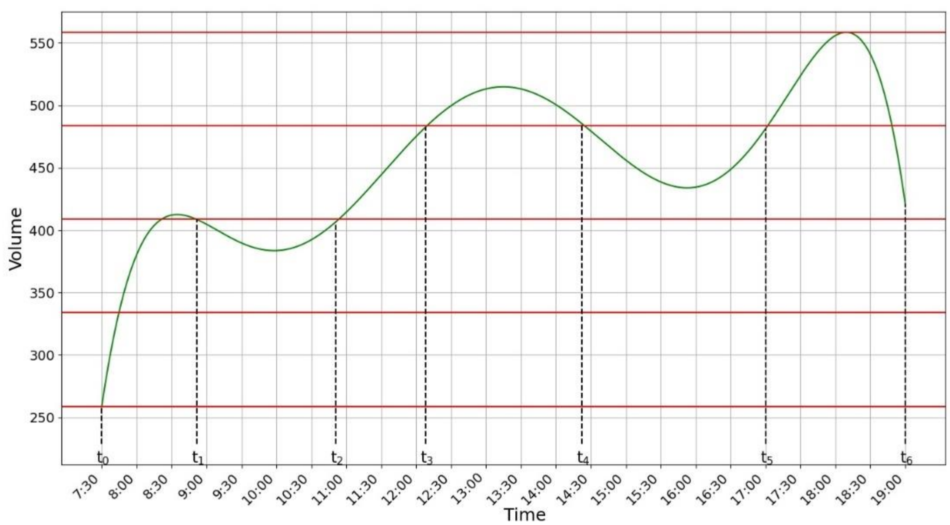

Figure 118: $\Delta V = Range/4$

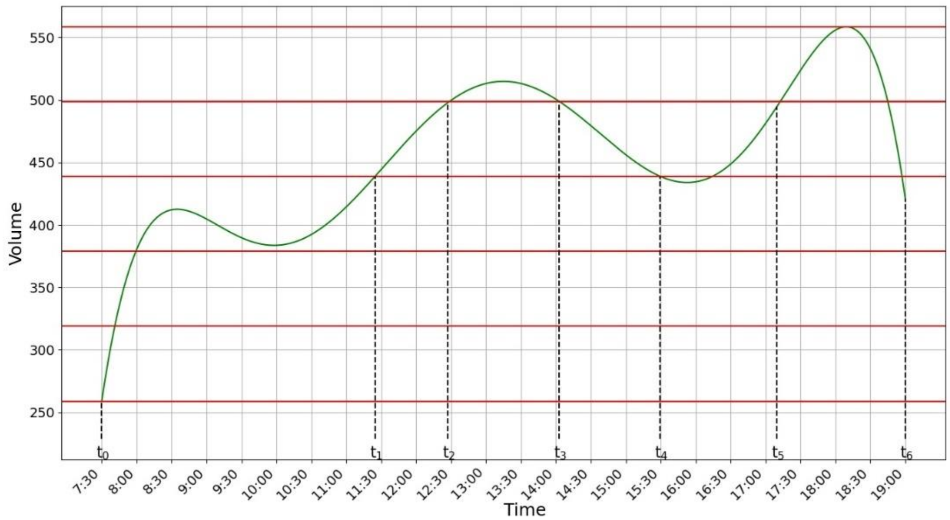

Figure 119: $\Delta V = Range/5$, Breakpoint Set 1

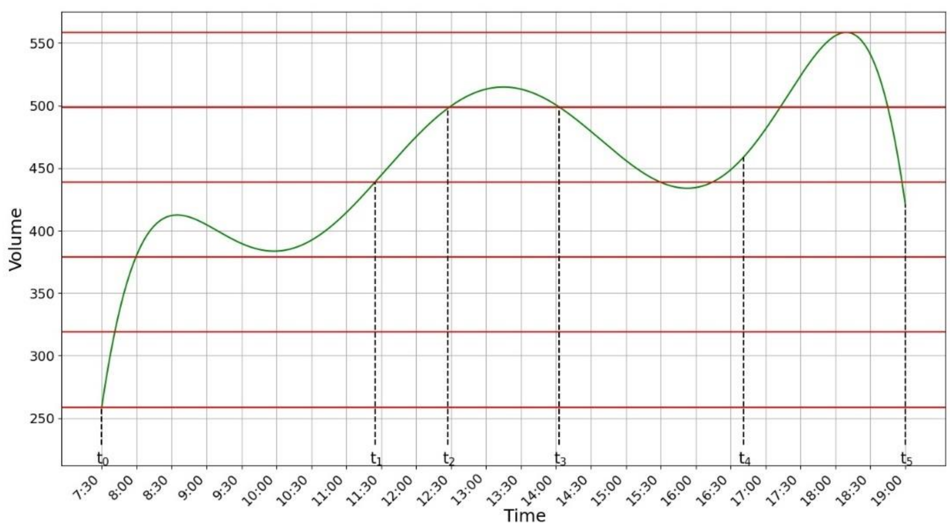

Figure 120: $\Delta V = Range/5$, Breakpoint Set 2

Table 8 includes the developed breakpoints along with the values of delay and the figure number of each set of timing plan breakpoints.

Table 8: Results of ΔV Optimization Method

ΔV	Start time	End time	Total Delay (sec/veh)	Figure Number
range/1	07:00	19:00	41.3	Figure 114
range/2	07:00	10:50	35.2	Figure 115
	10:50	19:00		
range/2	07:00	08:50	30	Figure 116
	08:50	10:50		
	10:50	19:00		
range/3	07:00	11:45	26.4	Figure 117
	11:45	15:00		
	15:00	16:40		
	16:40	19:00		
range/4	07:00	08:50	25.3	Figure 118
	08:50	10:50		
	10:50	12:10		
	12:10	14:20		
	14:20	17:00		
	17:00	19:00		
range/5	07:00	11:25	21.8	Figure 119
	11:25	12:25		
	12:25	14:05		
	14:05	15:30		
	15:30	17:10		
	17:10	19:00		
range/5	07:00	11:25	24	Figure 120
	11:25	12:25		
	12:25	14:05		
	14:05	16:40		
	16:40	19:00		

University Dr. and Texas Ave Intersection, Feb 13, 2019:

Below are the optimization results by using both of the developed optimization techniques for the traffic counts data of the intersection of University Dr. and Texas Ave. that were collected on February 13, 2019

Critical Zone Optimization Technique:

Figure 121 through Figure 167 show the developed breakpoints by using the critical zone optimization method.

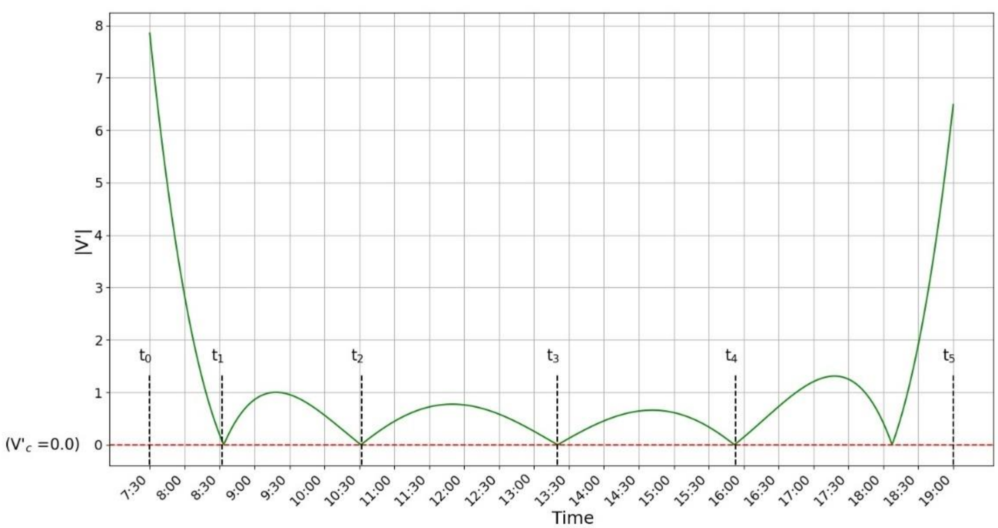

Figure 121: $V'(t)_{critical}$ = 0.0

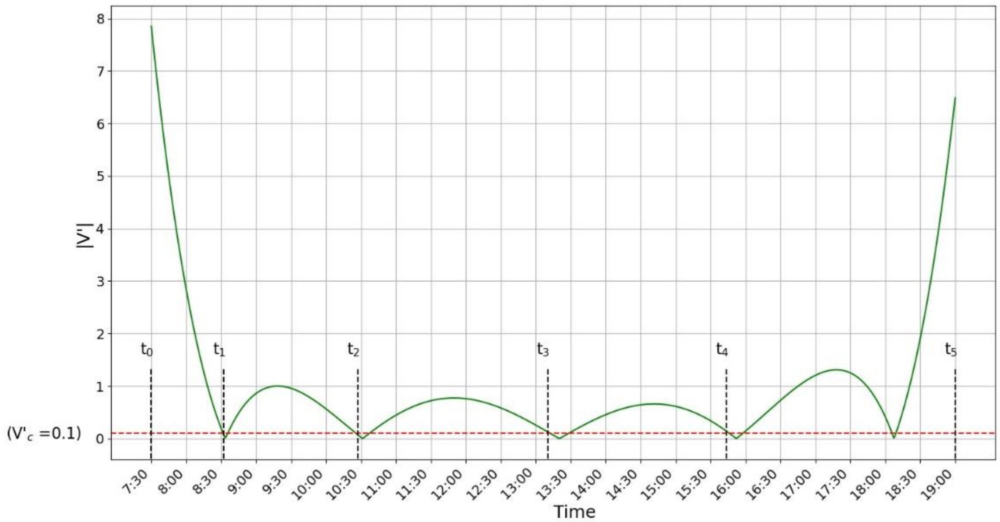

Figure 122: $V'(t)_{critical}$ = 0.1, Breakpoint Set 1

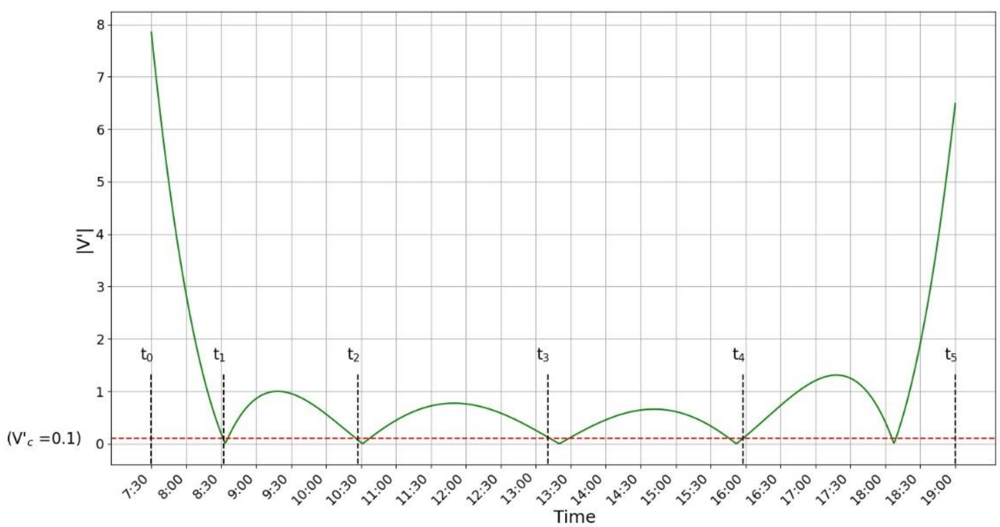

Figure 123: $V'(t)_{critical}$ = 0.1, Breakpoint Set 2

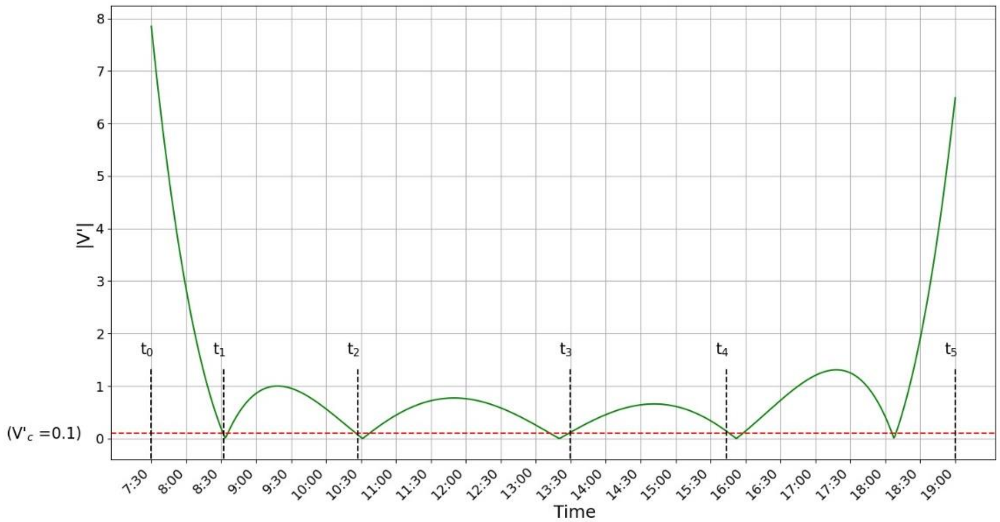

Figure 124: $V'(t)_{critical}$ = 0.1, Breakpoint Set 3

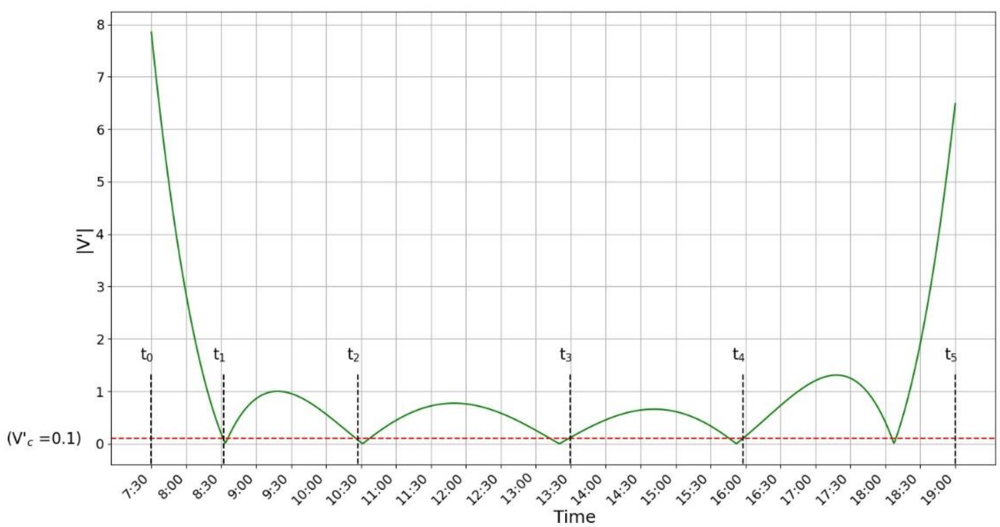

Figure 125: $V'(t)_{critical}$ = 0.1, Breakpoint Set 4

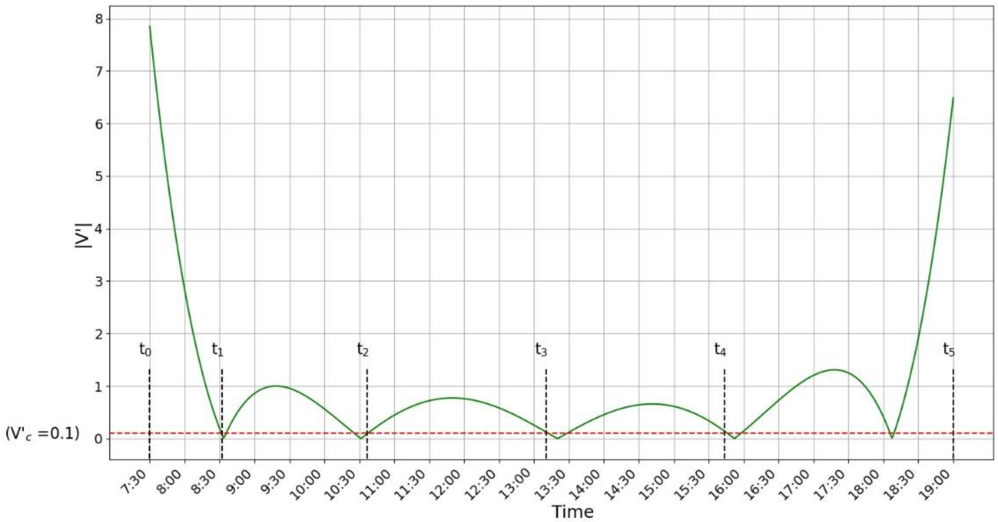

Figure 126: $V'(t)_{critical}$ = 0.1, Breakpoint Set 5

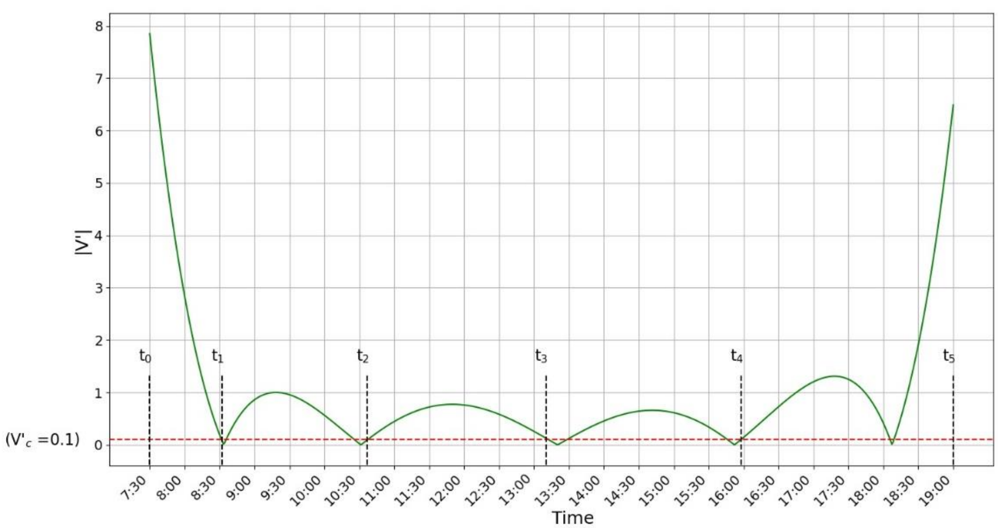

Figure 127: $V'(t)_{critical}$ = 0.1, Breakpoint Set 6

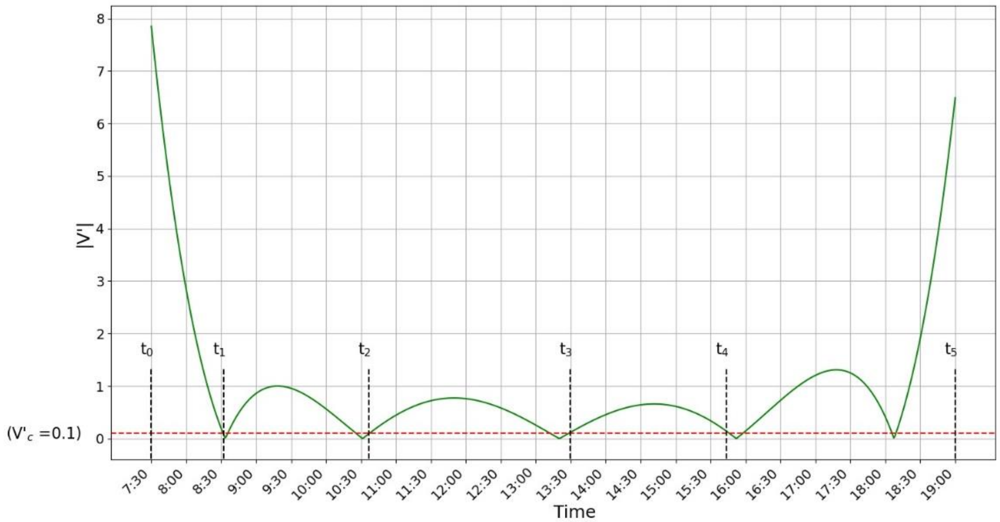

Figure 128: $V'(t)_{critical}$ = 0.1, Breakpoint Set 7

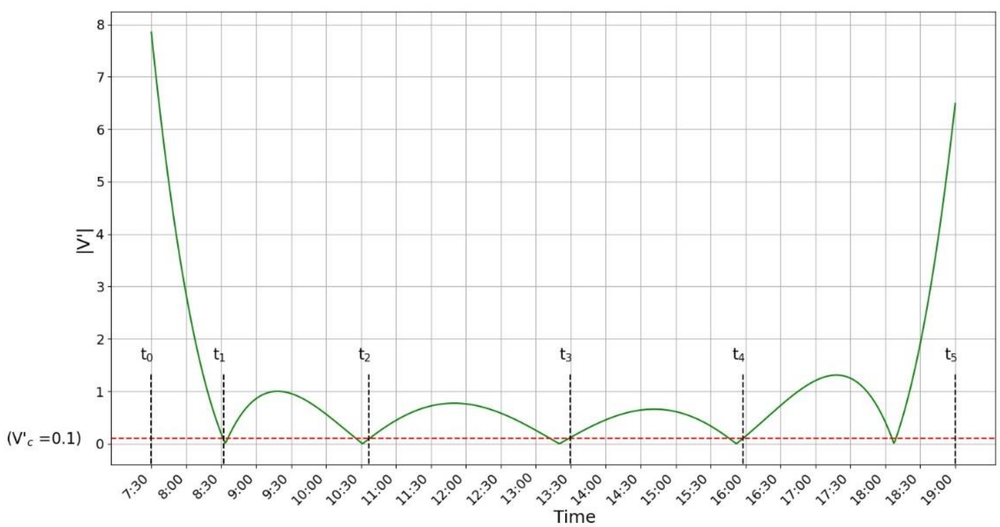

Figure 129: $V'(t)_{critical}$ = 0.1, Breakpoint Set 8

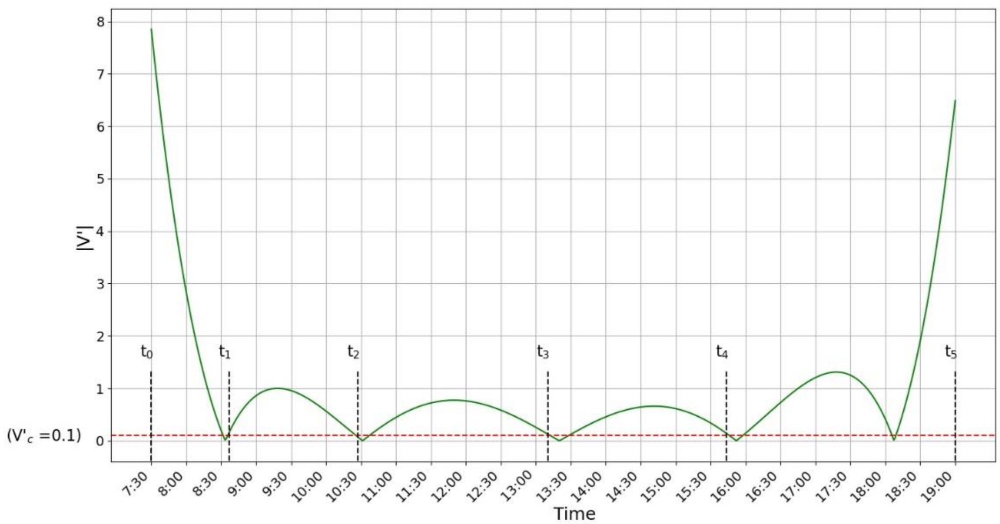

Figure 130: $V'(t)_{critical}$ = 0.1, Breakpoint Set 9

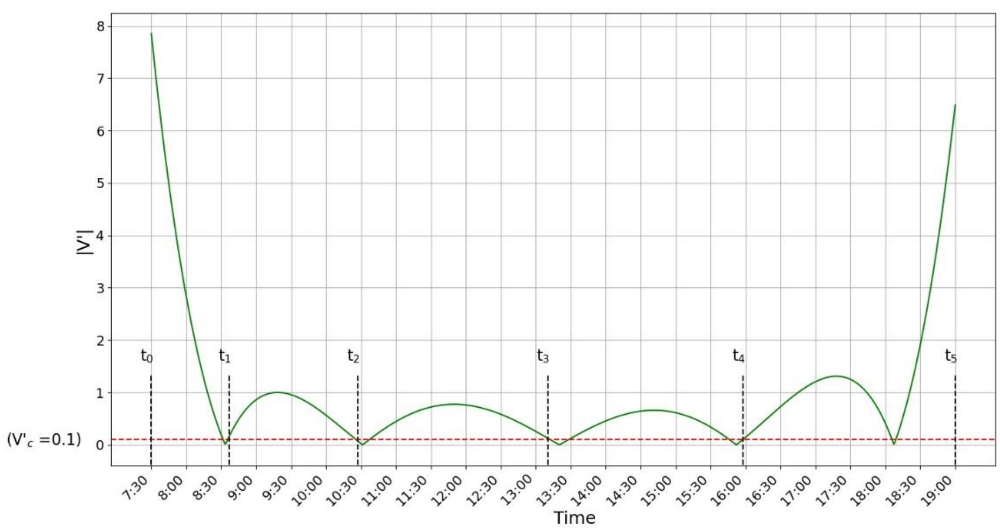

Figure 131: $V'(t)_{critical}$ = 0.1, Breakpoint Set 10

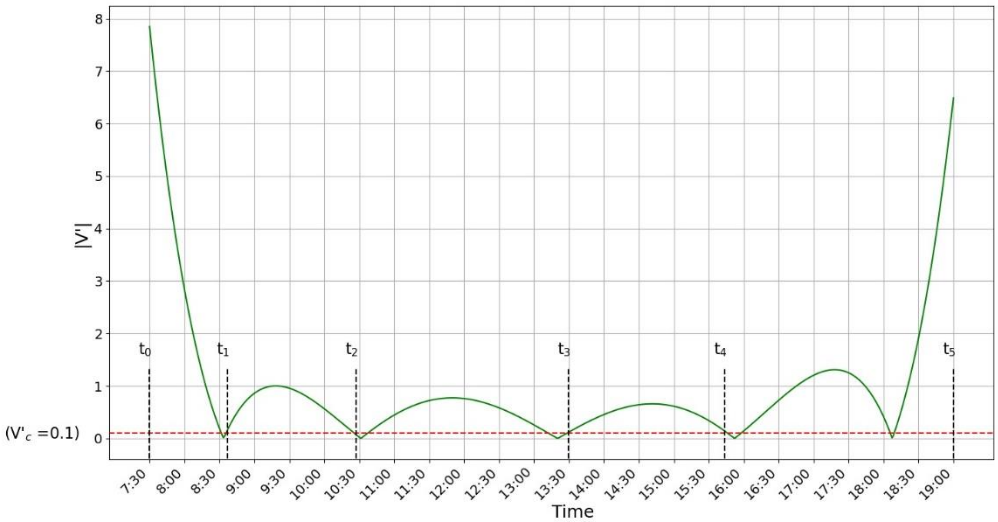

Figure 132: $V'(t)_{critical}$ = 0.1, Breakpoint Set 11

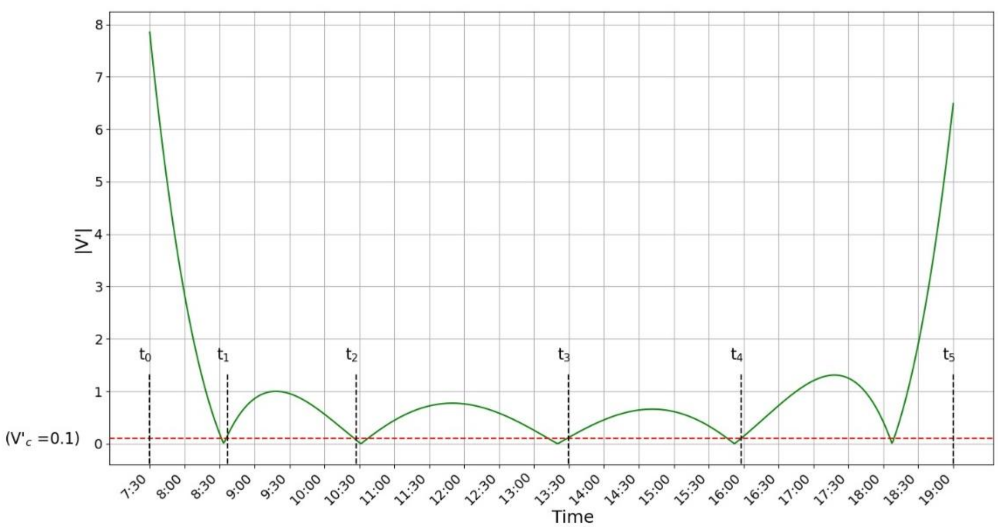

Figure 133: $V'(t)_{critical}$ = 0.1, Breakpoint Set 12

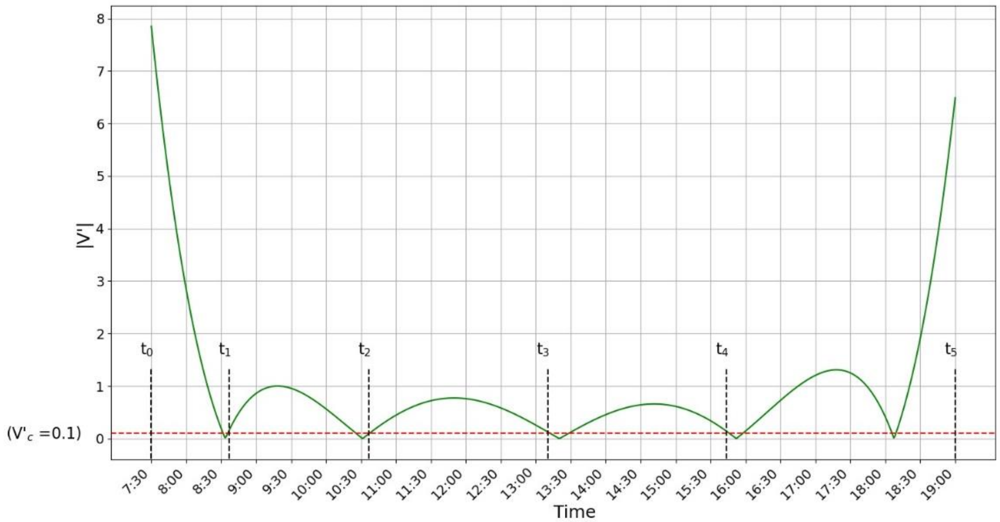

Figure 134: $V'(t)_{critical}$ = 0.1, Breakpoint Set 13

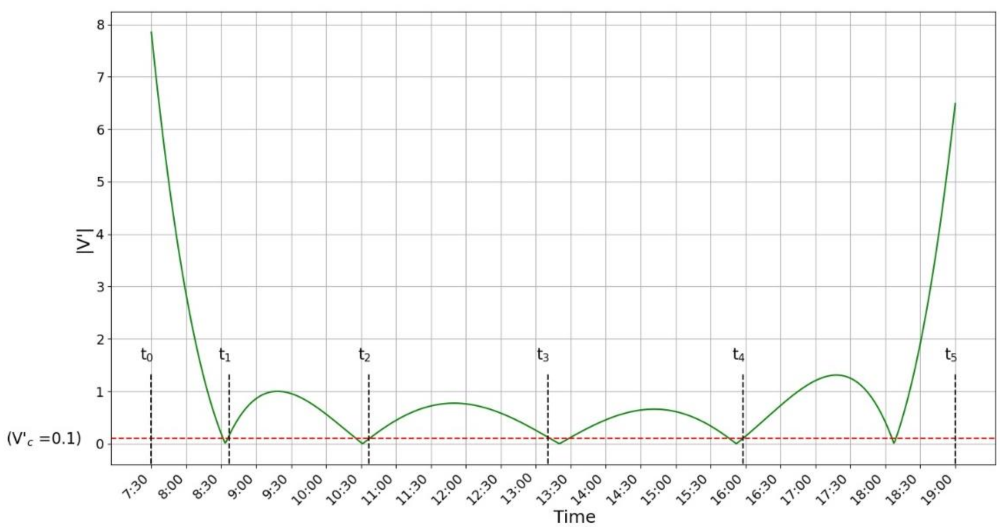

Figure 135: $V'(t)_{critical}$ = 0.1, Breakpoint Set 14

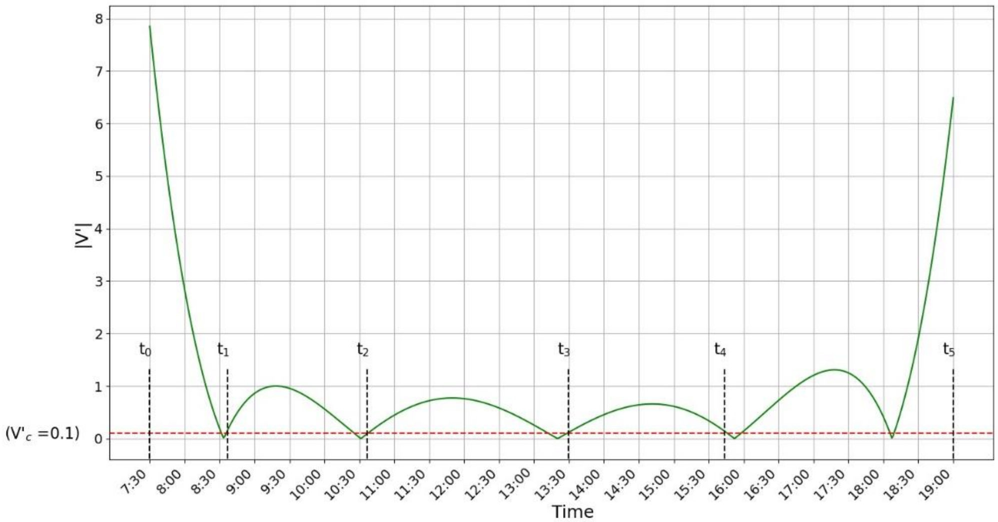

Figure 136: $V'(t)_{critical}$ = 0.1, Breakpoint Set 15

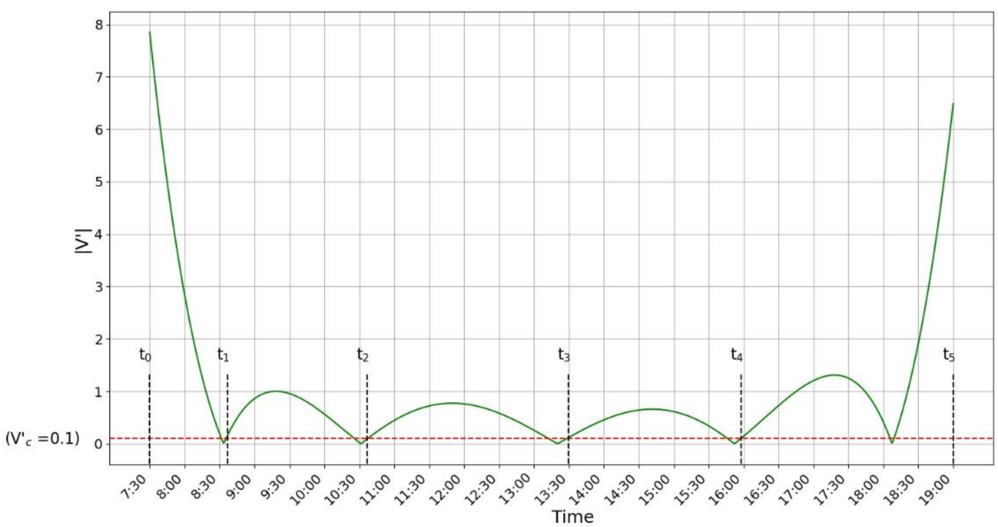

Figure 137: $V'(t)_{critical}$ = 0.1, Breakpoint Set 16

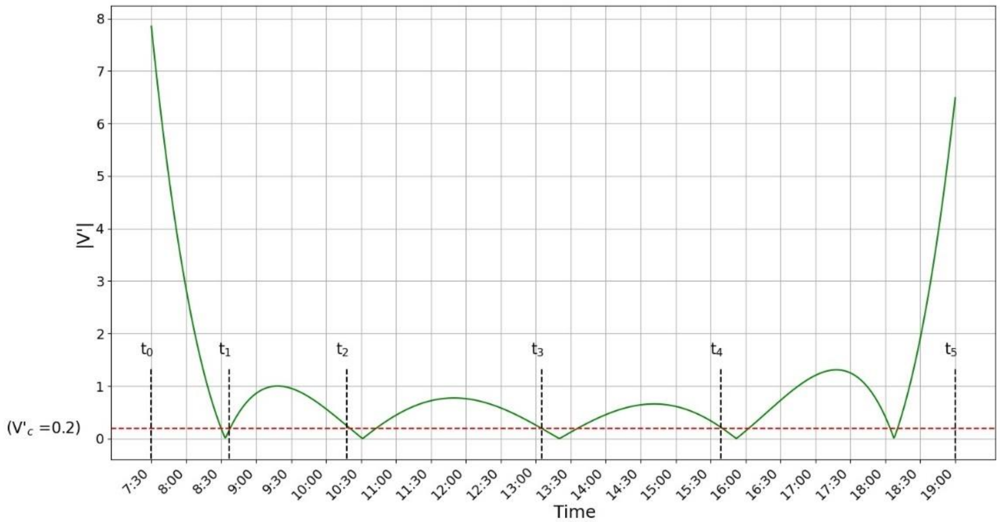

Figure 138: $V'(t)_{critical}$ = 0.2, Breakpoint Set 1

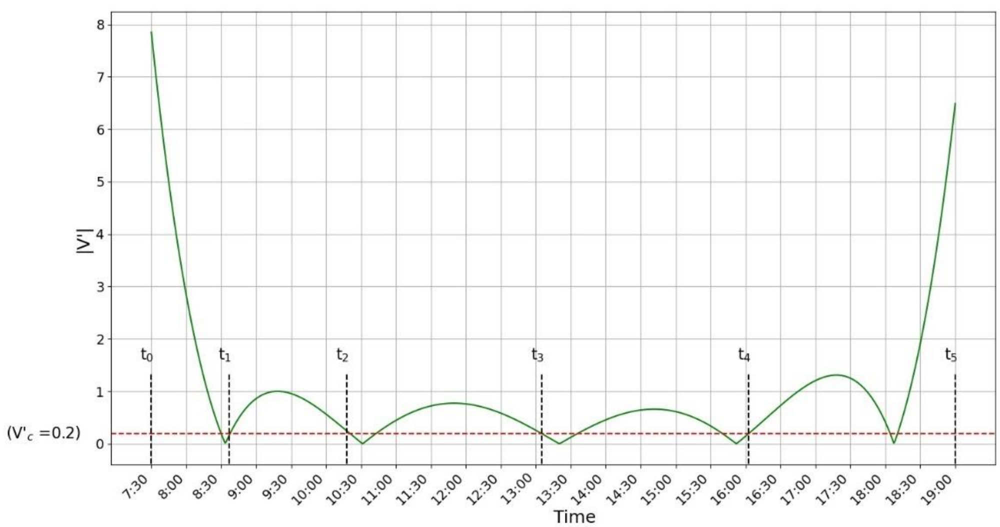

Figure 139: $V'(t)_{critical}$ = 0.2, Breakpoint Set 2

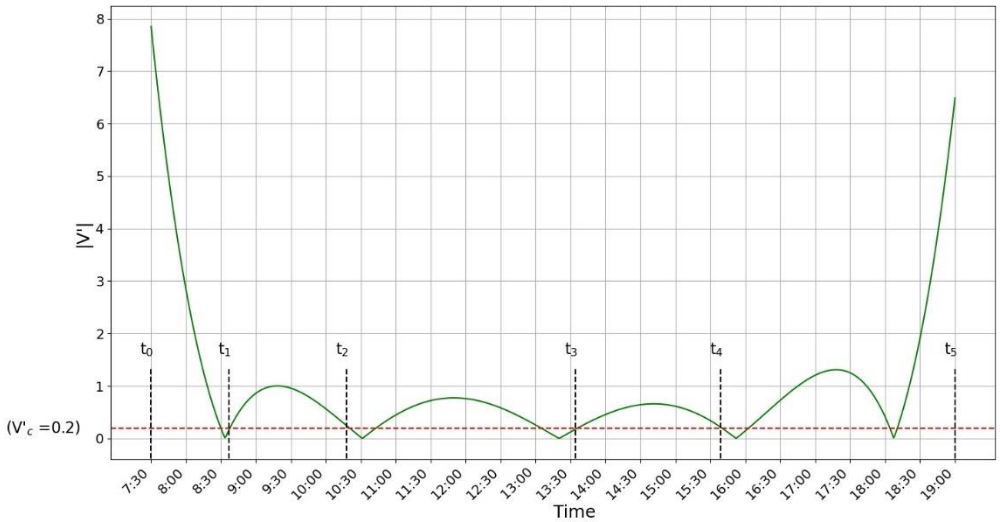

Figure 140: $V'(t)_{critical}$ = 0.2, Breakpoint Set 3

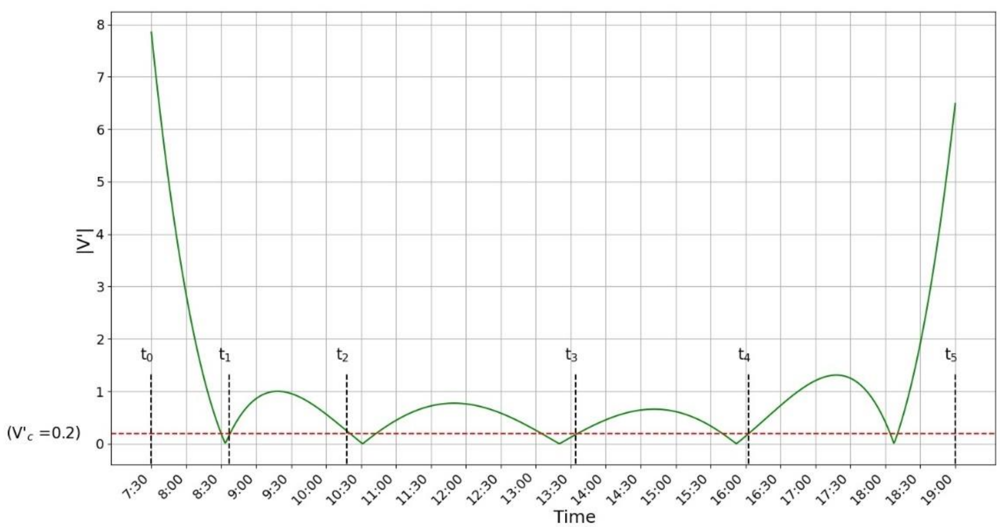

Figure 141: $V'(t)_{critical}$ = 0.2, Breakpoint Set 4

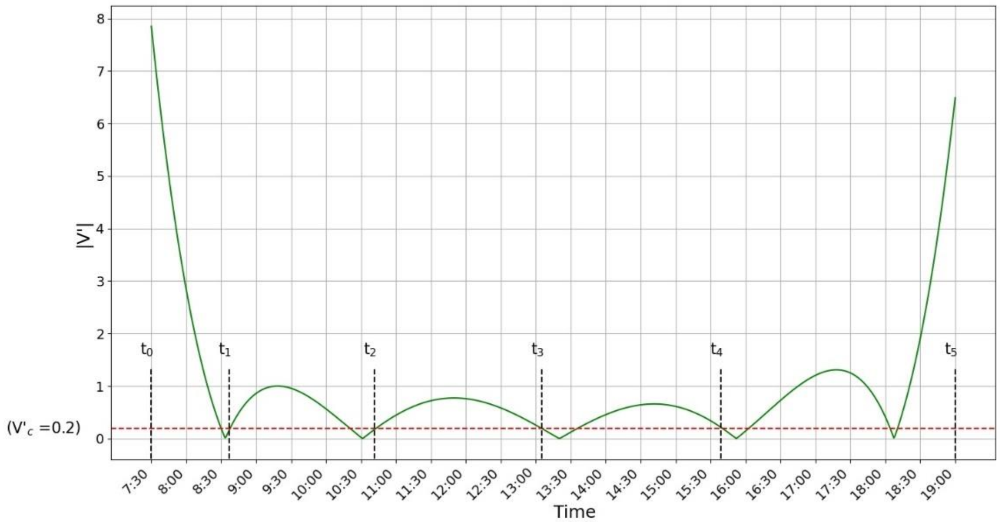

Figure 142: $V'(t)_{critical}$ = 0.2, Breakpoint Set 5

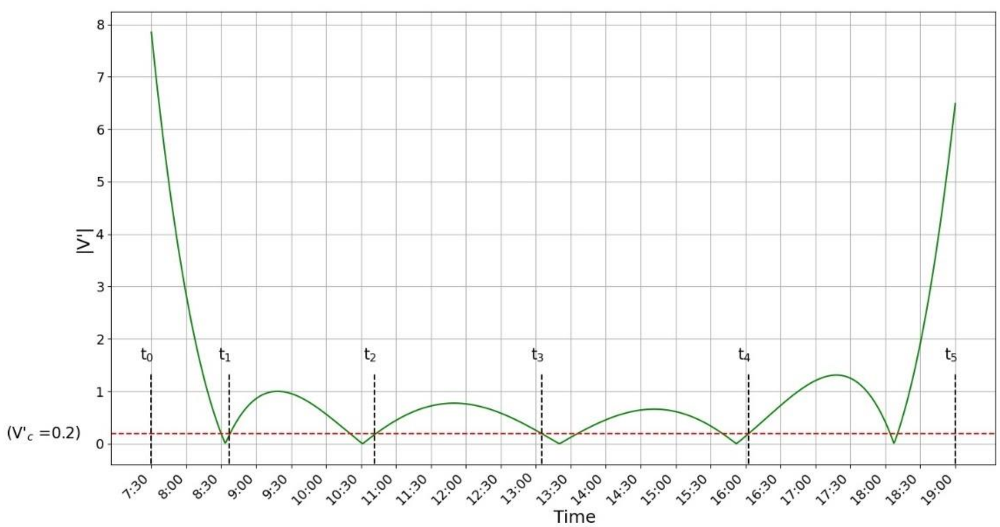

Figure 143: $V'(t)_{critical}$ = 0.2, Breakpoint Set 6

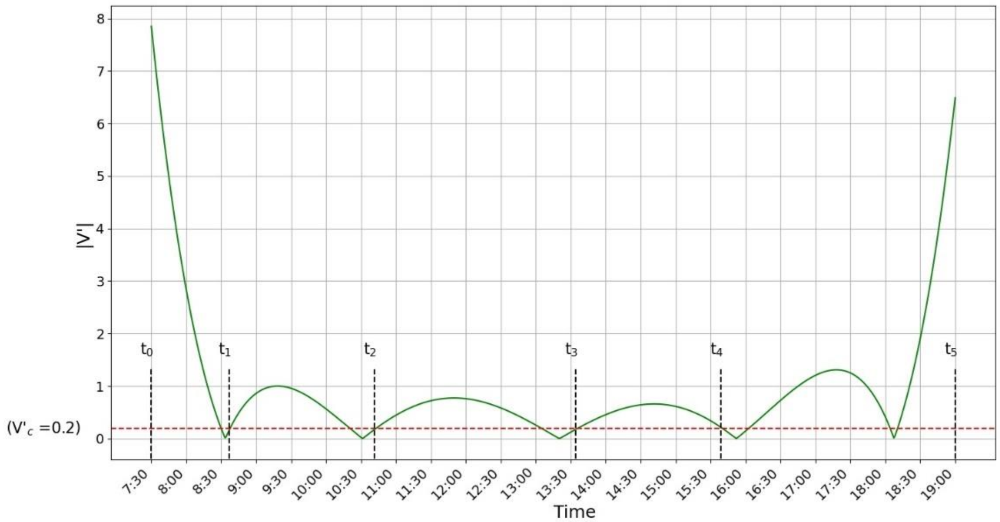

Figure 144: $V'(t)_{critical}$ = 0.2, Breakpoint Set 7

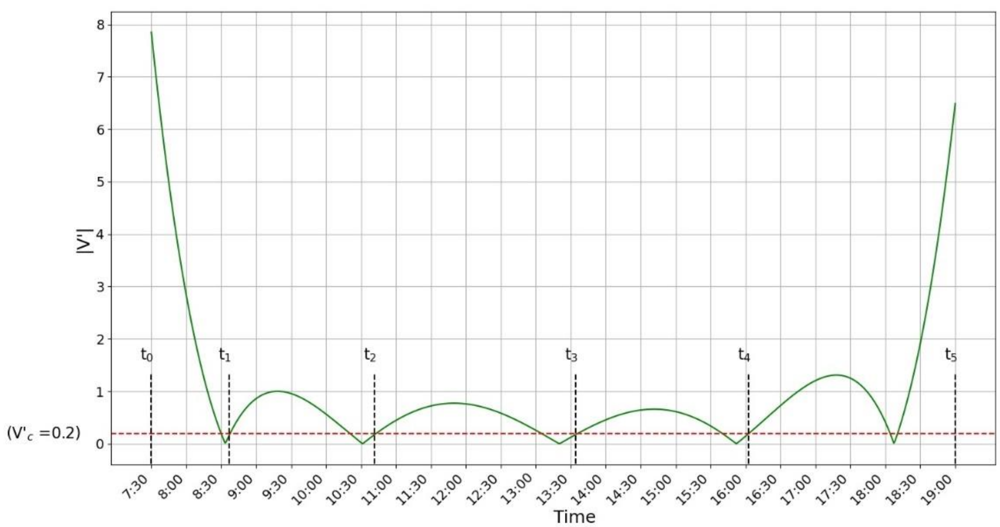

Figure 145: $V'(t)_{critical}$ = 0.2, Breakpoint Set 8

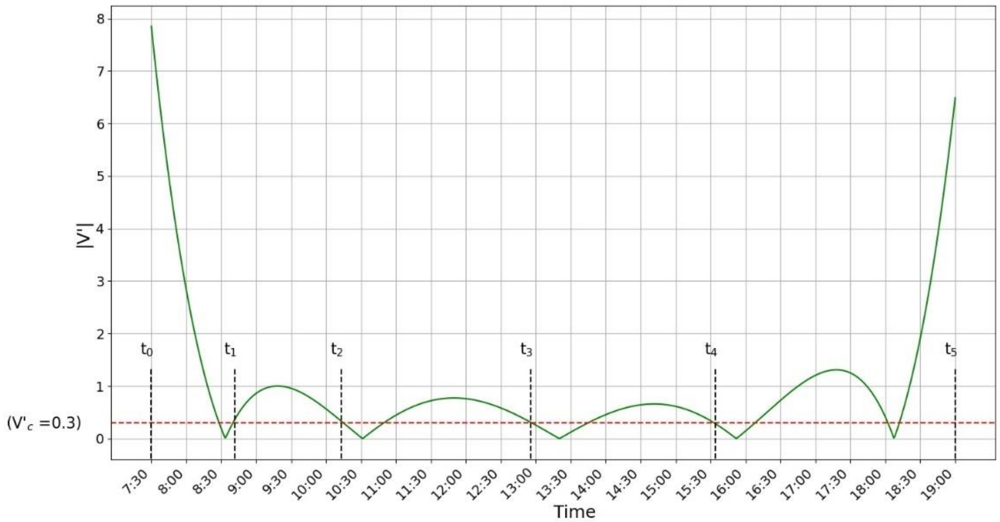

Figure 146: $V'(t)_{critical}$ = 0.3, Breakpoint Set 1

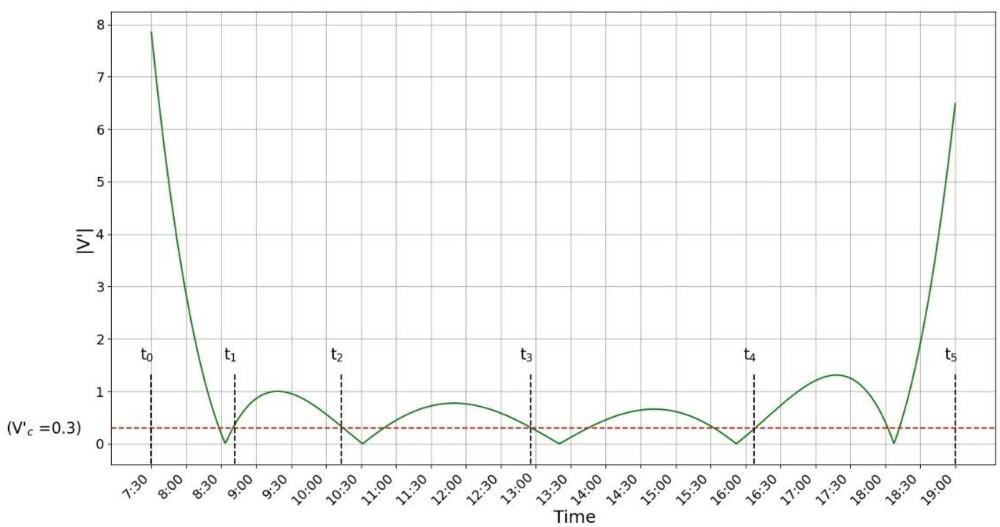

Figure 147: $V'(t)_{critical}$ = 0.3, Breakpoint Set 2

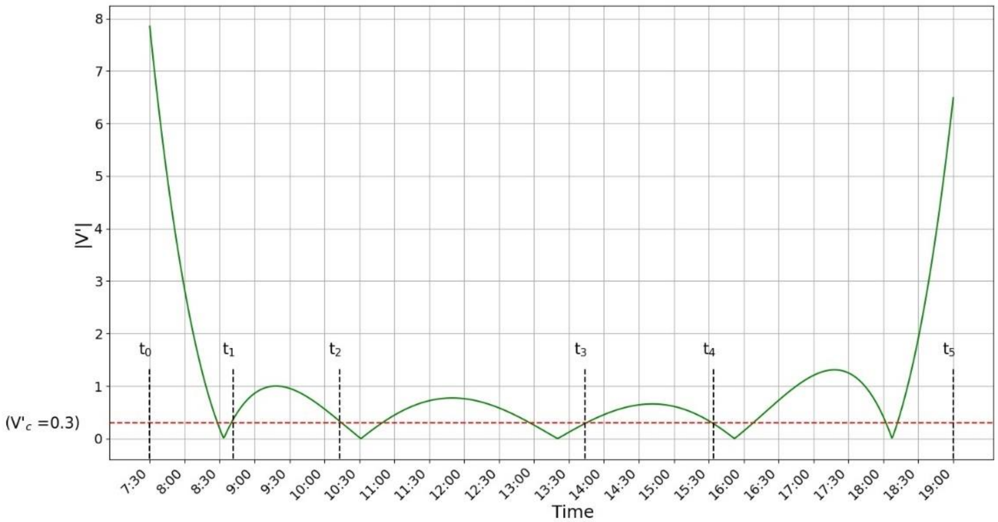

Figure 148: $V'(t)_{critical}$ = 0.3, Breakpoint Set 3

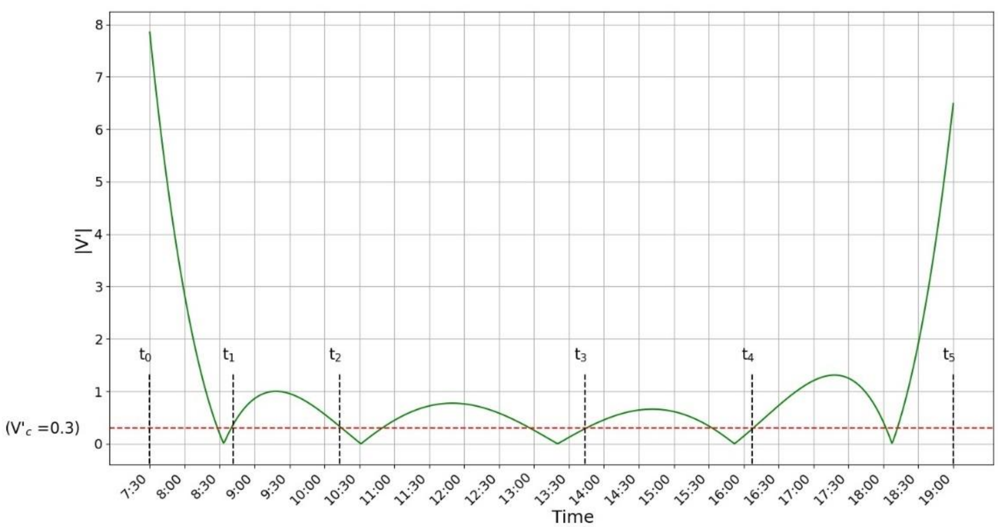

Figure 149: $V'(t)_{critical}$ = 0.3, Breakpoint Set 4

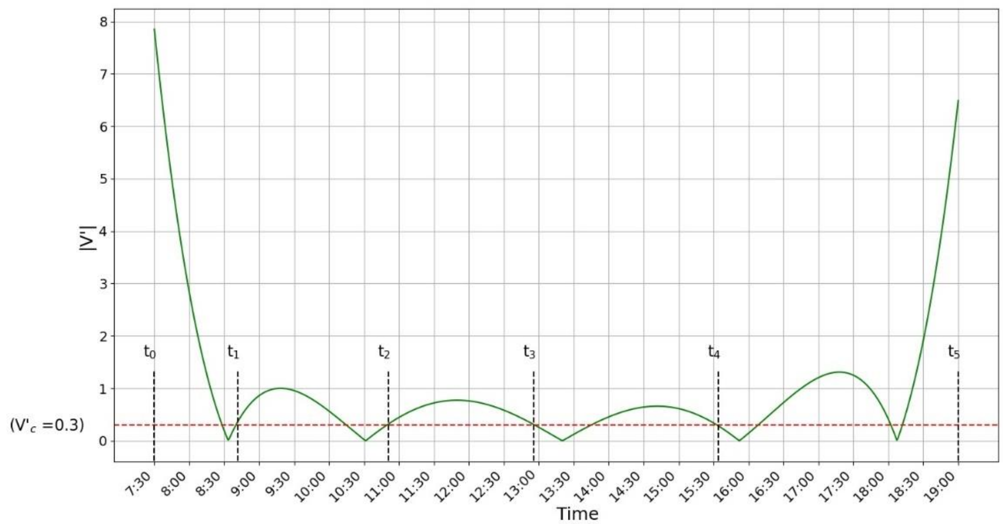

Figure 150: $V'(t)_{critical}$ = 0.3, Breakpoint Set 5

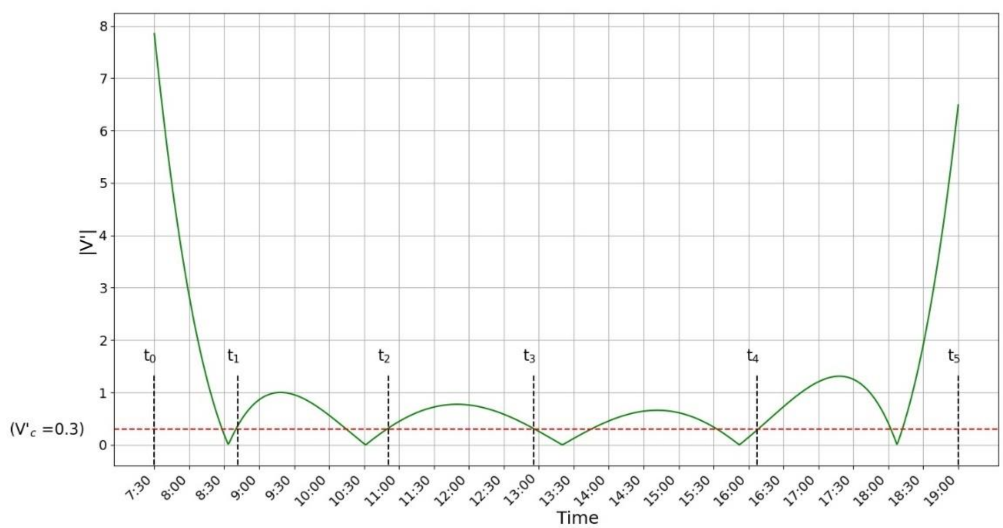

Figure 151: $V'(t)_{critical}$ = 0.3, Breakpoint Set 6

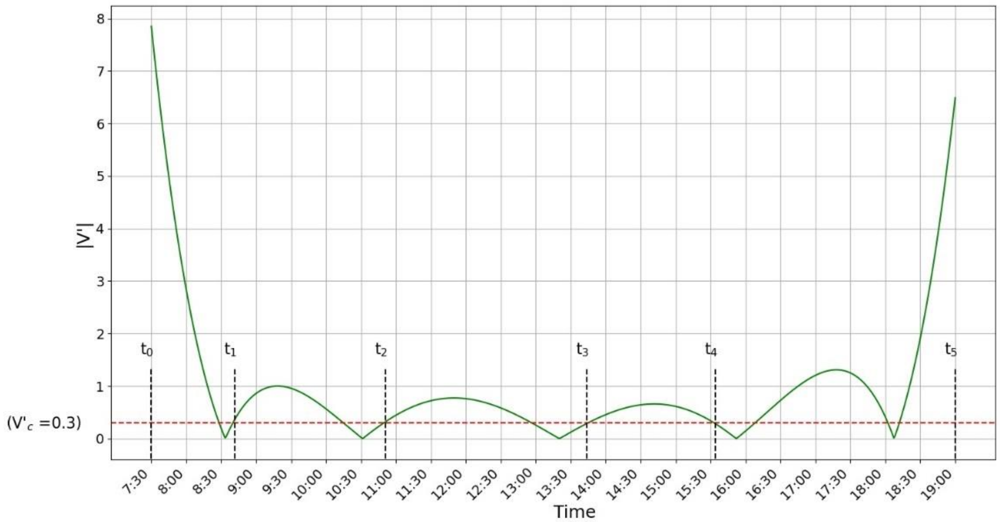

Figure 152: $V'(t)_{critical}$ = 0.3, Breakpoint Set 7

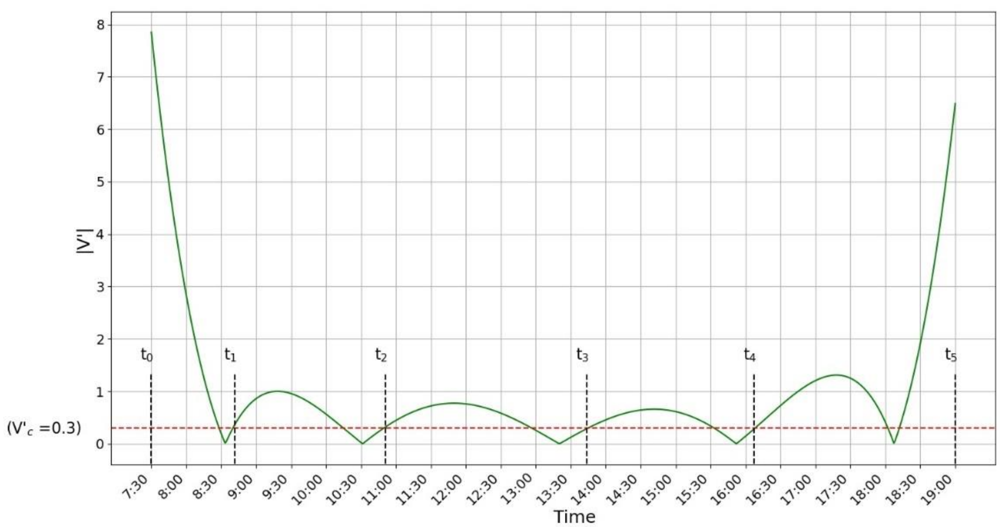

Figure 153: $V'(t)_{critical}$ = 0.3, Breakpoint Set 8

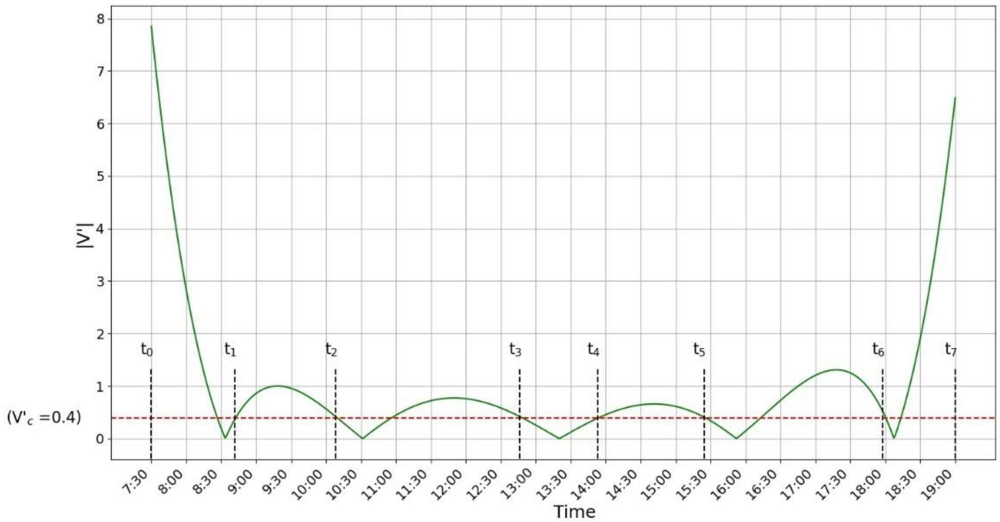

Figure 154: $V'(t)_{critical}$ = 0.4, Breakpoint Set 1

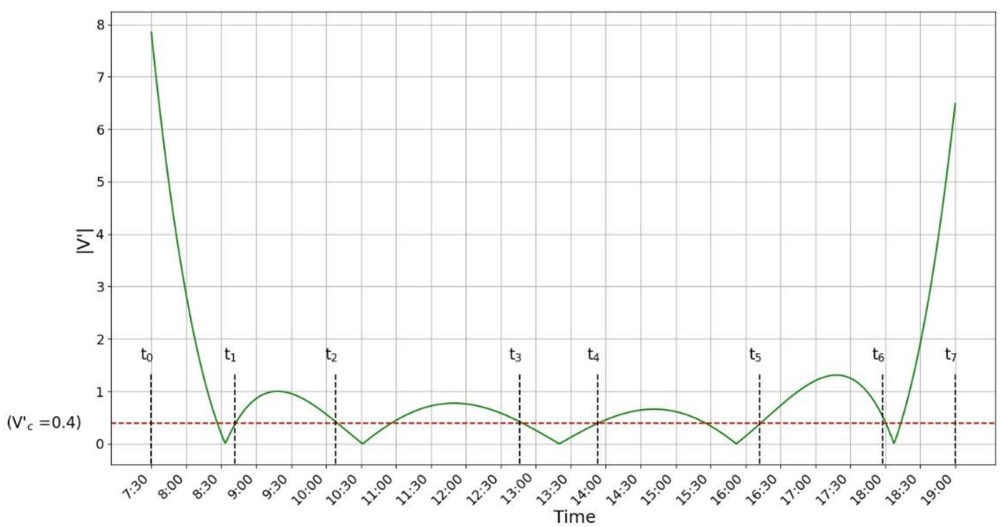

Figure 155: $V'(t)_{critical}$ = 0.4, Breakpoint Set 2

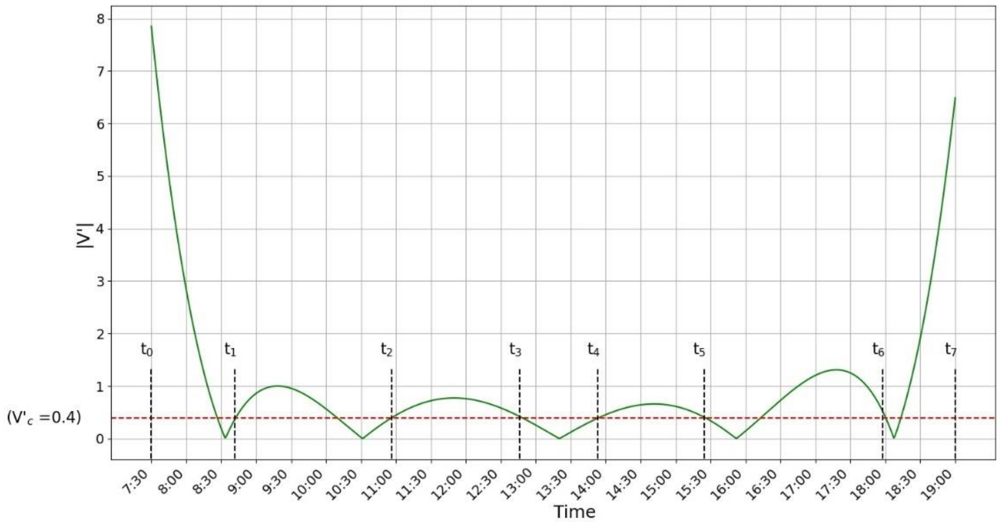

Figure 156: $V'(t)_{critical}$ = 0.4, Breakpoint Set 3

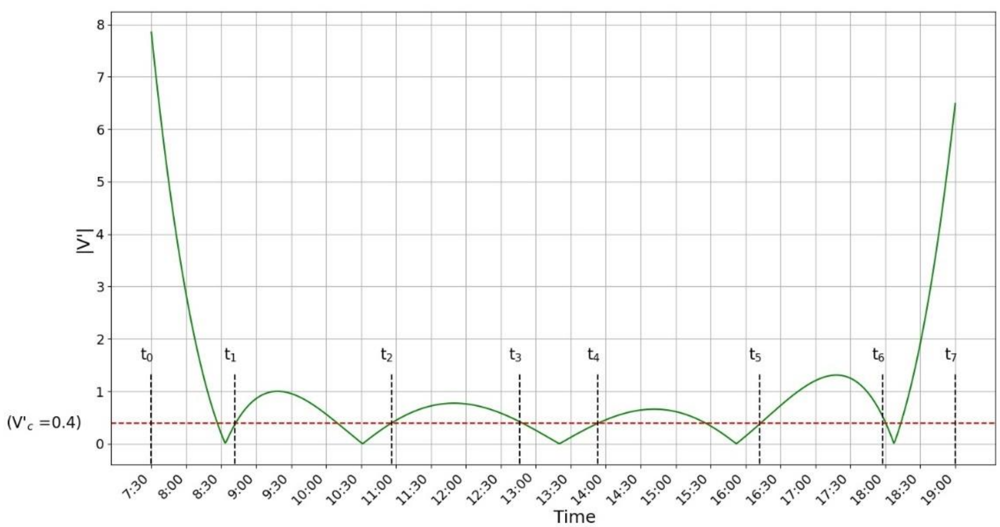

Figure 157: $V'(t)_{critical}$ = 0.4, Breakpoint Set 4

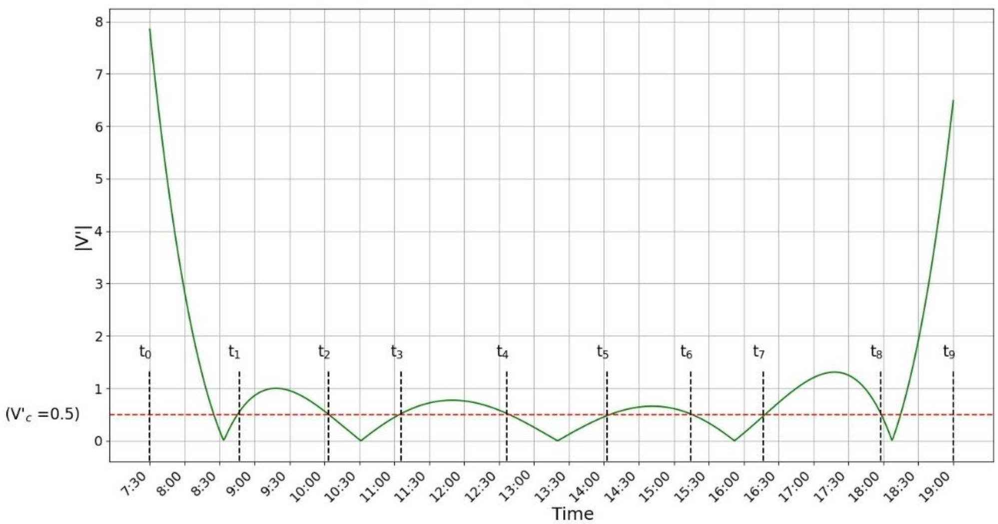

Figure 158: $V'(t)_{critical}$ = 0.5

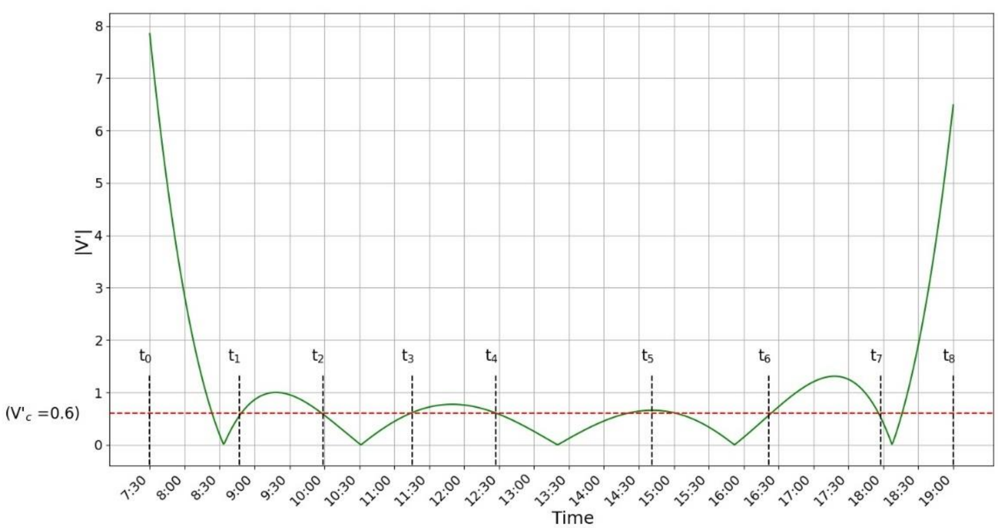

Figure 159: $V'(t)_{critical}$ = 0.6

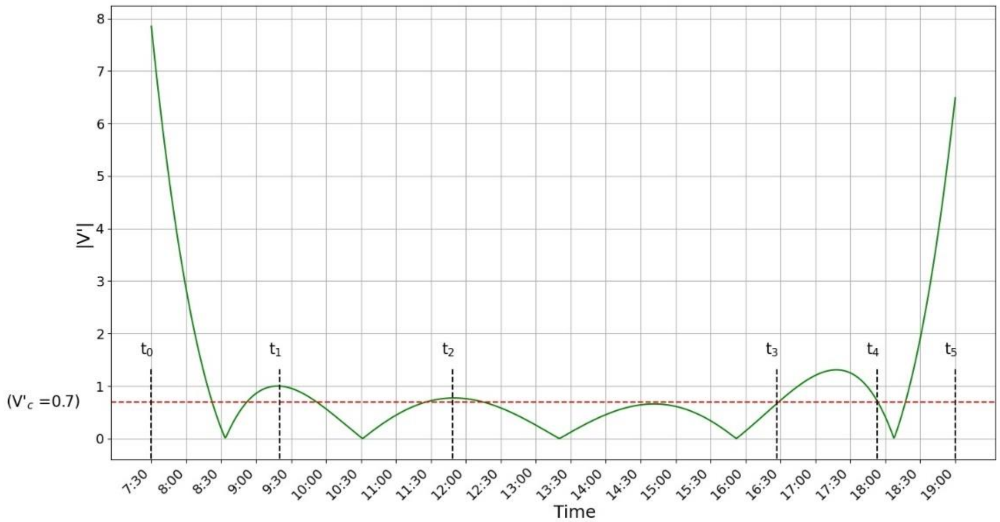

Figure 160: $V'(t)_{critical}$ = 0.7

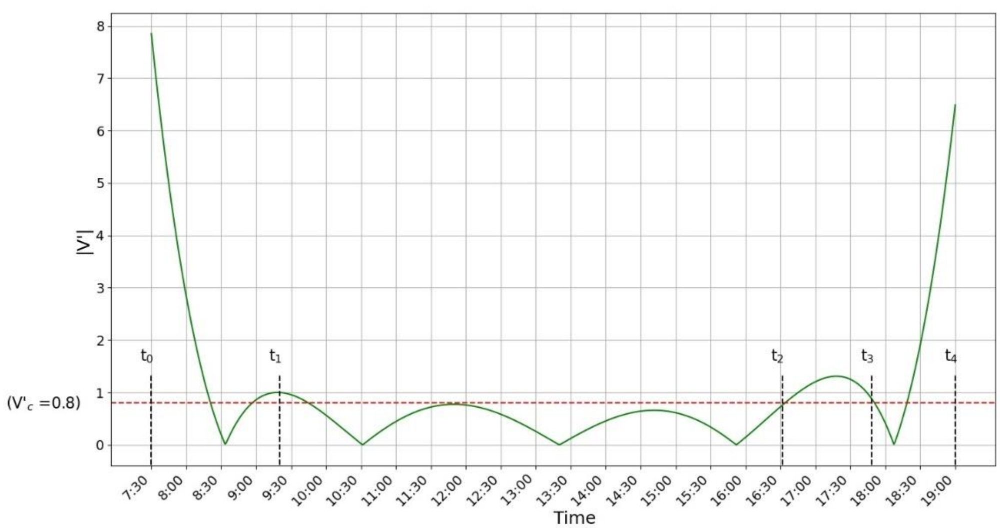

Figure 161: $V'(t)_{critical}$ = 0.8

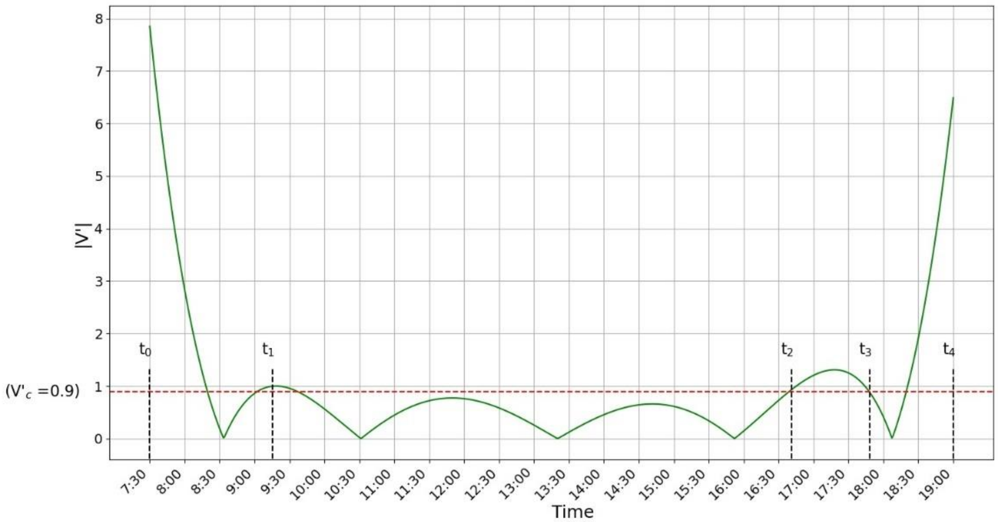

Figure 162: $V'(t)_{critical}$ = 0.9

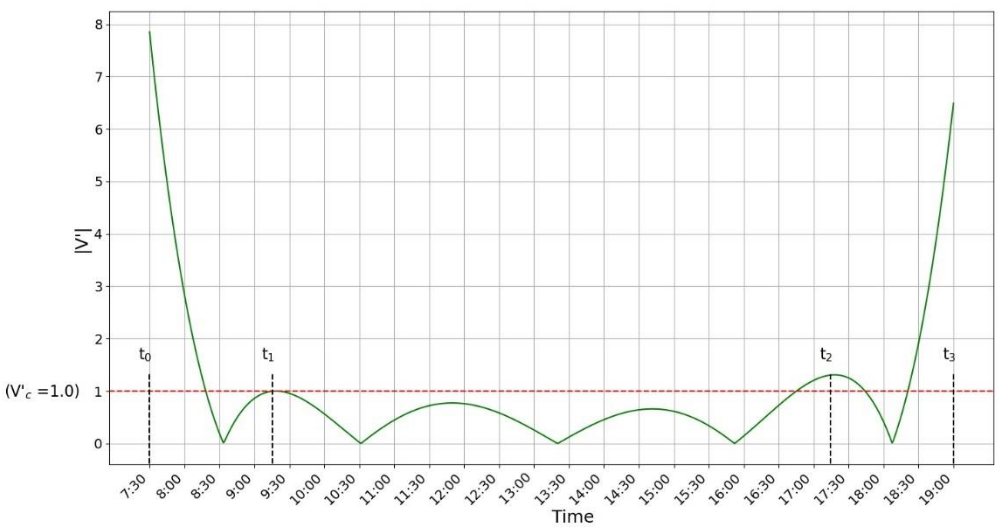

Figure 163: $V'(t)_{critical}$ = 1.0

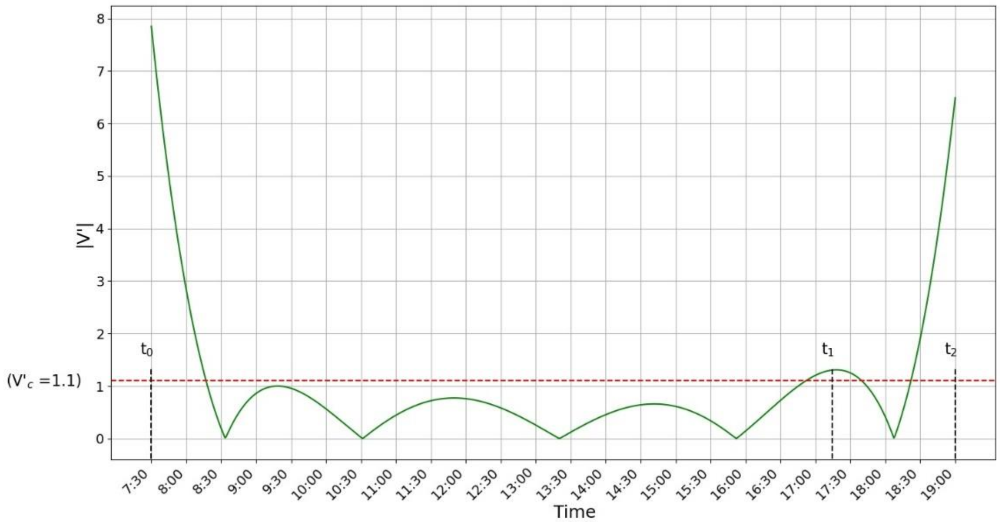

Figure 164: $V'(t)_{critical}$ = 1.1

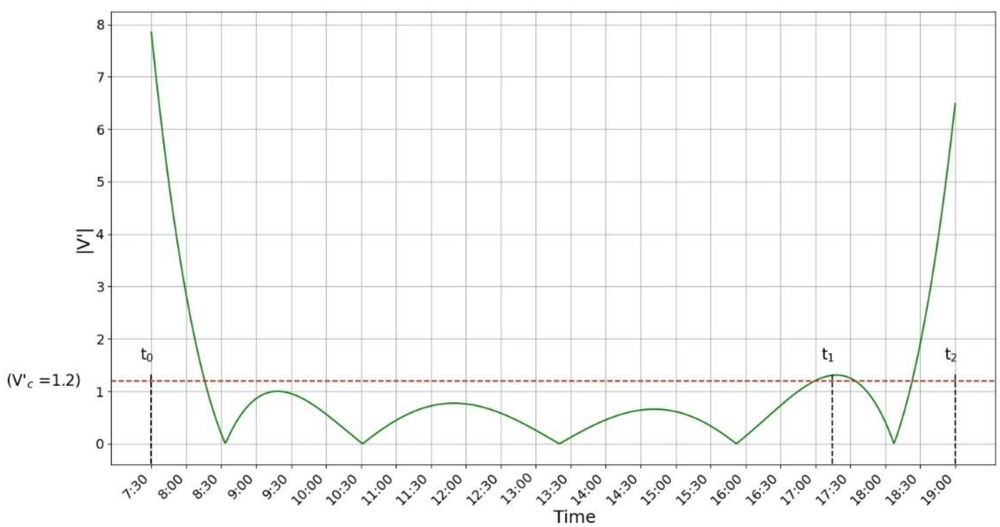

Figure 165: $V'(t)_{critical}$ = 1.2

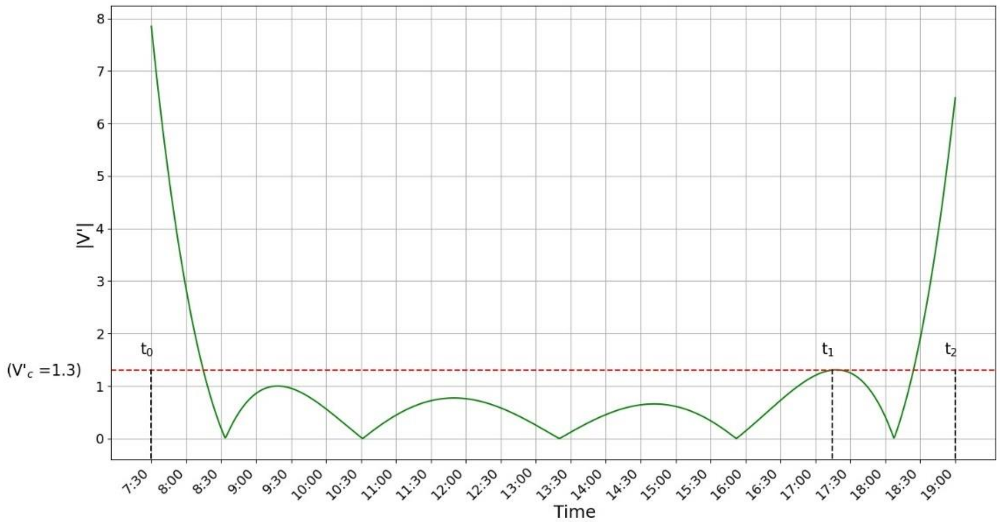

Figure 166: $V'(t)_{critical}$ = 1.3

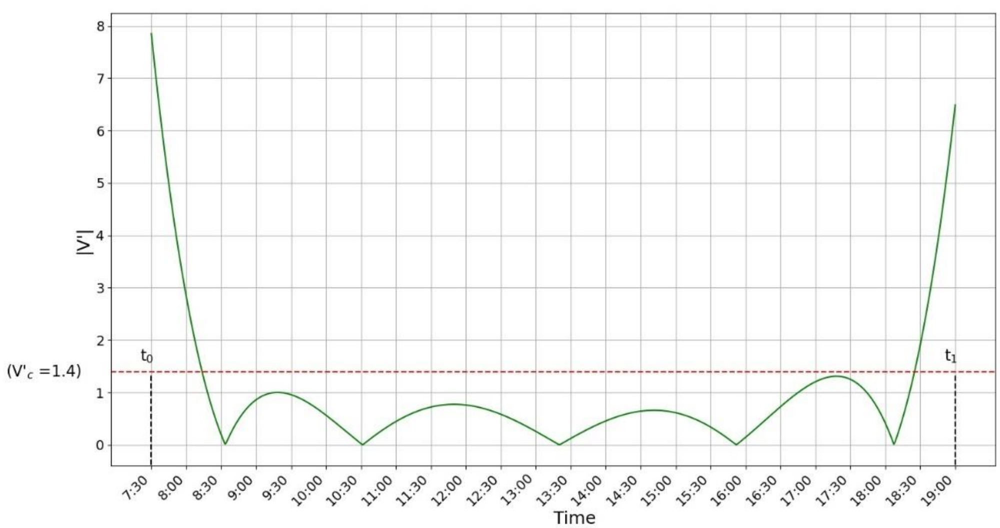

Figure 167: $V'(t)_{critical}$ = 1.4

Table 9 includes the developed breakpoints along with the values of delay and the figure number of each set of timing plan breakpoints.

Table 9: Results of Critical Zone Optimization Method

$V'(t)_{critical}$	Start time	End time	Total Delay (sec/veh)	Figure Number
0	07: 00	08:30	33.7	Figure 121
	08:30	10:30		
	10:30	13:20		
	13:20	16:00		
	16:00	19:00		
0.1	07:00	08:30	23.4	Figure 122
	08:30	10:25		
	10:25	13:10		
	13:10	15:45		
	15:45	19:00		
0.1	07:00	08:30	23.3	Figure 123
	08:30	10:25		
	10:25	13:10		
	13:10	16:00		
	16:00	19:00		
0.1	07:00	08:30	34.1	Figure 124
	08:30	10:25		
	10:25	13:30		
	13:30	15:45		
	15:45	19:00		
0.1	07:00	08:30	33.8	Figure 125
	08:30	10:25		
	10:25	13:30		
	13:30	16:00		
	16:00	19:00		
0.1	07:00	08:30	23.3	Figure 126
	08:30	10:35		
	10:35	13:10		
	13:10	15:45		
	15:45	19:00		
0.1	07:00	08:30	23.1	Figure 127
	08:30	10:35		
	10:35	13:10		
	13:10	16:00		
	16:00	19:00		
0.1	07:00	08:30	35	Figure 128

Table 9: Results of Critical Zone Optimization Method (Continued)

$V'(t)_{critical}$	Start time	End time	Total Delay (sec/veh)	Figure Number
	08:30	10:35		
	10:35	13:30		
	13:30	15:45		
	15:45	19:00		
0.1	07:00	08:30	34.8	Figure 129
	08:30	10:35		
	10:35	13:30		
	13:30	16:00		
	16:00	19:00		
0.1	07:00	08:35	23.1	Figure 130
	08:35	10:25		
	10:25	13:10		
	13:10	15:45		
	15:45	19:00		
0.1	07:00	08:35	23	Figure 131
	08:35	10:25		
	10:25	13:10		
	13:10	16:00		
	16:00	19:00		
0.1	07:00	08:35	34.2	Figure 132
	08:35	10:25		
	10:25	13:30		
	13:30	15:45		
	15:45	19:00		
0.1	07:00	08:35	33.9	Figure 133
	08:35	10:25		
	10:25	13:30		
	13:30	16:00		
	16:00	19:00		
0.1	07:00	08:35	22.9	Figure 134
	08:35	10:35		
	10:35	13:10		
	13:10	15:45		
	15:45	19:00		
0.1	07:00	08:35	22.8	Figure 135
	08:35	10:35		

Table 9: Results of Critical Zone Optimization Method (Continued)

$V'(t)_{critical}$	Start time	End time	Total Delay (sec/veh)	Figure Number
	10:35	13:10		
	13:10	16:00		
	16:00	19:00		
0.1	07:00	08:35	35.2	Figure 136
	08:35	10:35		
	10:35	13:30		
	13:30	15:45		
	15:45	19:00		
0.1	07:00	08:35	34.8	Figure 137
	08:35	10:35		
	10:35	13:30		
	13:30	16:00		
	16:00	19:00		
0.2	07:00	08:35	34.8	Figure 138
	08:35	10:20		
	10:20	13:05		
	13:05	15:40		
	15:40	19:00		
0.2	07:00	08:35	35.3	Figure 139
	08:35	10:20		
	10:20	13:05		
	13:05	16:05		
	16:05	19:00		
0.2	07:00	08:35	32.5	Figure 140
	08:35	10:20		
	10:20	13:35		
	13:35	15:40		
	15:40	19:00		
0.2	07:00	08:35	32.9	Figure 141
	08:35	10:20		
	10:20	13:35		
	13:35	16:05		
	16:05	19:00		
0.2	07:00	08:35	35.6	Figure 142
	08:35	10:40		
	10:40	13:05		

Table 9: Results of Critical Zone Optimization Method (Continued)

$V'(t)_{critical}$	Start time	End time	Total Delay (sec/veh)	Figure Number
	13:05	15:40		
	15:40	19:00		
0.2	07:00	08:35	36	Figure 143
	08:35	10:40		
	10:40	13:05		
	13:05	16:05		
	16:05	19:00		
0.2	07:00	08:35	34	Figure 144
	08:35	10:40		
	10:40	13:35		
	13:35	15:40		
	15:40	19:00		
0.2	07:00	08:35	34.5	Figure 145
	08:35	10:40		
	10:40	13:35		
	13:35	16:05		
	16:05	19:00		
0.3	07:00	08:40	37.4	Figure 146
	08:40	10:15		
	10:15	13:00		
	13:00	15:35		
	15:35	19:00		
0.3	07:00	08:40	37.1	Figure 147
	08:40	10:15		
	10:15	13:00		
	13:00	16:10		
	16:10	19:00		
0.3	07:00	08:40	32.7	Figure 148
	08:40	10:15		
	10:15	13:45		
	13:45	15:35		
	15:35	19:00		
0.3	07:00	08:40	32.5	Figure 149
	08:40	10:15		
	10:15	13:45		
	13:45	16:10		

Table 9: Results of Critical Zone Optimization Method (Continued)

$V'(t)_{critical}$	Start time	End time	Total Delay (sec/veh)	Figure Number
	16:10	19:00		
0.3	07:00	08:40	37.3	Figure 150
	08:40	10:50		
	10:50	13:00		
	13:00	15:35		
	15:35	19:00		
0.3	07:00	08:40	37.1	Figure 151
	08:40	10:50		
	10:50	13:00		
	13:00	16:10		
	16:10	19:00		
0.3	07:00	08:40	32.6	Figure 152
	08:40	10:50		
	10:50	13:45		
	13:45	15:35		
	15:35	19:00		
0.3	07:00	08:40	32.5	Figure 153
	08:40	10:50		
	10:50	13:45		
	13:45	16:10		
	16:10	19:00		
0.4	07:00	08:40	35.1	Figure 154
	08:40	10:10		
	10:10	12:45		
	12:45	14:00		
	14:00	15:25		
	15:25	18:00		
	18:00	19:00		
0.4	07:00	08:40	38	Figure 155
	08:40	10:10		
	10:10	12:45		
	12:45	14:00		
	14:00	16:10		
	16:10	18:00		
	18:00	19:00		
0.4	07:00	08:40	35	Figure 156

Table 9: Results of Critical Zone Optimization Method (Continued)

$V'(t)_{critical}$	Start time	End time	Total Delay (sec/veh)	Figure Number
	08:40	11:00		
	11:00	12:45		
	12:45	14:00		
	14:00	15:25		
	15:25	18:00		
	18:00	19:00		
	07:00	08:40		
	08:40	11:00		
	11:00	12:45		
0.4	12:45	14:00	37.9	Figure 157
	14:00	16:10		
	16:10	18:00		
	18:00	19:00		
	07:00	08:45		
	08:45	10:05		
	10:05	11:05		
	11:05	12:35		
0.5	12:35	14:05	52.3	Figure 158
	14:05	15:15		
	15:15	16:15		
	16:15	18:00		
	18:00	19:00		
	07:00	08:45		
	08:45	10:00		
	10:00	11:15		
0.6	11:15	12:25	54.8	Figure 159
	12:25	14:40		
	14:40	16:20		
	16:20	18:00		
	18:00	19:00		
	07:00	09:20		
	09:20	11:50		
0.7	11:50	16:25	46.3	Figure 160
	16:25	18:00		
	18:00	19:00		
0.8	07:00	09:20	57.6	Figure 161

Table 9: Results of Critical Zone Optimization Method (Continued)

$V'(t)_{critical}$	Start time	End time	Total Delay (sec/veh)	Figure Number
	09:20	16:30		
	16:30	17:50		
	17:50	19:00		
0.9	07:00	09:15	61.5	Figure 162
	09:15	16:40		
	16:40	17:50		
	17:50	19:00		
1	07:00	09:15	64.08	Figure 163
	09:15	17:15		
	17:15	19:00		
1.1	07:00	17:15	65.9	Figure 164
	17:15	19:00		
1.2	07:00	17:15	65.9	Figure 165
	17:15	19:00		
1.3	07:00	17:15	65.9	Figure 166
	17:15	19:00		
1.4	07:00	19:00	85.7	Figure 167

ΔV Optimization Method:

Figure 168 to Figure 171 show the developed breakpoints by using the ΔV optimization method.

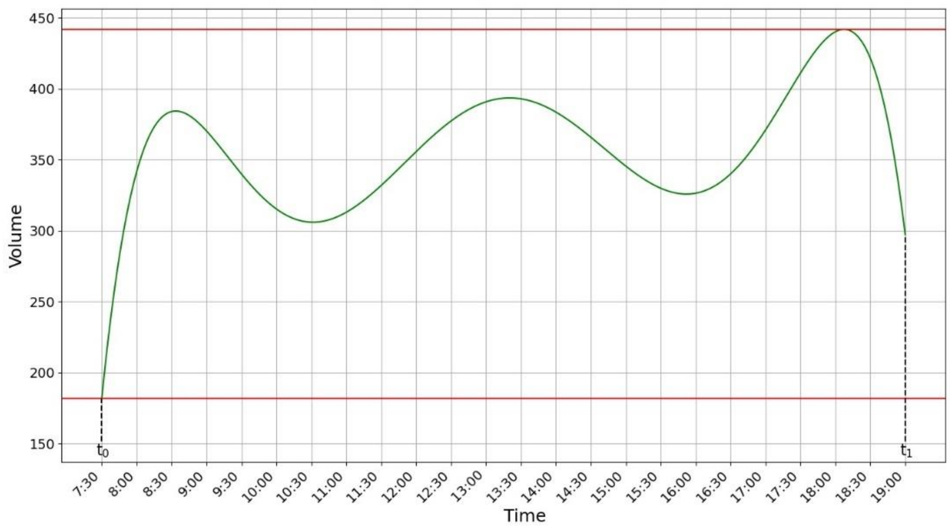

Figure 168: $\Delta V = \text{Range}/1$

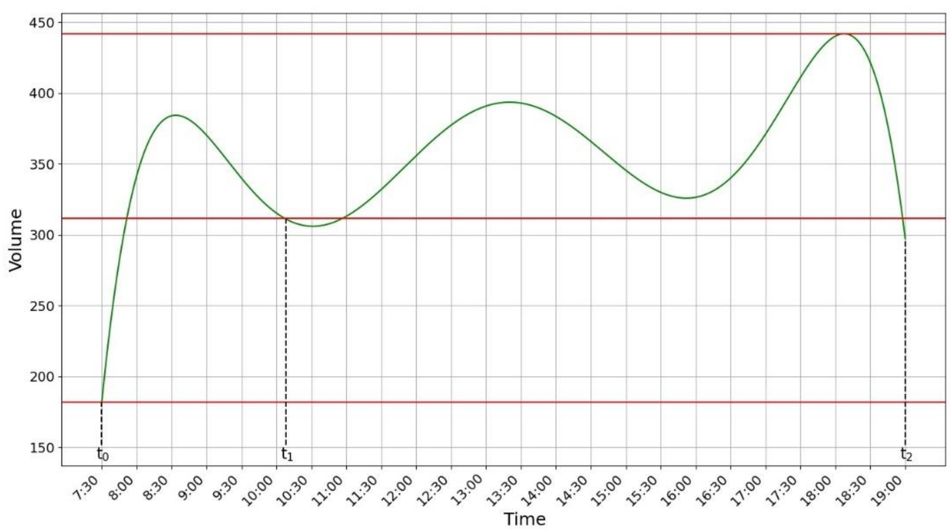

Figure 169: $\Delta V = \text{Range}/2$, Breakpoint Set 1

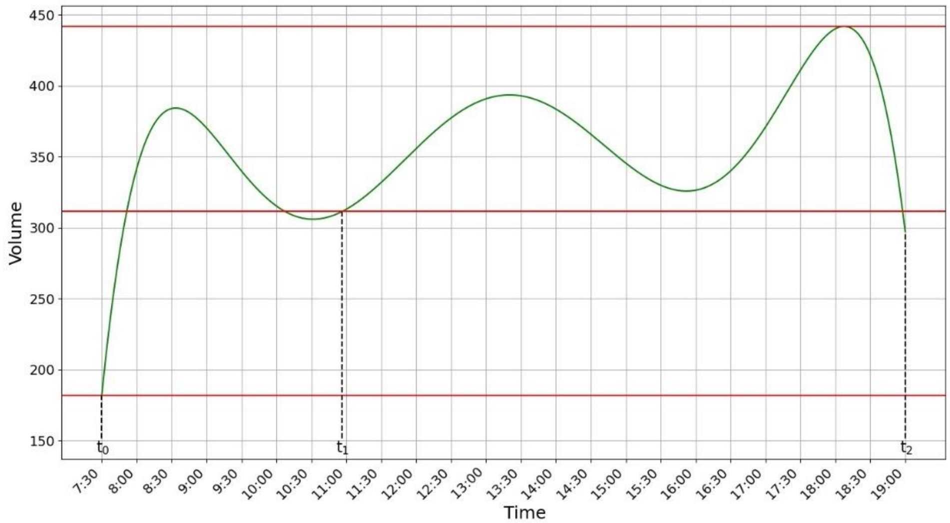

Figure 170: $\Delta\mathrm{V} = \mathrm{Range}/2$, Breakpoint Set 2

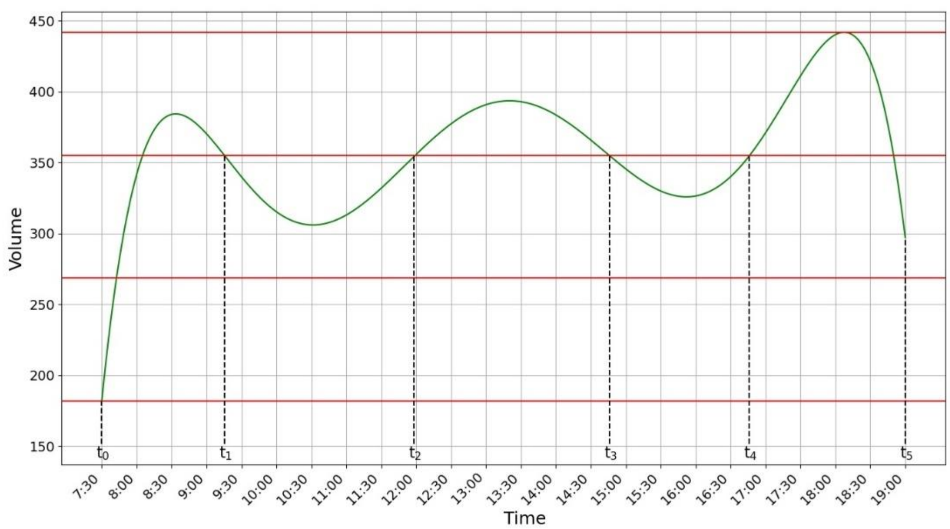

Figure 171: $\Delta\mathrm{V} = \mathrm{Range}/3$, Breakpoint Set 1

Table 10 includes the developed breakpoints along with the values of delay and the figure number of each set of timing plan breakpoints.

Table 10: Results of ΔV Optimization Method

ΔV	Start time	End time	Total Delay (sec/veh)	Figure Number
range/1	07:00	19:00	85.7	Figure 168
range/2	07:00	10:10	65.7	Figure 169
	10:10	19:00		
range/2	07:00	11:00	63.2	Figure 170
	11:00	19:00		
range/3	07:00	09:15	23.5	Figure 171
	09:15	12:00		
	12:00	14:45		
	14:45	16:45		
	16:45	19:00		

George Bush Dr. and Texas Ave Intersection, Feb 12, 2019:

Below are the optimization results by using both of the developed optimization techniques for the traffic counts data of the intersection of George Bush Dr. and Texas Ave. on February 12, 2019.

Critical Zone Optimization Technique:

Figure 172 to Figure 203 show the developed breakpoints by using the critical zone optimization method.

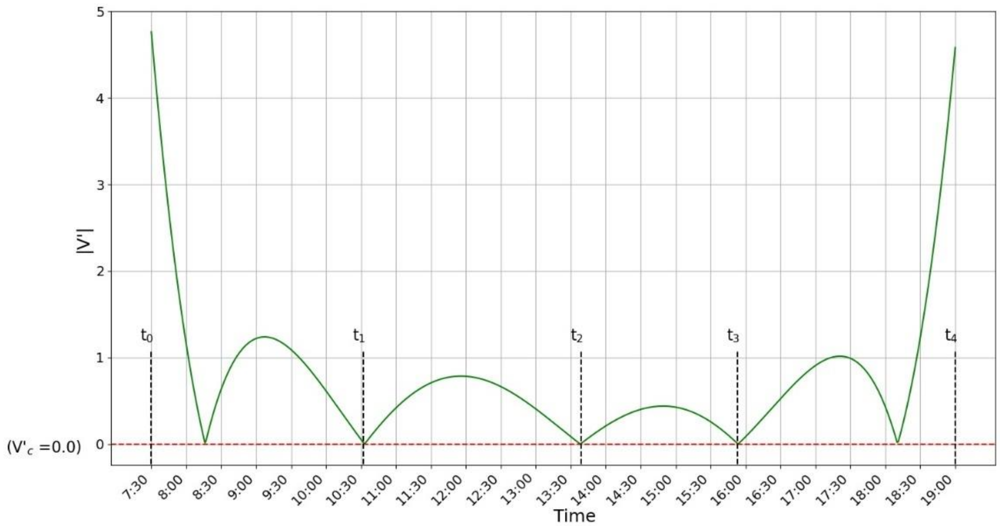

Figure 172: $\mathrm{V}'(\mathrm{t})_{\mathrm{critical}}$ = 0.0

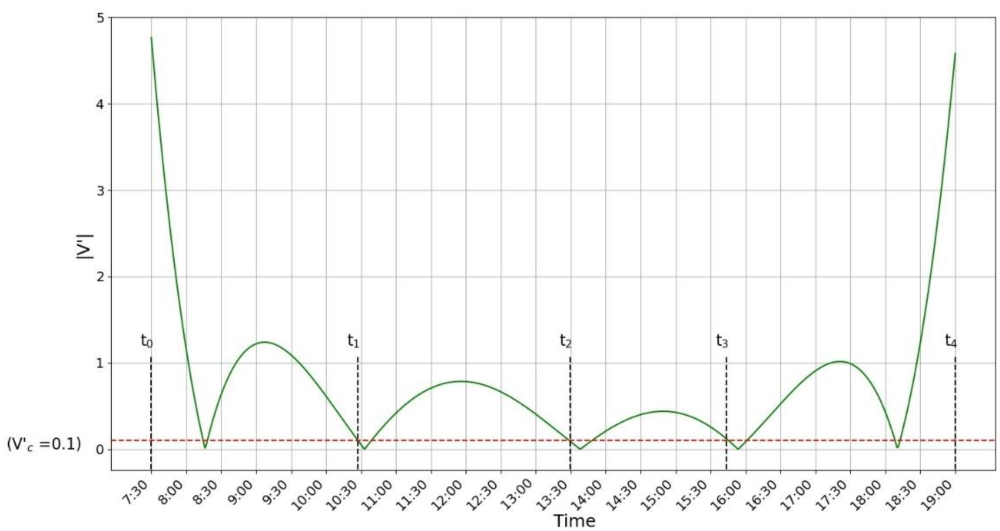

Figure 173: $\mathrm{V}'(\mathrm{t})_{\mathrm{critical}}$ = 0.1, Breakpoint Set 1

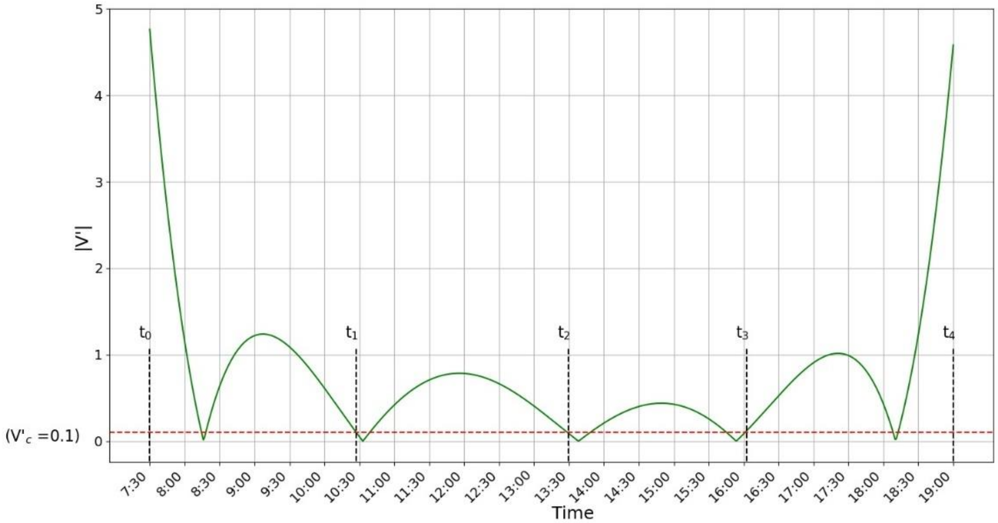

Figure 174: $V'(t)_{critical} = 0.1$, Breakpoint Set 2

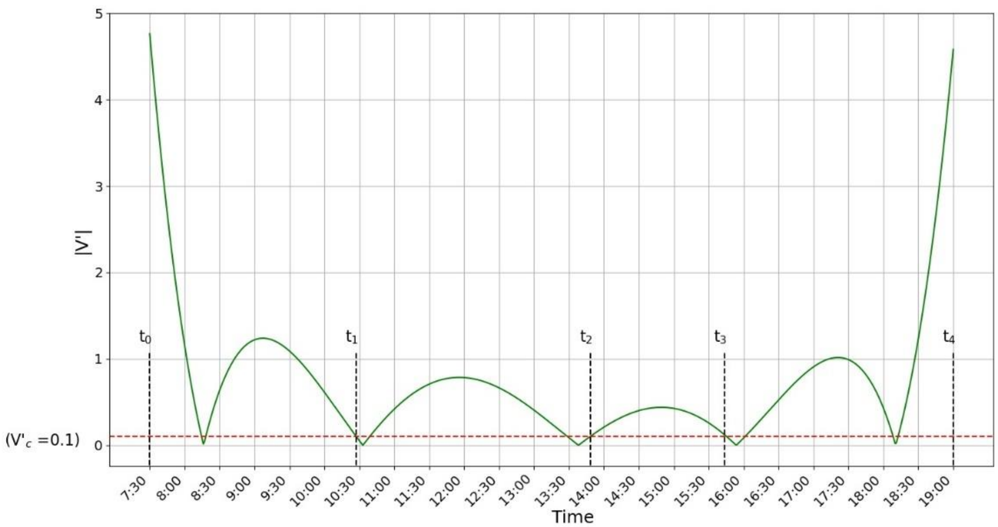

Figure 175: $V'(t)_{critical} = 0.1$, Breakpoint Set 3

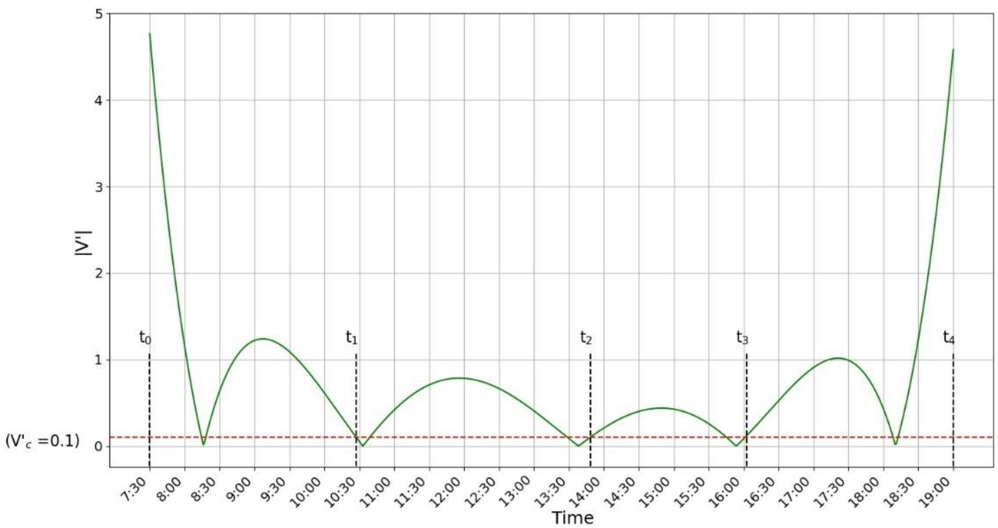

Figure 176: $V'(t)_{critical}$ = 0.1, Breakpoint Set 4

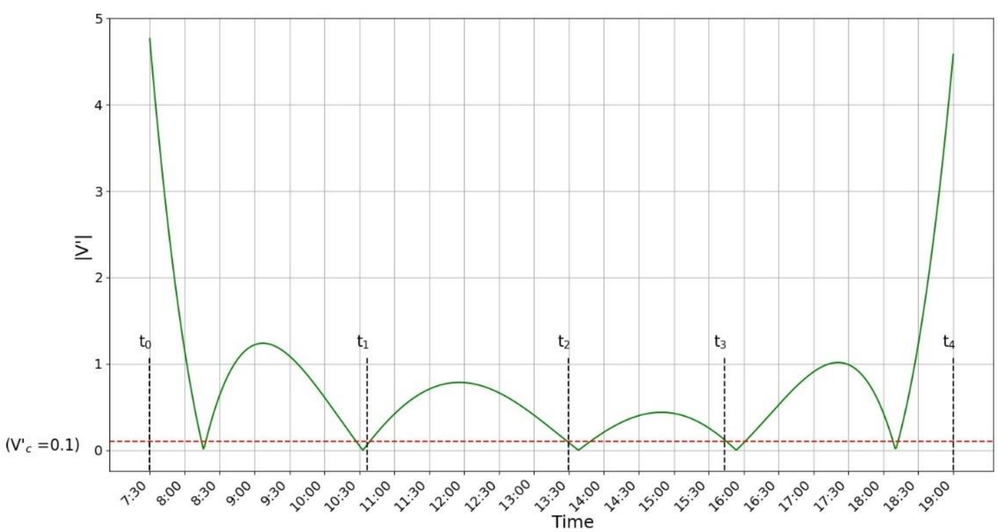

Figure 177: $V'(t)_{critical}$ = 0.1, Breakpoint Set 5

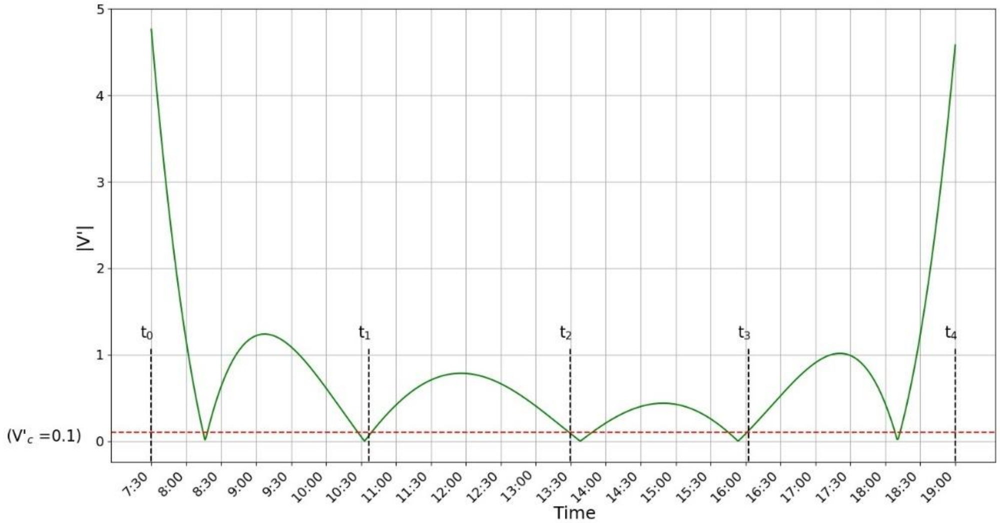

Figure 178: $V'(t)_{critical}$ = 0.1, Breakpoint Set 6

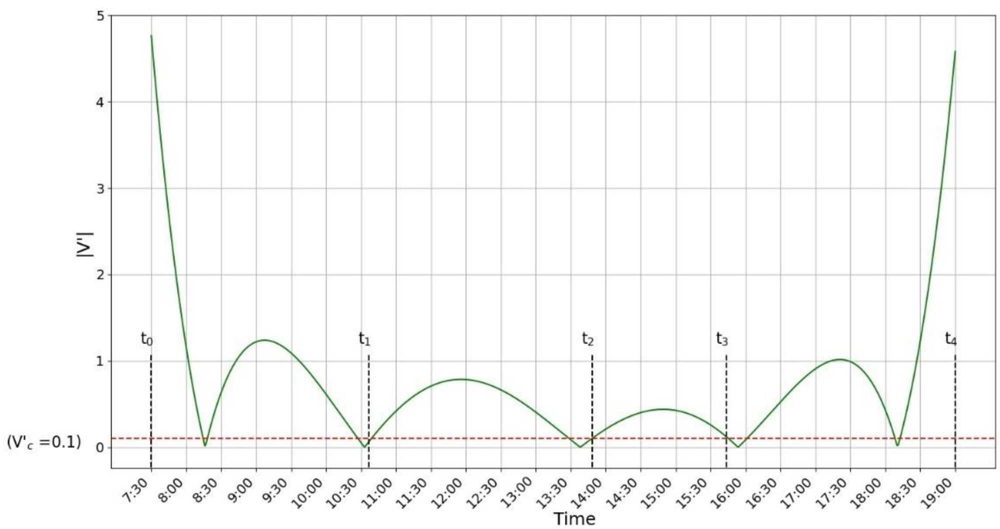

Figure 179: $V'(t)_{critical}$ = 0.1, Breakpoint Set 7

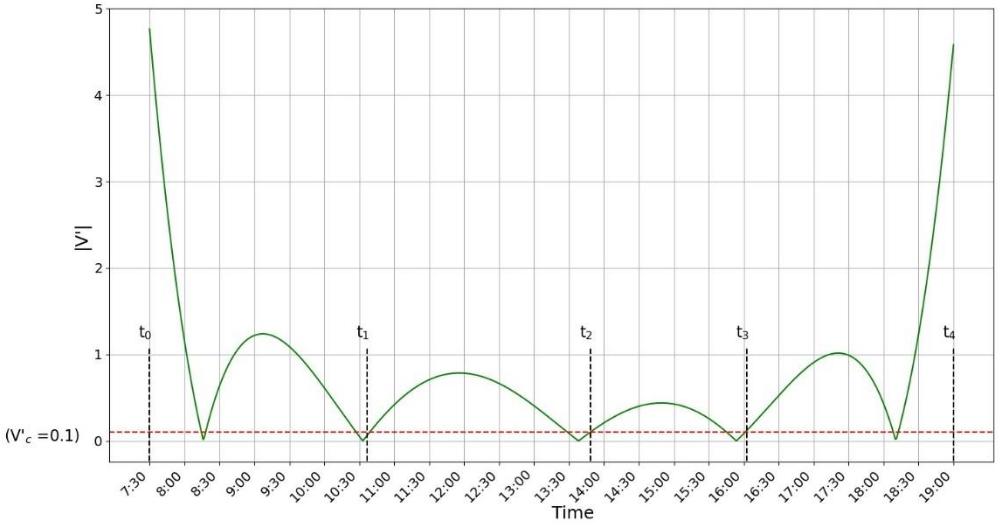

Figure 180: $V'(t)_{critical}$ = 0.1, Breakpoint Set 8

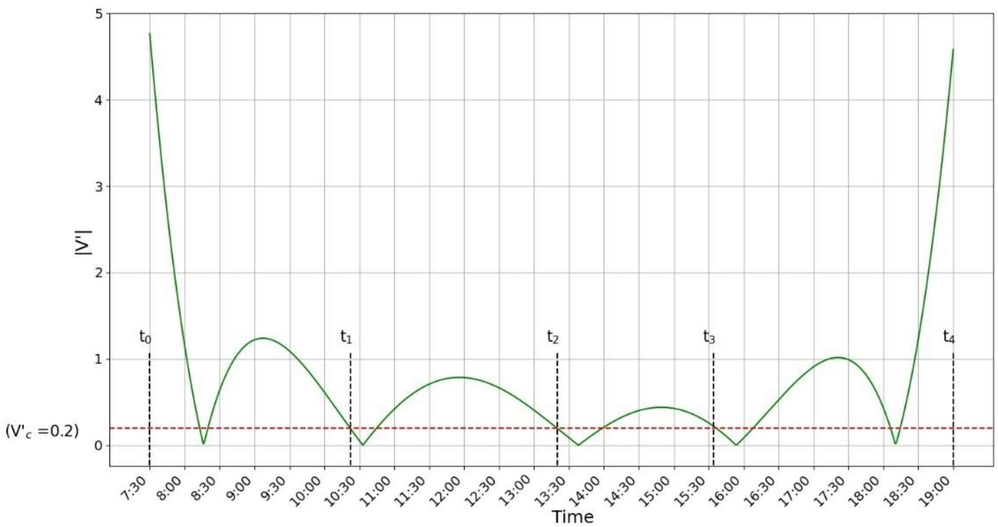

Figure 181: $V'(t)_{critical}$ = 0.2, Breakpoint Set 1

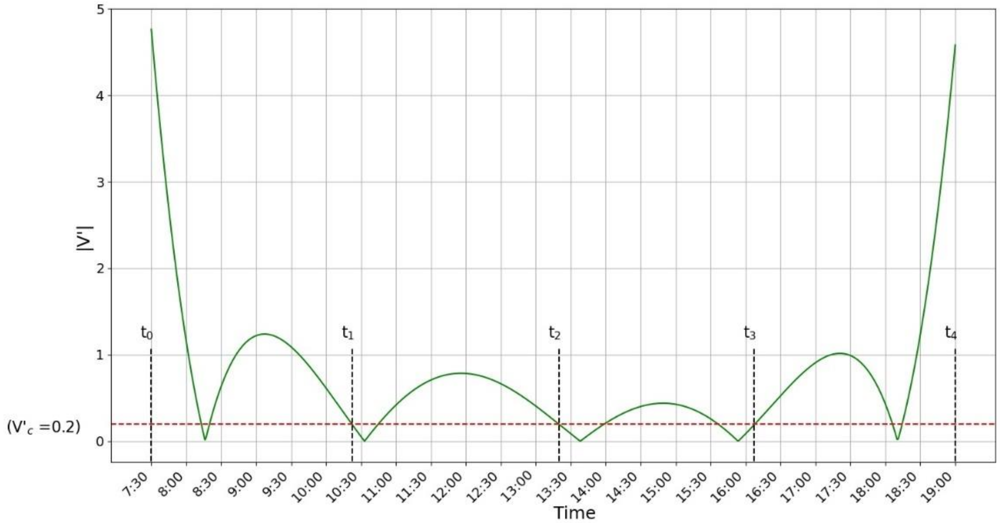

Figure 182: $V'(t)_{critical}$ = 0.2, Breakpoint Set 2

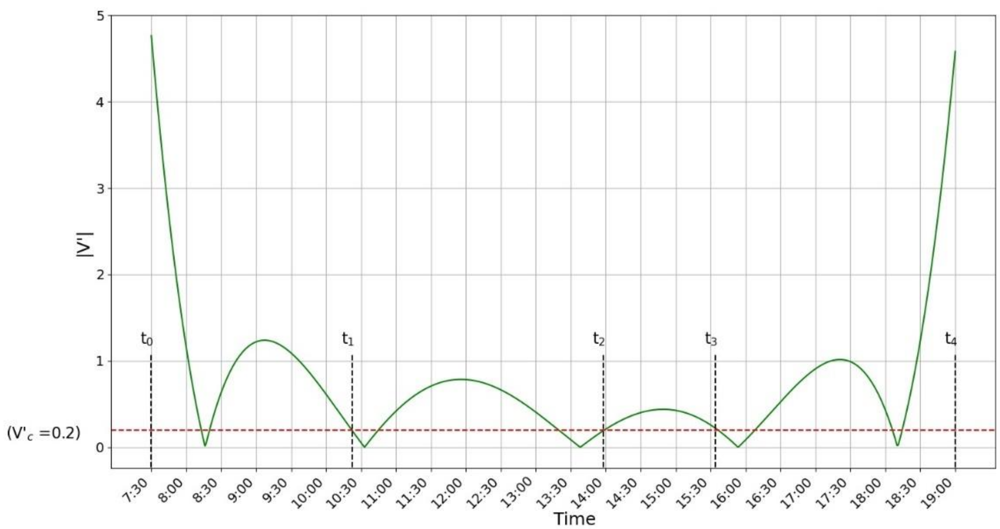

Figure 183: $V'(t)_{critical}$ = 0.2, Breakpoint Set 3

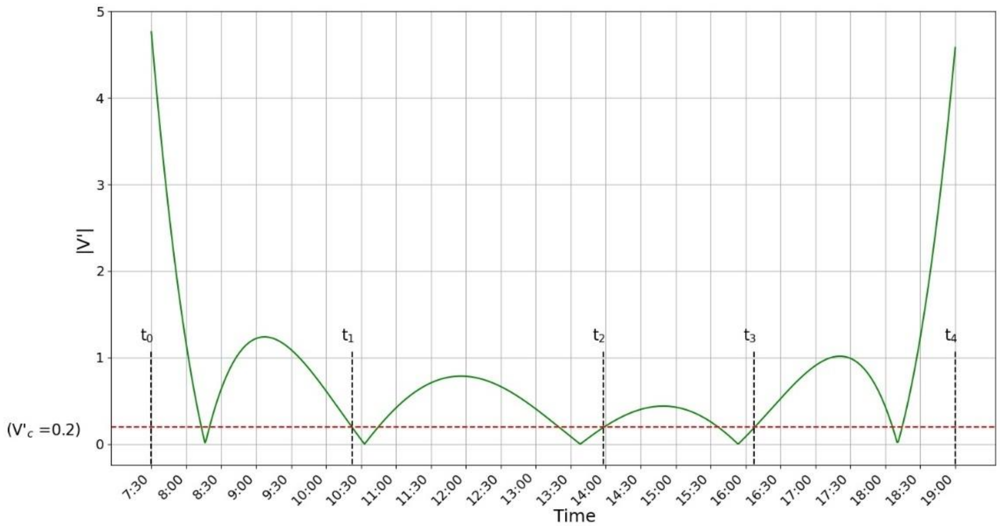

Figure 184: $V'(t)_{\text{critical}}$ = 0.2, Breakpoint Set 4

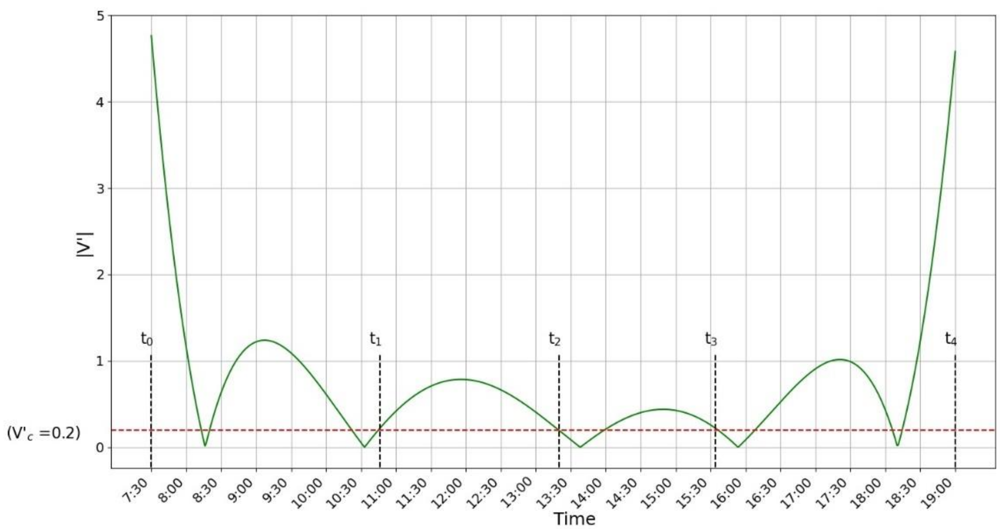

Figure 185: $V'(t)_{\text{critical}}$ = 0.2, Breakpoint Set 5

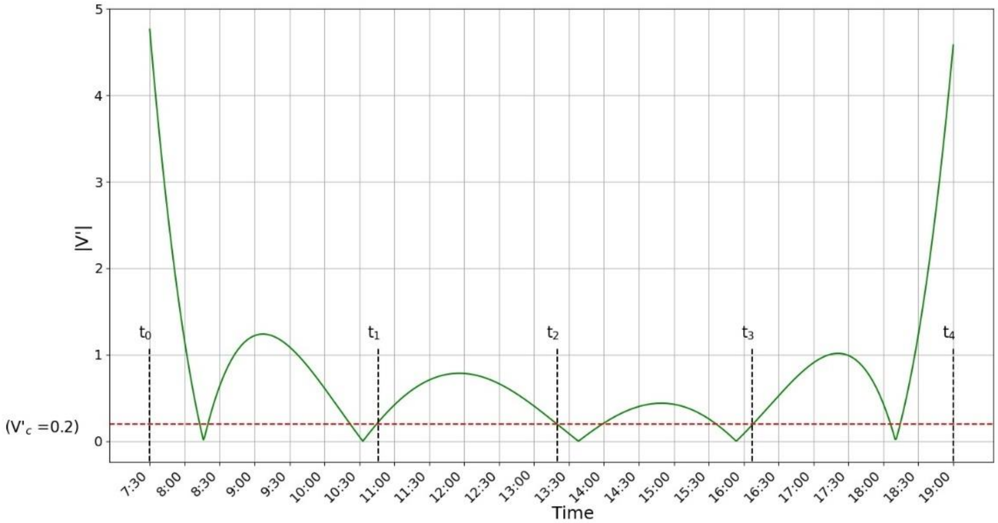

Figure 186: $V'(t)_{critical}$ = 0.2, Breakpoint Set 6

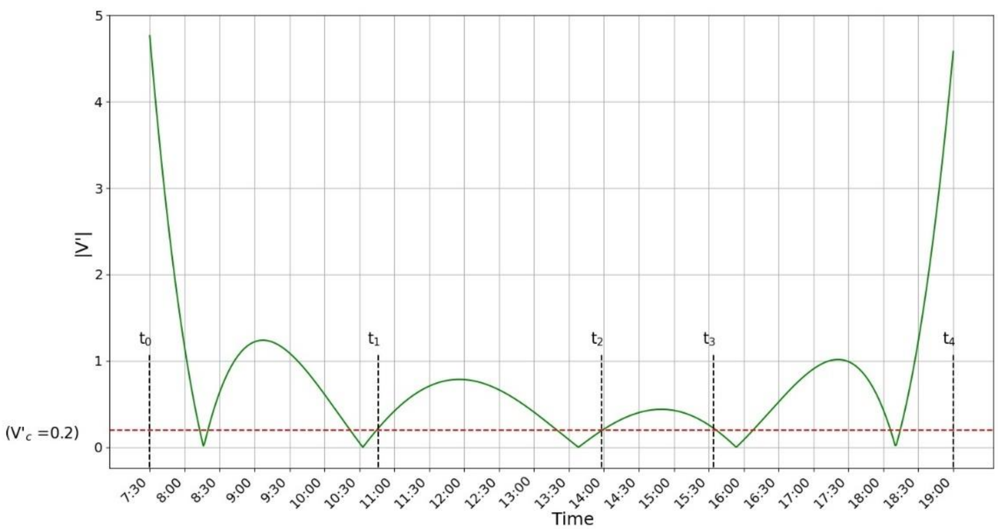

Figure 187: $V'(t)_{critical}$ = 0.2, Breakpoint Set 7

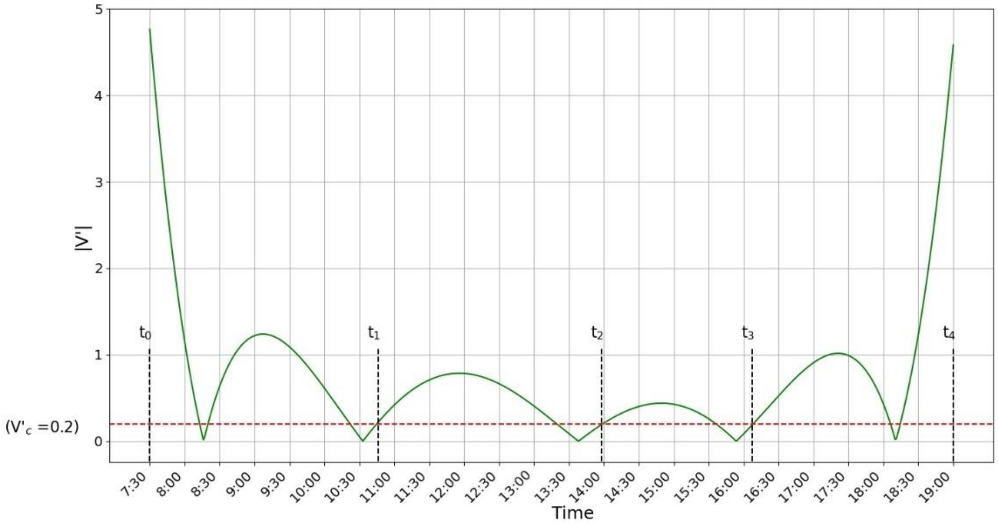

Figure 188: $\mathrm{V}'(\mathrm{t})_{\mathrm{critical}} = 0.2$, Breakpoint Set 8

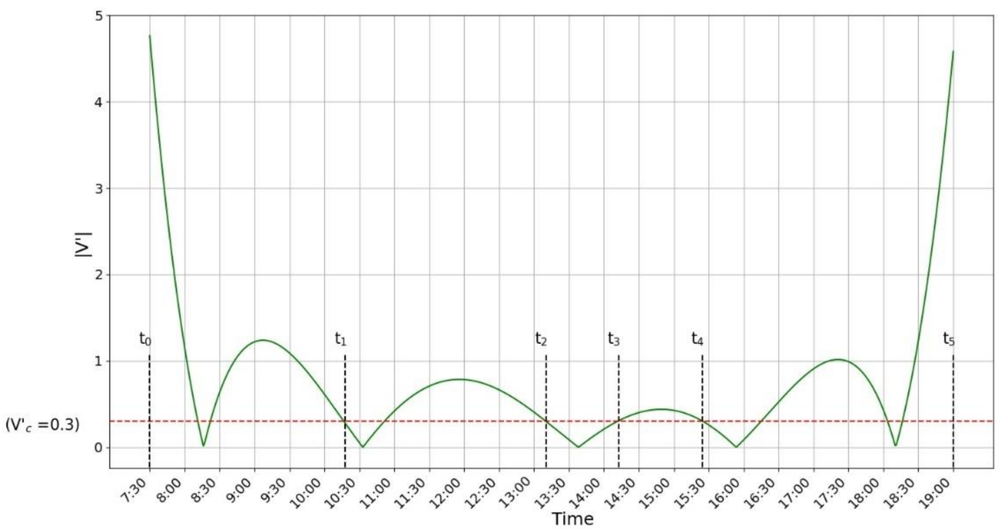

Figure 189: $\mathrm{V}'(\mathrm{t})_{\mathrm{critical}} = 0.3$, Breakpoint Set 1

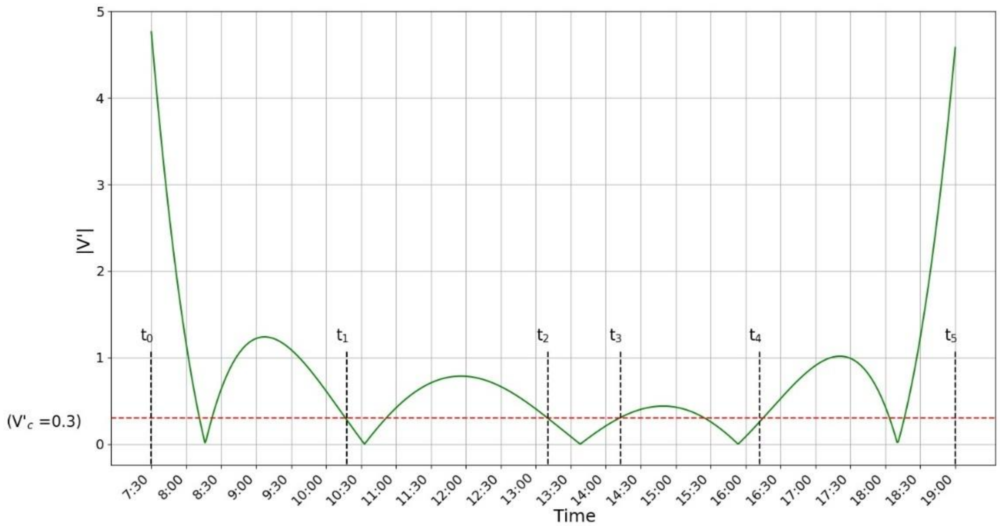

Figure 190: $V'(t)_{critical}$ = 0.3, Breakpoint Set 2

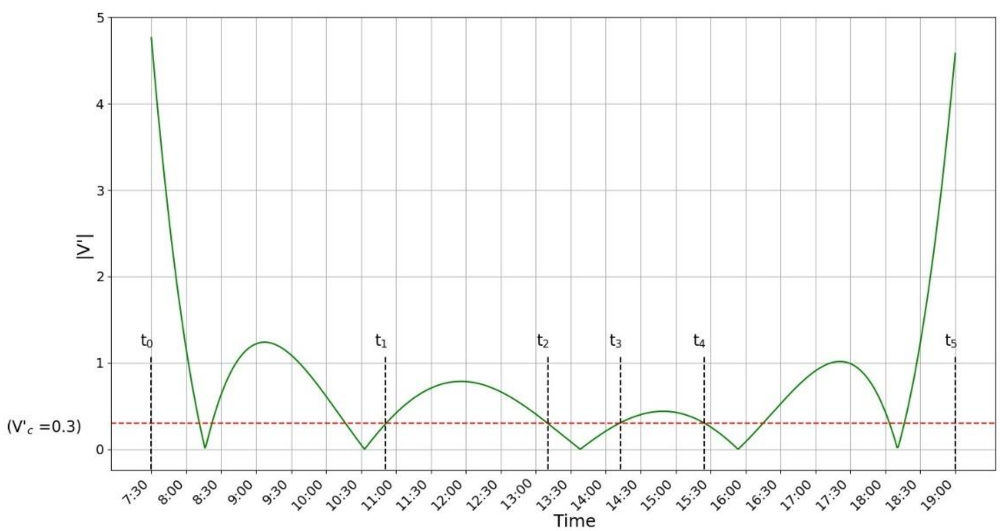

Figure 191: $V'(t)_{critical}$ = 0.3, Breakpoint Set 3

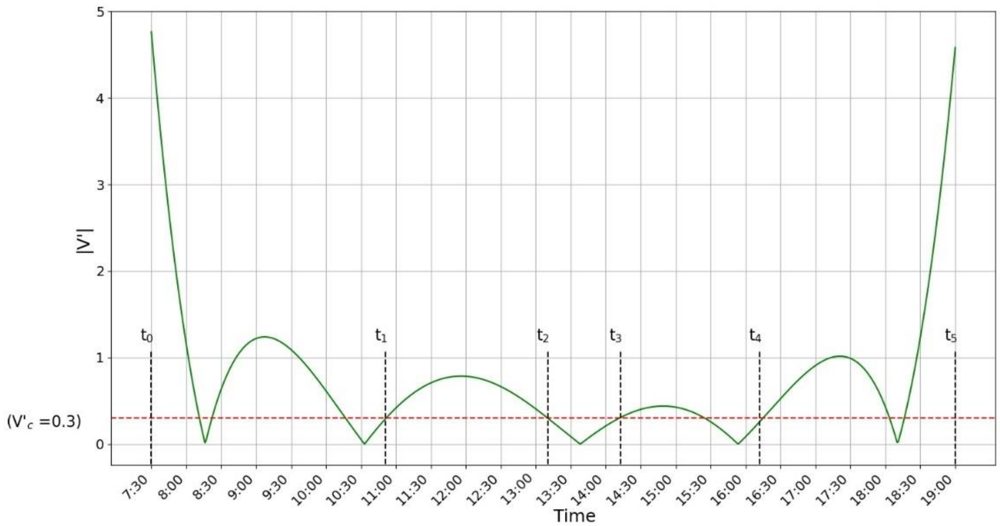

Figure 192: $V'(t)_{critical}$ = 0.3, Breakpoint Set 4

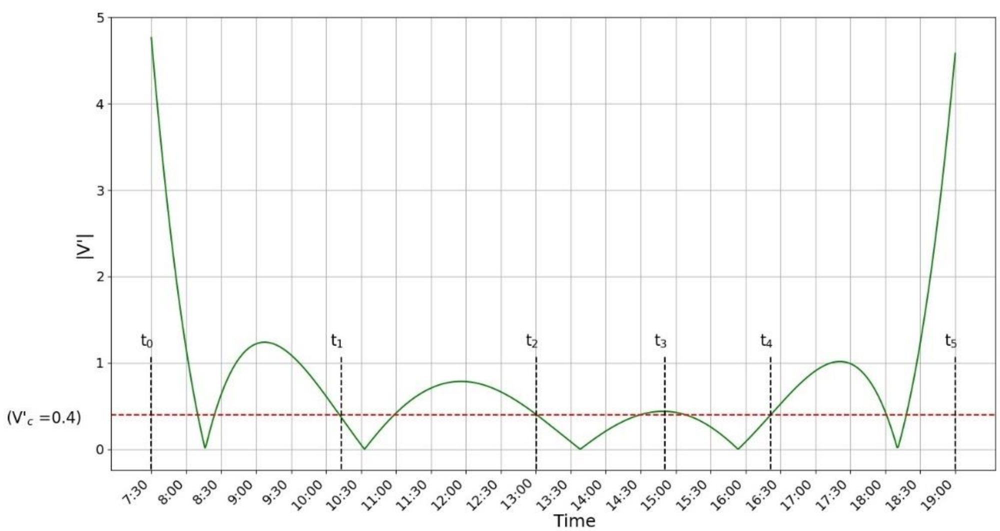

Figure 193: $V'(t)_{critical}$ = 0.4, Breakpoint Set 1

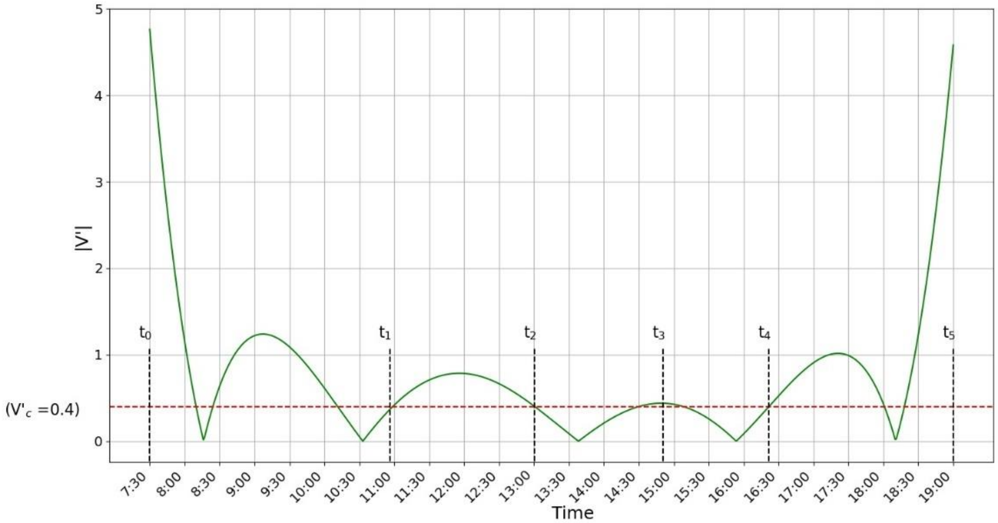

Figure 194: $V'(t)_{critical}$ = 0.4, Breakpoint Set 2

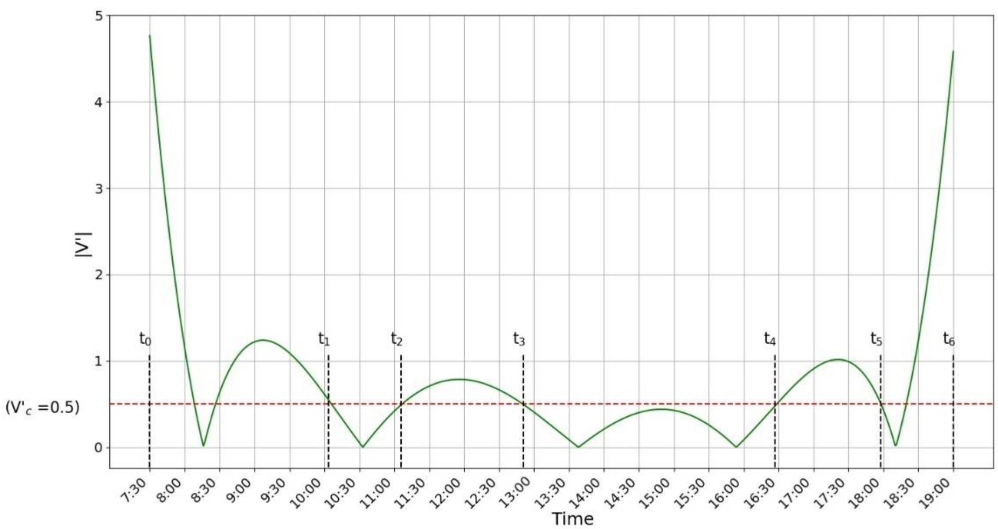

Figure 195: $V'(t)_{critical}$ = 0.5

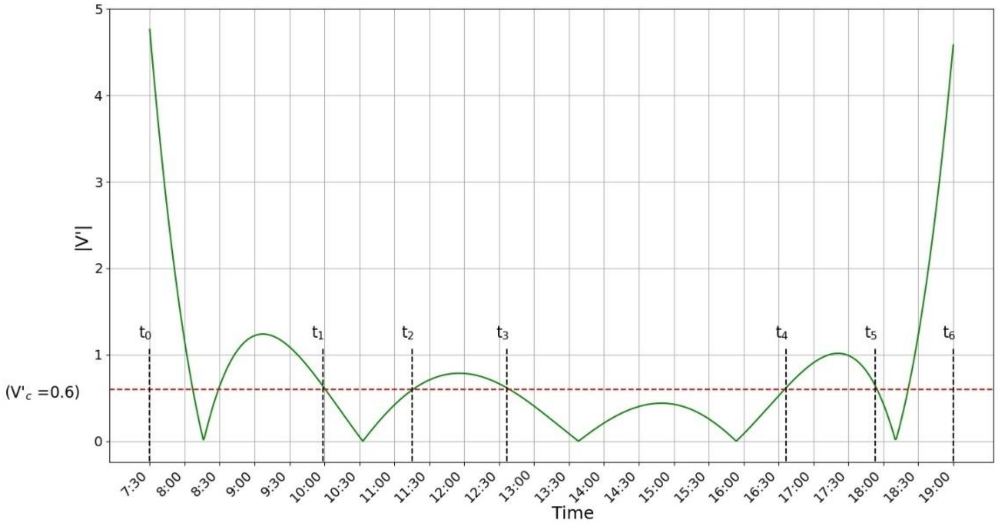

Figure 196: $V'(t)_{critical} = 0.6$

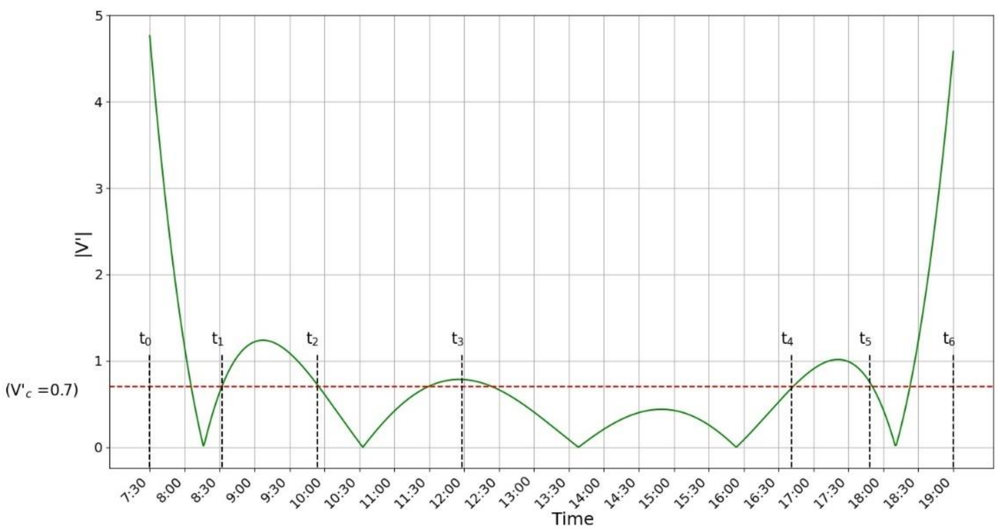

Figure 197: $V'(t)_{critical} = 0.7$

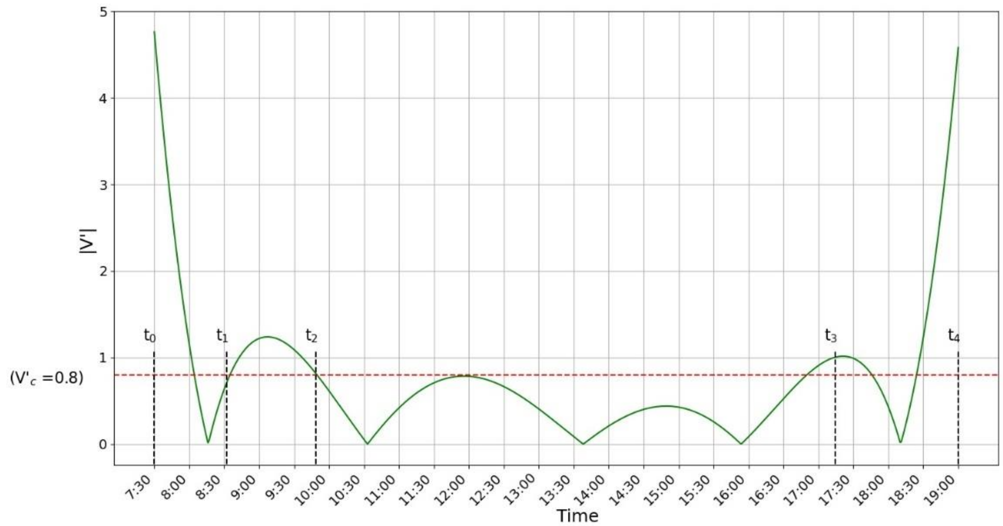

Figure 198: $\mathrm{V}'(\mathrm{t})_{\mathrm{critical}} = 0.8$

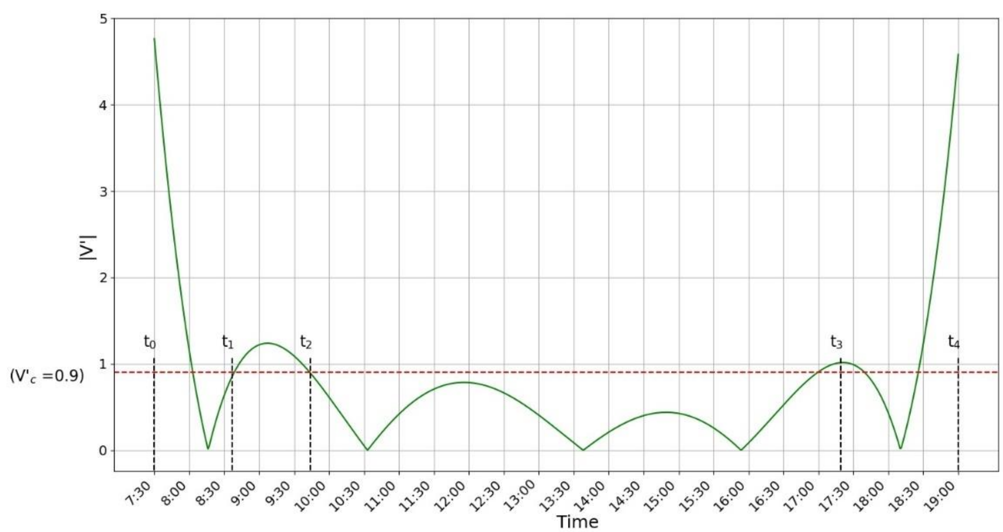

Figure 199: $\mathrm{V}'(\mathrm{t})_{\mathrm{critical}} = 0.9$

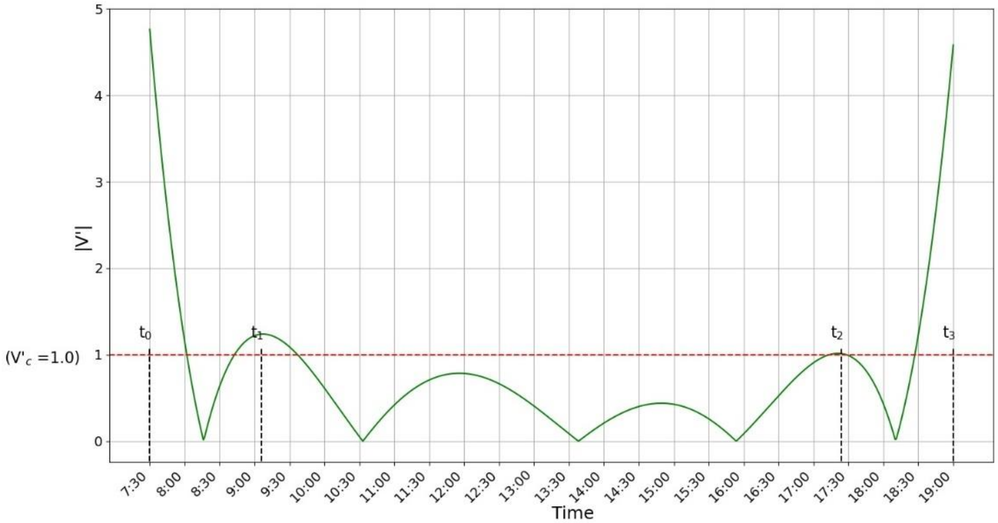

Figure 200: $\mathrm{V}'(\mathrm{t})_{\mathrm{critical}} = 1.0$

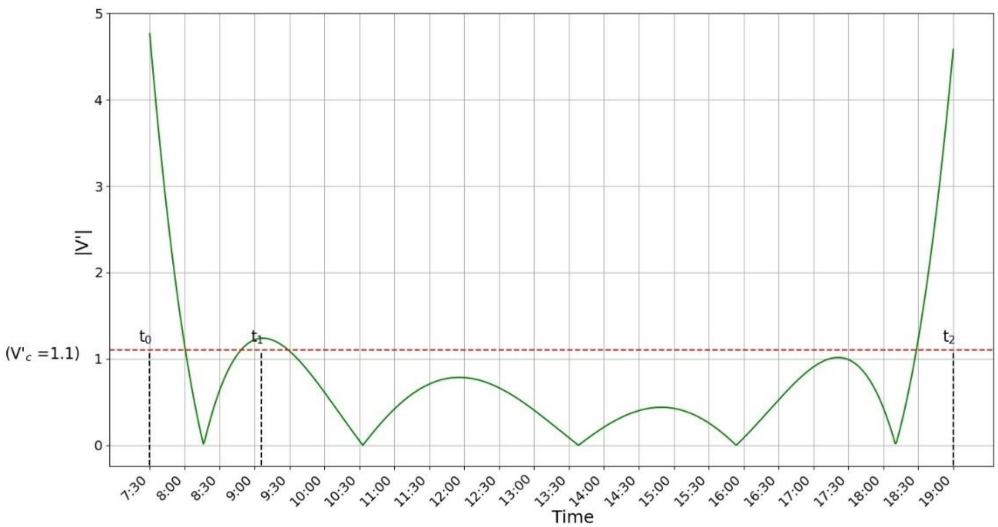

Figure 201: $\mathrm{V}'(\mathrm{t})_{\mathrm{critical}} = 1.1$

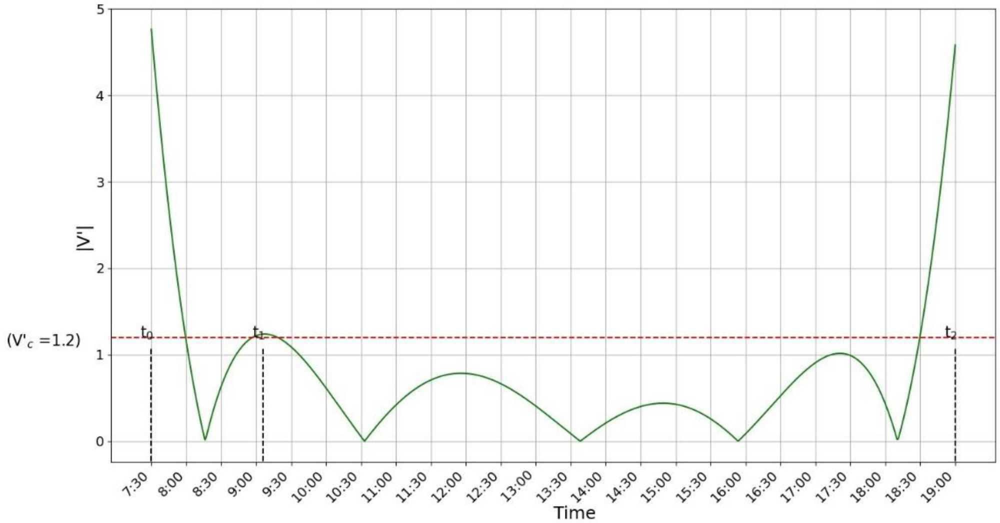

Figure 202: $V'(t)_{critical}$ = 1.2

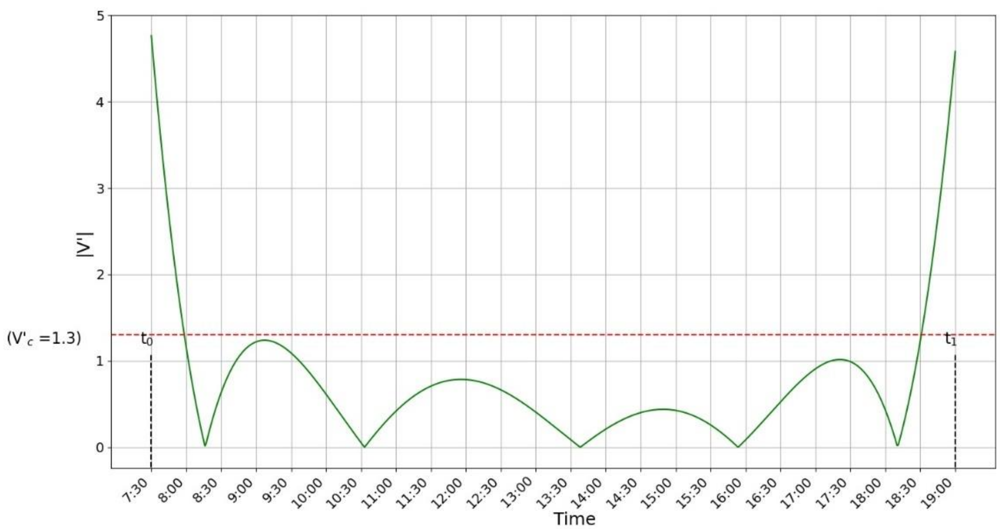

Figure 203: $V'(t)_{critical}$ = 1.3

Table 11 includes the developed breakpoints along with the values of delay and the figure number of each set of timing plan breakpoints.

Table 11: Results of Critical Zone Optimization Method

$V'(t)_{critical}$	Start time	End time	Total Delay (sec/veh)	Figure Number
0	07:00	10:30	50	Figure 172
	10:30	13:40		
	13:40	16:00		
	16:00	19:00		
0.1	07:00	10:25	46	Figure 173
	10:25	13:30		
	13:30	15:45		
	15:45	19:00		
0.1	07:00	10:25	45.7	Figure 174
	10:25	13:30		
	13:30	16:05		
	16:05	19:00		
0.1	07:00	10:25	45.5	Figure 175
	10:25	13:50		
	13:50	15:45		
	15:45	19:00		
0.1	07:00	10:25	45.2	Figure 176
	10:25	13:50		
	13:50	16:05		
	16:05	19:00		
0.1	07:00	10:35	46.7	Figure 177
	10:35	13:30		
	13:30	15:45		
	15:45	19:00		
0.1	07:00	10:35	46.3	Figure 178
	10:35	13:30		
	13:30	16:05		
	16:05	19:00		
0.1	07:00	10:35	46.3	Figure 179

Table 11: Results of Critical Zone Optimization Method (Continued)

$V'(t)_{critical}$	Start time	End time	Total Delay (sec/veh)	Figure Number
	10:35	13:50		
	13:50	15:45		
	15:45	19:00		
0.1	07:00	10:35	45.9	Figure 180
	10:35	13:50		
	13:50	16:05		
	16:05	19:00		
0.2	07:00	10:20	48.6	Figure 181
	10:20	13:20		
	13:20	15:35		
	15:35	19:00		
0.2	07:00	10:20	46.9	Figure 182
	10:20	13:20		
	13:20	16:10		
	16:10	19:00		
0.2	07:00	10:20	37.5	Figure 183
	10:20	14:00		
	14:00	15:35		
	15:35	19:00		
0.2	07:00	10:20	36	Figure 184
	10:20	14:00		
	14:00	16:10		
	16:10	19:00		
0.2	07:00	10:45	49	Figure 185
	10:45	13:20		
	13:20	15:35		
	15:35	19:00		
0.2	07:00	10:45	47.3	Figure 186
	10:45	13:20		
	13:20	16:10		
	16:10	19:00		
0.2	07:00	10:45	37.6	Figure 187
	10:45	14:00		
	14:00	15:35		
	15:35	19:00		
0.2	07:00	10:45	36.1	Figure 188

Table 11: Results of Critical Zone Optimization Method (Continued)

$V'(t)_{critical}$	Start time	End time	Total Delay (sec/veh)	Figure Number
	10:45	14:00		
	14:00	16:10		
	16:10	19:00		
0.3	07:00	10:20	30.7	Figure 189
	10:20	13:10		
	13:10	14:10		
	14:10	15:25		
	15:25	19:00		
0.3	07:00	10:20	30.8	Figure 190
	10:20	13:10		
	13:10	14:10		
	14:10	16:10		
	16:10	19:00		
0.3	07:00	10:50	30.8	Figure 191
	10:50	13:10		
	13:10	14:10		
	14:10	15:25		
	15:25	19:00		
0.3	07:00	10:50	30.9	Figure 192
	10:50	13:10		
	13:10	14:10		
	14:10	16:10		
	16:10	19:00		
0.4	07:00	10:15	29.3	Figure 193
	10:15	13:00		
	13:00	14:50		
	14:50	16:20		
	16:20	19:00		
0.4	07:00	11:00	29.3	Figure 194
	11:00	13:00		
	13:00	14:50		
	14:50	16:20		
	16:20	19:00		
0.5	07:00	10:05	33.1	Figure 195
	10:05	11:05		
	11:05	12:50		

Table 11: Results of Critical Zone Optimization Method (Continued)

$V'(t)_{critical}$	Start time	End time	Total Delay (sec/veh)	Figure Number
	12:50	16:25		
	16:25	18:00		
	18:00	19:00		
0.6	07:00	10:00	26.8	Figure 196
	10:00	11:15		
	11:15	12:35		
	12:35	16:35		
	16:35	18:00		
	18:00	19:00		
0.7	07:00	08:30	56.6	Figure 197
	08:30	10:00		
	10:00	12:00		
	12:00	16:40		
	16:40	17:50		
	17:50	19:00		
0.8	07:00	08:30	74	Figure 198
	08:30	09:50		
	09:50	17:15		
	17:15	19:00		
0.9	07:00	08:35	78.3	Figure 199
	08:35	09:45		
	09:45	17:20		
	17:20	19:00		
1	07:00	09:05	55	Figure 200
	09:05	17:25		
	17:25	19:00		
1.1	07:00	09:05	119.6	Figure 201
	09:05	19:00		
1.2	07:00	09:05	119.6	Figure 202
	09:05	19:00		
1.3	07:00	19:00	159.3	Figure 203

***ΔV Optimization Method*:**

Figure 204 to Figure 217 show the developed breakpoints by using the ΔV optimization method.

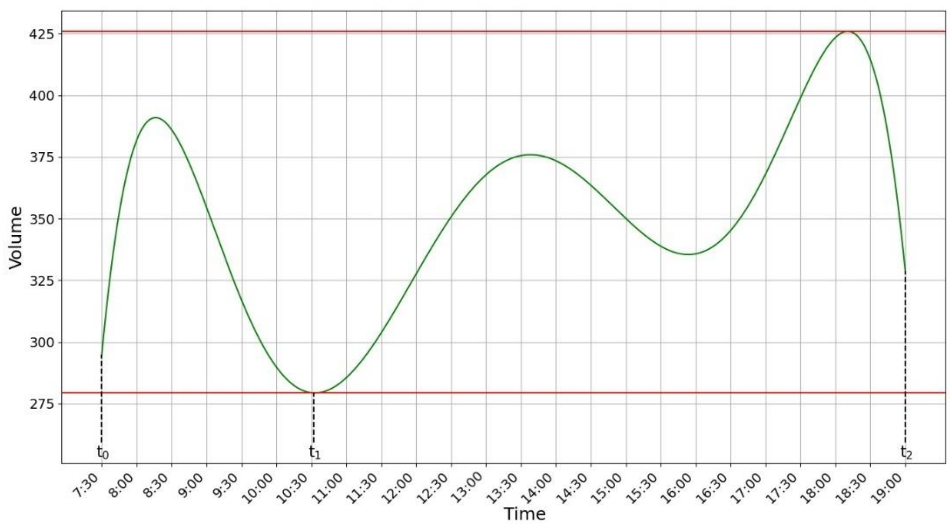

Figure 204: $\Delta\mathrm{V} = \mathrm{Range}/1$

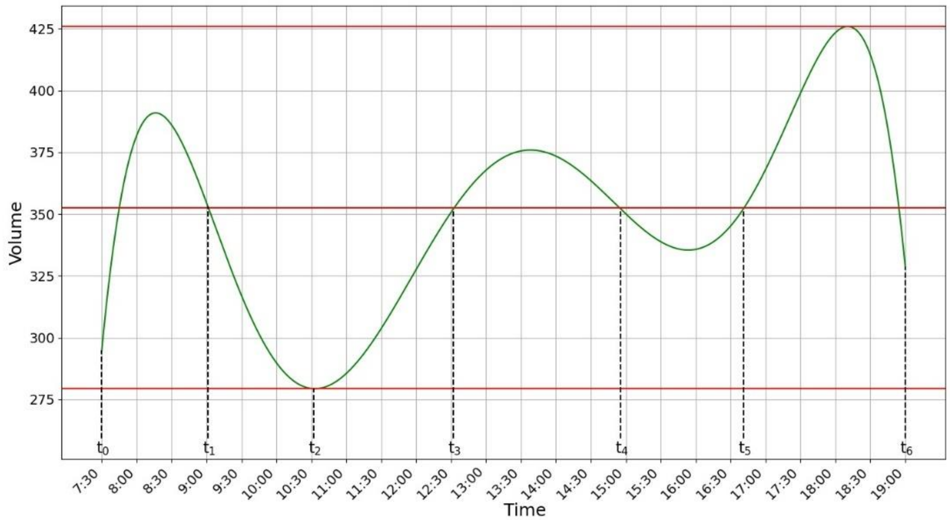

Figure 205: $\Delta V = \text{Range}/2$

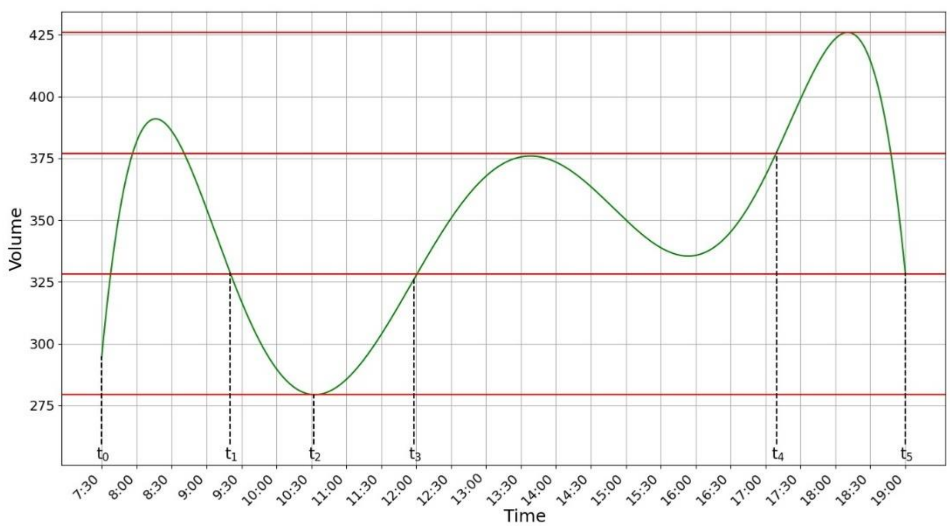

Figure 206: $\Delta V = \text{Range}/3$, Breakpoint Set 1

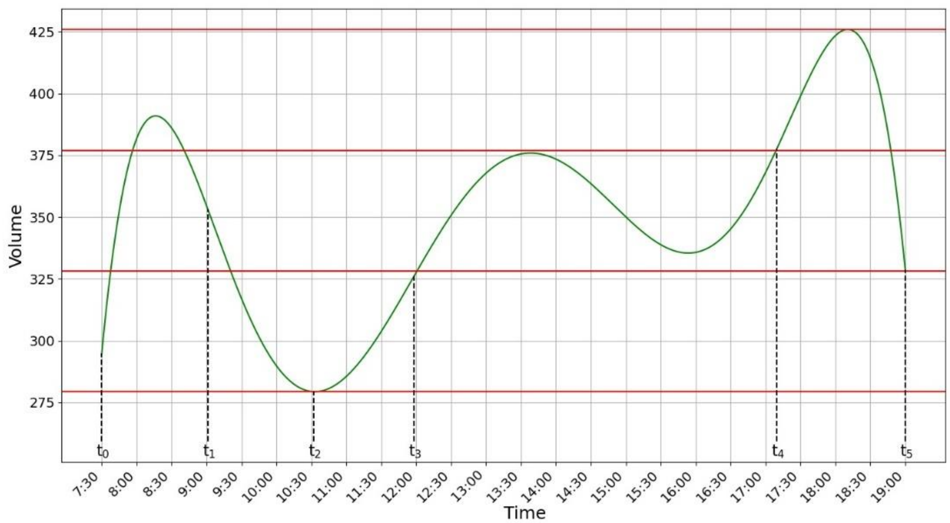

Figure 207: $\Delta V = \text{Range}/3$, Breakpoint Set 2

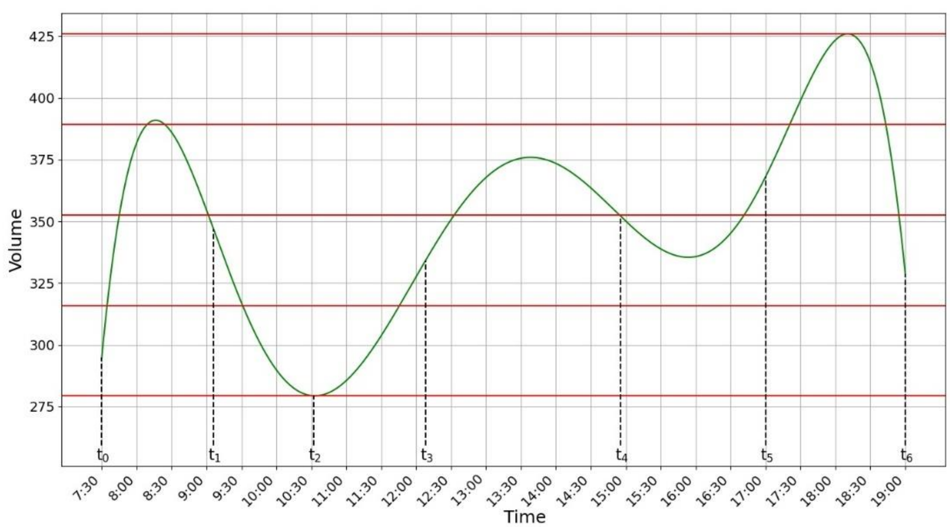

Figure 208: $\Delta V = \text{Range}/4$, Breakpoint Set 1

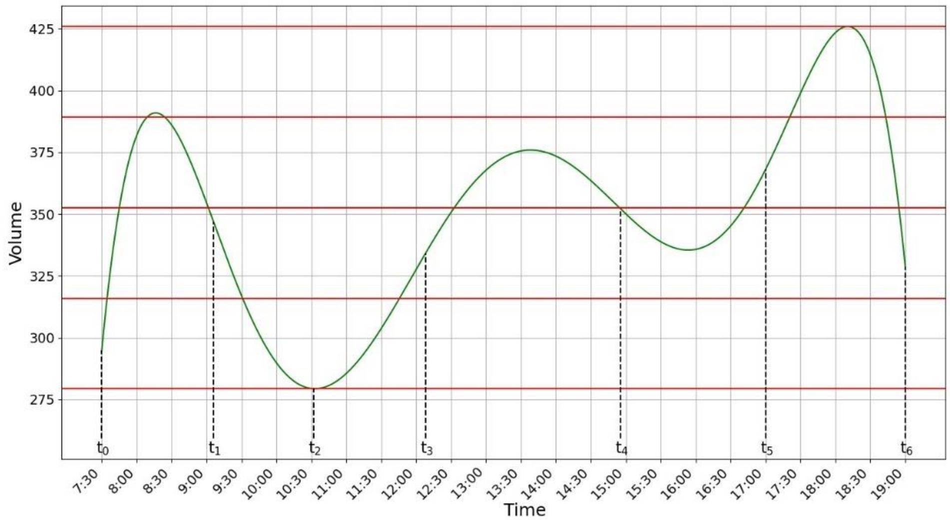

Figure 209: $\Delta V = \text{Range}/4$, Breakpoint Set 2

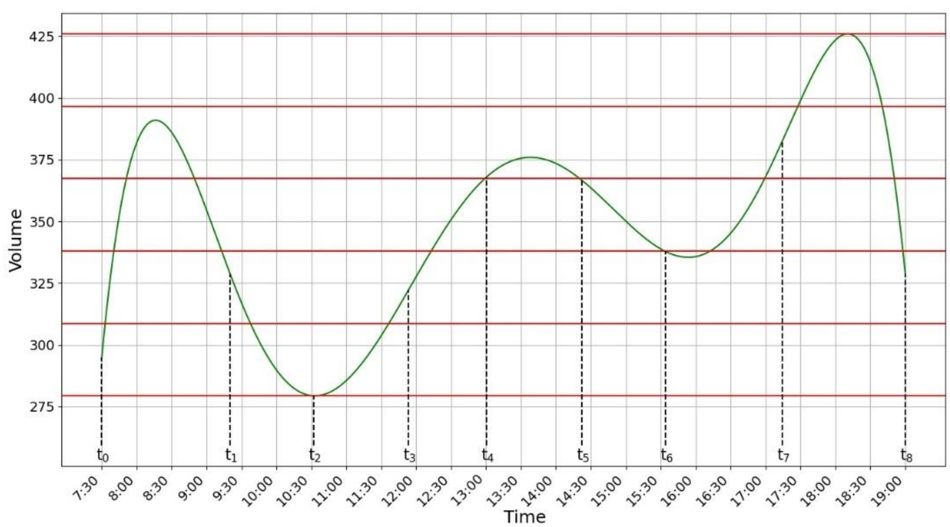

Figure 210: $\Delta V = \text{Range}/5$, Breakpoint Set 1

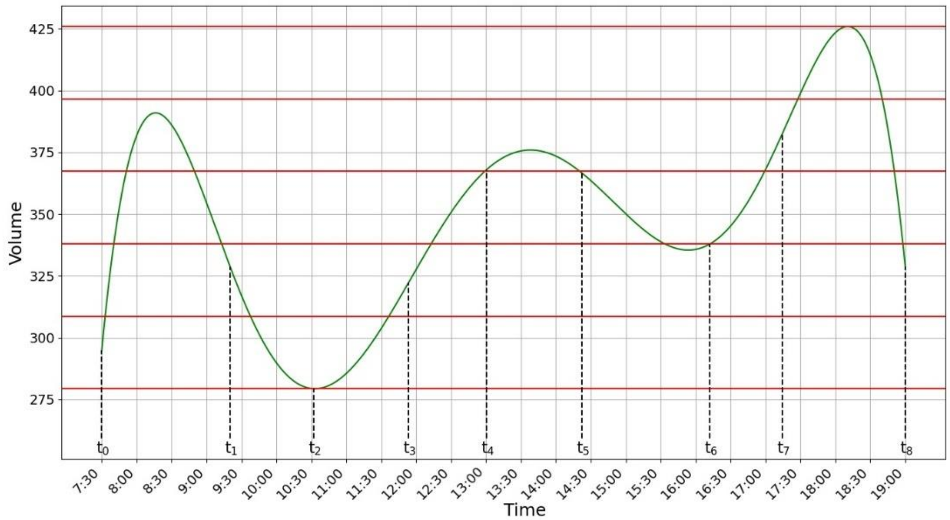

Figure 211: $\Delta V = \text{Range}/5$, Breakpoint Set 2

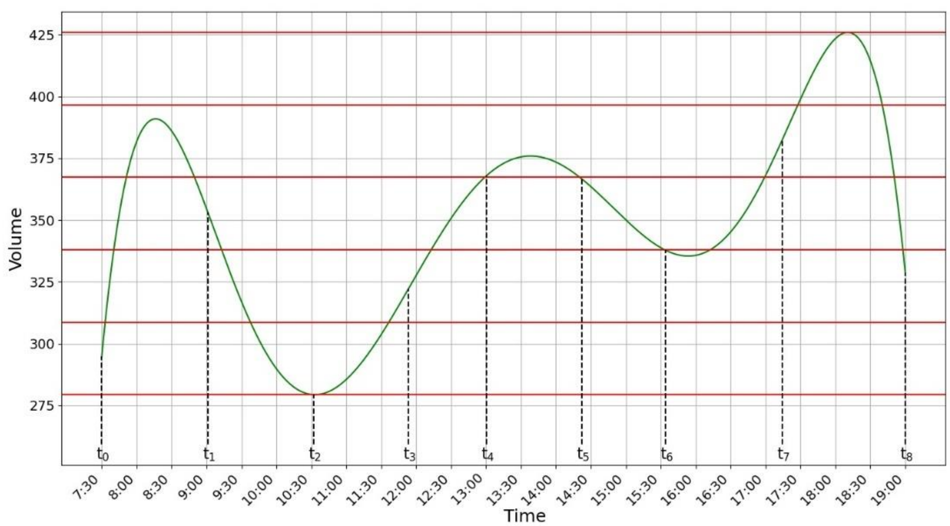

Figure 212: $\Delta V = \text{Range}/5$, Breakpoint Set 3

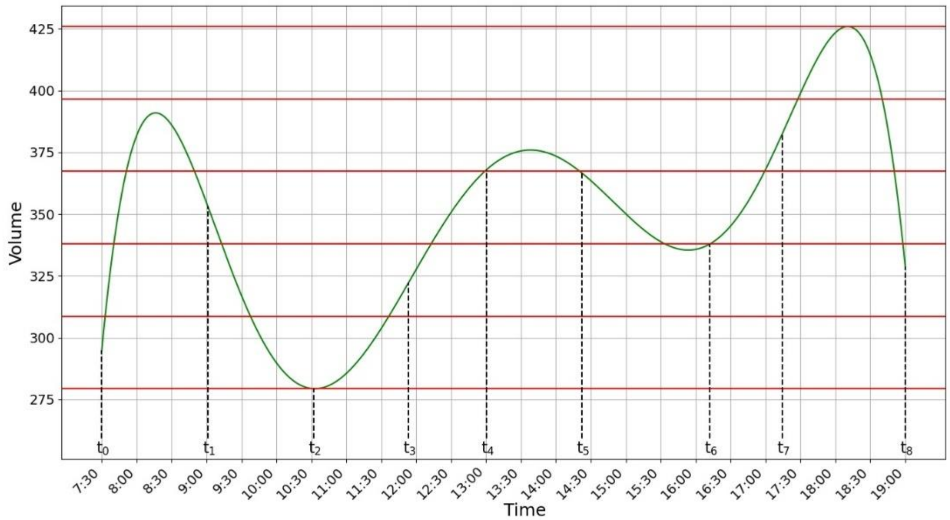

Figure 213: $\Delta\text{V} = \text{Range}/5$, Breakpoint Set 4

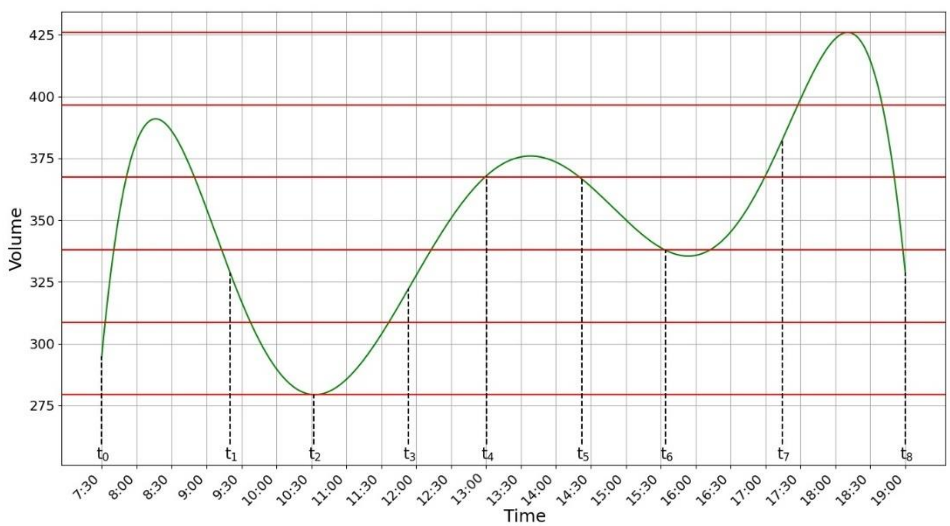

Figure 214: $\Delta\text{V} = \text{Range}/5$, Breakpoint Set 5

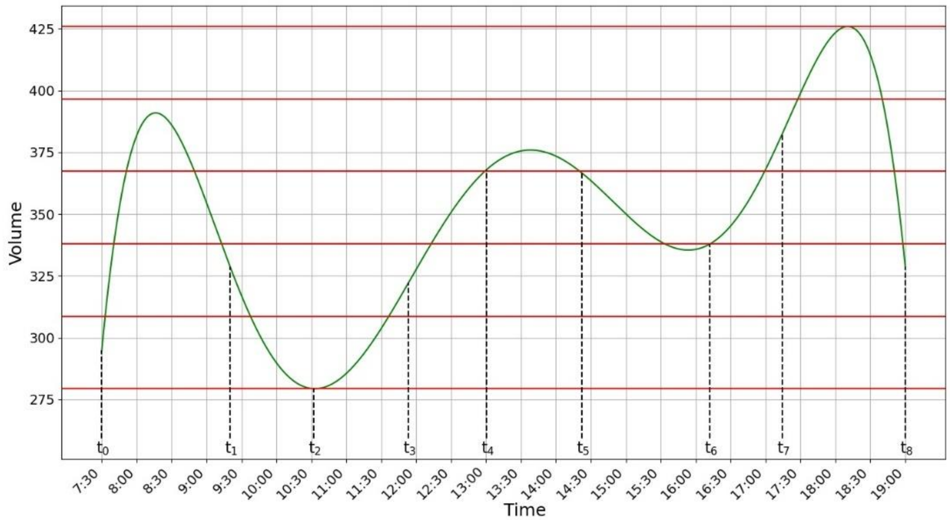

Figure 215: $\Delta V = \text{Range}/5$, Breakpoint Set 6

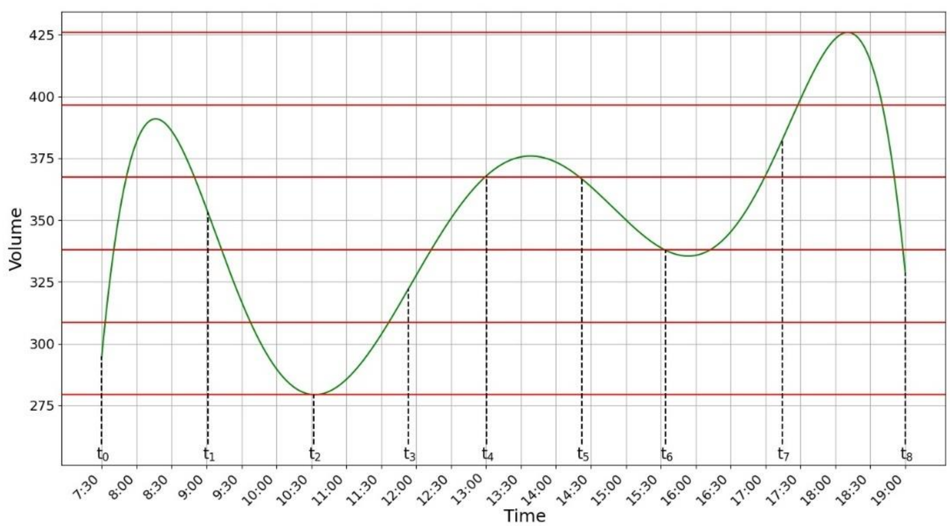

Figure 216: $\Delta V = \text{Range}/5$, Breakpoint Set 7

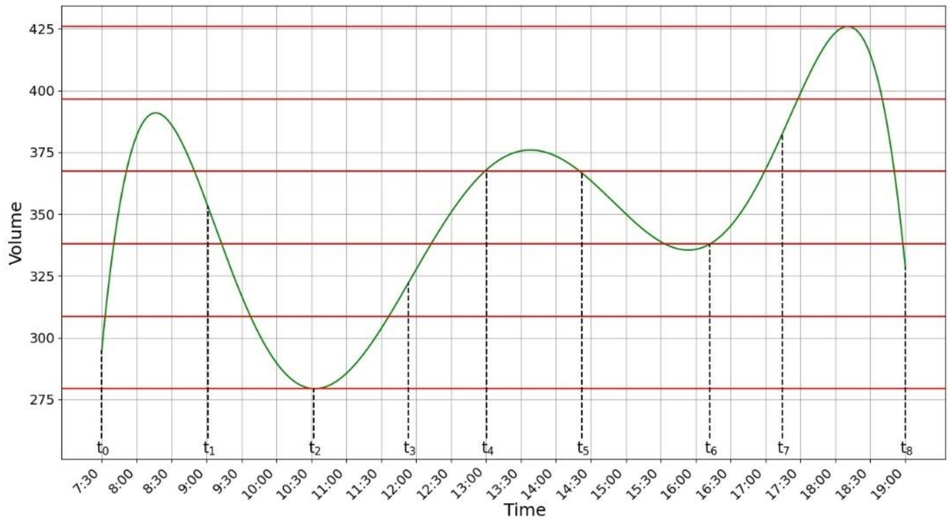

Figure 217: $\Delta V = \text{Range}/5$, Breakpoint Set 8

Table 12 includes the developed breakpoints along with the values of delay and the figure number of each set of timing plan breakpoints.

Table 12: Results of ΔV Optimization Method

ΔV	Start time	End time	Total Delay (sec/veh)	Figure Number
range/1	07:00	10:30	105.3	Figure 204
	10:30	19:00		
range/2	07:00	09:00	33.2	Figure 205
	09:00	10:30		
	10:30	12:30		
	12:30	15:00		
	15:00	16:40		
	16:40	19:00		
range/3	07:00	09:20	52.7	Figure 206
	09:20	10:30		
	10:30	12:00		
	12:00	17:10		
	17:10	19:00		
range/3	07:00	09:00	52.5	Figure 207
	09:00	10:30		
	10:30	12:00		
	12:00	17:10		
	17:10	19:00		
range/4	07:00	09:05	41.2	Figure 208
	09:05	10:30		
	10:30	12:10		
	12:10	15:00		
	15:00	17:00		
	17:00	19:00		
range/4	07:00	09:05	41.2	Figure 209
	09:05	10:30		
	10:30	12:10		
	12:10	15:00		
	15:00	17:00		
	17:00	19:00		
range/5	07:00	09:20	27.2	Figure 210
	09:20	10:30		
	10:30	12:00		
	12:00	13:00		
	13:00	14:20		
	14:20	15:35		

Table 12: Results of ΔV Optimization Method (Continued)

ΔV	Start time	End time	Total Delay (sec/veh)	Figure Number
	15:35	17:15		
	17:15	19:00		
range/5	07:00	09:20	29.5	Figure 211
	09:20	10:30		
	10:30	12:00		
	12:00	13:00		
	13:00	14:20		
	14:20	16:10		
	16:10	17:15		
	17:15	19:00		
range/5	07:00	09:00	27.1	Figure 212
	09:00	10:30		
	10:30	12:00		
	12:00	13:00		
	13:00	14:20		
	14:20	15:35		
	15:35	17:15		
	17:15	19:00		
range/5	07:00	09:00	29.4	Figure 213
	09:00	10:30		
	10:30	12:00		
	12:00	13:00		
	13:00	14:20		
	14:20	16:10		
	16:10	17:15		
	17:15	19:00		
range/5	07:00	09:20	27.2	Figure 214
	09:20	10:30		
	10:30	12:00		
	12:00	13:00		
	13:00	14:20		
	14:20	15:35		
	15:35	17:15		
	17:15	19:00		
range/5	07:00	09:20	29.5	Figure 215
	09:20	10:30		

Table 12: Results of ΔV Optimization Method (Continued)

ΔV	Start time	End time	Total Delay (sec/veh)	Figure Number
	10:30	12:00		
	12:00	13:00		
	13:00	14:20		
	14:20	16:10		
	16:10	17:15		
	17:15	19:00		
range/5	07:00	09:00	27.1	Figure 216
	09:00	10:30		
	10:30	12:00		
	12:00	13:00		
	13:00	14:20		
	14:20	15:35		
	15:35	17:15		
	17:15	19:00		
range/5	07:00	09:00	29.4	Figure 217
	09:00	10:30		
	10:30	12:00		
	12:00	13:00		
	13:00	14:20		
	14:20	16:10		
	16:10	17:15		
	17:15	19:00		

George Bush Dr. and Texas Ave Intersection, Feb 13, 2019:

Below are the optimization results by using both of the developed optimization techniques for the traffic counts data of the intersection of George Bush Dr. and Texas Ave. on February 13, 2019.

Critical Zone Optimization Technique:

Figure 218 to Figure 255 show the developed breakpoints by using the critical zone optimization method.

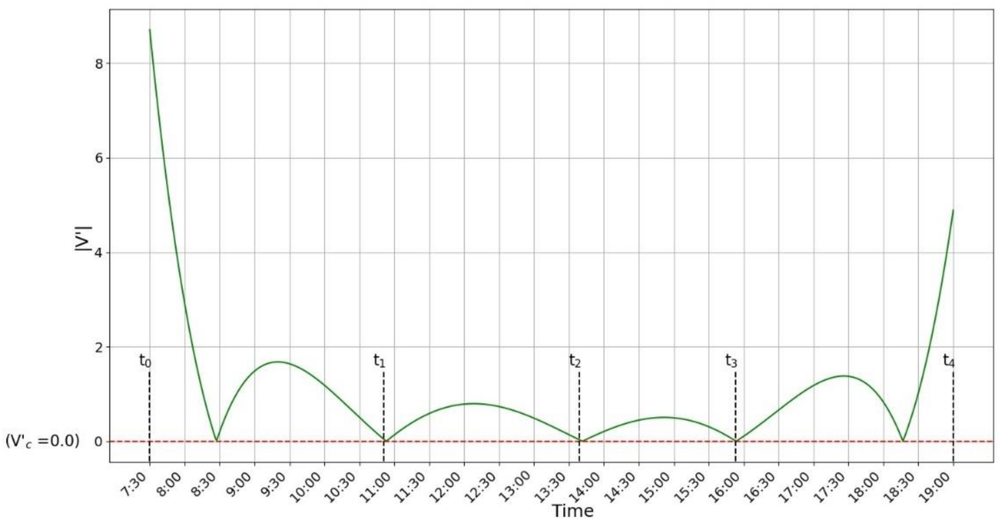

Figure 218: $V'(t)_{critical}$ = 0.0

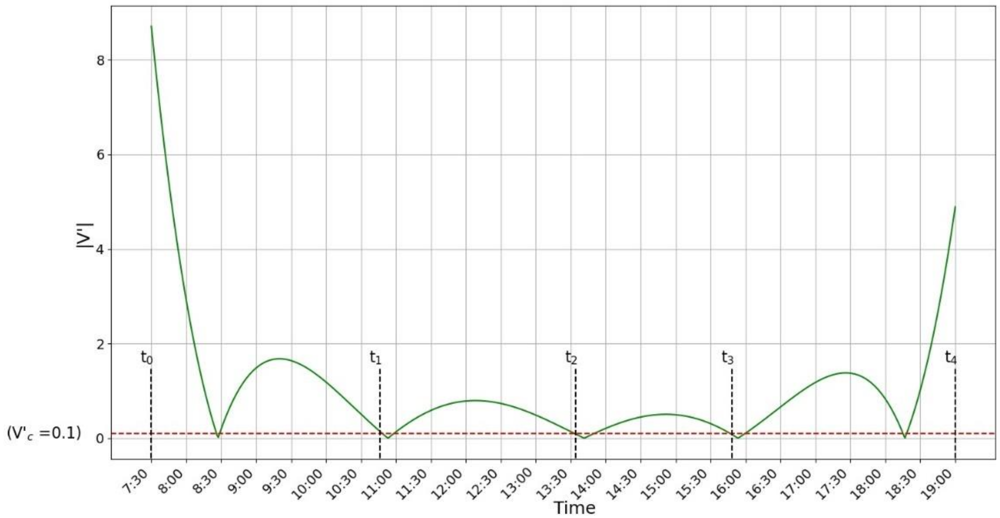

Figure 219: $V'(t)_{critical}$ = 0.1, Breakpoint Set 1

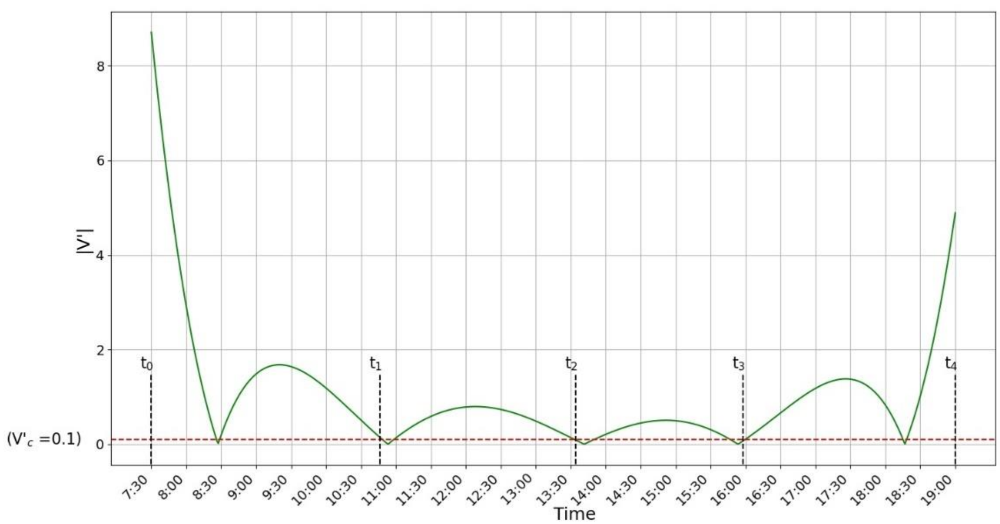

Figure 220: $V'(t)_{critical}$ = 0.1, Breakpoint Set 1

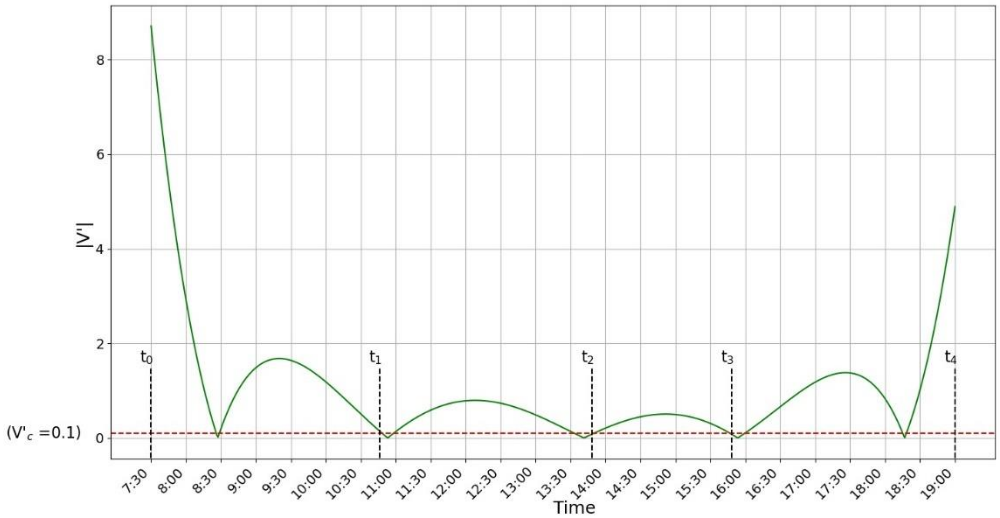

Figure 221: $V'(t)_{critical}$ = 0.1, Breakpoint Set 1

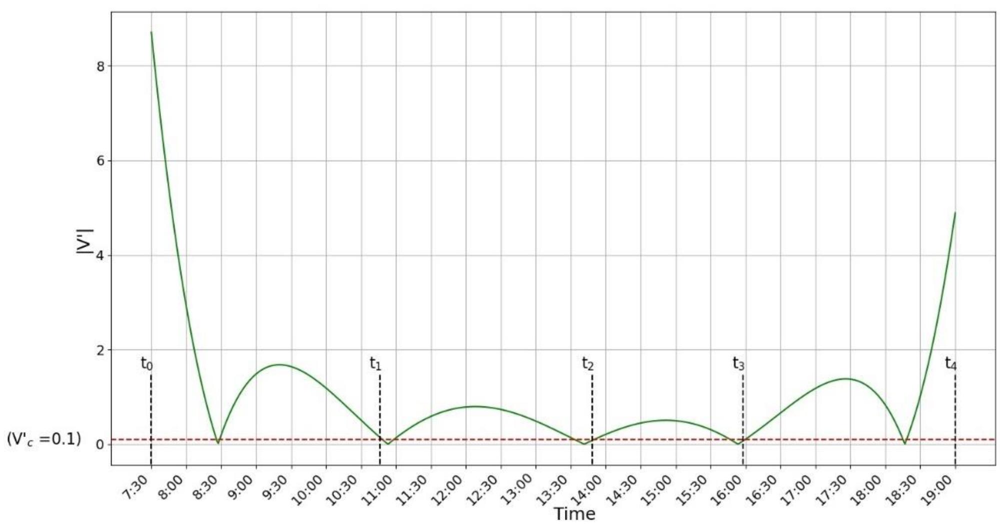

Figure 222: $V'(t)_{critical}$ = 0.1, Breakpoint Set 1

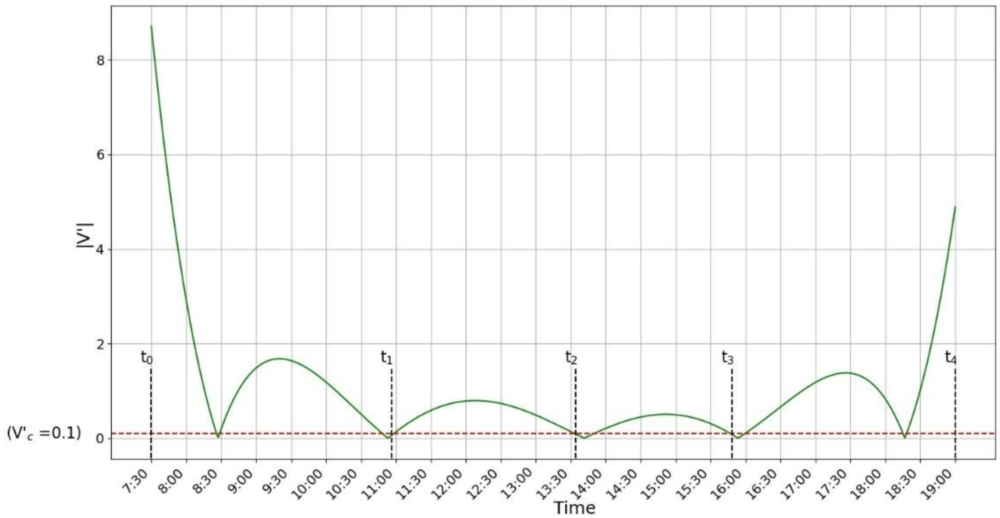

Figure 223: $V'(t)_{critical}$ = 0.1, Breakpoint Set 1

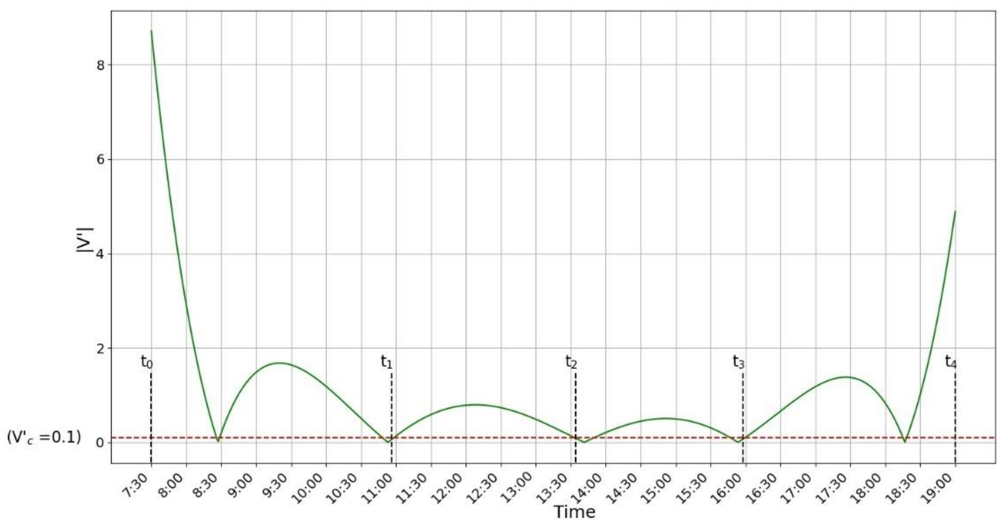

Figure 224: $V'(t)_{critical}$ = 0.1, Breakpoint Set 1

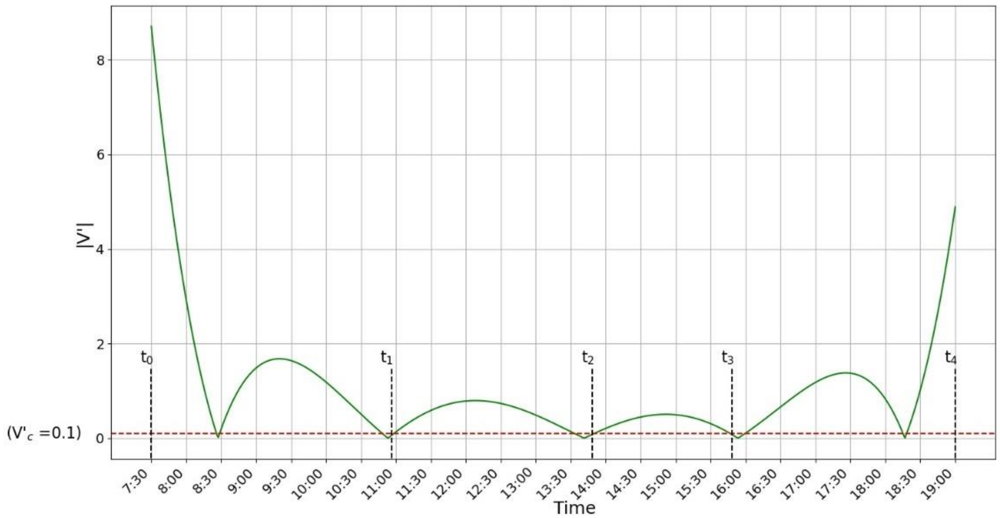

Figure 225: $V'(t)_{critical}$ = 0.1, Breakpoint Set 1

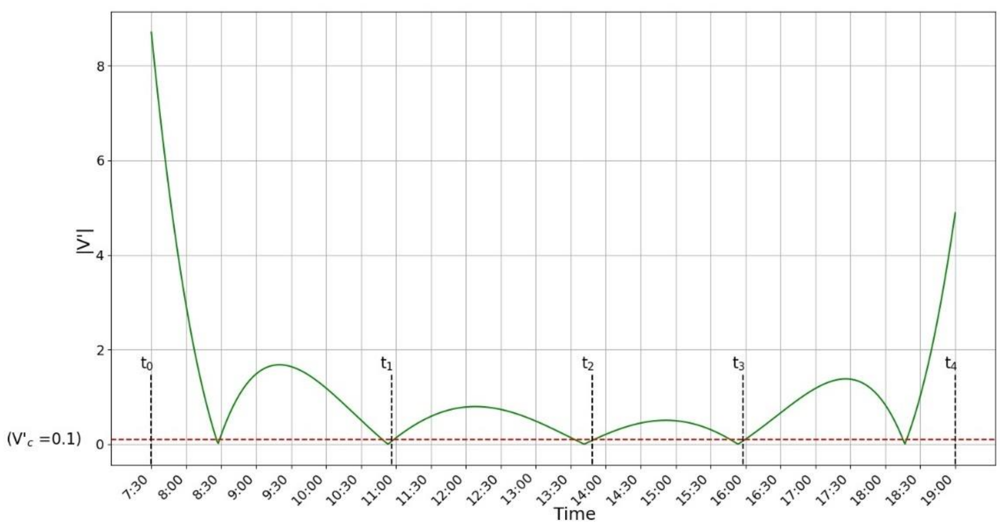

Figure 226: $V'(t)_{critical}$ = 0.1, Breakpoint Set 1

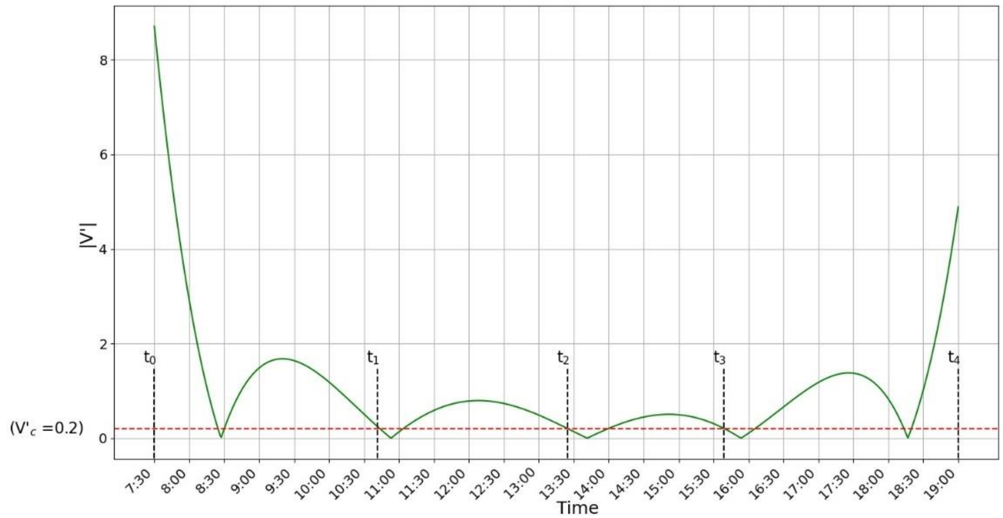

Figure 227: $V'(t)_{critical}$ = 0.2, Breakpoint Set 1

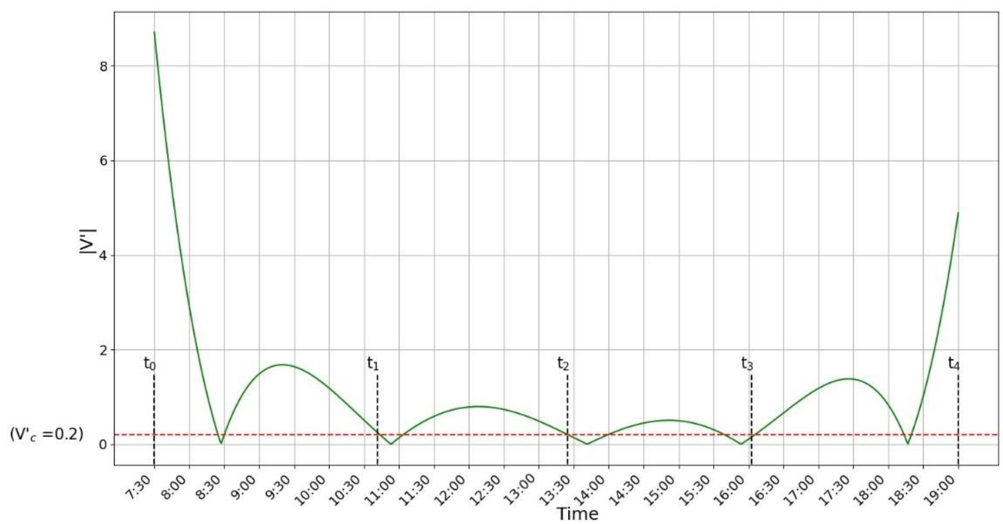

Figure 228: $V'(t)_{critical}$ = 0.2, Breakpoint Set 1

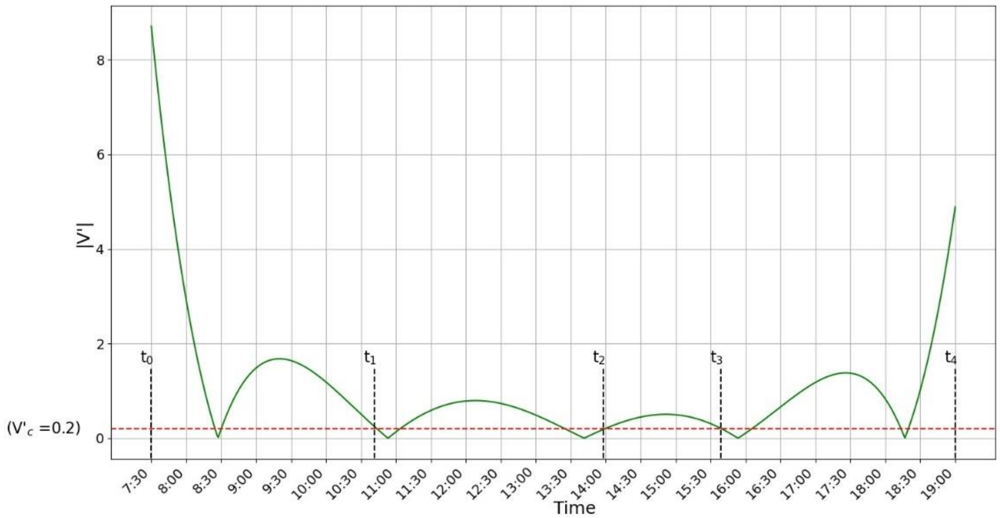

Figure 229: $V'(t)_{critical}$ = 0.2, Breakpoint Set 1

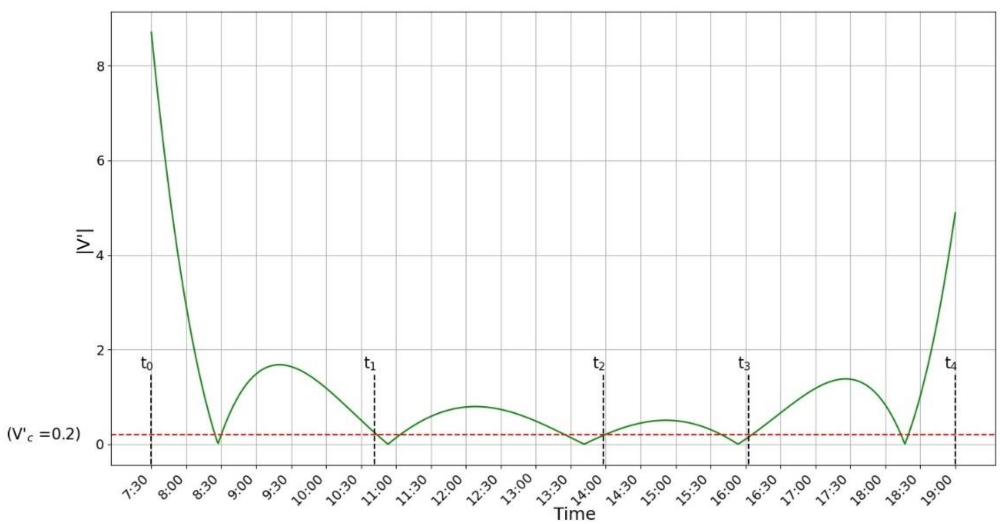

Figure 230: $V'(t)_{critical}$ = 0.2, Breakpoint Set 1

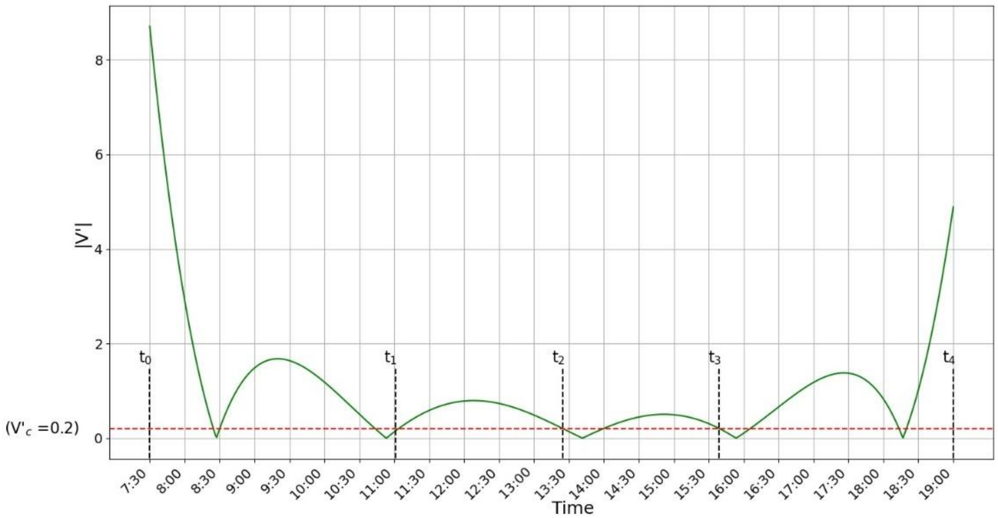

Figure 231: $V'(t)_{critical}$ = 0.2, Breakpoint Set 1

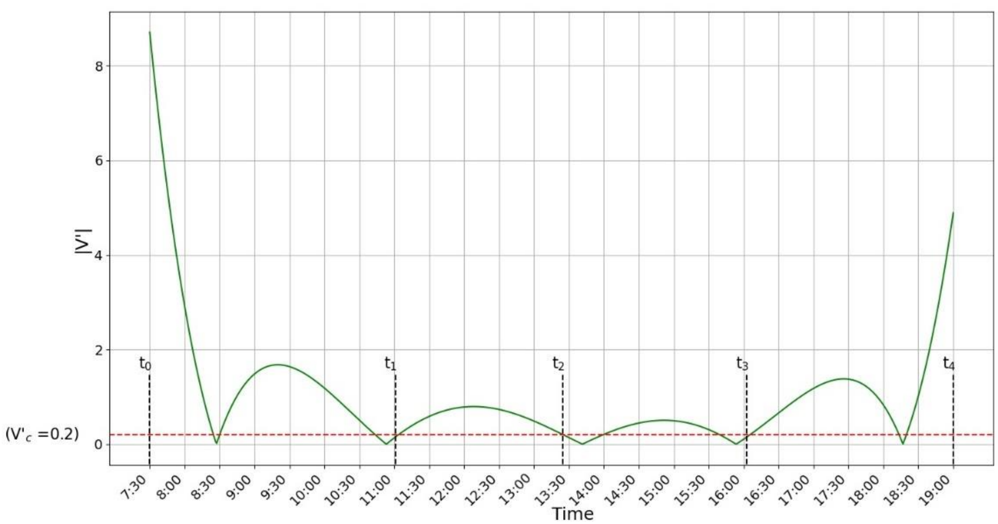

Figure 232: $V'(t)_{critical}$ = 0.2, Breakpoint Set 1

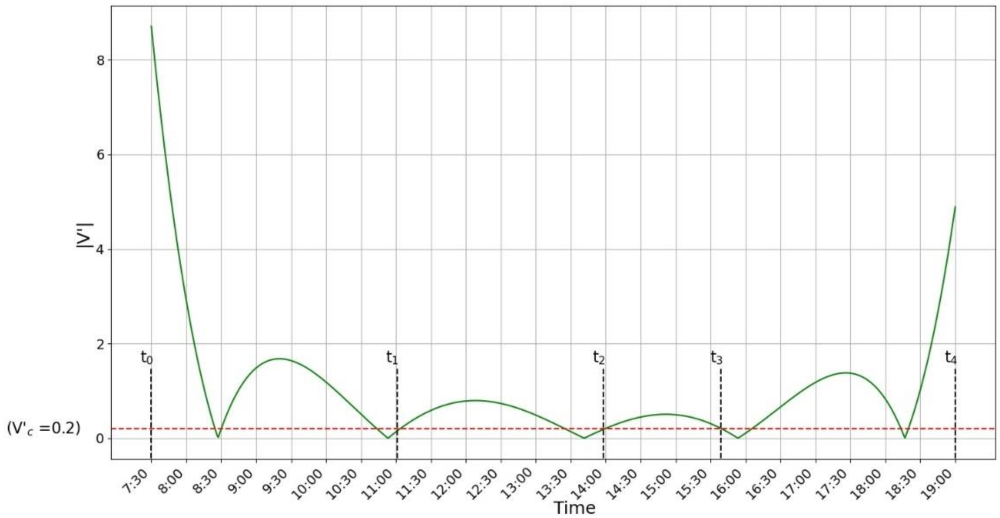

Figure 233: $V'(t)_{critical}$ = 0.2, Breakpoint Set 1

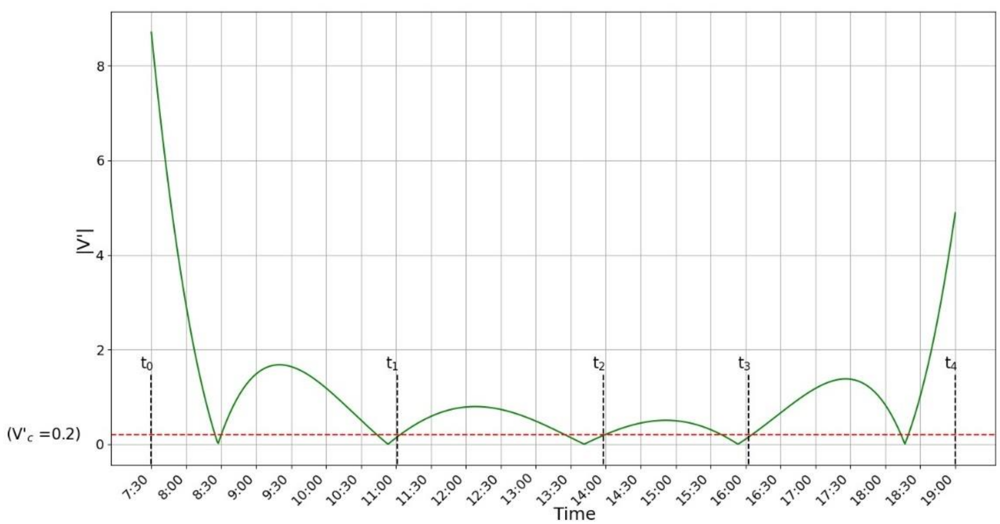

Figure 234: $V'(t)_{critical}$ = 0.2, Breakpoint Set 1

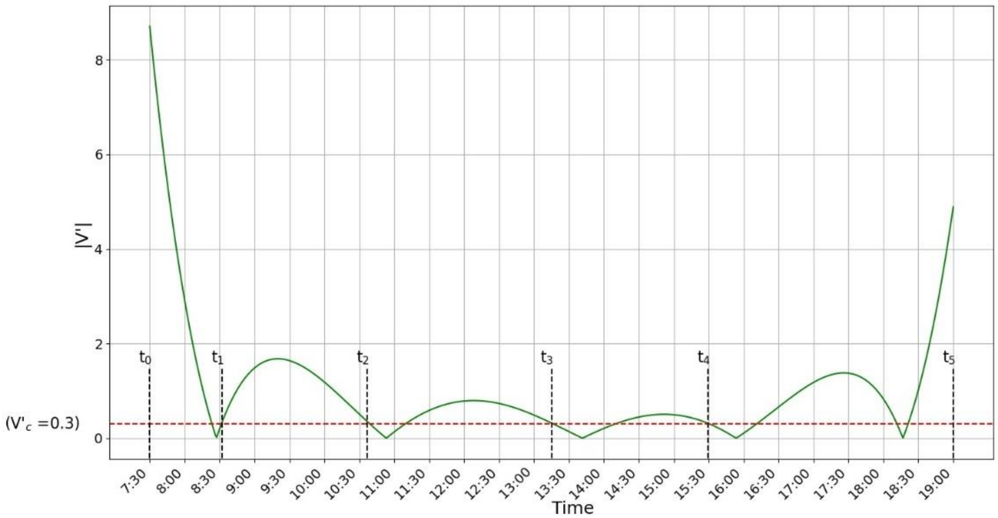

Figure 235: $V'(t)_{critical}$ = 0.3, Breakpoint Set 1

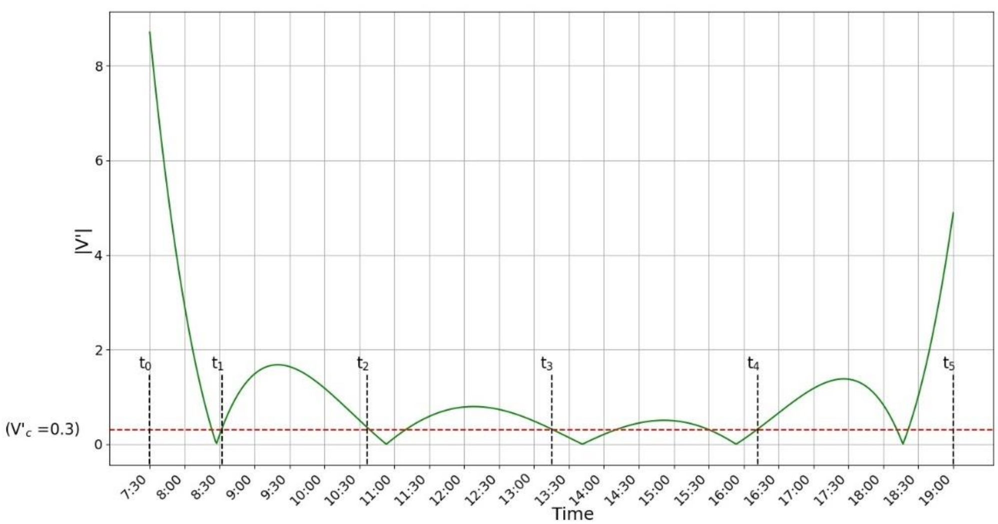

Figure 236: $V'(t)_{critical}$ = 0.3, Breakpoint Set 1

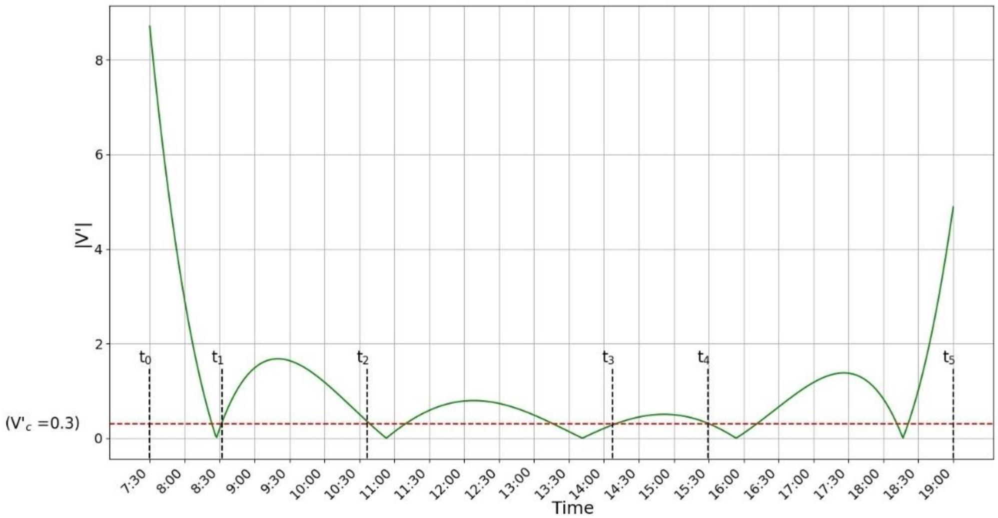

Figure 237: $V'(t)_{critical}$ = 0.3, Breakpoint Set 1

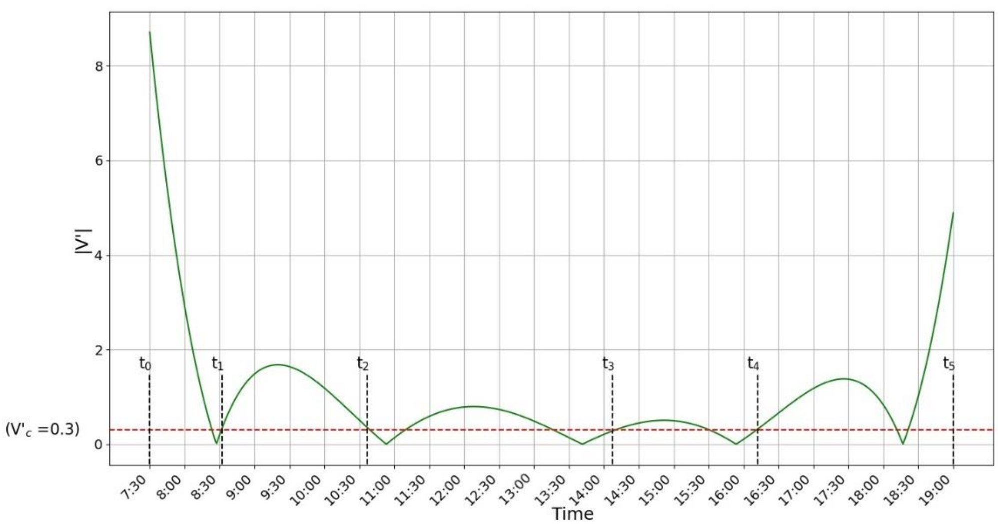

Figure 238: $V'(t)_{critical}$ = 0.3, Breakpoint Set 1

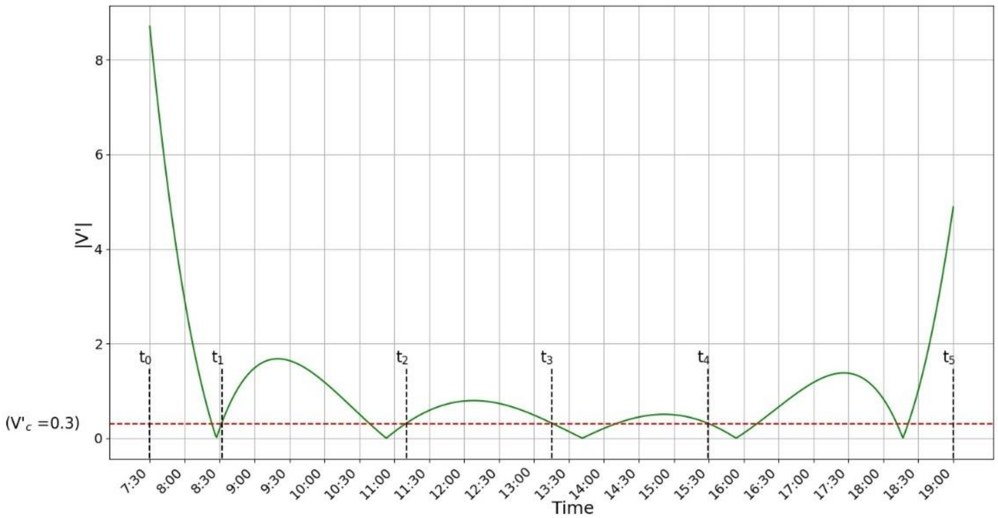

Figure 239: $V'(t)_{critical}$ = 0.3, Breakpoint Set 1

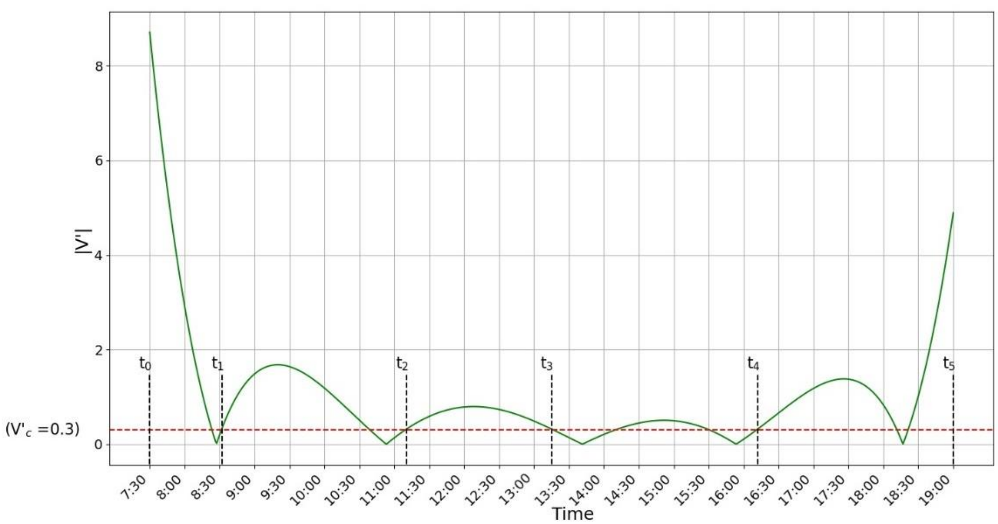

Figure 240: $V'(t)_{critical}$ = 0.3, Breakpoint Set 1

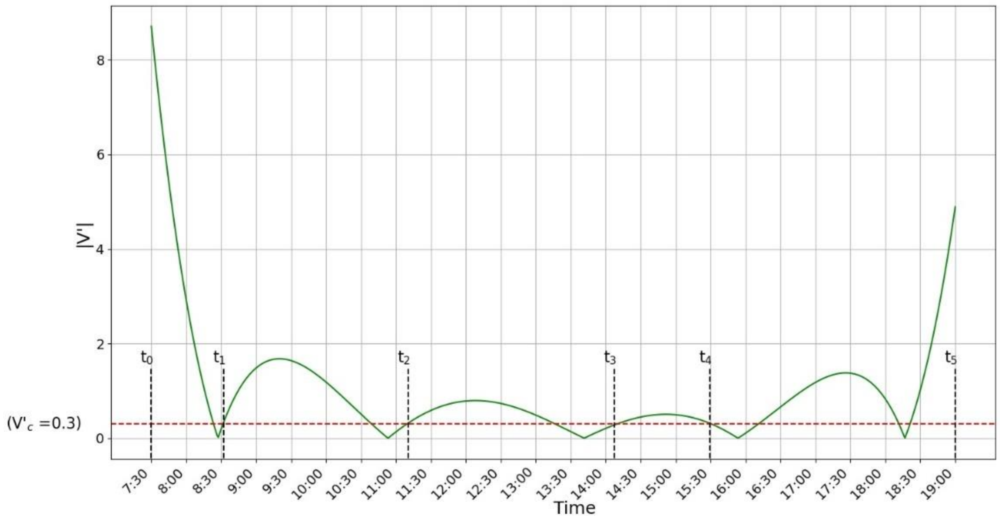

Figure 241: $V'(t)_{critical}$ = 0.3, Breakpoint Set 1

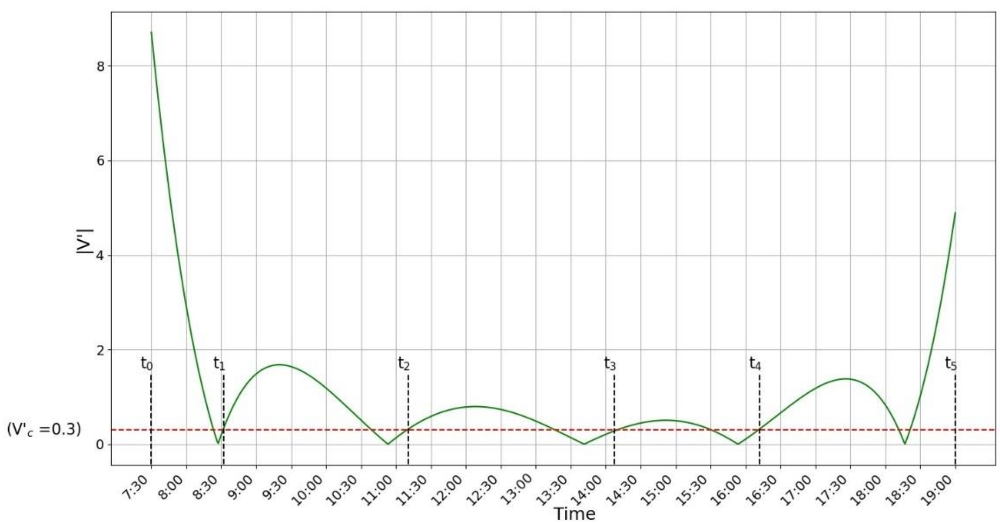

Figure 242: $V'(t)_{critical}$ = 0.3, Breakpoint Set 1

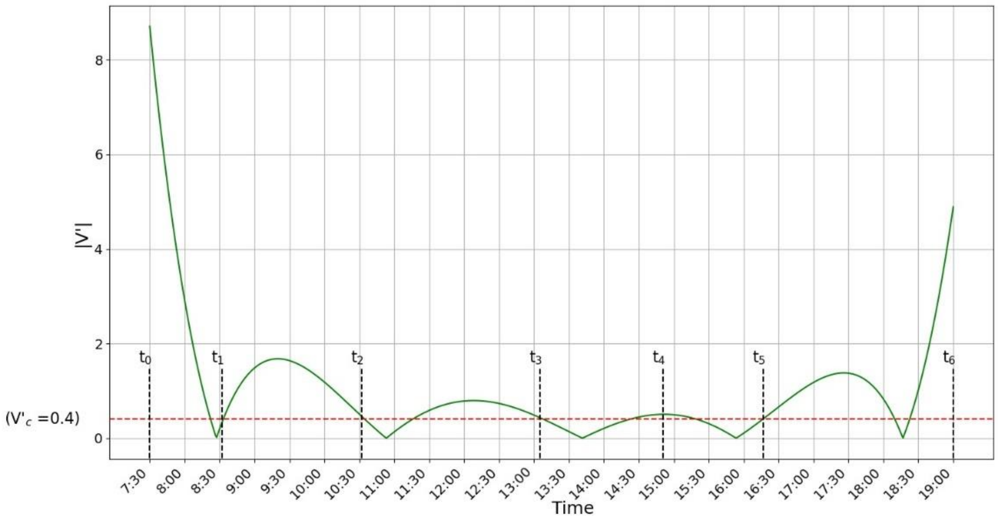

Figure 243: $V'(t)_{critical}$ = 0.4, Breakpoint Set 1

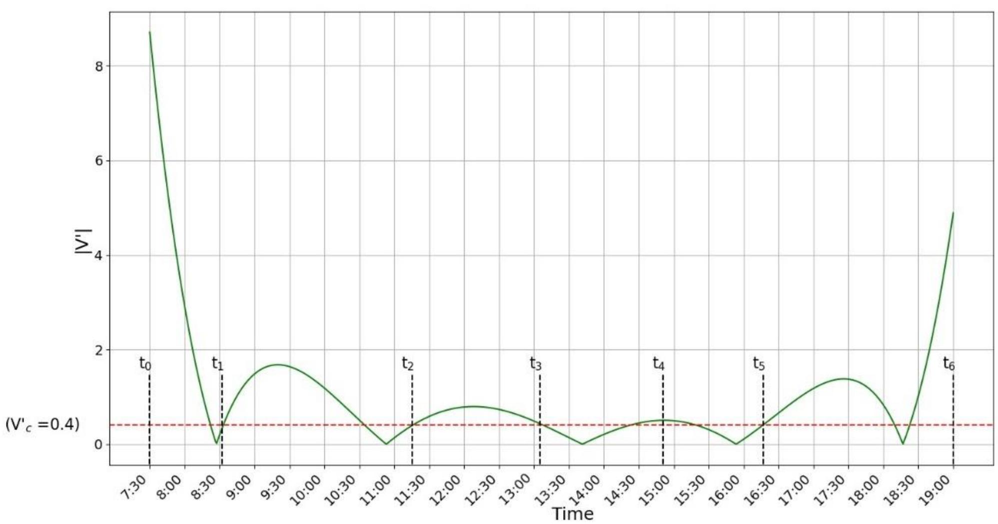

Figure 244: $V'(t)_{critical}$ = 0.4, Breakpoint Set 1

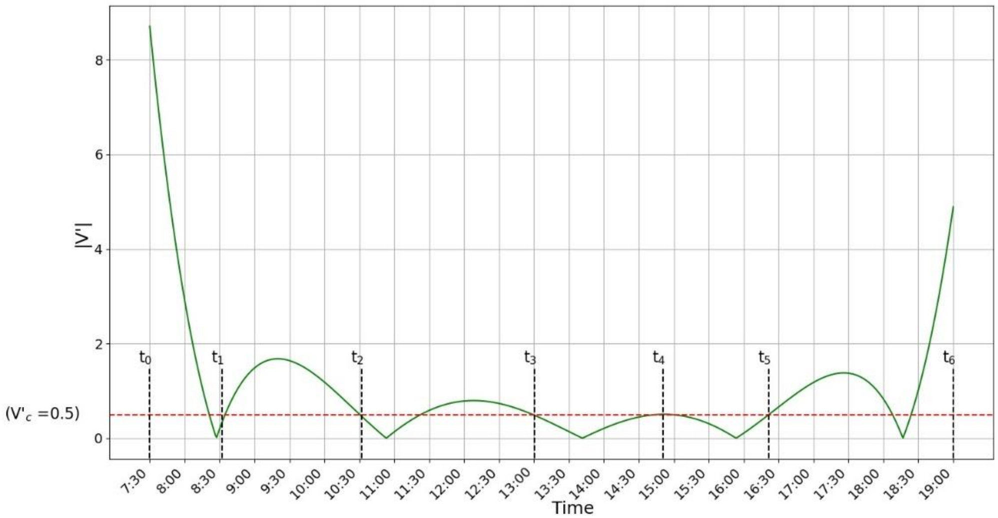

Figure 245: $V'(t)_{critical}$ = 0.5, Breakpoint Set 1

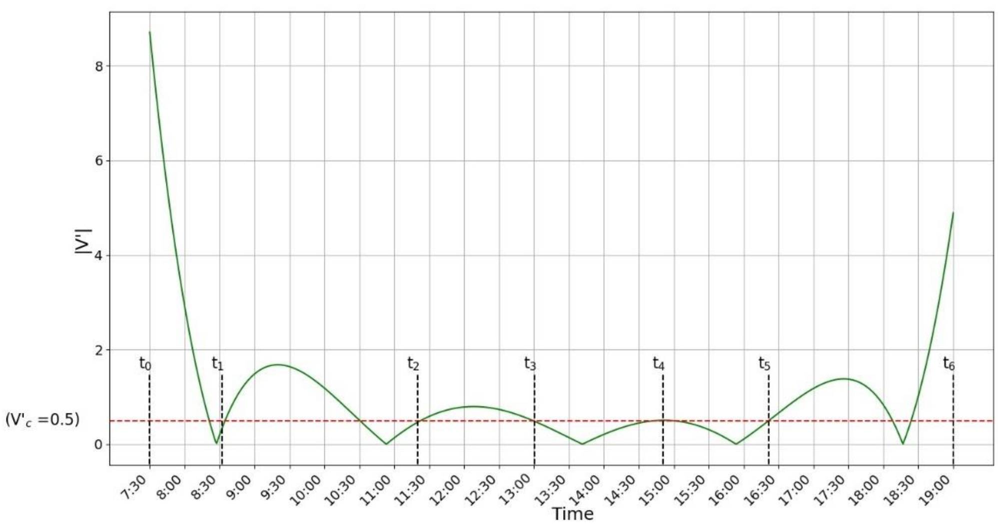

Figure 246: $V'(t)_{critical}$ = 0.5, Breakpoint Set 1

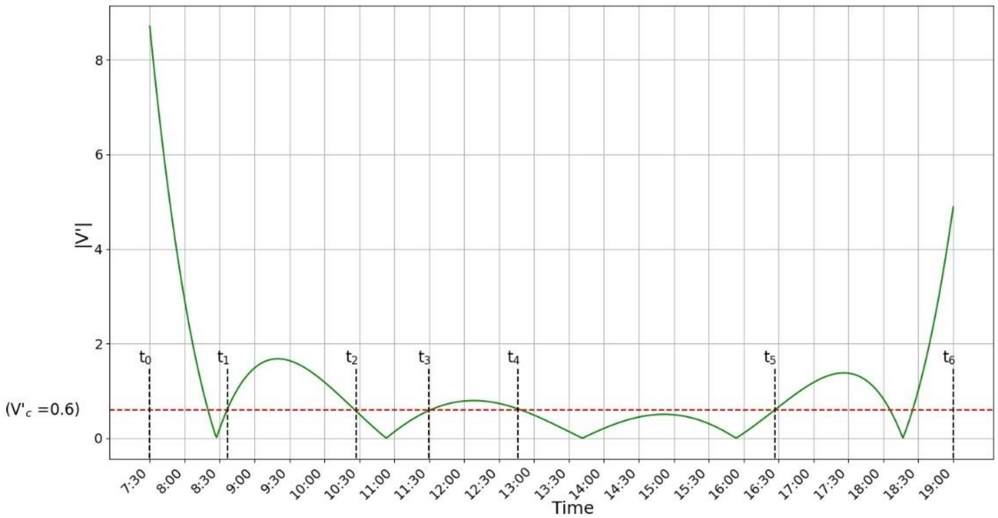

Figure 247: $V'(t)_{critical}$ = 0.6

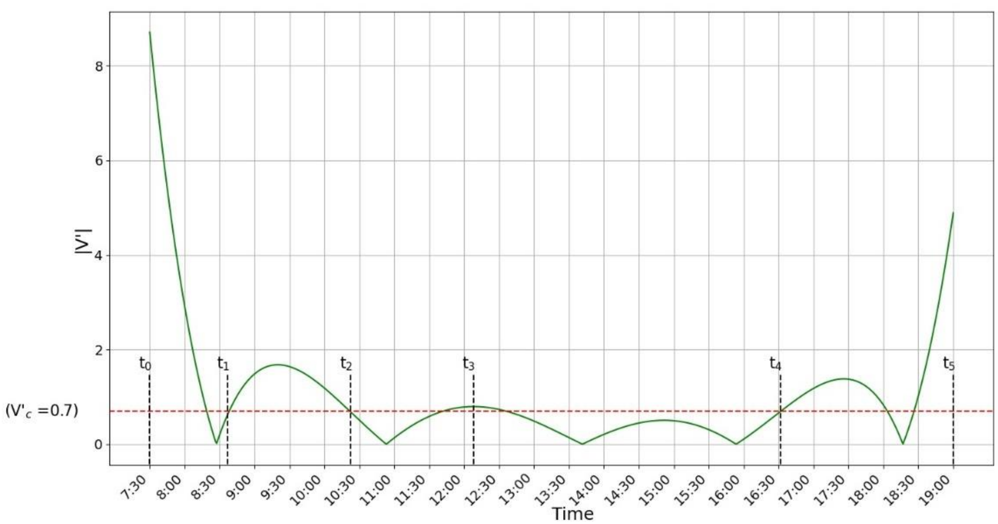

Figure 248: $V'(t)_{critical}$ = 0.7

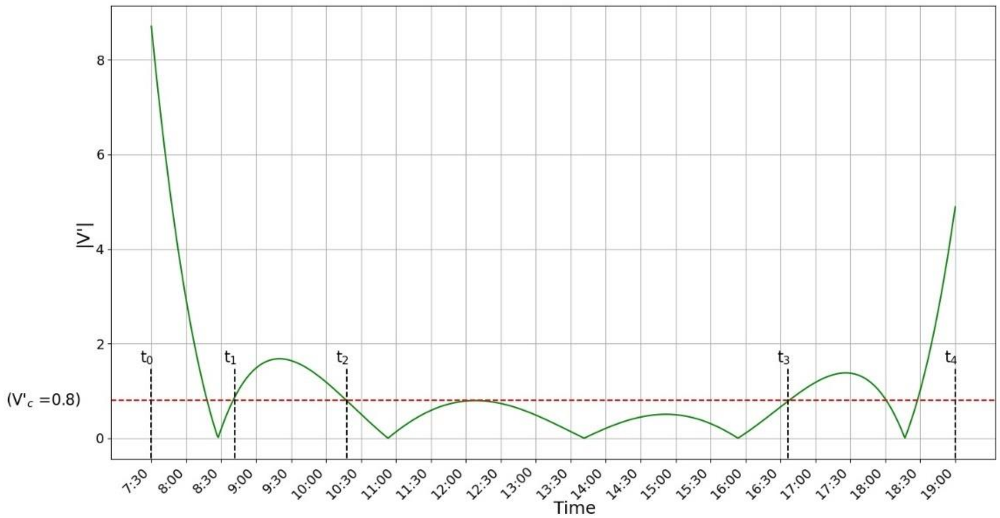

Figure 249: $V'(t)_{critical}$ = 0.8

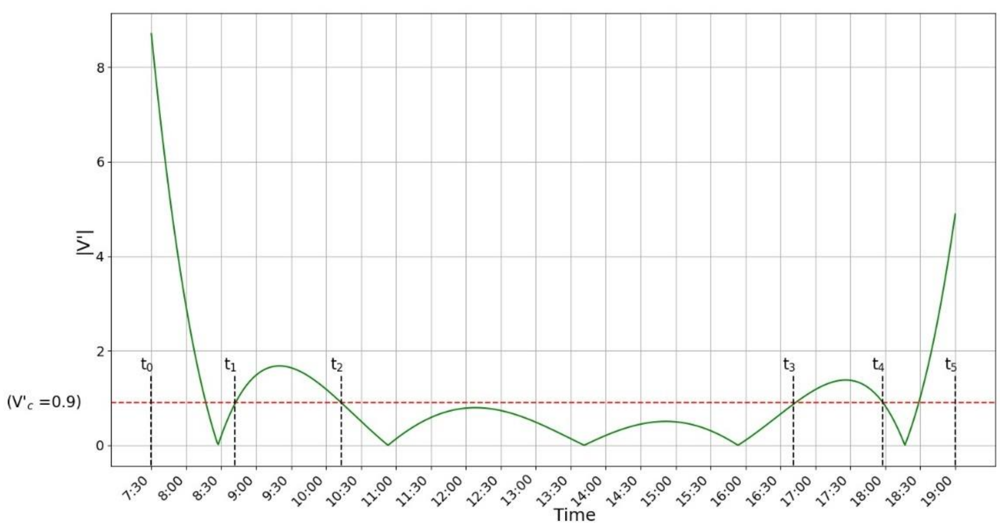

Figure 250: $V'(t)_{critical}$ = 0.9

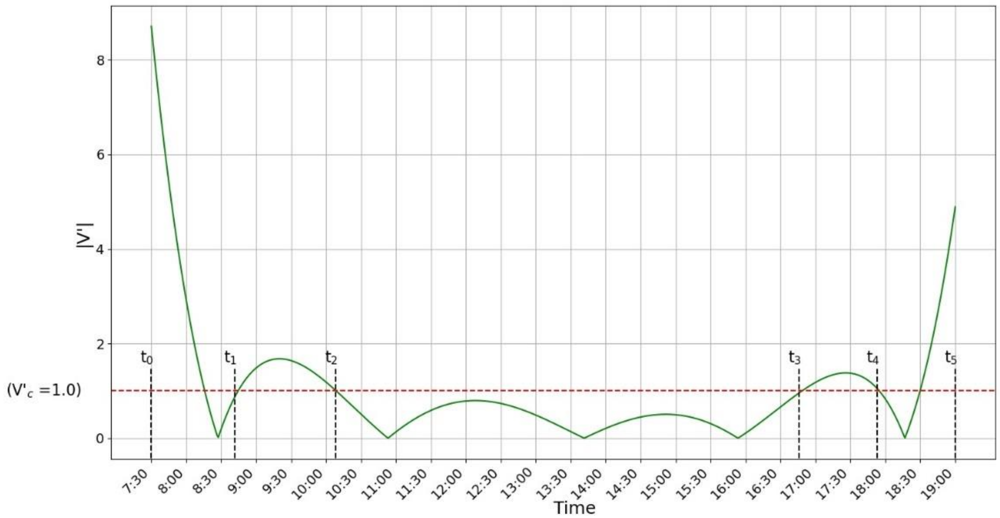

Figure 251: $V'(t)_{critical}$ = 1.0

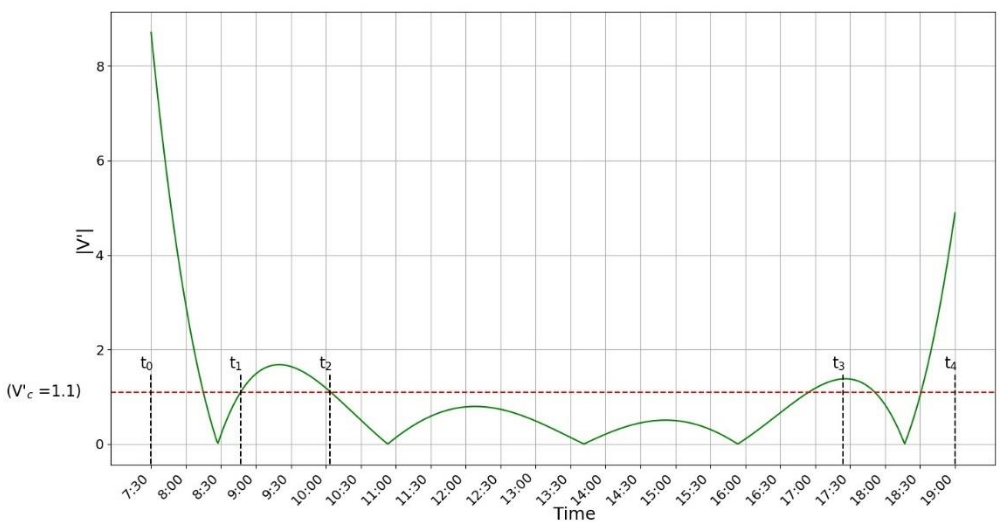

Figure 252: $V'(t)_{critical}$ = 1.1

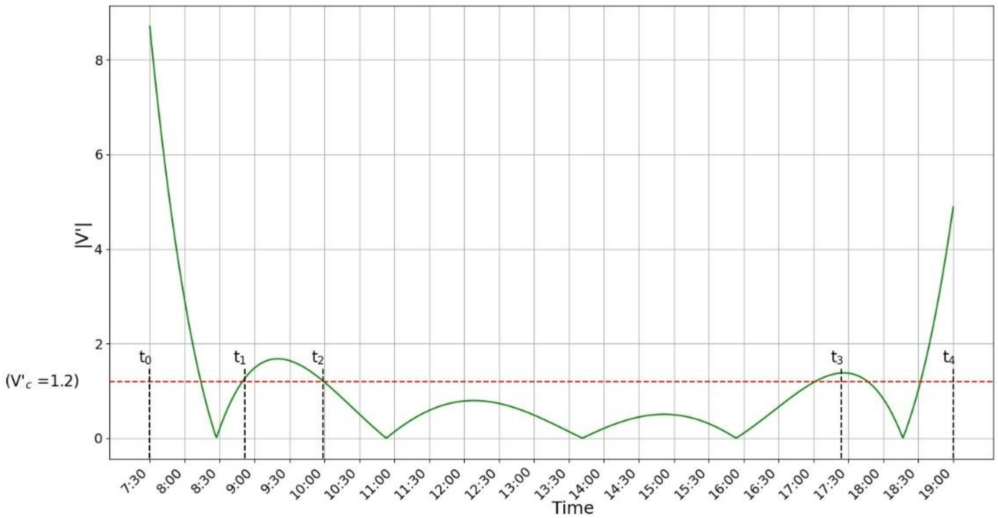

Figure 253: $V'(t)_{critical}$ = 1.2

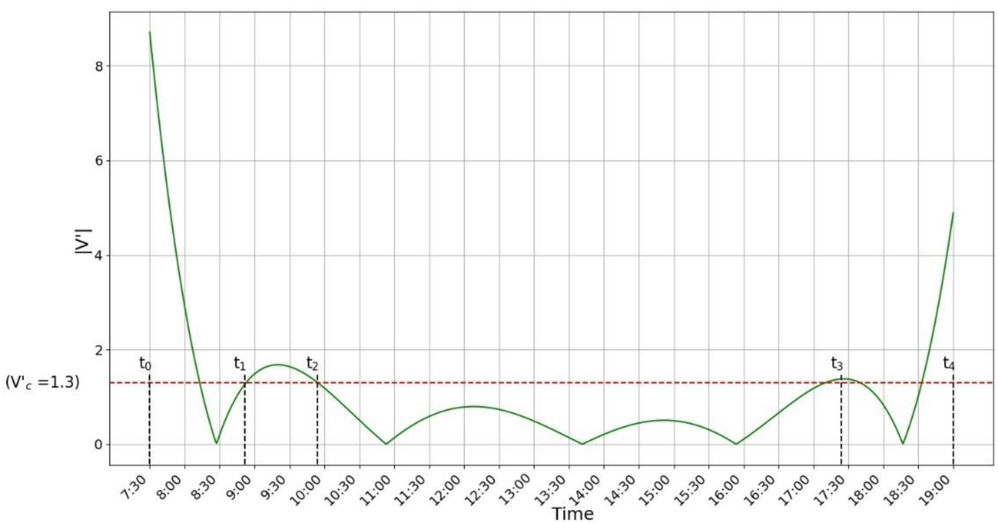

Figure 254: $V'(t)_{critical}$ = 1.3

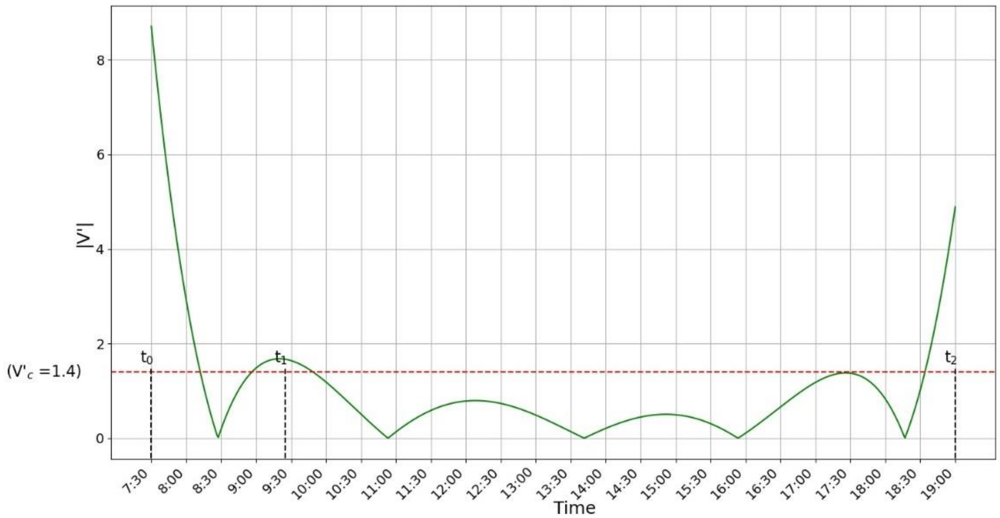

Figure 255: $V'(t)_{critical}$ = 1.4

Table 13 includes the developed breakpoints along with the values of delay and the figure number of each set of timing plan breakpoints.

Table 13: Results of Critical Zone Optimization Method

$V'(t)_{critical}$	Start time	End time	Total Delay (sec/veh)	Figure Number
0	07:00	10:50	54.8	Figure 218
	10:50	13:40		
	13:40	16:00		
	16:00	19:00		
0.1	07:00	10:45	46.8	Figure 219
	10:45	13:35		
	13:35	15:50		
	15:50	19:00		
0.1	07:00	10:45	48.3	Figure 220
	10:45	13:35		
	13:35	16:00		
	16:00	19:00		
0.1	07:00	10:45	45.5	Figure 221
	10:45	13:50		
	13:50	15:50		
	15:50	19:00		
0.1	07:00	10:45	46.9	Figure 222
	10:45	13:50		
	13:50	16:00		
	16:00	19:00		
0.1	07:00	11:00	46.8	Figure 223
	11:00	13:35		
	13:35	15:50		
	15:50	19:00		
0.1	07:00	11:00	48.2	Figure 224
	11:00	13:35		
	13:35	16:00		
	16:00	19:00		
0.1	07:00	11:00	45.5	Figure 225
	11:00	13:50		
	13:50	15:50		
	15:50	19:00		
0.1	07:00	11:00	46.9	Figure 226
	11:00	13:50		
	13:50	16:00		
	16:00	19:00		

Table 13: Results of Critical Zone Optimization Method (Continued)

$V'(t)_{critical}$	Start time	End time	Total Delay (sec/veh)	Figure Number
0.2	07:00	10:40	47.7	Figure 227
	10:40	13:25		
	13:25	15:40		
	15:40	19:00		
0.2	07:00	10:40	43.6	Figure 228
	10:40	13:25		
	13:25	16:05		
	16:05	19:00		
0.2	07:00	10:40	48.4	Figure 229
	10:40	14:00		
	14:00	15:40		
	15:40	19:00		
0.2	07:00	10:40	44.3	Figure 230
	10:40	14:00		
	14:00	16:05		
	16:05	19:00		
0.2	07:00	11:00	46	Figure 231
	11:00	13:25		
	13:25	15:40		
	15:40	19:00		
0.2	07:00	11:00	42	Figure 232
	11:00	13:25		
	13:25	16:05		
	16:05	19:00		
0.2	07:00	11:00	46.8	Figure 233
	11:00	14:00		
	14:00	15:40		
	15:40	19:00		
0.2	07:00	11:00	42.8	Figure 234
	11:00	14:00		
	14:00	16:05		
	16:05	19:00		
0.3	07:00	08:30	33.2	Figure 235
	08:30	10:35		
	10:35	13:15		
	13:15	15:30		

Table 13: Results of Critical Zone Optimization Method (Continued)

$V'(t)_{critical}$	Start time	End time	Total Delay (sec/veh)	Figure Number
	15:30	19:00		
0.3	07:00	08:30	34	Figure 236
	08:30	10:35		
	10:35	13:15		
	13:15	16:10		
	16:10	19:00		
0.3	07:00	08:30	34.6	Figure 237
	08:30	10:35		
	10:35	14:10		
	14:10	15:30		
	15:30	19:00		
0.3	07:00	08:30	35.4	Figure 238
	08:30	10:35		
	10:35	14:10		
	14:10	16:10		
	16:10	19:00		
0.3	07:00	08:30	31.4	Figure 239
	08:30	11:10		
	11:10	13:15		
	13:15	15:30		
	15:30	19:00		
0.3	07:00	08:30	32.2	Figure 240
	08:30	11:10		
	11:10	13:15		
	13:15	16:10		
	16:10	19:00		
0.3	07:00	08:30	32.9	Figure 241
	08:30	11:10		
	11:10	14:10		
	14:10	15:30		
	15:30	19:00		
0.3	07:00	08:30	33.6	Figure 242
	08:30	11:10		
	11:10	14:10		
	14:10	16:10		
	16:10	19:00		

Table 13: Results of Critical Zone Optimization Method (Continued)

$V'(t)_{critical}$	Start time	End time	Total Delay (sec/veh)	Figure Number
0.4	07:00	08:30	29.9	Figure 243
	08:30	10:30		
	10:30	13:05		
	13:05	14:50		
	14:50	16:15		
	16:15	19:00		
0.4	07:00	08:30	29.4	Figure 244
	08:30	11:15		
	11:15	13:05		
	13:05	14:50		
	14:50	16:15		
	16:15	19:00		
0.5	07:00	08:30	30.1	Figure 245
	08:30	10:30		
	10:30	13:00		
	13:00	14:50		
	14:50	16:20		
	16:20	19:00		
0.5	07:00	08:30	30	Figure 246
	08:30	11:20		
	11:20	13:00		
	13:00	14:50		
	14:50	16:20		
	16:20	19:00		
0.6	07:00	08:35	28.6	Figure 247
	08:35	10:25		
	10:25	11:30		
	11:30	12:45		
	12:45	16:25		
	16:25	19:00		
0.7	07:00	08:35	25.4	Figure 248
	08:35	10:20		
	10:20	12:10		
	12:10	16:30		
	16:30	19:00		
0.8	07:00	08:40	44.6	Figure 249

Table 13: Results of Critical Zone Optimization Method (Continued)

$V'(t)_{critical}$	Start time	End time	Total Delay (sec/veh)	Figure Number
	08:40	10:20		
	10:20	16:35		
	16:35	19:00		
0.9	07:00	08:40	67.8	Figure 250
	08:40	10:15		
	10:15	16:40		
	16:40	18:00		
	18:00	19:00		
1	07:00	08:40	43.5	Figure 251
	08:40	10:10		
	10:10	16:45		
	16:45	18:00		
	18:00	19:00		
1.1	07:00	08:45	49.9	Figure 252
	08:45	10:05		
	10:05	17:25		
	17:25	19:00		
1.2	07:00	08:50	50.4	Figure 253
	08:50	10:00		
	10:00	17:25		
	17:25	19:00		
1.3	07:00	08:50	48	Figure 254
	08:50	10:00		
	10:00	17:25		
	17:25	19:00		
1.4	07:00	09:25	94.5	Figure 255
	09:25	19:00		

ΔV Optimization Method:

Figure 256 to Figure 261 show the developed breakpoints by using the ΔV optimization method.

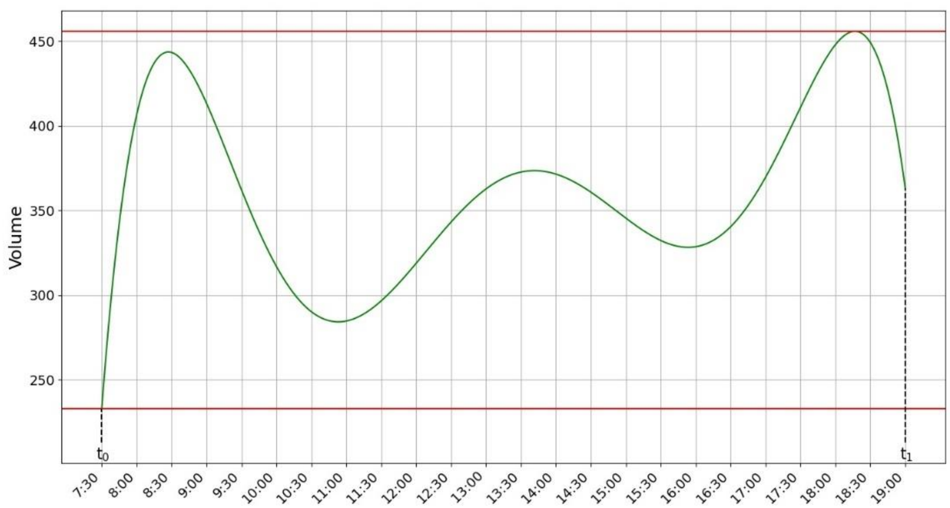

Figure 256: $\Delta V = \text{Range}/1$

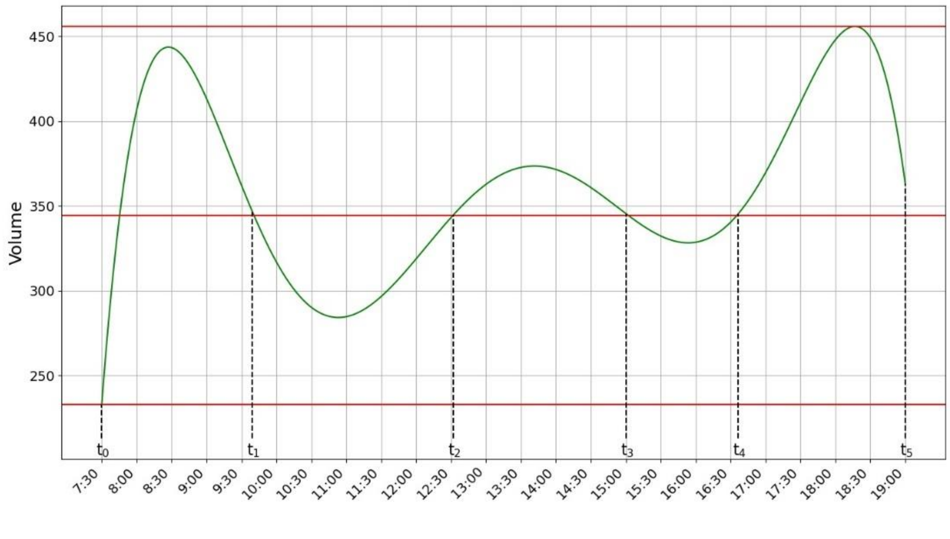

Figure 257: $\Delta V = \text{Range}/2$

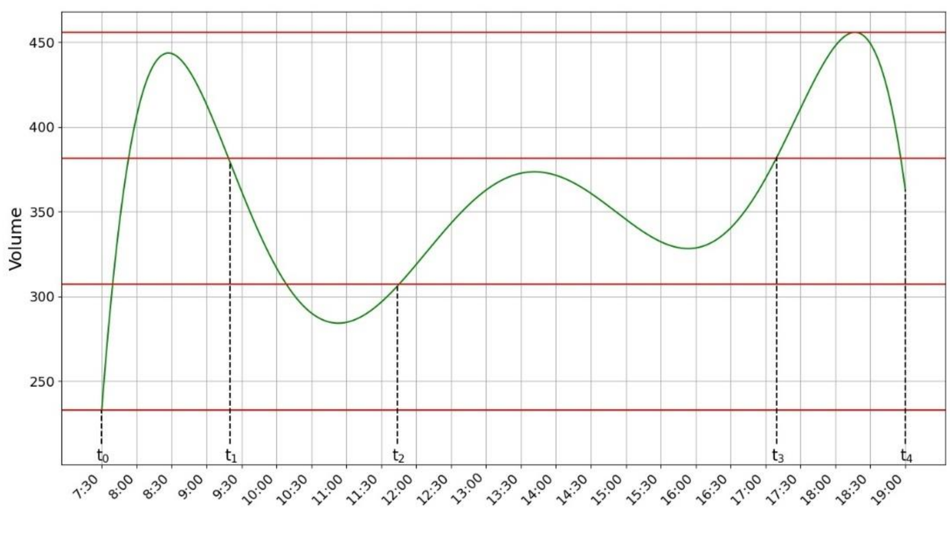

Figure 258: $\Delta V = \text{Range}/3$, Breakpoint Set 1

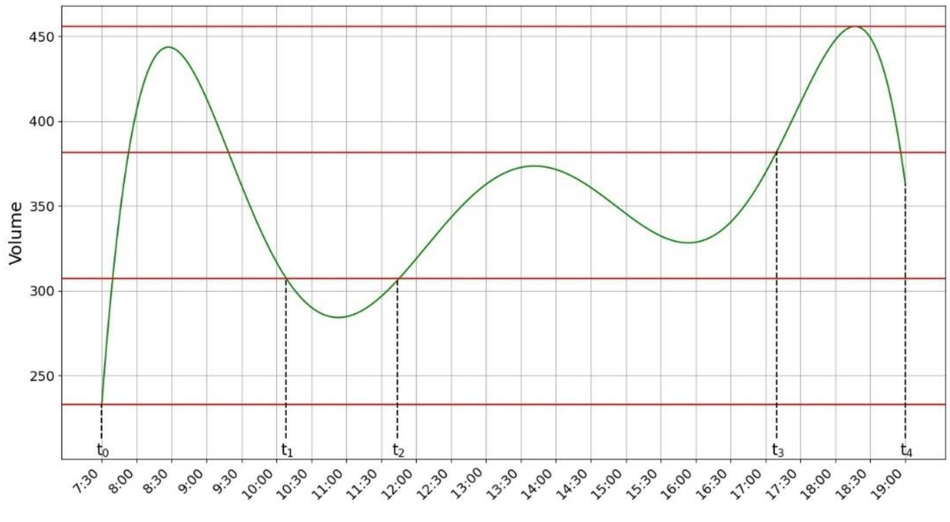

Figure 259: $\Delta V = \text{Range}/3$, Breakpoint Set 2

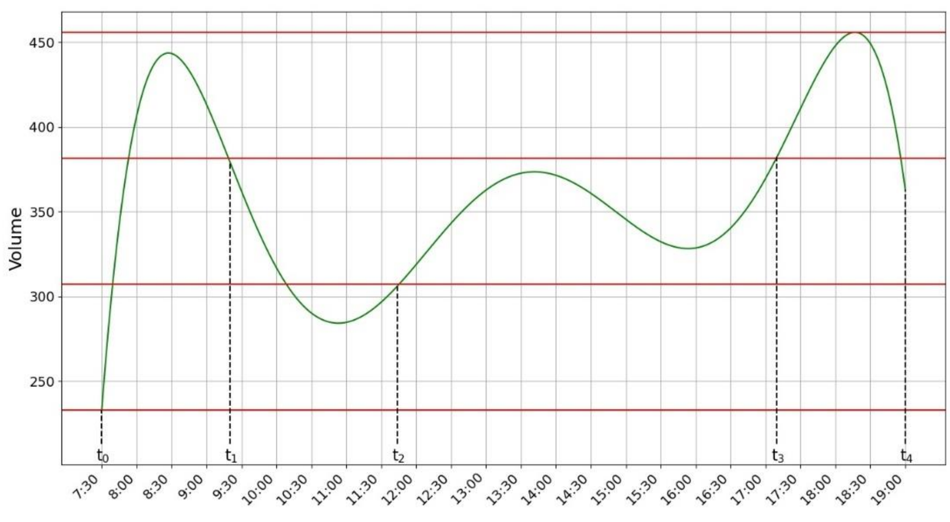

Figure 260: $\Delta V = \text{Range}/3$, Breakpoint Set 3

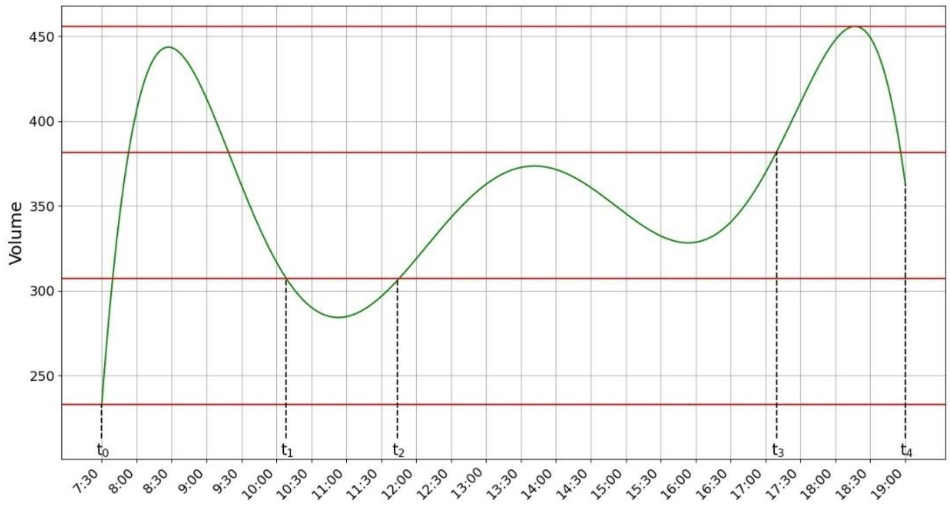

Figure 261: $\Delta V = \text{Range}/3$, Breakpoint Set 4

Table 14 includes the developed breakpoints along with the values of delay and the figure number of each set of timing plan breakpoints.

Table 14: Results of ΔV Optimization Method

ΔV	Start time	End time	Total Delay (sec/veh)	Figure Number
range/1	07:00	19:00	104.8	Figure 256
range/2	07:00	09:40	25.3	Figure 257
	09:40	12:30		
	12:30	15:00		
	15:00	16:35		
	16:35	19:00		
range/3	07:00	09:20	34.2	Figure 258
	09:20	11:45		
	11:45	17:10		
	17:10	19:00		
range/3	07:00	10:10	35.1	Figure 259
	10:10	11:45		
	11:45	17:10		
	17:10	19:00		
range/3	07:00	09:20	34.2	Figure 260
	09:20	11:45		
	11:45	17:10		
	17:10	19:00		
range/3	07:00	10:10	35.1	Figure 261
	10:10	11:45		
	11:45	17:10		
	17:10	19:00		